

DTIC FILE COPY

(2)

STRUCTURE AND PROPERTIES OF HIGH SYMMETRY COMPOSITES

AD-A226 479

Final Report

Grant No. AFOSR-88-0075

Program Monitor: Dr. Liselotte Schioler

DTIC

SELECTE
AUG 28 1990

by

**Frank K. Ko
Albert S.D. Wang
Charles Lei
Eileen Armstrong Carroll
and
Yun Jia Cai**

Fibrous Materials Research Laboratory

Drexel University

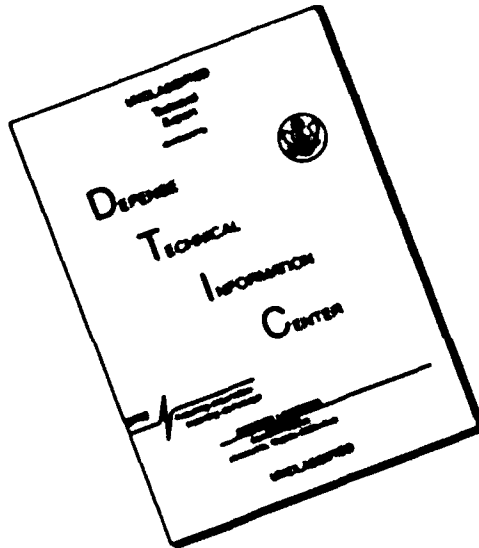
DISTRIBUTION STATEMENT A

Approved for public release;
Distribution Unlimited



ADP...

DISCLAIMER NOTICE



THIS DOCUMENT IS BEST
QUALITY AVAILABLE. THE COPY
FURNISHED TO DTIC CONTAINED
A SIGNIFICANT NUMBER OF
PAGES WHICH DO NOT
REPRODUCE LEGIBLY.

REPORT DOCUMENTATION PAGE

1. REPORT SECURITY CLASSIFICATION Unclassified		1b. RESTRICTIVE MARKINGS	
2. SECURITY CLASSIFICATION AUTHORITY		3. DISTRIBUTION/AVAILABILITY STATEMENT Approved for Public Release Distribution Unlimited	
5. DECLASSIFICATION/DOWNGRADING SCHEDULE		5. MONITORING ORGANIZATION REPORT NUMBER AFOSR-TR-90-0873	
1. PERFORMING ORGANIZATION REPORT NUMBER(S) 010004-1		5. NAME OF MONITORING ORGANIZATION Same as 5a	
6a. NAME OF PERFORMING ORGANIZATION Drexel University Department of Materials Eng.	6b. OFFICE SYMBOL (If applicable)	7a. NAME OF MONITORING ORGANIZATION Same as 5a	
6c. ADDRESS (City, State, and ZIP Code) Philadelphia, PA 19104		7b. ADDRESS (City, State, and ZIP Code) Same as 5c	
8a. NAME OF FUNDING/SPONSORING ORGANIZATION Office of Scientific Research	8b. OFFICE SYMBOL (If applicable) AFOSR/NE	9. PROCUREMENT INSTRUMENT IDENTIFICATION NUMBER AFOSR-88-0075	
8c. ADDRESS (City, State, and ZIP Code) Bldg. 410, Bolling AirForce Base, DC 20332		10. SOURCE OF FUNDING NUMBERS PROGRAM ELEMENT NO: 61102F PROJECT NO: 2366 TASK NO: A2 WORK UNIT ACCESSION NO:	
11. TITLE (Include Security Classification) Structure and Properties of High Symmetry Ceramic Matrix Composites			
12. PERSONAL AUTHOR(S) Frank K. Ko and Albert S. D. Yang			
13a. TYPE OF REPORT Final	13b. TIME COVERED FROM 87/12/1 TO 90/11/30	14. DATE OF REPORT (Year, Month, Day) 90/7/27	15. PAGE COUNT 180
16. SUPPLEMENTARY NOTATION			
17. COSATI CODES FIELD: GROUP: SUB-GROUP:		18. SUBJECT TERMS (Continue on reverse if necessary and identify by block number) High Symmetry Composite, 3-D fiber Architecture. Spherical Reinforcement, Finite Cell Modelling	
19. ABSTRACT (Continue on reverse if necessary and identify by block number) This report describes the concept formulation and demonstration for high symmetry composites by examination of the combination of spheres in 3-D fiber architectures. By computer simulation, the level of geometric symmetry of fiber architectures and spheres were examined. To establish a basis for the analysis of the mechanical response of high symmetry composites, a finite cell model and a finite element code for the analysis of sphere have been developed. A method for the fabrication of the high symmetry system has also been developed.			
20. DISTRIBUTION/AVAILABILITY OF ABSTRACT <input checked="" type="checkbox"/> UNCLASSIFIED/UNLIMITED <input type="checkbox"/> SAME AS RPT. <input type="checkbox"/> DTIC USERS		21. ABSTRACT SECURITY CLASSIFICATION Unclassified	
22a. NAME OF RESPONSIBLE INDIVIDUAL Dr. Liselotte Schioler		22b. TELEPHONE (Include Area Code) 202-767-4933	22c. OFFICE SYMBOL NE

Table of Contents

I.	Background	1
II.	3-D Fiber Architecture	9
III.	Symmetry of 3-D Fiber Architecture	53
IV.	Geometric Modelling	68
V.	Mechanical Modelling	132
VI.	Fabrication of High Symmetry Structures	164
VII.	Conclusions and Recommendations	172
References		177
Appendices		

- A. Listing of FCM program
- B. Listing of Finite Element Code for Hollow Sphere
- C. List of Publications



Accepted _____
 Date _____
 By _____
 Date _____
 A-1

CHAPTER ONE

BACKGROUND

The advent of multiphase engineering materials, in particular fiber reinforced composites, has opened the door for tailored engineering materials. Depending on the nature of packing, order and symmetry of the different phases, a wide range of material properties and structural stability can be achieved. To address the technological needs for structural applications in space and on the ground wherein multidirectional reinforcement and high level of thermo-mechanical stability are required, a great deal of effort has been devoted to the development of strong and tough composite material in the past decade.

It has been recognized that fiber architecture, being the structural backbone of composites, has much to contribute to the structural toughening of composites. As it is often found in nature, e.g., bee's honeycomb, and crystal of reticulated cerussite, a well ordered triangular packing with material symmetry provides the most efficient and structurally stable material system. To reduce this material concept into practice, it has been found that fiber replacement by textile processes in an economical and practical way to create the desirable fiber architecture.

For example, as shown in Figure 1.1, a triaxially woven fabric produces a well regulated, symmetric network of hexagons. As a result, this structure has the highest level of planar stability and isotropy comparing to other planar fibrous assemblies. For thick structures, on the other hand, the concept of close-to-cubic (CTC) symmetry was explored for hardened structure for re-entry applications utilizing a 4-directional reinforcement. Reducing the close-to-cubic symmetry concept into practice in our laboratory by a three-dimensional braiding process, the concept of structural toughening by 3-D fiber architecture has been successfully demonstrated.

Another significant outcome of our research is the demonstration of the direct formation of structural shapes by the 3-D braiding process. The idealized unit cell structure from a 3-D braided 1-beam is shown in Figure 1.2. While the idea of net shape, tough composite is very attractive for structural applications, the question often asked is the compressive resistance of the 3-D integrated structures.

The major concern, as seen in Figure 1.3, is the apparent structural weakness at yarn cross-overs or where the yarns are bent. To address this problem or to elevate the level of compressive resistance of this 3-D structures, it appears that an additional reinforcement system or an incompressible phase would be needed.

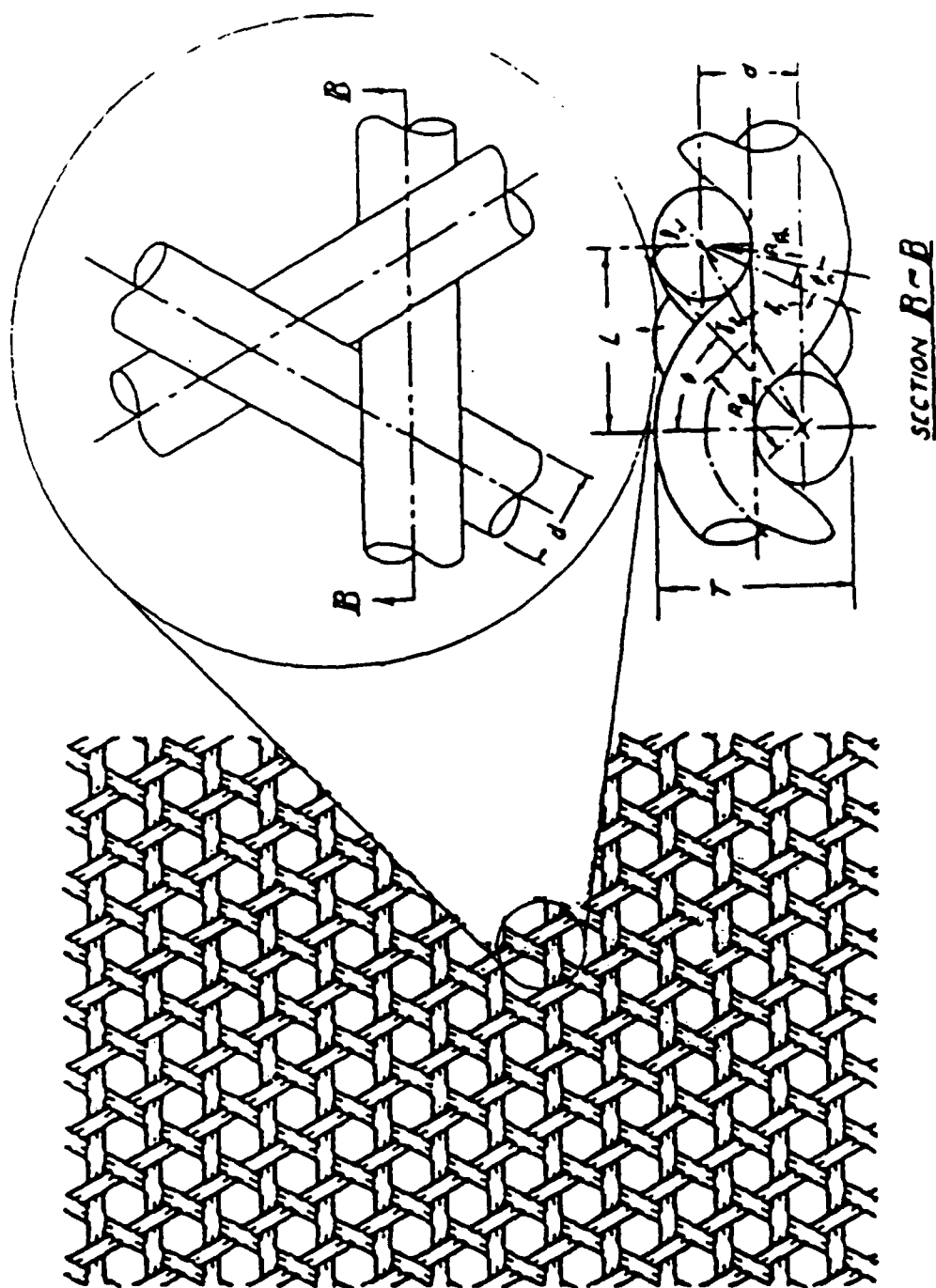


Figure 1.1 Development of Planar Stability by Triaxial Weaving.

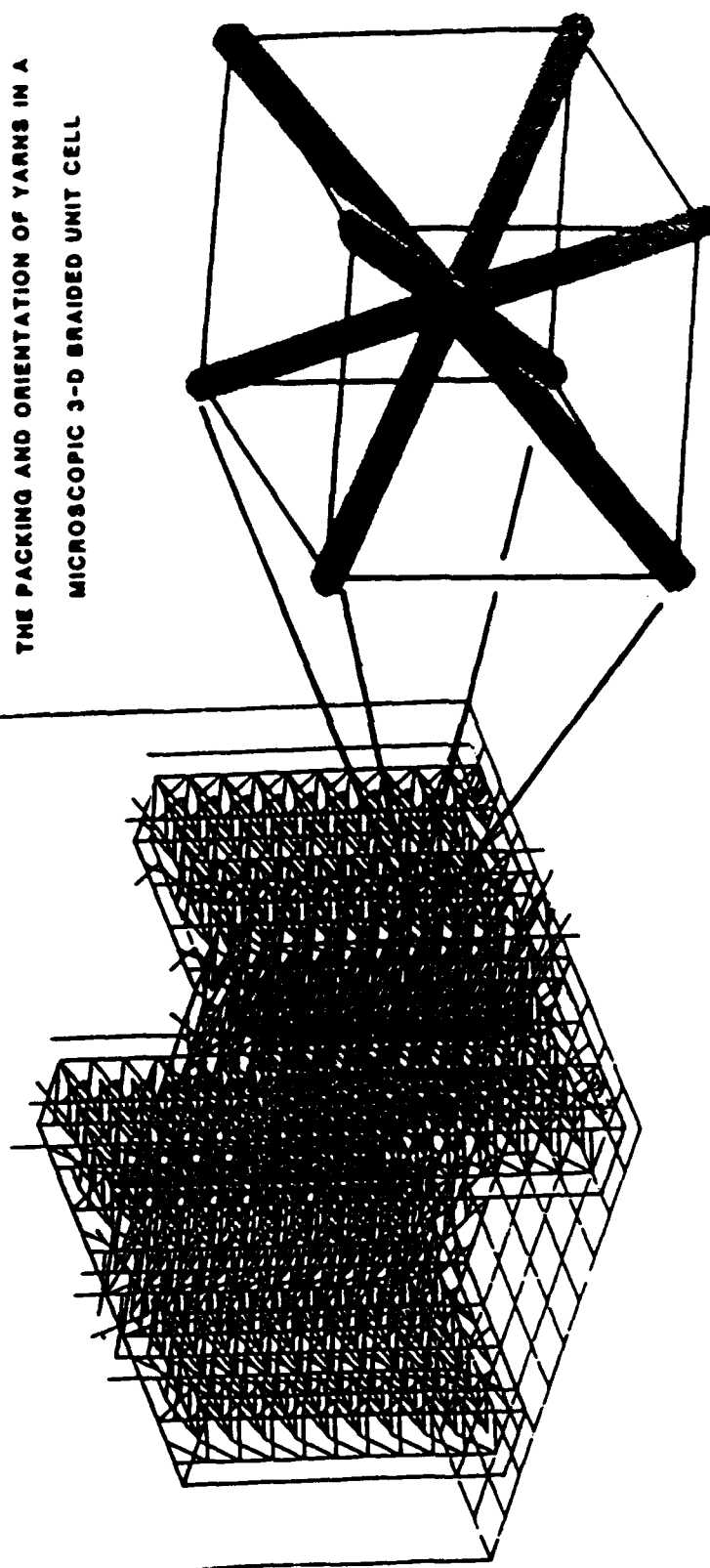


Figure 1.2 Close-to-Cubic Symmetry by 3-D Braiding.

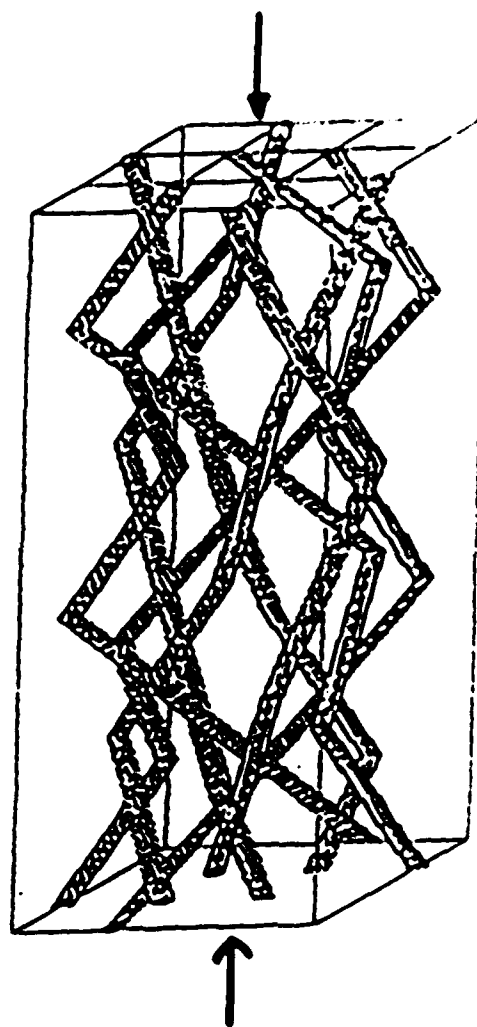


Figure 1.3 Isometric View of Yarn Geometry in a 3-D Braid.

As we experience in ball bearings and many other applications, it is well known that, for the same material, spherical shape provides the best compressive resistance. If one introduces a spherical phase in the reinforcement system and allows the spheres to bear the compressive stresses, a hybrid geometrical structure having tensile, shear and compressive resistance can be produced. This can conceivably be achieved as shown in Figure 1.4 by the superposition of a closest packing of spheres in a tetrahedral/octahedral fiber network.

Equally as important as the development of the High Symmetry Composites (HSC) system, the issue of prediction of macro-structural performance from microstructure on a unit cell level must be addressed. Although some initial work has been carried out on the modelling of unit cell geometry of 3-D braid composites, there is currently no satisfactory theoretical framework linking microstructural unit cell to macrostructural performance as called for in a recent ASME meeting. The mesomechanics of HSC is quite necessary in order to provide guidance to the creation of the multiphase material system and to explore the potential of structural systems from these materials for end use requirements yet to be defined. What is needed is the precise identification and quantification of the unit cell geometry with a combination of spheres and fiber network.

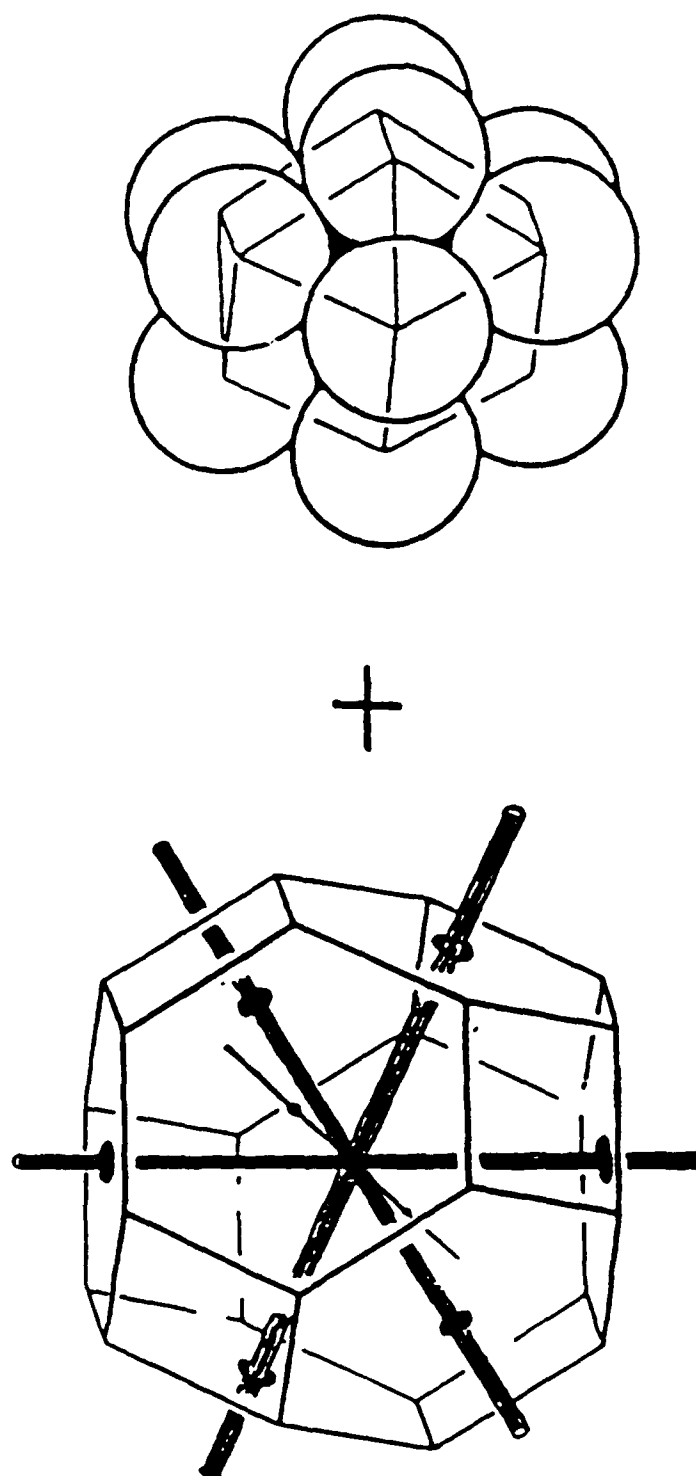


Figure 1.4 High Symmetry Composites by Closest Packing of Spheres in a 3-D Braided Fiber Network.

Treating this cell as a finite structural unit, a Fine Cell Model (FCM) can be developed. The FCM, on one hand, account for the detail design of the unit cell structure and, on the other hand, it allows the exploration of global structural behavior, therefore bridging the communication gap between material scientists and structural mechanicians.

Accordingly, the objectives of this proposed study are:

1. To demonstrate the feasibility and potential of composite material system with high level of tensile, compressive and damage resistance by the concept of High Structural Symmetry.
2. To establish a theoretical framework for the design, analysis and prediction of structural performance of the High Symmetry Composite through Finite Cell Modelling.

To achieve our objectives, this study begins with a review of the technology of 3-D fiber architecture. To provide a basis for discussion, the 3-D fiber architectures are classified according to the level of symmetry. After establishing a framework for the modelling of the geometry of the mechanical responses of high symmetry structures are modelled by the finite cell methodology. In order to transform the geometric concepts to reality, a method for the fabrication of the high symmetry structures is illustrated. It was planned, in the subsequent Phase of the program, that the fabrication method will be demonstrated and employed to produce high symmetry ceramic matrix composites. Verifications of the geometric and mechanical models were also planned in the subsequent Phase of the program by mechanical testing and geometric characterization.

CHAPTER TWO

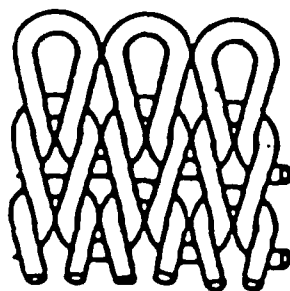
3-D FIBER ARCHITECTURE

In order to develop a classification system for 3D fiber architectures one needs to examine the state of the art of these architectures. The result of this examination provides information which can be used to develop new classes based on the distinguishing and the common properties of the 3D fiber architectures which are produced today and which will be produced tomorrow.

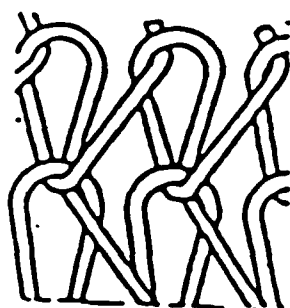
This chapter provides the reader with a review of the state of the art of 3D fiber architectures. The different fiber architectures are grouped in this chapter by their traditional classifications.

Knits

Knitting involves the interlooping of yarns. The knitting process involves two steps; the formation of loops in the yarns, and the linking of the formed loops together with needles. There are two basic types of knitting. These types are called warp knitting and weft knitting. Basic warp and weft knit structures are shown in Figure 2-1.



Basic Weft Knit Stitch [20]



Basic Warp Knit Stitch [20]

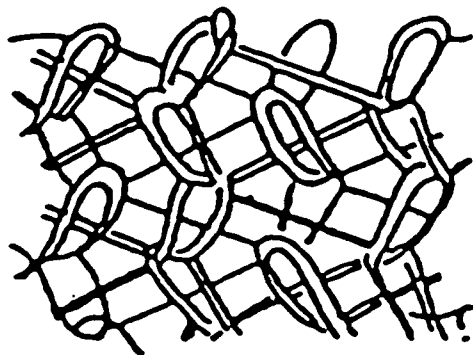
Figure 2-1

Weft knitting is the oldest form of knitting. The first weft knit machine was invented about 1589 [12]. Weft knitting involves the formation of a whole row of loops from one yarn. These loops are then pulled through the previous row of loops to form the knit. Most apparel is formed by weft knitting. Hand knitting is a special case of weft knitting.

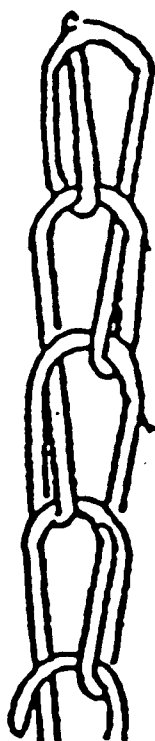
Warp knitting is always machine generated. The first warp knitting machine was invented in 1847 [12]. In warp knitting many yarns are feed as a sheet to the knitting machine. Each yarn goes through its own needle. The needles simultaneously form a loop and interloop of the yarn. This knitting style possesses a higher production rate but also possesses a lower extensibility compared to weft knitting.

Today, warp knitting is the most popular type of knitting for three dimensional textiles. The general form of the warp knit style used in engineering applications is Multiaxial Warp Knits (MWK). MWK typically are composed of lay-ins in the 0° , 90° , and $\pm\theta$ directions. The lay-in are knitted together with a warp knit stitch. The lay-in yarns usually possess a much larger cross-sectional area than the knitting yarns and are therefore the major load bearing component of the fabric. These fabrics are produced by many companies including: Kyntex of Sequin Texas, HiTech of Reno Nevada, and Bean Fiberglass Company of Jaffrey New Hampshire.

The warp knit stitch typically used in MWK is a chain or tricot stitch. Both stitches are shown in Figure 2-2. For many applications the tricot stitch is the most popular. This stitch allows for more flexibility in the shear and weft directions [36]. In a certain type of MWK, weft insert warp knits



Tricot Stitch [32]



Chain Stitch [32]

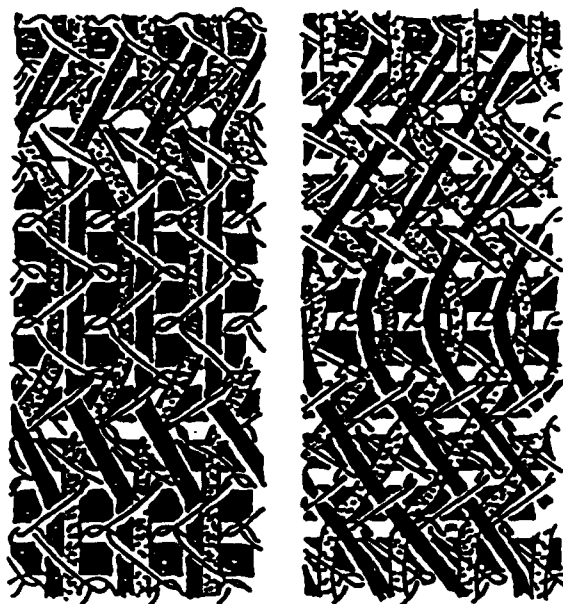
Figure 2-2

(WIWK), the weft inserted yarns can form sinusoidal or linear paths. WIWK are distinguished by two sets of lay-in yarns orthogonal to each other. A WIWK with nonlinear weft yarns and a MWK are shown in Figure 2-3.

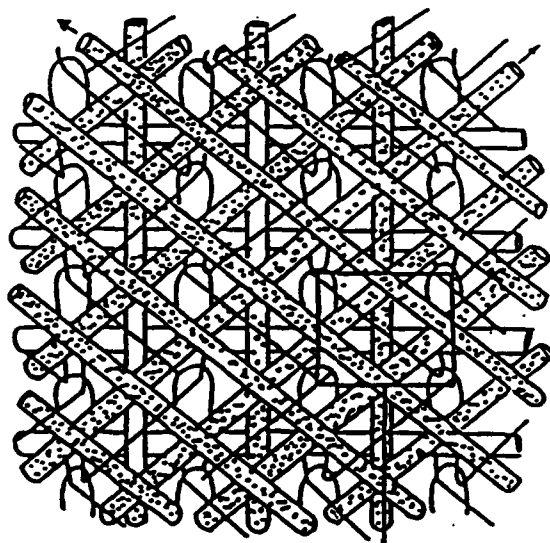
Most MWK machines can precisely control the placement of the warp knitting needle. However impalement of weft inserted yarns in the bias direction often occurs. Impalement breaks and displaces fibers. Thus impalement results in reduced in-plane strength and structural consistency in the fabric.

The Karl Mayer Textile Machine Company of West Germany has invented a WMK machine which does not impale yarns [36]. This affords a higher yarn to fabric translation efficiency. However these fabrics are more voluminous than the other weft insert warp knits. This bulkiness leads to a lower fiber volume fraction. This lower fiber volume fraction leads to reduced composite strength.

MWK knitting allows for much design flexibility. This flexibility partly arises from the variability in the direction, and linearity of the weft inserts. The effect of the direction of yarn placement on the strength efficiency of a fabric is shown in Figure 2-4. In this figure the strength efficiency in the machine (fabric takeoff) direction and the weft (cross or normal to machine) direction are shown as a function of lay in yarn orientation at various volume fractions, ranging from 0% to 40%, of longitudinal lay-in yarns. The strength efficiency is defined as the fractional part of the strength of the yarns transferred to the fabric [21]. When tested in the machine direction,

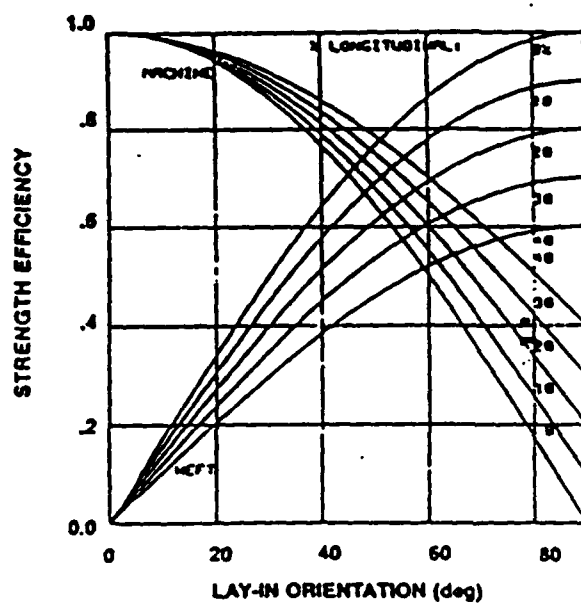


WIWK [32]



MWK [32]

Figure 2-3



Strength Efficiency of a MWK as a Function of Lay-In Yarn Orientation [21]

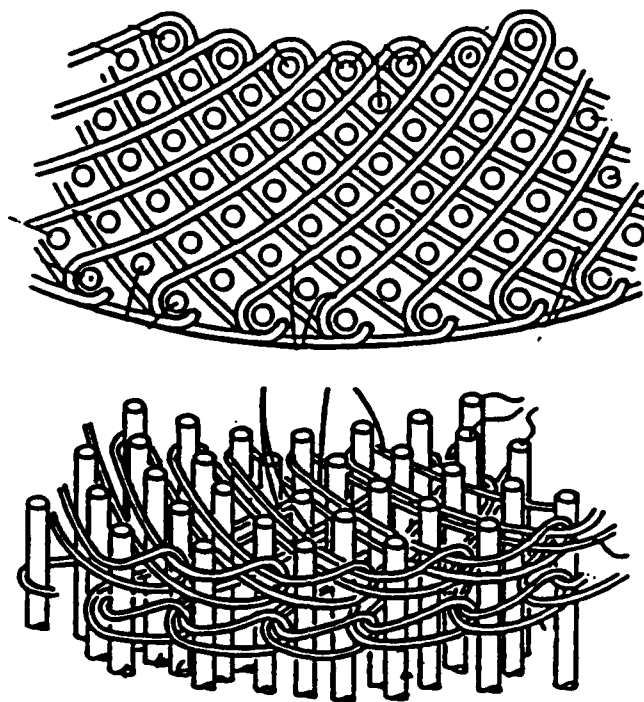
Figure 2-4

the strength efficiency decreases as the lay in yarn angle increases. An increase in the longitudinal yarn fiber volume fraction increases the strength efficiency in the machine direction. Since the weft direction is normal to the longitudinal lay-ins, an increase in longitudinal yarn fiber volume fraction decreases the strength efficiency.

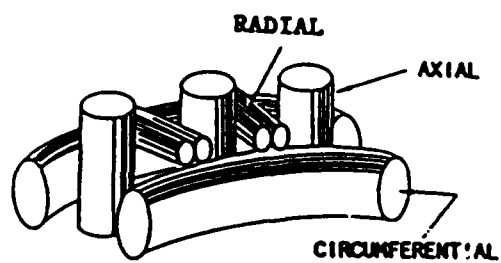
The effect of linearity can be discussed by comparing linear and nonlinear $\pm 45^\circ$ weft inserted warp knits [24]. Linear weft inserted warp knits possess an higher initial modulus than nonlinear. The strength of the nonlinear knit is slightly higher in the 0 and 90 degree direction. However, the bias strength of the linear knit is much greater than the nonlinear, since in the linear knit more fiber is aligned in this direction. The flexibility of these knits can vary greatly depending on the number of layers and the direction of the weft yarn inserts.

MWK can produce fabrics up to 1.3 centimeters thick. By using another technique, a thick warp knitted fabric can be formed. The Aerospatiale Company of France pioneered this technique.

Aerospatiale developed a three dimensional circular knitting machine. Presently there are two models of this machine [1,2,8]. These machines are capable of producing the fabric geometries shown in Figure 2-5. The different knit geometries are a result of the different templates used for the longitudinal yarns. The two different template structures are shown in Figure 2-6. These templates define the paths of two of the three constituent yarns. In the first geometry, which will be referred to as XXYZ, circumferential yarns are laid in and radial yarns are knitted. The radial

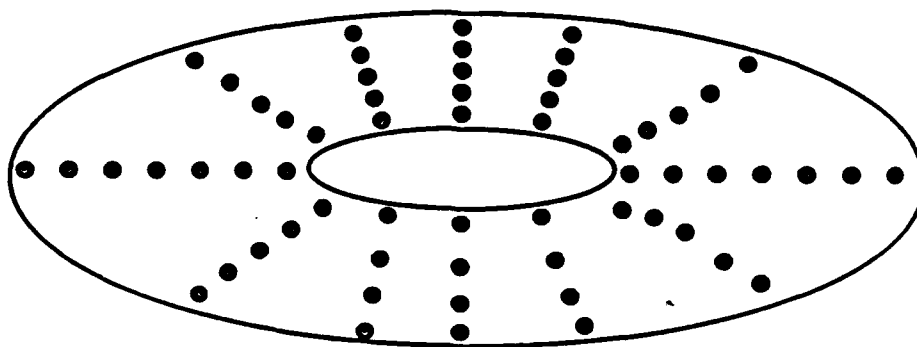


Aerospatiale XXYYZ Geometry [8]

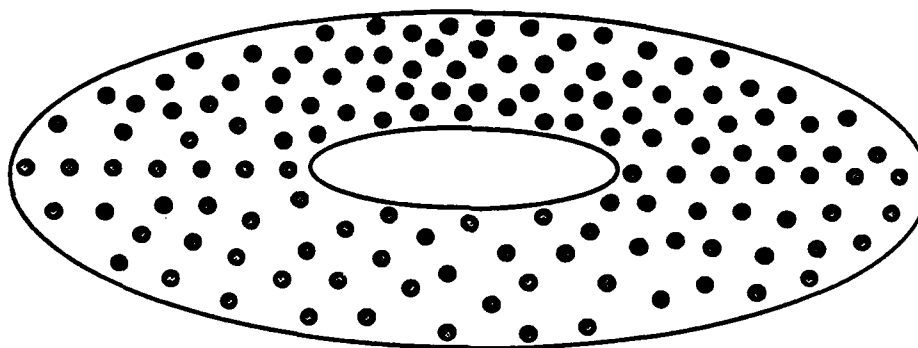


Aerospatiale XXYZ Geometry [7]

Figure 2-5



XXYZ Geometry Template



XXYYZ Geometry Template

Aerospatiale Templates

Figure 2-6

yarns form a series of chain stitches on the outer side the the fabric. In the second geometry, XXYYZ, two sets of radial yarns form chain stitches in different directions and on alternating levels. Both these geometries provide high tensile and shear strength in all directions. The XXYYZ geometry is more flexible as a result of the substitution of a second radial knitting yarn for the circumferential yarn.

The fabric formation process used for each geometry is slightly different. This paragraph describes the formation process for the XXYZ geometry [7]. First metallic rods are inserted in the template in the longitudinal yarn position. Then the radial yarns are knitted by an hook-shaped needle which is inserted between the longitudinal rods and the circumferential yarns are feed into circumferential corridors. The apparatus on which the template is set rotates, allowing the knitting of the chain stitches and the laying down of the circumferential yarns. After each layer is formed, it is compacted. After all the radial and circumferential yarns are added, the longitudinal wire rods are pushed out using lacing needles. The eye of both needles then hooks a yarn strand and inserts it into the proper longitudinal position.

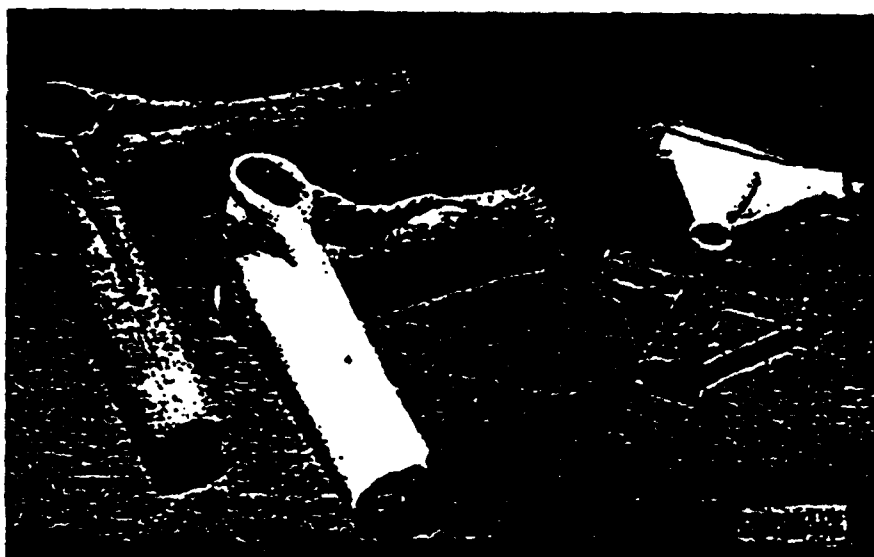
The following is the fabric formation process for the XXYYZ geometry [8]. First metallic rods are inserted in the template in the longitudinal yarn position. Then the two radial yarns are knitted by hook-shaped needles which are inserted between the longitudinal rods. The two different radial knitting machines move around the template structure. After each layer is formed, it is compacted. After all the radial yarns are added, the longitudinal wire rods are pushed out using lacing needles. The eye of

each needle then hooks a yarn strand and inserts it into the proper longitudinal position.

Although warp knitting is the most popular form of knitting for three dimensional textile structures, Courtaulds produces a modified computer controlled weft knitting machine to knit three dimensional preforms [36]. This modification allows individual needle control. This control is important with high modulus fibers. The brittle nature of high modulus fibers cause them to be more susceptible to breakage with variations in tension. The individual needle control maintains constant tension on each yarn during the knitting process.

Examples of the complex three dimensional shapes that can be knitted with this process are shown in Figure 2-7. A substantial amount of the fiber lies in a loop configuration. Since the loop configuration is comprised of so many orientations, this configuration is similar to that of a random mat. Because of this configuration, these fabrics possess moduli comparable to those of a random mat. The tensile strength of these fabrics is lower than that of a random mat [39]. The key advantage of this structure is the ability to form integral structures without fiber discontinuities at key joints in the structure. These structures are three dimensional in shape but their thickness is small.

In general, because of the toughness needed by the knitting yarn, there are some material restrictions on this yarn. With the weft insert warp knits, the knitting yarn is usually a polyester yarn with a diameter a tenth the



Three Dimensional Shapes Produced by Weft Knitting [39]

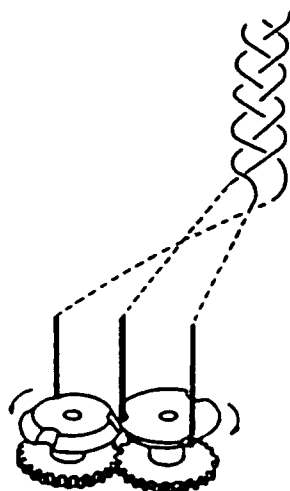
Figure 2-7

size of the weft yarns. The presence of the loop make knits tougher and more conformable to complex shapes.

Braids

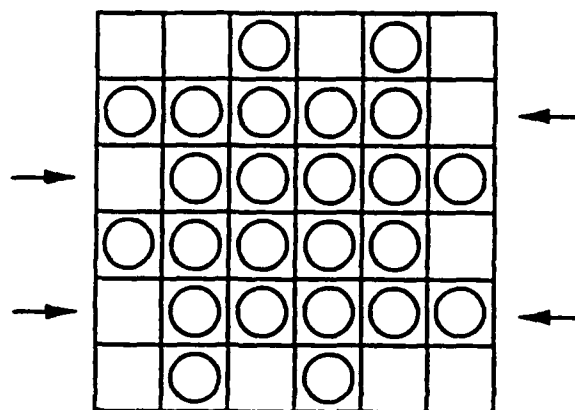
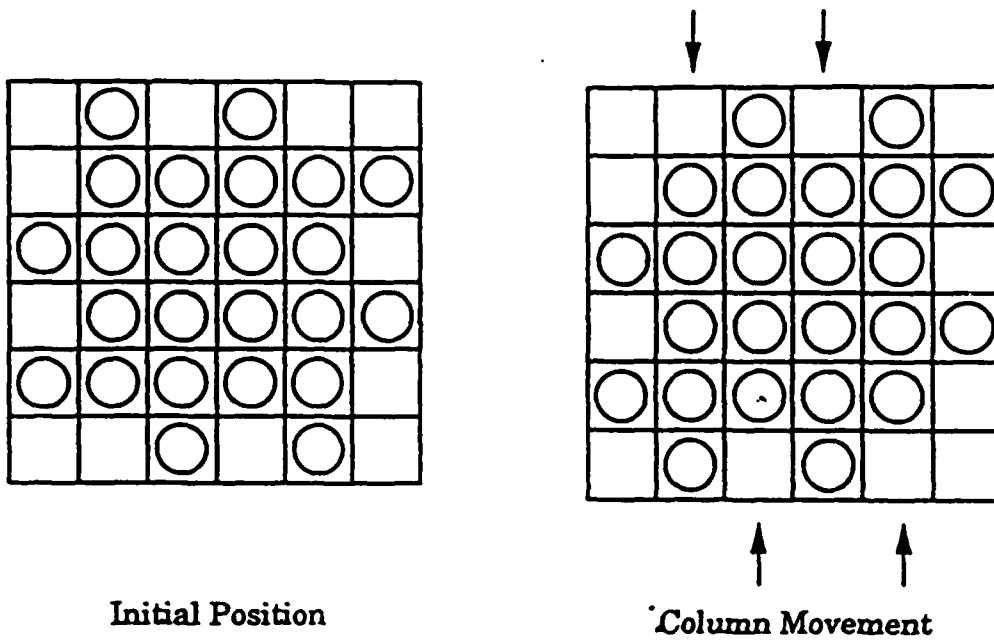
Braids are formed by the intertwining of yarns. The basic braiding method is shown in Figure 2-8. The intertwining is accomplished by the crossing of yarns on individual yarn carriers. The oldest recorded use of braiding is between 1500 and 1000 B.C. [12]. Although this technique has been used since prehistoric times, in general, it has never been as popular as the other textile techniques. One of the factors that limited the use of braids is that the braiding machine size must be much larger than the actual braid produced. However in the field of three dimensional textiles, braiding techniques are becoming very popular. This popularity is a result of their high damage tolerance, delamination resistance, and conformability.

Three dimensional Euclidean braiding involves the steps shown in Figure 2. This sequence can be performed on circular or rectangular looms. In this process yarns gradually move through the thickness of the fabric, through alternate track and column motion. Thus the yarns traverse a circular path with a zig-zag motion. The resultant yarn path, projected onto the braidplane, of one yarn following this sequence in both types of looms is shown in Figure 2-10. The three dimensional path of one yarn in an Euclidean braid is shown in Figure 2-11. The discrete lattice shown in this figure is used to locate the yarn in the braid. The presence of this lattice has generated the nomenclature, Euclidean braiding, to describe the track/column braiding process.



Basic Braiding Motion [19]

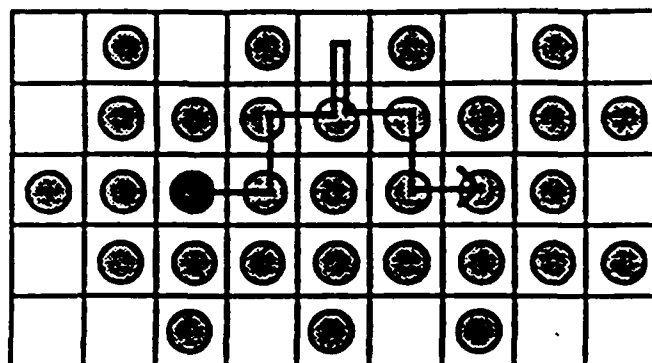
Figure 2-8



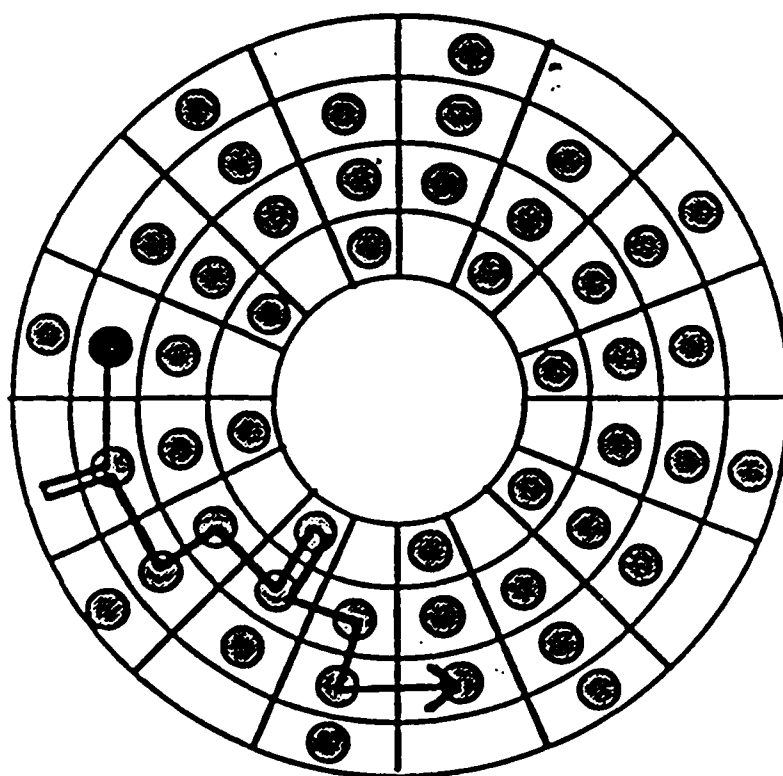
Track Movement

Loom Motions of Euclidean Braiding

Figure 2-9

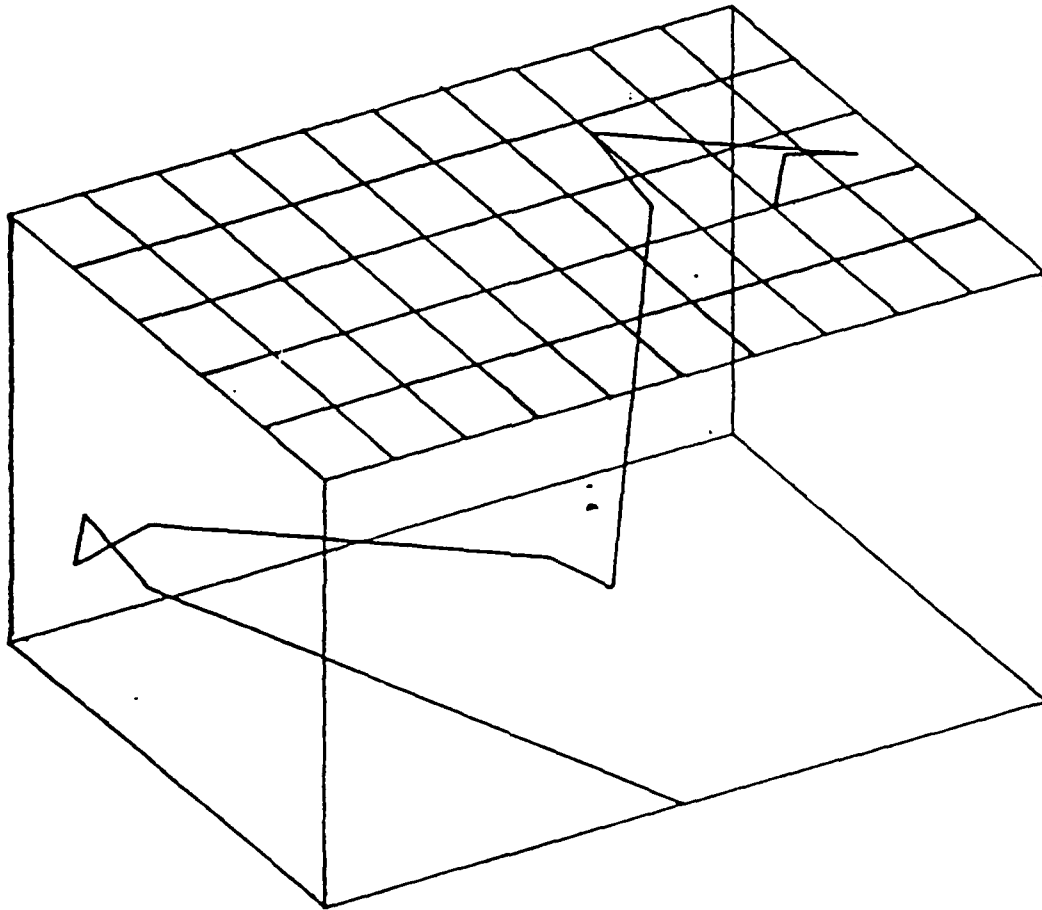


Yarn Path in the Braiding Plane in a Rectangular Loom [31]



Yarn Path in the Braiding Plane in a Circular Loom [31]

Figure 2-10



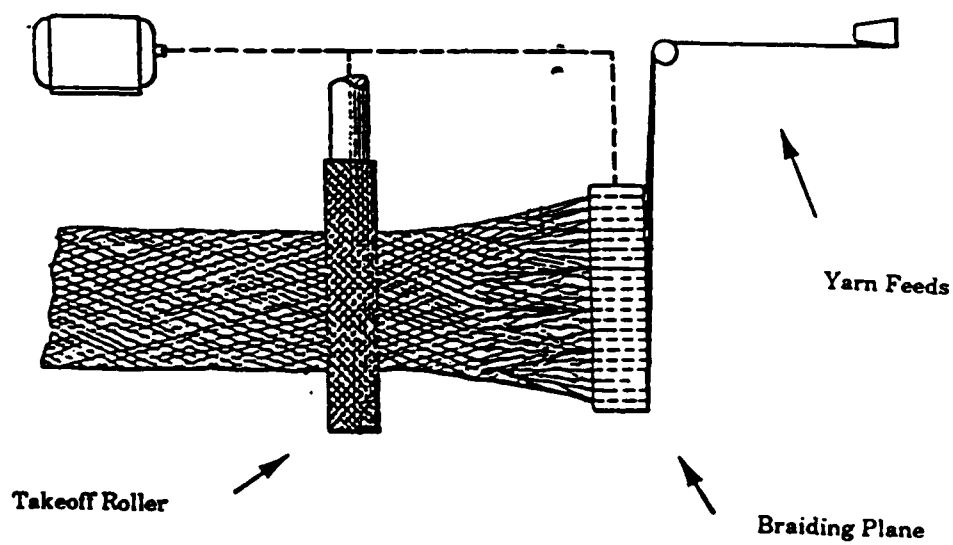
Isolated Path of a Single Yarn in a 3D Braided Fabric [31]

Figure 2-11

After each set of track and column movements, the yarns are compacted. In this process body diagonal yarn pairs resulting from a track/column movement are compacted against body diagonal pairs arising from the previous track/column motion. The compacting motion intertwines the yarns. The braiding process just mentioned is the result of many developments in braiding machine technology. The following paragraphs trace the development of three dimensional braiding machines.

This first patent for this method of yarn placement was granted to Bluck in 1969 [3]. Bluck's machine moved the tracks and columns of the braiding plane with cams connected by gears to a driveshaft. Each yarn is fed into the braiding plane through holes in individual yarn guides. The yarn guides move in the braiding sequence as mentioned above. The speed of braiding is controlled by takeoff rollers which grip the fabric a certain distance from the braiding plane and pull the fabric away from this plane. A schematic of this machine is shown in Figure 2-12.

In 1973 Maistre patented a braiding process [27]. In this process, the yarns are attached to a rigid frame which arranges the yarns into a vertical net. The distance between the yarns comprising the net is constant in the vertical and horizontal directions. In Maistre's machine the yarn feeding mechanism is not in the braiding plane and there is no takeoff roller. Braiding occurs as a result of the alternate displacement of the row and columns of the yarns. Though Maistre's machine differs from Bluck's in the yarn feeding mechanism and the absence of a takeoff roller, the resultant yarn path of both machines is the same.



Bluck's Braiding Apparatus [3]

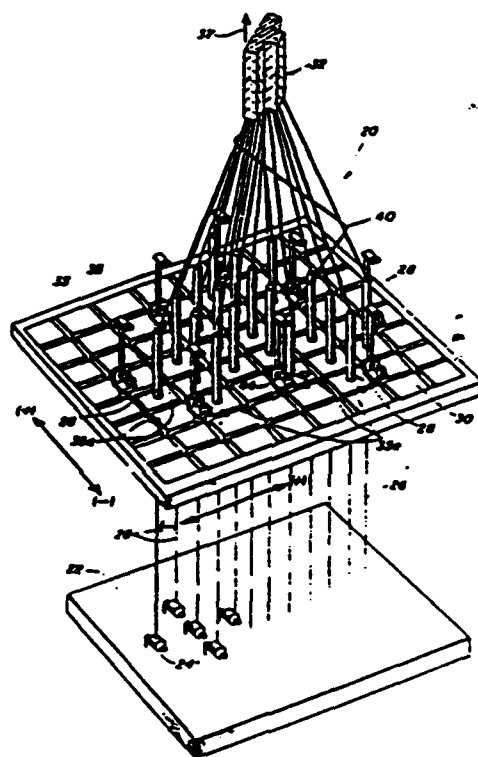
Figure 2-12

In 1982 Florentine improved Bluck's braiding machine. Florentine's machine [13], called "Magnaweave", uses solenoids to move the yarn carriers. The yarn carriers are properly aligned with respect to each other by bar magnets on the yarn carrier. Each yarn carrier contains a spool of yarn. A series of pins to beat up the braided fabric are added between the braiding plane and the takeoff rollers. These pins are removed during each braiding sequence and are engaged again after said sequence.

In 1986 Brown [6] addressed the problem of machine jamming in the braiding machine of Florentine. Jamming is minimized by moving a track or column of yarns carriers sequentially, and by applying a tamping stroke after each movement to insure that the yarn carriers are in their proper place. Brown's yarn carrier design is also different. In Brown's setup, a finite length of yarn is attached to a smaller length of an elastic yarn. The looped end of the elastic yarn is attached to a hook on the yarn carrier.

In 1988 Brown [5] modified the design of the circular braiding machine to allow for interchangeable rings of the same diameter. These rings replace the concentric rings used in Florentine's machine. The capacity of the machine as measured by the number of rings could not be easily expanded with the concentric rings.

Another three dimensional braiding process is the Two Step Braid. The Two Step Braid was patented by Popper of DuPont in 1988 [29]. This apparatus is shown in Figure 2-13. The Two Step Braid is composed of axial and braider yarns. The axials are placed in the fabric forming direction and remain approximately straight in the structure. The



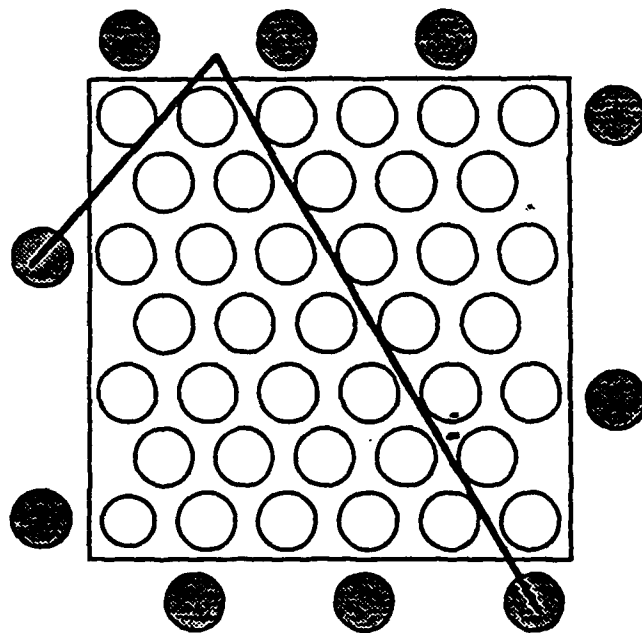
Two-Step Braid Apparatus [29]

Figure 2-13

braiders move between the stationary axials in a special pattern, which cinches the axials and stabilizes the shape of the braid. The path of one yarn during a braiding sequence is shown in Figure 2-14. The zig-zag motion of a yarn constitutes one sequence. Although the resultant yarn path is the same for the Two Step Braid as for the other three dimensional braids mentioned above, the method of achieving this path differs. The Two Step Braid path differs from the other 3D braids by passing each braiding yarn through the whole fabric thickness during each movement. In the Two Step process a smaller number of braiding sequences is needed for the yarn to travel back to its initial point in the braiding plane.

It is important to note that with the Euclidean braiding process, non braiding yarns, called longitudinal yarns can be positioned between the columns, as shown in Figure 2-15. These yarns are subjected only to a slight zig-zag motion as the rows move back and forth. The effect of this zig-zag motion upon the straightness of the longitudinal yarns has not been examined. These yarns act in the same way as the the axial yarns of the Two Step Braid. Since the longitudinal yarns are more aligned with the fabric's vertical axis than the braiding yarns, these yarns increase the tensile strength of an Euclidean braid in this direction. The normalized tensile strength of 3D braids with and without axial yarns is compared in Figure 2-16. The value of the normalized tensile strength is determined by dividing the tensile strength measured by the number of yarns in the braid and the breaking strength of a constituent yarn.

Figure 2-17 shows the effect of varying the braid angle of both braid types. The braid angle is the angle a braiding yarn makes with the vertical axis of

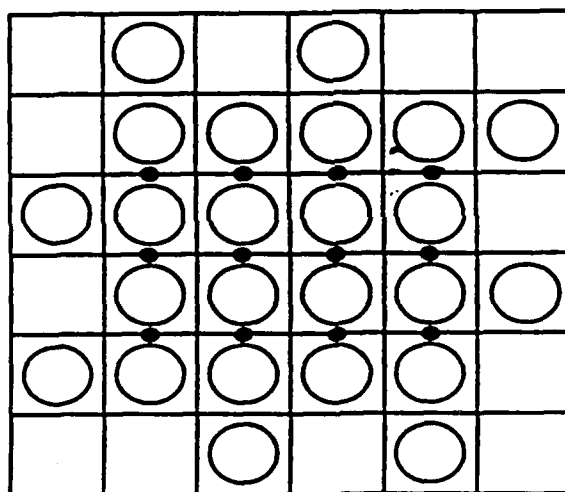


● Braider Yarns

○ Axial Yarns

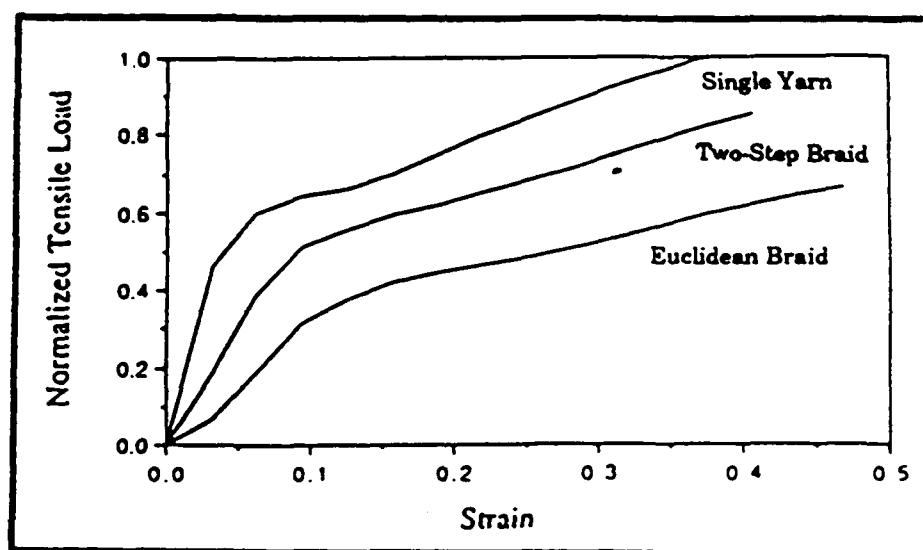
2-Step Loom Design

Figure 2-14



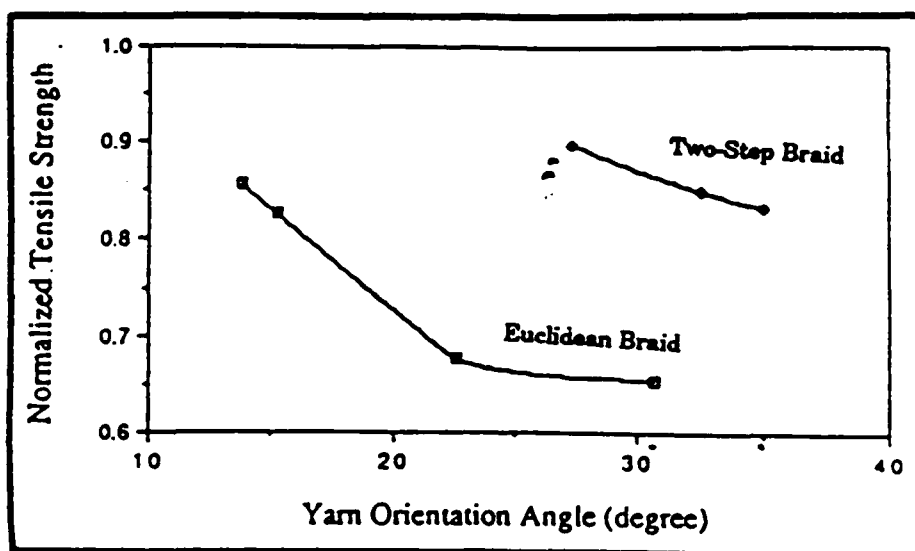
Euclidean Braid Loom Design with Longitudinal Lay-ins

Figure 2-15



Typical Load-Elongation Curves [26]

Figure 2-16



Normalized Tensile Strength as a Function of Braid Angle [26]

Figure 2-17

the braid. Though the tensile strength of the Two Step braid is greater than that of a Euclidean braid (with no longitudinal yarns), the comformability and compressability of a Euclidean braid is greater than that of the Two Step braid.

Nonwovens

Two dimensional nonwovens are formed by fiber entanglements. The means of entanglement may be chemical or mechanical. Nonwoven felts are considered the oldest textile structures produced. The first machine made nonwoven, paper, was made in 1804 [37]. Today nonwovens form the largest percentage of the two dimensional industrial textile market.

The simplest three dimensional nonwoven is an assembly of chopped fiber. This nonwoven is held together in composite form by the matrix material. Ideally this structure is the most isotropic reinforcement geometry. But usually the resultant fiber orientation is skewed to favor melt flow paths. This deviation is a result of the fabricating conditions of the composite. A composite with this geometry is tough, but possesses a small strength translation efficiency. The fibers act as crack deflectors, but do not carry a significant part of the load. The load bearing capacity of the fibers is increased if the aspect ratio of the fibers is large. As the length of the fibers increases, the capacity of the fiber to transfer stress along this dimension necessarily increases.

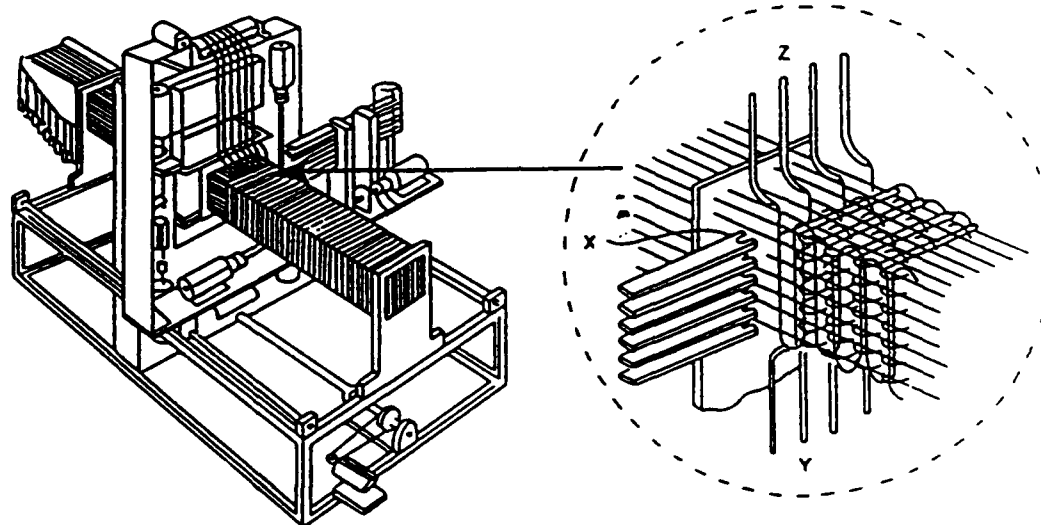
Three dimensional nonwovens lay ups are formed from continuous yarns. Thus these nonwovens possess a high strength translation efficiency. These fabrics differ from the nonwovens mentioned before. In most three

dimensional nonwovens the constituent yarns are laid in from various directions and are not entangled. These nonwovens form stable structures by means of the resultant frictional forces between fibers.

In 1971 General Electric introduced "Omniweave" [4] In this nonwoven the path of the yarns forming the fabric is straight through the thickness direction. When a yarn reaches a surface, the x-y orientation is reversed. The z directional motion is maintained. A three directional orthogonal placement of the yarns was most common with this loom. However a four directional yarn placement along the body diagonals of a parallelepiped unit cell can also be achieved.

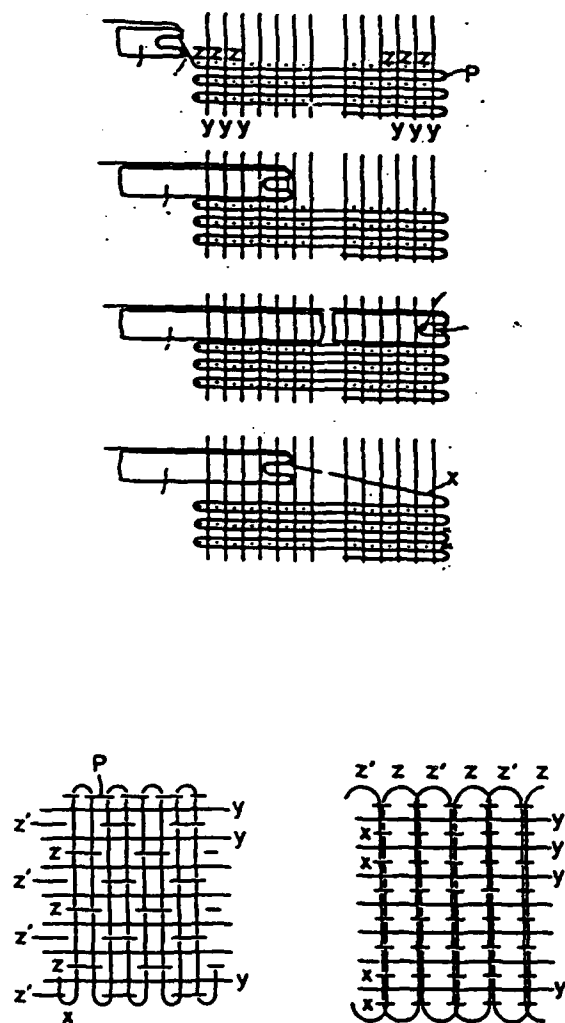
In 1974 Fukuta was granted a patent [14] for a process to make a orthogonal three dimensional fabric. Fukuta's apparatus and the fabric made with this machine is shown in Figure 2-18. The yarns in the y direction are fixed. A yarn inserted in the xy plane follows the path shown in Figure 2-19. P is a binder yarn which maintains the two yarn diameter distance between the z yarns in the y direction. A new set of z yarns is inserted after each x yarn. A set of z yarns is inserted by the simultaneous lowering of the z curved arm and raising of the z' curved arm.

In 1976 Crawford [9] was granted a patent for a method of laying in yarns from various directions. The different yarn geometries formed by this process are shown in Figure 2-20. These geometries differ from that of the other 3D nonwovens through the combinations of orthogonal and diagonal yarns lay-ins.



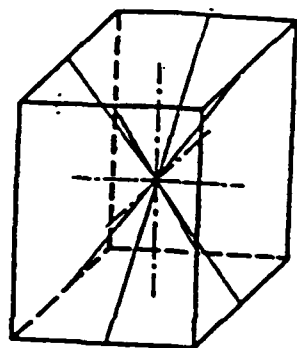
Fukuta's Nonwoven Apparatus [14]

Figure 2-18

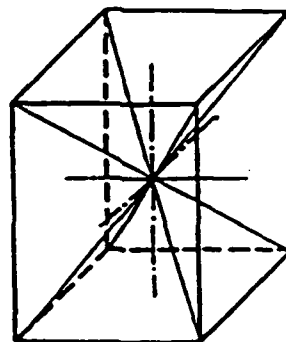


Yarn Path in Fukuta's Nonwoven Apparatus [14]

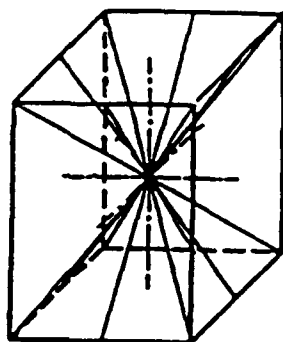
Figure 2-19



7D Face Diagonal Geometry



7D Body Diagonal Geometry



11D Geometry

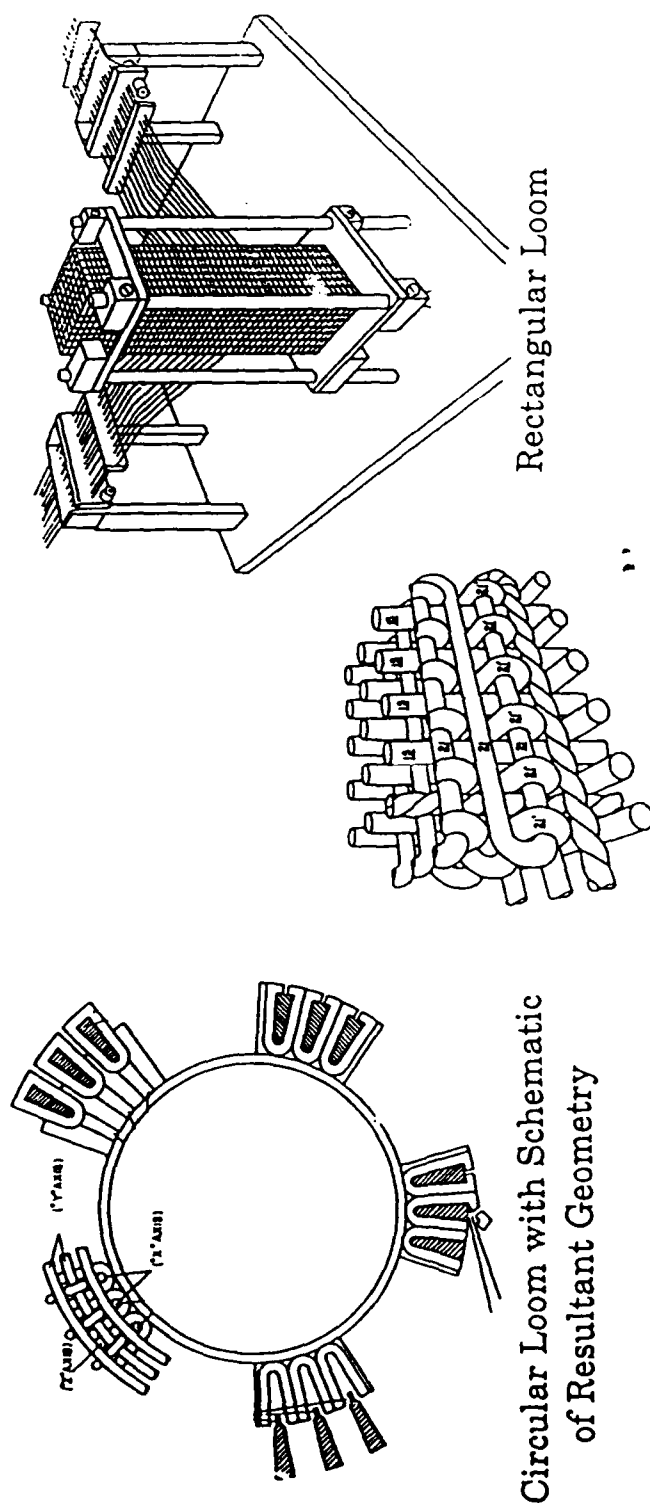
Crawford's Nonwoven Geometries [9]

Figure 2-20

In 1977 King was granted a patent for a three dimensional orthogonal rectangular and circular loom [18]. These looms and the resultant fabric geometries are shown in Figure 2-21. The rectangular loom creates a fabric with a distance of one yarn diameter between adjacent parallel yarns. The circular loom creates a fabric with a distance of two yarn diameters between adjacent yarns in one direction and a distance of one yarn diameter between parallel yarns in the orthogonal direction. The rectangular loom can be easily adjusted so that the x and y yarns are fed in at an angle.

In 1978 Kallmeyer invented a three dimensional orthogonal nonwoven rectangular loom [16]. The operation sequence of this loom is diagramed in Figure 2-22. In this process a shed is created at the center row of the z array. Then a x yarn is added. The shed is closed. Two adjacent sheds are then opened. The first x yarn is doubled back through the adjacent shed. An additional x yarn is inserted through the other shed. The two sheds are closed. Then two additional adjacent sheds open. This process continues until a x yarn is inserted through all the z rows. At this point the loom is rotated ninety degrees and the above process is carried out with y yarns.

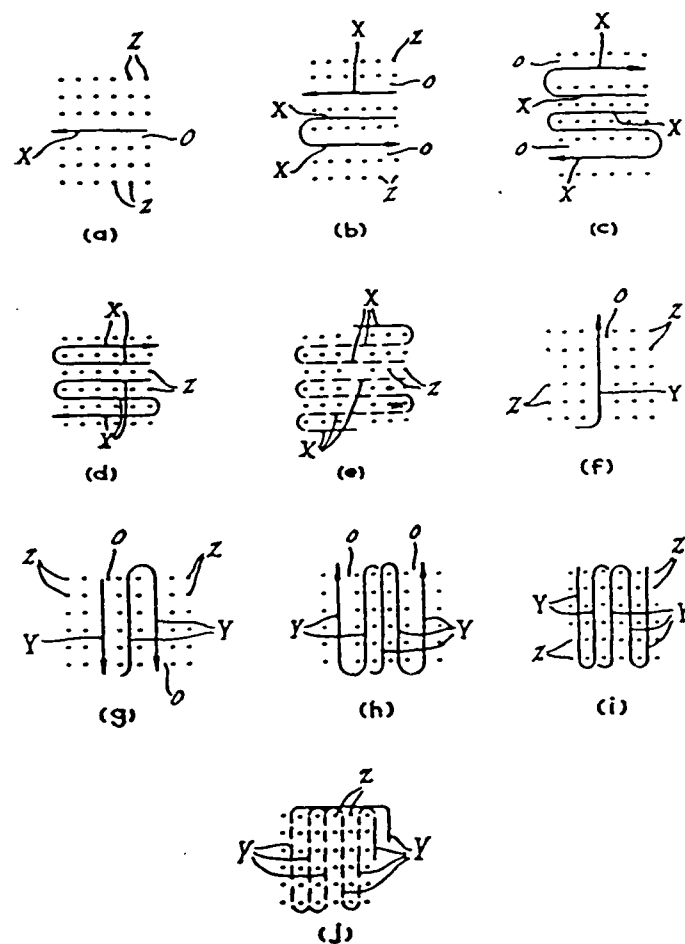
"Autoweave" [35] is another circular three dimensional nonwoven machine. In this apparatus a prepreg cable is simultaneously cut and inserted into a foam mandrel, known as a porcupine, normal to its surface. These radial rods form helical corridors. Axial yarns are fed by a shuttle which loops the axial yarn around the crown at each end of the mandrel before passing through the next corridor. The circumferential yarns are



Resultant Geometry of Rectangular Loom

King's Nonwoven Apparatus [18]

Figure 2-21



Yarn Path in Kallmeyer's Nonwoven [16]

Figure 2-22

tensioned and fed into the radial corridors by a shuttle. This process can be adapted for four and five directional yarn lay ins.

Of the processes mentioned above the Autoweave process is the most flexible and rapid. These structures possess high strength and moduli in the direction of fiber reinforcement. However these structures are not as conformable as other structures such as the 3D braids.

Another type of three dimensional nonwoven, called Noveltex [15], is a modification of needle punch technology. In this process a roll of a 2D fabric is placed under needles which pierce the fabric. The needles pierce through one to two 2D fabric layers. More 2D fabric from the same roll is then placed under the needles. In this way a thick fabric with some orientation in the through thickness direction is formed. This orientation hinders delamination. The resultant three dimensional fabric possesses high compressive and shear strength. However the fabric's tensile and flexural strength is lower than the other continuous fiber three mentioned before.

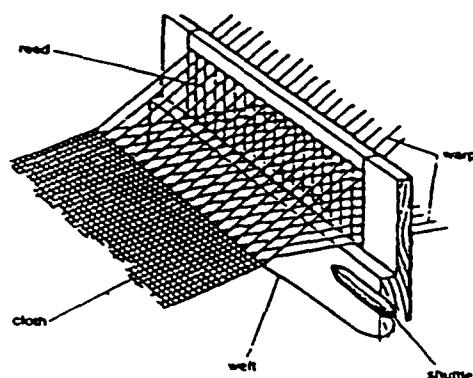
Many of the nonwoven fabrication processes described in this section form similar unit cells. The orthogonal nonwoven structures of the Omniweave, King's rectangular loom, Autoweave, and Kallmeyer processes will be henceforth referred to as XYZ nonwovens. The orthogonal nonwovens of Fukuta and King's circular loom will be referred to as XXYZ nonwovens. This structure is similar to a XYZ nonwoven composed of x yarns which possess a cross-sectional area that is twice the size of the other constituent yarns.

Wovens

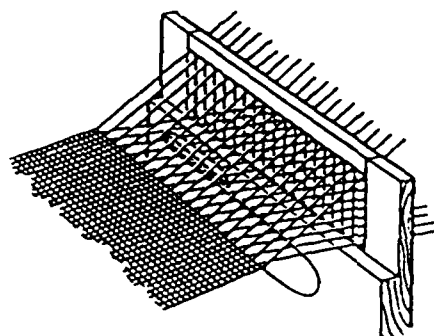
Woven fabrics are formed by yarn interlacing. The weaving process consists of three basic steps. This process is shown in Figure 2-23. The first step is called shedding. Shedding is the separation of warp yarns (the set of yarns in the machine direction) into top and bottom sheets. In the next step, weft insertion, a weft yarn (set of yarns not in the machine direction) is inserted between the two sheets. The final step is the compacting of the weft yarn, in which a reed forces the weft yarn tightly into the shed of the fabric. When this process is repeated, the position of at least some of the warp yarns forming the two sheets is reversed. The reversal of the warp yarns creates a sinusoidal path for these yarns. The actual length of the curved yarn divided by the net distance traveled, is known as the crimp of the fabric.

The earliest evidence of the use of a loom was in Egypt at 4400 B.C. [12]. By the 13th century the standard horizontal loom design, which is still used, had evolved. This loom was automated in a series of steps during the 18th century. For intricate weaves a draw loom is used. A draw loom possesses cords attached to the warp yarns. These cords allow for more control in forming the upper and lower sheet in the shedding process. In 1805 Jacquard introduced a draw loom with an automatic shedding device [12]. Ever since this time, a loom which allows for custom tailoring of each warp yarn motion is called a Jacquard loom.

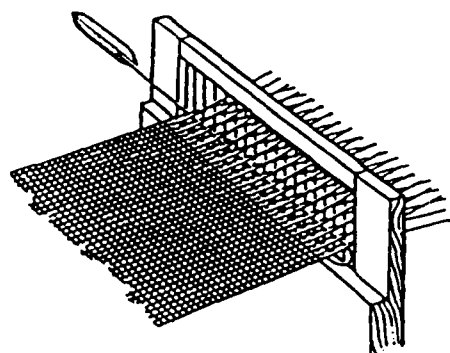
Adaptations are made to two dimensional weaving techniques when used for engineering applications [10]. For engineering applications a



Shedding



Weft Insertion



Compacting

The Basic Weaving Sequence [12]

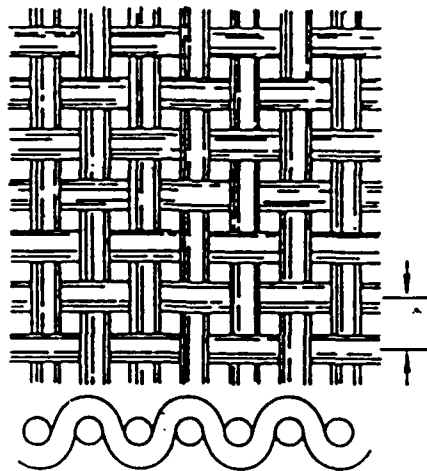
Figure 2-23

minimum amount of crimp is desired. The greater the amount of crimp, the greater the magnitude of the components of the fiber position vector not aligned with the fabric axis. This misalignment leads to diminished strength. Crimp is minimized by using weaving techniques such as the satin weave. In Figure 2-24 a five harness satin and a plain weave are shown. Note the number of interlacings is smaller in the satin weave. A lower number of interlacings in a fabric results in a smaller amount of crimp.

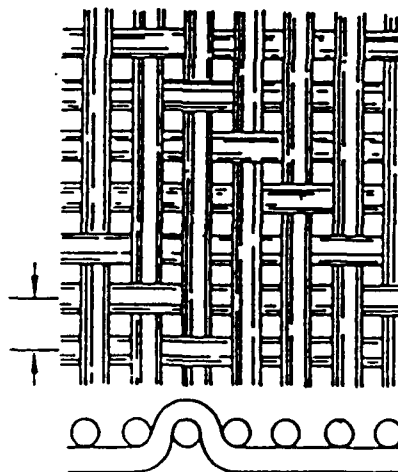
Crimp also needs to be minimized since the high modulus yarns typical of engineering applications possess a large critical bending radius. The critical bending radius is inversely proportional to the amount of curvature a yarn can maintain without breaking. Special high modulus weaves are available which avoid this problem by keeping the high modulus yarns straight and performing the actual weaving with a low modulus yarn possessing a much smaller cross-sectional area.

There are two forms of three dimensional weaves. In the first form, a thin fabric is woven in such a way as to obtain a three dimensional form. This form of three dimensional weaving is shown in Figure 2-25. The second form of three dimensional weaving results in the formation of a fabric of substantial thickness. It is this form of weaving that is addressed in the following paragraphs.

A weave geometry for thick fabrics is mentioned in Rheume's 1973 patent [34]. This geometry is shown in Figure 2-26. This figure is a schematic of the weave's geometry normal and parallel to the warp yarn plane. The



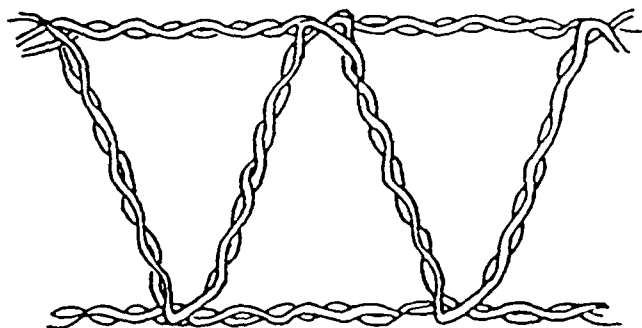
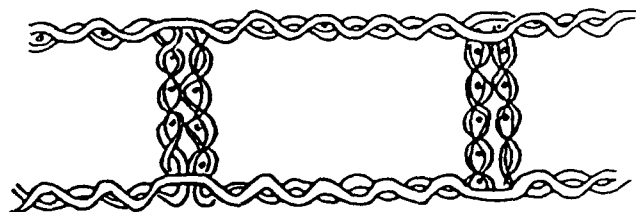
Plain Weave



Five Harness Satin

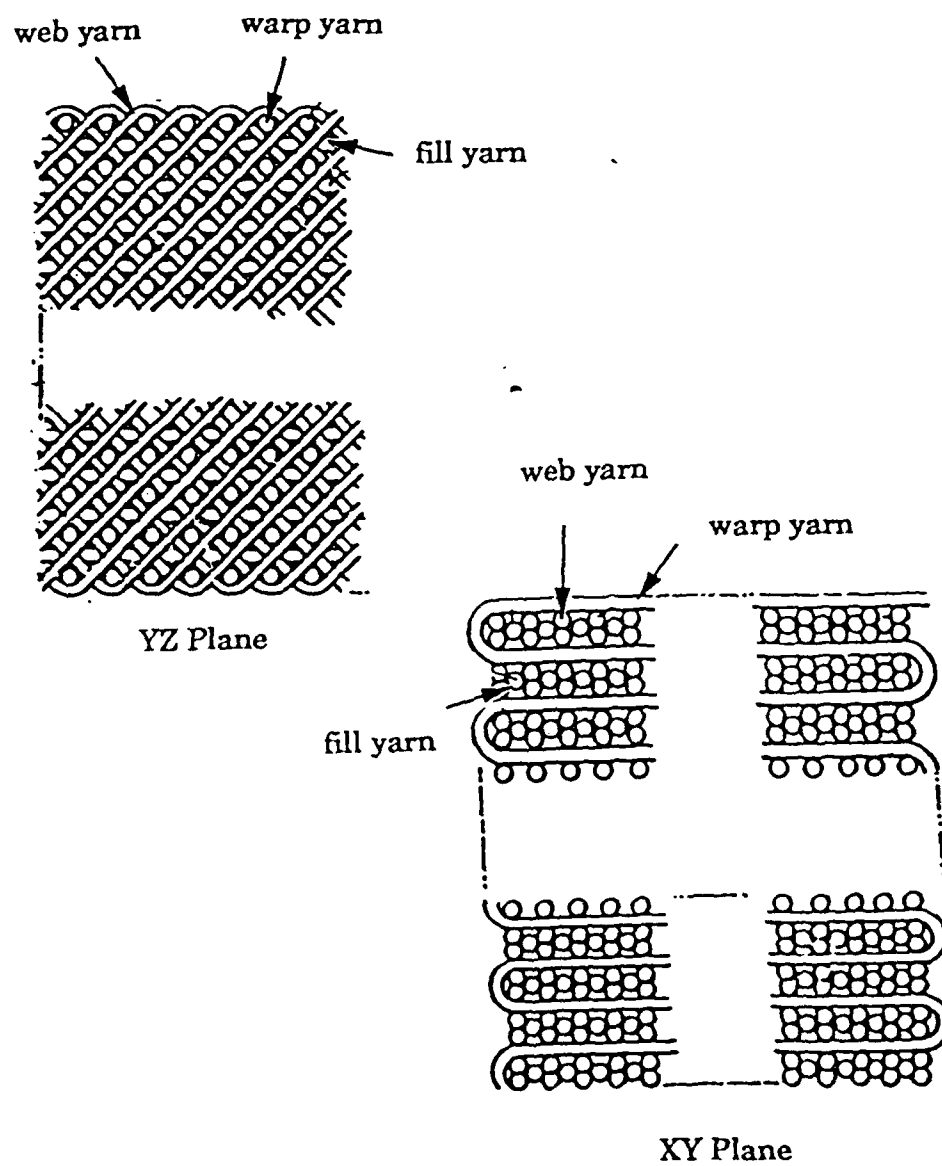
Different Weave Geometries [28]

Figure 2-24



Weaving Three Dimensional Shapes [32]

Figure 2-25

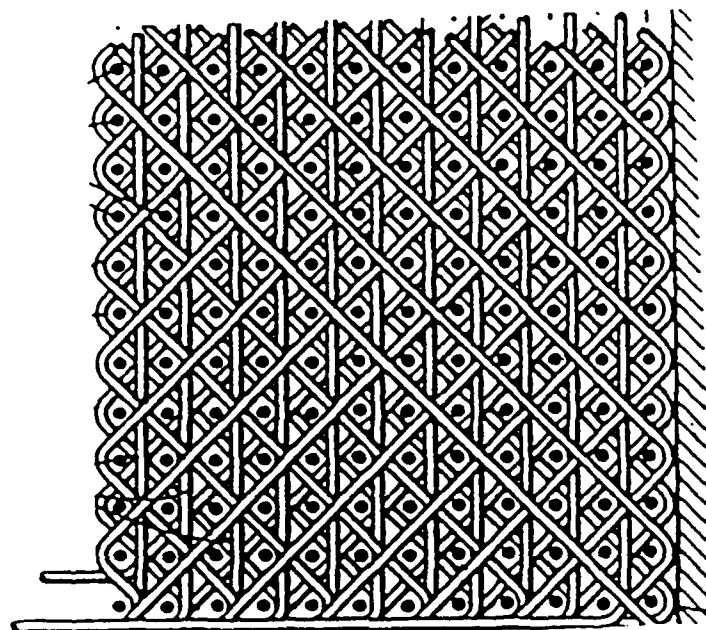


Rheaume's Weave Geometries [34]

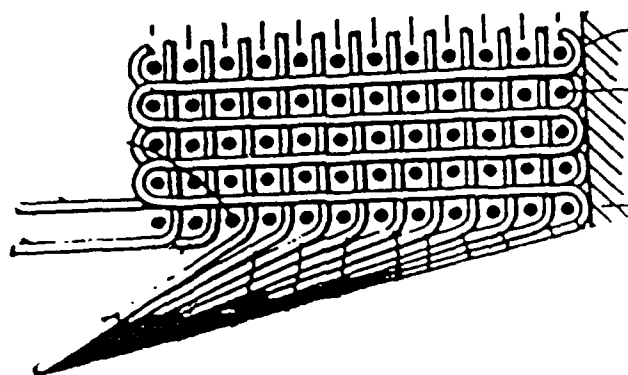
Figure 2-26

weaving of the warp yarns is controlled by a series of Jacquard heads. This three dimensional geometry is created by adding a web yarn in the through thickness direction. Although in this patent the web yarns transverse the fabric thickness, thick weaves are also made with not all layers being transversed. Using web yarns fabrics up to seventeen layers thick have been woven. There is no inherent limit to the thickness of these weaves. The current limit is a result of the machinery currently available. These fabrics are produced by companies such as Textile Technologies in Hatboro, Pa and Woven Structures in Compton, Ca.

An apparatus for creating thick weaves was patented by Emerson in 1973 [11]. Emerson's machine is a circular loom controlled by a plurality of Jacquard heads. These heads control the placement of stuffer and locker warp yarns (analogous to the web yarns mentioned above). There is also a filler yarn system which follows an helical path. Insertion of the filler yarns is controlled by an inserter which moves around the mandrel. The stuffer yarns are parallel to the mandrel axis. The locker yarns follow a sinusoidal path around the stuffer and filler yarns. This path is in the radial direction with respect to the mandrel axis. A fabric compactor comprised of a perforated plate compacts the fabric after each filler yarn insertion. Possible weave geometries resulting from this machine are shown in Figure 2-27. The complexity of this machine leads to problems in fabrication and as a result this process is not currently popular.



XY Plane of an Alternative Weave Geometry



XY Plane of an Orthogonal Weave

Weave Geometries Possible with Emerson's Apparatus [11]

Figure 2-27

CHAPTER THREE

SYMMETRY OF THREE DIMENSIONAL FIBER ARCHITECTURES

Introduction

Since the interior unit cells of many fabric structures from different textile classes possess the same elements of symmetry, a classification system based on these symmetry elements has been developed. This chapter will explain the underlying principles of symmetry used to develop this model. The symmetry present in the three dimensional fiber architectures mentioned in chapter two will be explained. Additionally, the performance properties of fiber architectures can be modelled by utilizing the different elastic strain energy expressions produced by different combinations of symmetry elements.

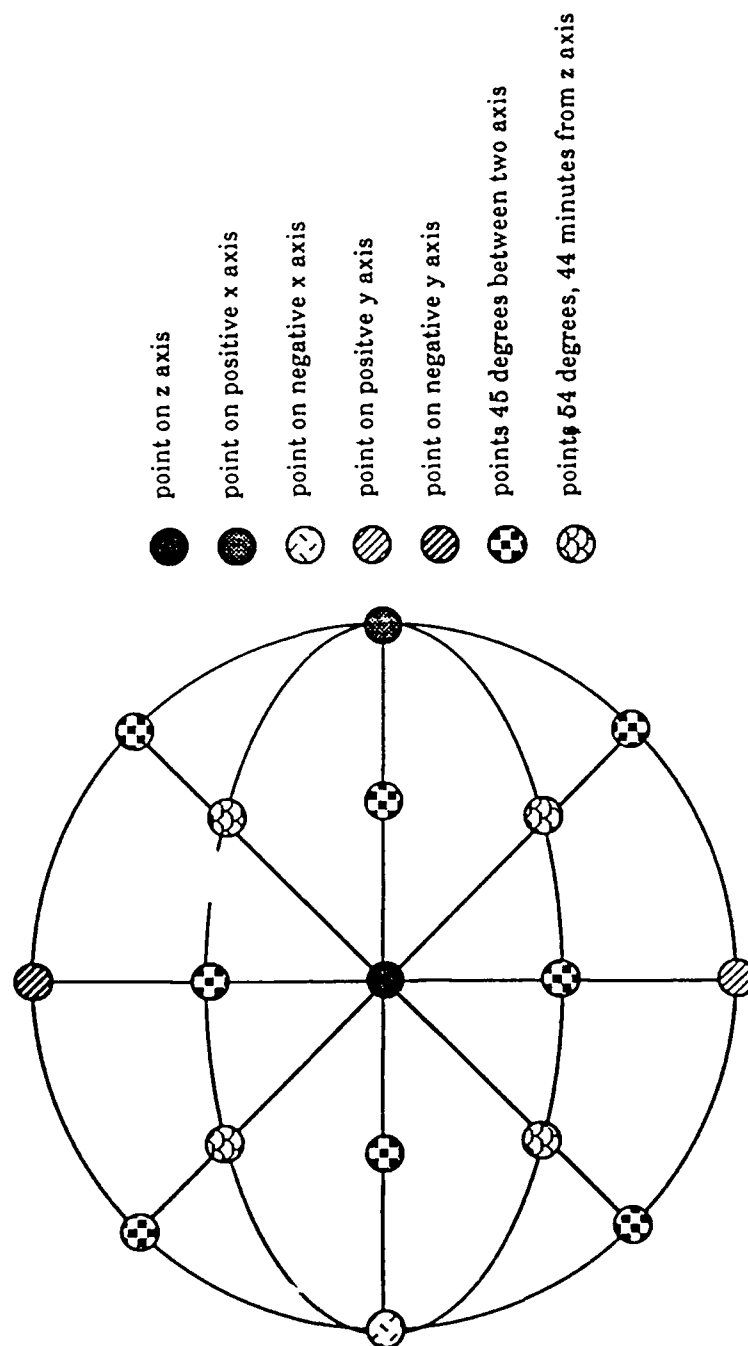
Symmetry in Materials

The symmetry concepts employed in the description of the various textile structures are adapted from the field of crystallography. There are three basic type of operations used to determine symmetry. These operations are: rotation about an axis, reflection in a plane, and rotoinversion (rotation followed by reflection). A material is symmetric under one of the above operations if it appears as it did initially after a symmetry operation.

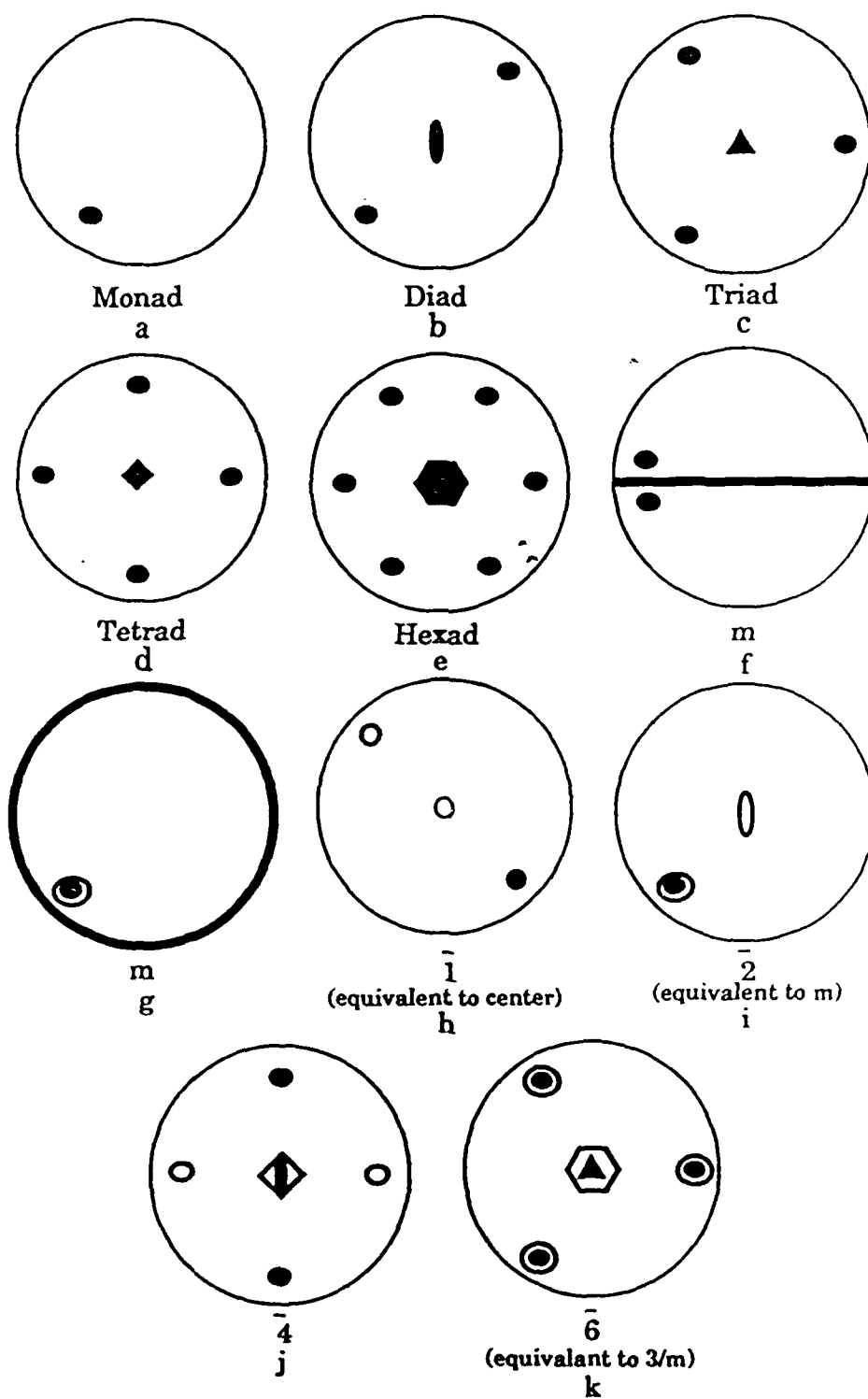
A restriction is placed on the allowable types of rotation operations. This restriction is that rotation operations must be performed in such a manner that the translational symmetry of the material is maintained. Translational symmetry is maintained when the distance between adjacent lattice sites remains constant. Besides a rotation of 360 degrees, this symmetry can only be maintained with rotations of 60, 90, 120, and 180 degrees about a symmetry axis. The rotational symmetries corresponding to the above rotations are hexad, tetrad, triad, and diad respectively.

For a three dimensional object, the symmetry operations about three mutually orthogonal axes must be coherent. When coherence is achieved, a combination of a symmetry operation on one axis followed by an operation on a second axis is equivalent to one operation about the third axis. There are 32 combinations of symmetry elements for three dimensional figures which satisfy this requirement. These combinations are referred to as the 32 crystallographic point groups. When these operations are performed, the position of only one point, the point through which they pass, is unmoved.

These point groups are usually diagrammed on stereograms. Stereograms are two dimensional representations of a three dimensional body. Figure 3-1 diagrams a stereogram with the z axis normal to the stereograph plane and intersecting said plane at the center of the stereogram. Figure 3-2 (adapted from [17]) diagrams the different positions of a point as it undergoes different symmetry operations. Figure 3-2a represents a rotation of 360 degrees about the z axis (central point on stereogram). Figure 3-2b to e represents a diad axis, triad axis, tetrad axis, and a hexad



Schematic of the Components of a Stereogram
Figure 3-1



Symmetry Operations

Figure 3-2

axis, respectively. A reflection through a mirror plane along the x axis is shown in figure 3.2f. A reflection through a mirror plane in the xy plane is shown in figure 3.2g. Figure 3.2h is a rotoinversion operation consisting of a rotation of 360 degrees followed by inversion through the center of the sphere of projection. The effect of the other rotoinversion operations is shown in Figures 3-2i, j, and k.

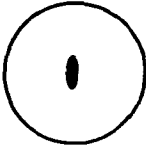
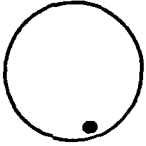
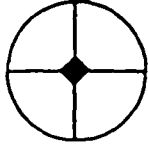
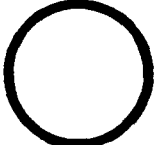
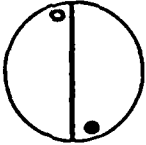
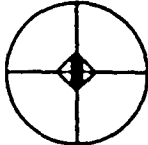


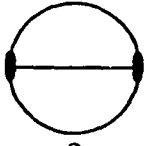
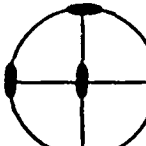
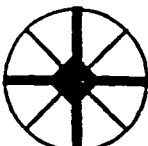
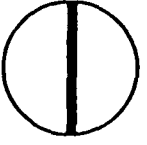
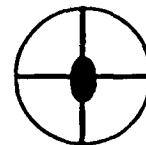
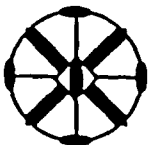
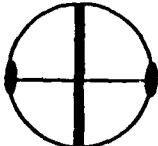
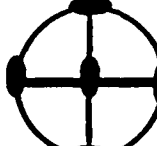
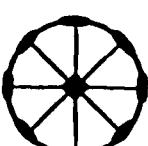
Figure 3-3 (adapted from [17]) diagrams the 32 possible point groups. These point groups are classified by the shape of the unit cell in which they occur. Each unit cell class is ordered in terms of increasing symmetry. The state of highest symmetry for a certain class is known as the holosymmetric state. The different criteria for classifying these unit cells and the shape of these unit cells is given in Table 3-1. The lattice parameters a , b , and c correspond to the length of the unit cell in the x , y , and z directions, respectively. The directional cosines are denoted by angles α , β , and γ .

Symmetry Elements in 3D Fiber Architectures

The symmetry considerations described above were devised for materials with symmetric atomic structure. The textile structures described here consist of continuous lengths of yarn oriented in various directions with respect to one another. When these yarns intersect, they offset each other in space. This offset will be ignored when describing the symmetry elements present in the 3D fiber architectures. The area of the yarn's intersection is reduced to a point when performing symmetry operations. A schematic of a yarn intersection before and after the above simplification

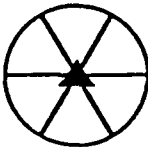
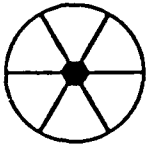
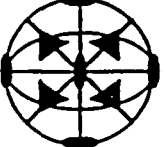
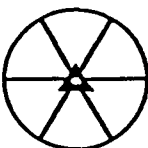
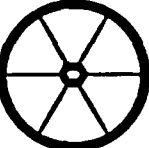


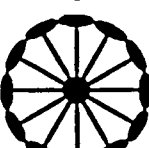
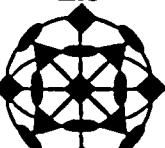
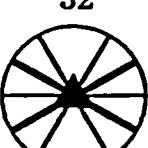
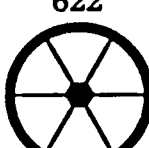

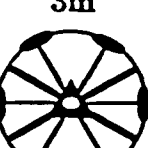
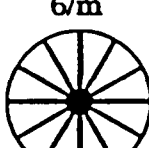

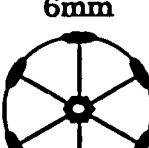
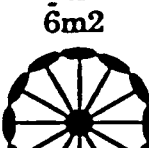
System	Symmetry	Conventional Cell
Triclinic	No axes of symmetry	$a \neq b \neq c; \alpha \neq \beta \neq \gamma$
Monoclinic	One Diad	$a \neq b \neq c; \alpha = \gamma = 90^\circ$
Orthorhombic	Three Orthogonal Perpendicular Diads	$a \neq b \neq c; \alpha = \beta = \gamma = 90^\circ$
Trigonal	One Triad	$a = b \neq c; \alpha = \beta = \gamma = 120^\circ$
Tetragonal	One Tetrad	$a = b \neq c; \alpha = \beta = \gamma = 90^\circ$
Hexagonal	One Hexad	$a = b \neq c; \alpha = \beta = 90^\circ, \gamma = 120^\circ$
Cubic	Four Triads	$a = b = c; \alpha = \beta = \gamma = 90^\circ$

Crystallographic Unit Cells (adapted from [17])
Table 3-1

Monoclinic (1st Setting)	Triclinic	Tetragonal
 2	 1	 4
 $\bar{2}$ (equivalent to m)	 $\bar{1}$	 $\bar{4}$
 $2/m$		 $4/m$
Monoclinic (2nd Setting)	Orthorhombic	
 2	 222	 422
 m	 $2mm$	 $\bar{4}2m$
 $2/m$	 mmm	 $4/mmm$

Stereograms of the 32 Symmetry Point Groups
 (adapted from [17])

Figure 3-3

Trigonal	Hexagonal	Cubic
		
3	6	23
		
$\bar{3}$	$\bar{6}$	m3
		
32	622	432
		
3m	6/m	43m
		
$\bar{6}m$	6mm	m3m
		
	$\bar{6}m2$	
		
	6/mmm	

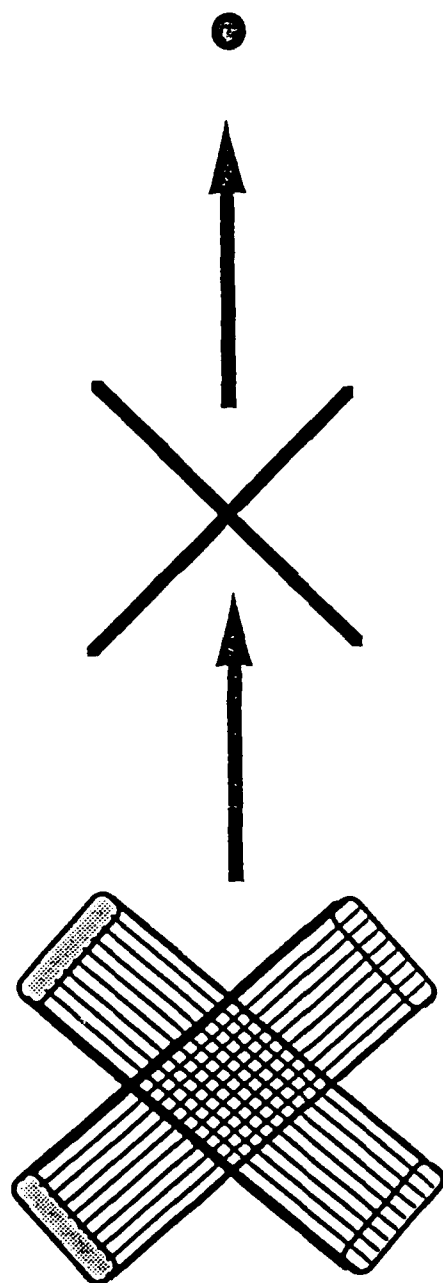
Stereograms of the 32 Symmetry Point Groups
(adapted from [17])

Figure 3-3

is shown in Figure 3-4. Other assumptions concerning the geometry of the yarns that have been made are: the yarns possess a circular cross-sectional area, and in the limit of the lattice parameter scale the yarns are linear. There are additional simplifying assumptions that must be made to generate rectilinear unit cells for fabrics formed on circular looms. Since the lattice parameter of each unit cell is on the order of the distance between two parallel yarns, the circumferential yarns were approximated to be linear. As the distance between interlacings increases, the curvature of the circumferential yarns increases and this approximation cannot be used. Another assumption is that the difference in distance between z yarns in the adjacent concentric rings is insignificant.

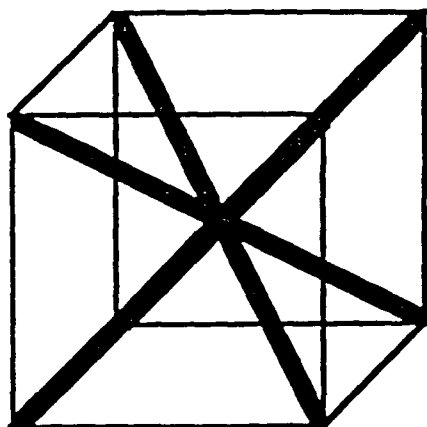
Utilizing the above assumptions, numerous textile structures possess holosymmetric cubic symmetry. This symmetry state is found in certain three dimensional braids, nonwovens, and knits. An Euclidean braid with 100% braiding yarns and the fourfold body diagonal lay-in architecture of the Omniweave with a yarn orientation angle of 45 degrees with respect to three orthogonal axes, possesses this symmetry. This symmetry is also possessed by the XYZ geometries of Omniweave, King's nonwoven, Kallmeyer's nonwoven, the thick weave with a web angle of 0° , and Autoweave when all the constituent yarns possess similar circular cross-sectional areas and are therefore equidistant.

There are a number of symmetry elements in the holosymmetric cubic state. The simplified unit cell of these two geometry types and their point group symmetry is shown in Figure 3-5. The position of some of these symmetry elements is projected onto the cubic unit cell in Figure 3-6.

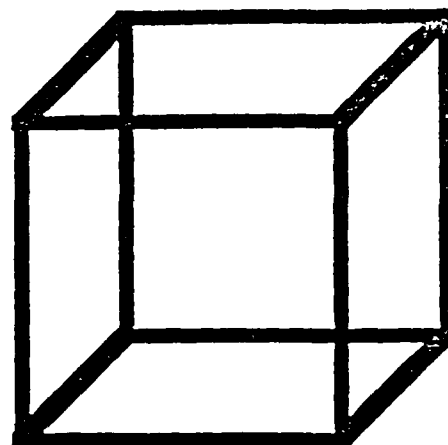


Schematic of Yarn Intersection, Simplification

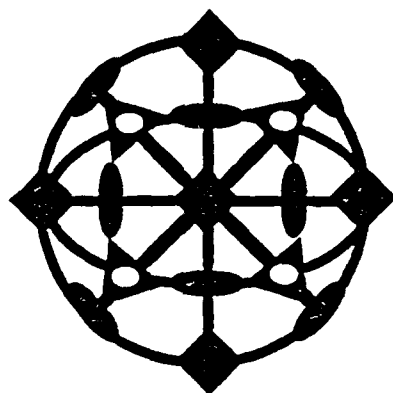
Figure 3-4



Simplified Unit Cell for
Body Diagonal Geometries



Simplified Unit Cell for
XYZ Geometries



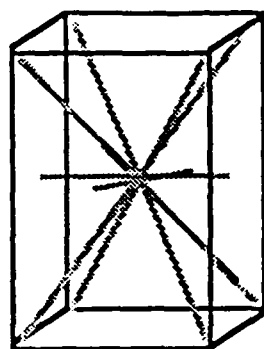
m3m

m3m Symmetry Shown by Above Unit Cells

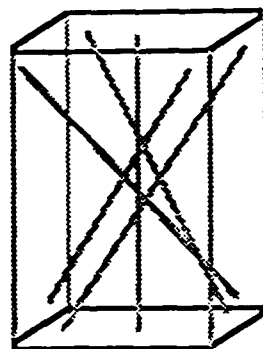
Figure 3-5

The addition of two orthogonal lateral lay-in yarns in the xy plane to the unit cell of an Euclidean braid comprised of 100% braiding yarns 100% reduces the x and y tetrad axis of symmetry to a diad axis, and also destroys all triad axis of symmetry. This unit cell possesses holosymmetric tetrahedral symmetry. This symmetry state also occurs with a two-step braid possessing equal a and b lattice parameters, with the body diagonal geometries possessing a braid angle not equal to 45° in one of the orthogonal planes, and with the XXYYZ Aerospatale geometry. The $4/mmm$ symmetry corresponding to this state and the unit cell of these geometries is shown in Figure 3-7.

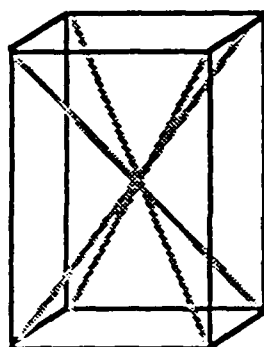
Another common symmetry type is mmm, which is the holosymmetric symmetry state of an orthorhombic unit cell. This symmetry state is possessed by: Crawford's nonwovens, Euclidean braids with one lateral or longitudinal lay-in, body diagonal geometries with the braid angle not equal to 45° in all orthogonal planes, a Two-Step braid with unequal lattice parameters, and the XXYZ fiber architectures of Aerospatale, King, and Fukuta. Crawford's nonwovens possess this symmetry state since the combination of three orthogonal and either four or eight diagonal yarns reduces all symmetry axes to diads. The XXYZ fiber architectures are mmm since the presence of two x yarns for every unit cell destroys all tetrad and triad axes of symmetry. The highest axis of symmetry for the holosymmetric orthorhombic geometry is diad. The unit cells of fiber architectures possessing this symmetry and the projection of the mmm point group onto an orthorhombic cell is shown in Figure 3-8



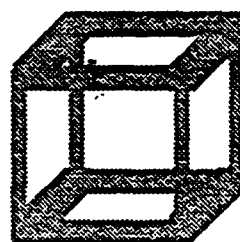
Euclidean Braid with
2 Orthogonal
Lateral Lay-in Yarns
 $a = b$



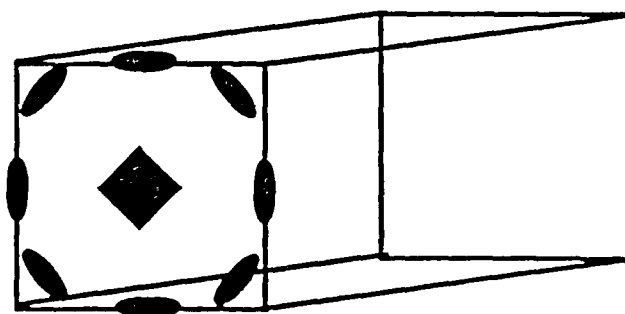
Two-Step
Braid
 $a = b$



Body Diagonal
Unit Cell
Braid angle $\neq 45^\circ$
in one plane

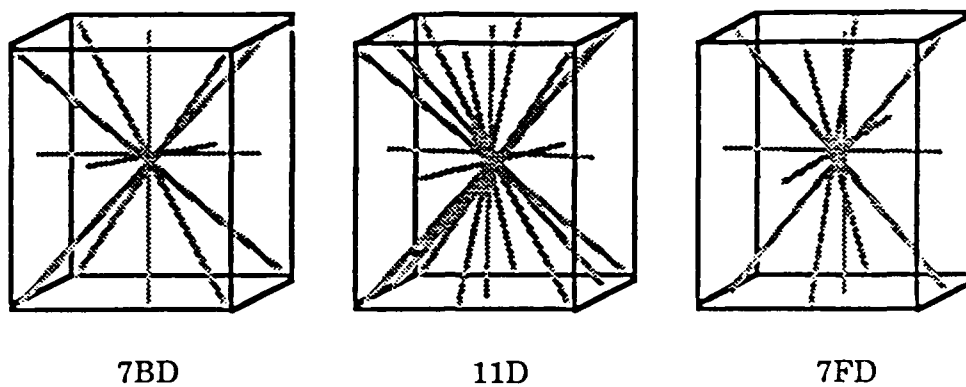


XXXXYZ
Geometry

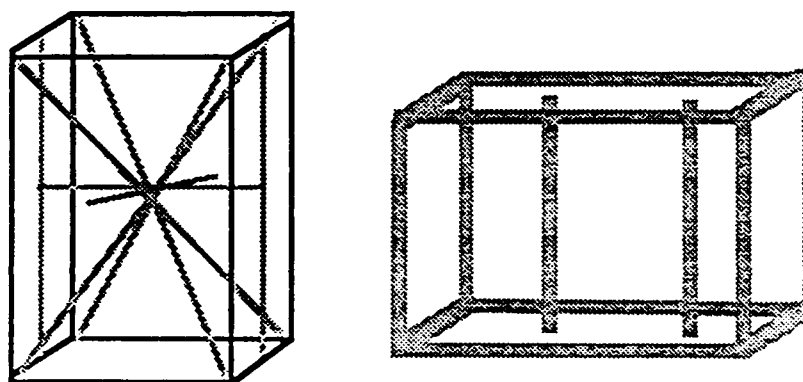


4/mmm Symmetry elements in relationship to the xy plane
of a tetrahedral unit cell

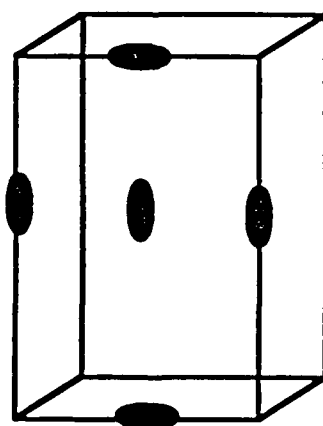
Figure 3-7



Crawford's Nonwovens

3D Braid with Longitudinal
Lay-in

XXYZ Geometry

mmm Symmetry Elements shown in relationship to the
xz plane of an orthorhombic unit cellFigure
3-8

The remaining textile structures do not possess three dimensional symmetry. Although there is through thickness fiber integration, the unit cell shape of these structures is similar to that of a laminate. Like laminates, these structures possess symmetry in the xy plane, not in the through thickness planes.

The Effect of Symmetry on the Elastic Stiffness Matrix

The elastic stiffness matrix describes the relationship between strain and stress in a material at a specific point. The theory of elasticity governs the creation of the stiffness matrix. The assumptions made in the theory of elasticity are: the body is a continuous medium, strains experienced by said body are small, the stress/strain relationship is linear, initial stresses are ignored, and deformation is reversible.

Strain is a measure of the deformation experienced by a body. The strain state of a point can be expressed as a second order tensor. The components of this tensor are shown below.

$$\epsilon_{ij} = \begin{pmatrix} \epsilon_{xx} & \epsilon_{xy} & \epsilon_{xz} \\ \epsilon_{yx} & \epsilon_{yy} & \epsilon_{yz} \\ \epsilon_{zx} & \epsilon_{zy} & \epsilon_{zz} \end{pmatrix} \quad (3-1)$$

CHAPTER FOUR

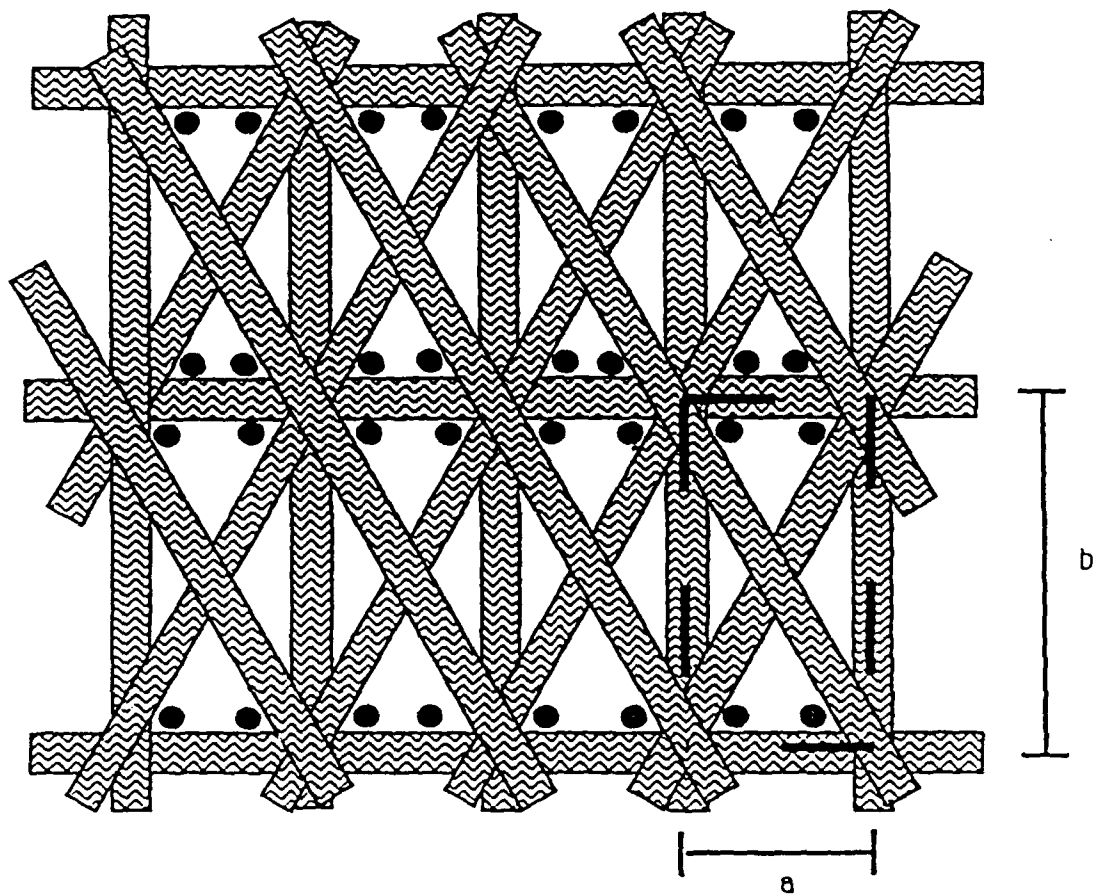
GEOMETRIC MODELLING OF 3D FIBER ARCHITECTURES

Introduction

In this chapter the unit cell geometries of various 3D fiber architectures are modelled. In all the models the yarns are assumed to be incompressible and to possess a circular cross-sectional area. Except where noted, all yarns comprising the fiber architectures are identical. The effect of varying geometric parameters on the fiber volume fraction is studied. Also the percent fiber volume fraction in different fiber orientations is stated. The effective volume of fiber oriented towards an arbitrary angle is given for each fiber architecture.

Multiaxial Warp Knits

The MWK possesses an orthogonal unit cell. The a and b parameters of a MWK unit cell are shown in Figure 4-1. In this figure, the dashed box contains the ab plane of one unit cell. The length of the a parameter is equivalent to the distance between the centers of two adjacent orthogonal yarns in the x direction. The length of the b parameter is equivalent to the distance between the centers of two adjacent orthogonal yarns in the y direction.



The Unit Cell of a Multiaxial Warp Knit

Figure 4-1

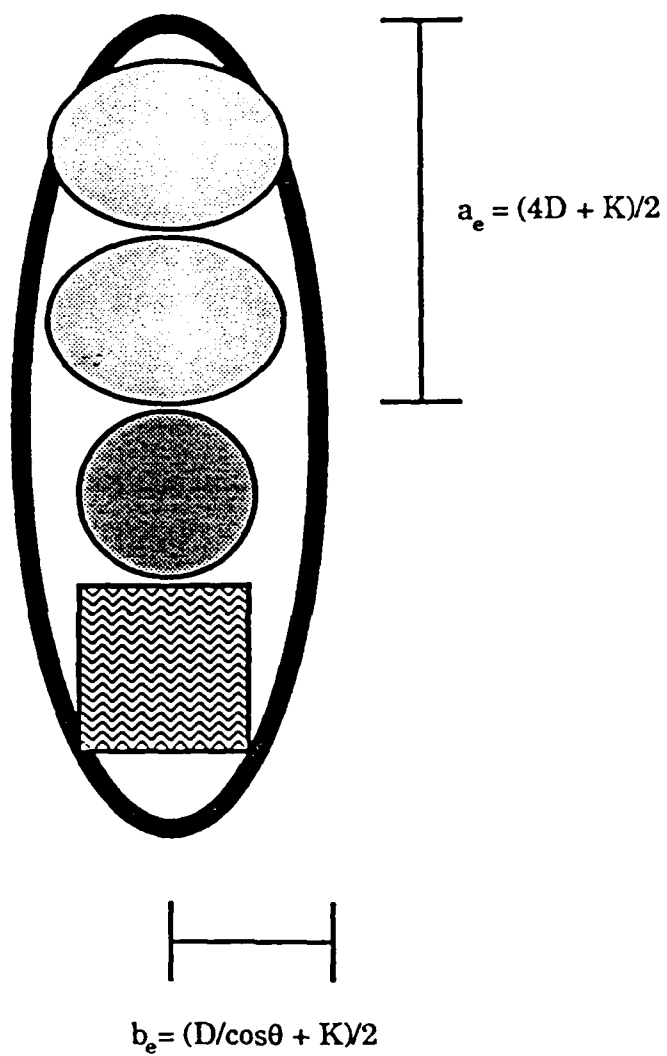
The circles in each unit cell in Figure 4.1 represent the intersection of the knitting yarns with the ab plane. The knitting yarn is assumed to have a cross-sectional area one tenth the size of the lay-in yarns. The shape of each knitted loop completed by the knitting yarn is modelled as an ellipse. Figure 4.2 shows the relationship of the geometric parameters of the knitting yarn ellipse to the MWK unit cell. As shown in Figure 4.1, there are four spots in each unit cell where a knitting yarns intersects with the ab plane. The three dimensional shape represented by each circle in the unit cell is one-half of an ellipse. Thus there are two knitting yarn ellipses in each unit cell. The length of knitting yarn in the unit cell is equal to the circumference of two ellipses. The circumference of an ellipse is equal to:

$$C = 4a_e \int_0^{\pi/2} \sqrt{1 - \epsilon^2 \sin^2 \phi} d\phi = 2\pi a_e (1 - 0.25\epsilon^2 - .047\epsilon^4)$$

$$\text{with } \epsilon_e = \frac{\sqrt{a_e^2 - b_e^2}}{a_e} \quad (4-1)$$

Each MWK cell consists of yarn lay-ins in the x, y, and +/- θ directions. The c parameter of the MWK unit cell is equivalent to $4D + K$. D is defined as the diameter of the lay-in yarns and K is defined as the diameter of the knitting yarn. This distance results from the four lay-ins, and the one-half diameter of the knitting yarn on the top and bottom of the unit cell.

The length of the a parameter of the MWK unit cell is $D + S$, where S is the distance between yarns of like orientations. The length of b depends on the angle of the bias yarns. If θ is 45° , $b = a$. When θ is not 45° , $b = (D + S)\tan\theta$.



The Elliptical Path of a Knitting Yarn in a Multi-axial Warp Knit

Figure 4-2

The two angled lay-ins each possess a length of $L_a = a/\cos\theta = (D + S)/\cos\theta$.

The fiber volume fraction of yarn in the unit cell is equal to:

$$V_f = \frac{(a + b + 2L_a)\frac{\pi D^2}{4} + 2C\frac{\pi K^2}{4}}{abc} \quad (4-2)$$

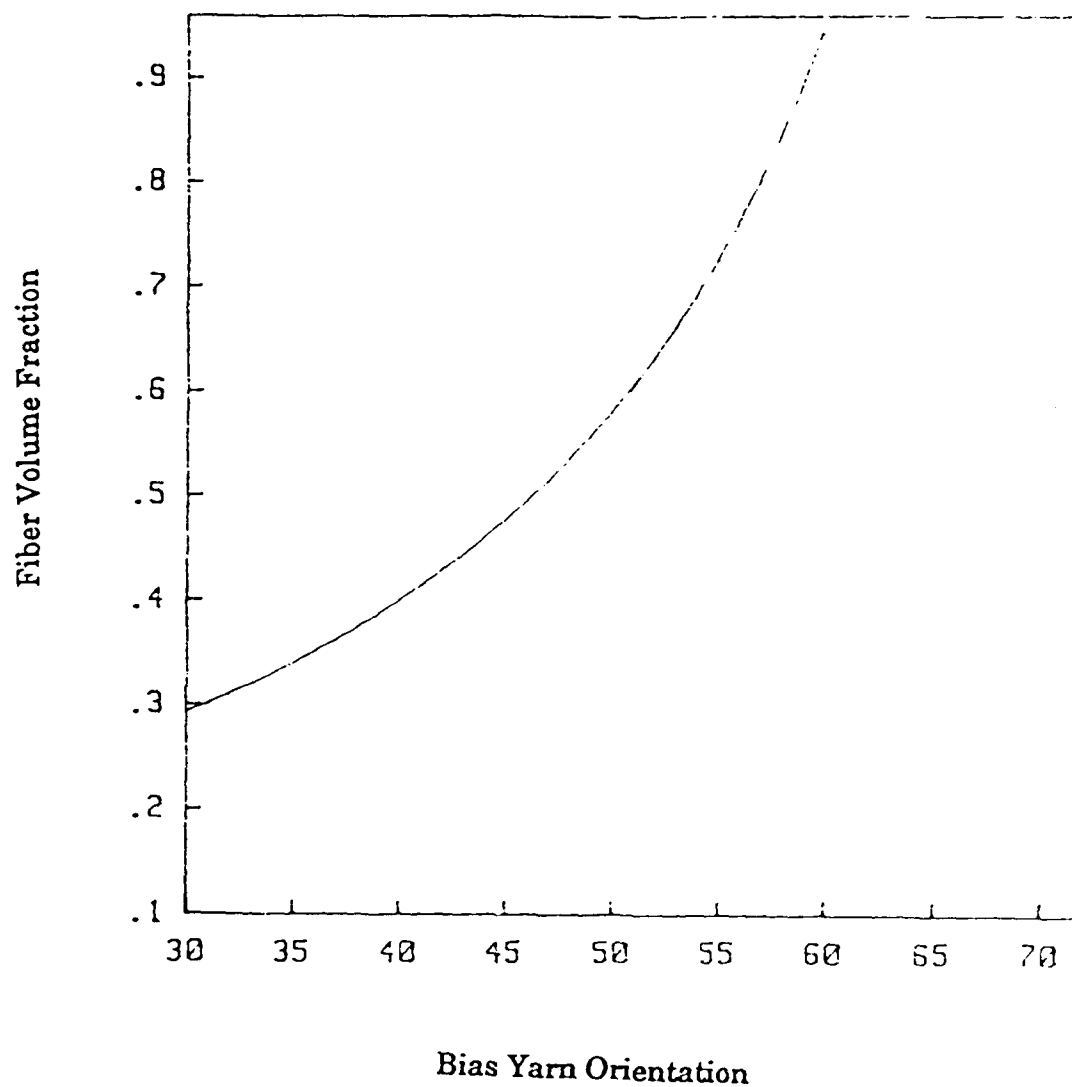
where $\frac{\pi K^2}{4}$ is the cross-sectional area of a yarn

with diameter K

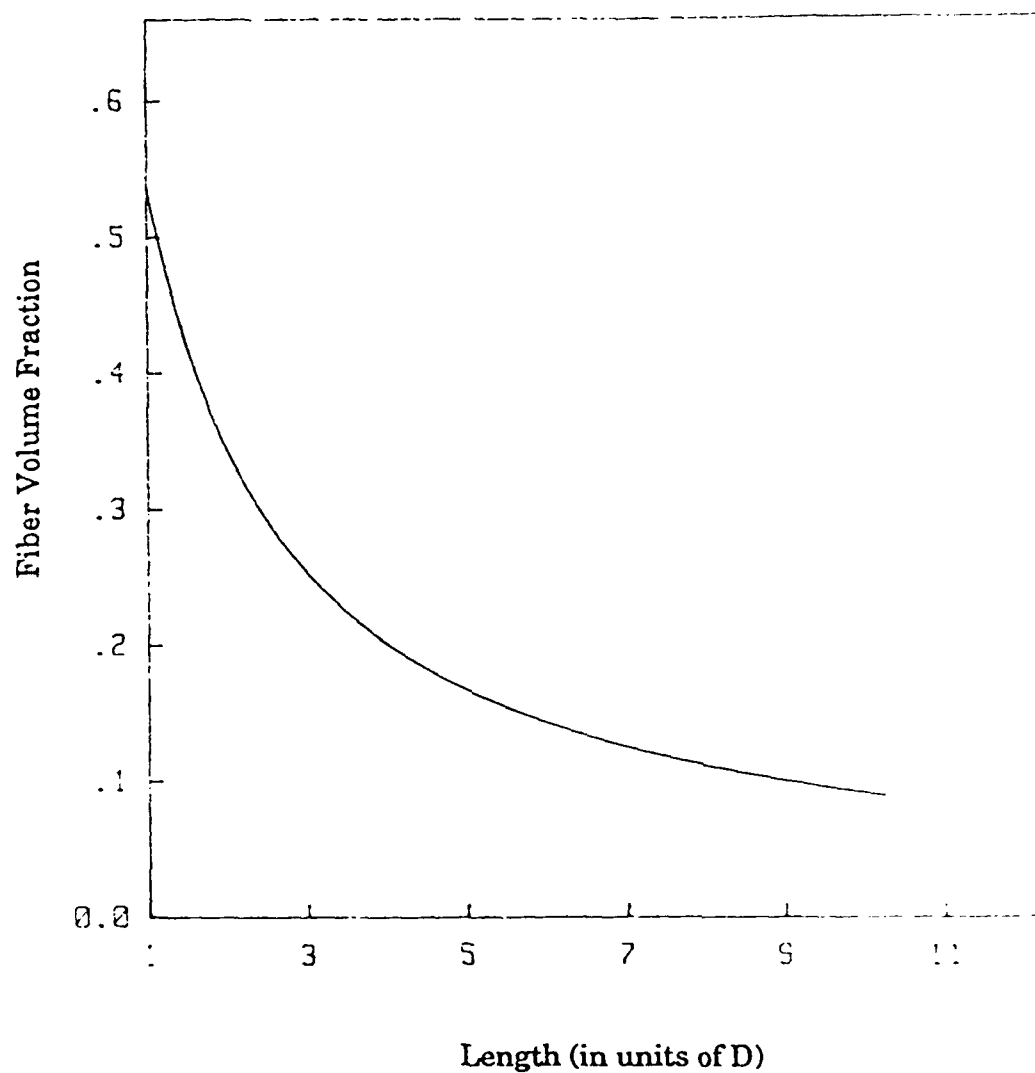
The fiber volume fraction of yarn in the unit cell is the volume of yarn in the unit cell divided by the unit cell volume. The volume of a MWK unit cell is the product of the three unit cell parameters.

The effect of varying the angle of the angled lay-ins on the fiber volume fraction is plotted in Figure 4-3. In this plot, the space between adjacent yarns in the x direction is assumed to be one yarn diameter and the diameter of the knitting yarn is assumed to be one-tenth that of the lay-in yarns. The fiber volume fraction increases rapidly after 45°. This increase is a result of the a parameter being greater than the b parameter. In this region of the curve the space between yarns in the b direction is decreasing. Varying the angle of the bias yarn changes the fiber volume significantly.

Figure 4-4 plots the effect of varying the distance between the yarns in the closest-packed direction. The dependence of fiber volume fraction on the distance between closest-packed yarns is harmonic. The fiber volume fraction between two integral S values approximately decreases by $1/(S_H+1)$ with S_H being the higher S value. The biggest reduction in fiber volume



Dependence of the Fiber Volume Fraction of a Multiaxial Warp Knit
on Bias Yarn Orientation
Figure 4-3



Dependence of the Fiber Volume Fraction of a Multiaxial Warp Knit
on the Distance Between Adjacent Parallel Yarns
Figure 4-4

fraction, 50%, occurs in the region of zero to one yarn diameter of space between the closest-packed yarns.

The effect of assuming a different relative diameter of the knitting yarn to that of the lay-in yarns for a MWK with $\theta = 45^\circ$ is shown in Figure 4-5. Varying K by an order of magnitude of ten changes the fiber volume fraction by 11%.

Orthogonal Fiber Architectures

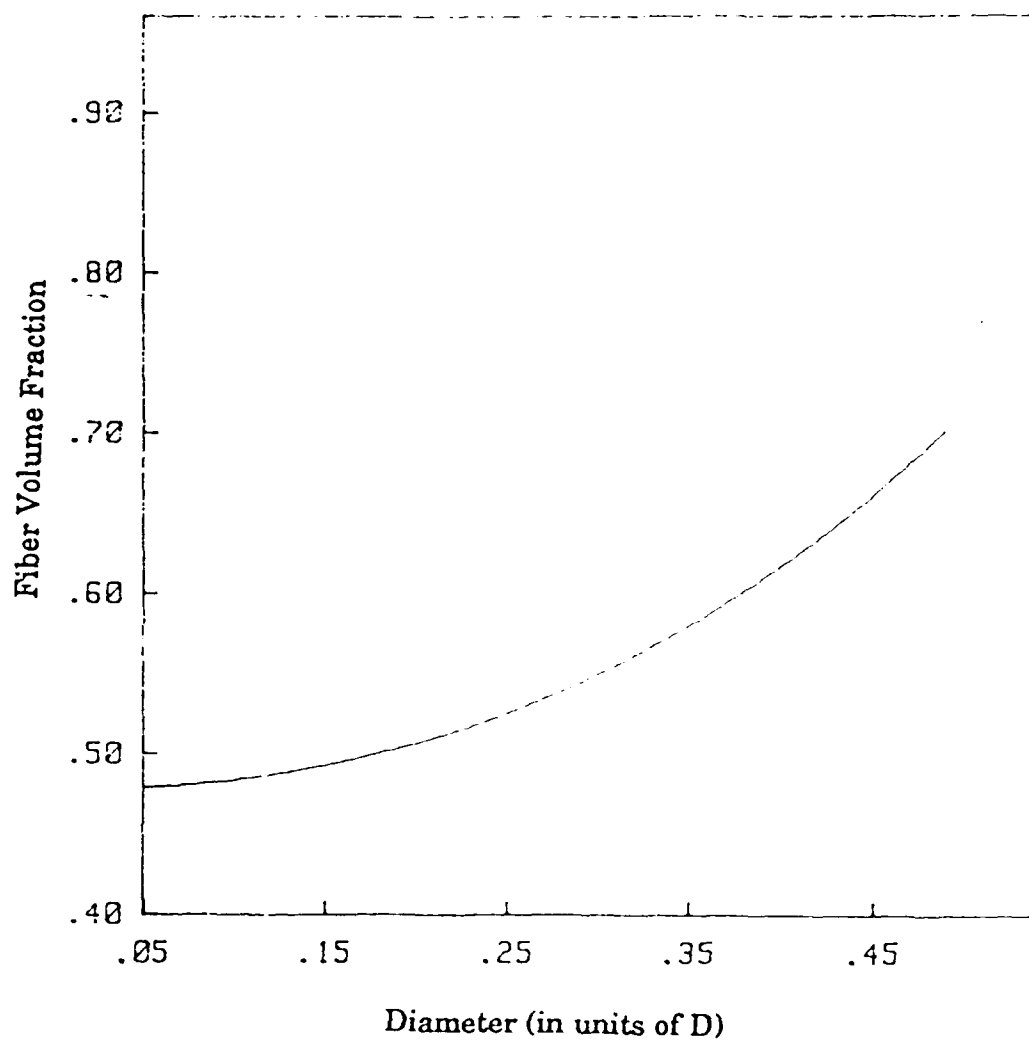
XYZ Geometry

In this section the XYZ, XXYYZ and the XXYZ orthogonal geometries will be discussed. The XYZ geometry possesses a cubic unit cell. The geometry of each $\langle 100 \rangle$ plane in this cell is shown in Figure 4-6. As shown in this figure, the unit cell parameters are equal to $2D$, where D is the diameter of the constituent yarns. The fiber volume fraction of the XYZ geometry equals:

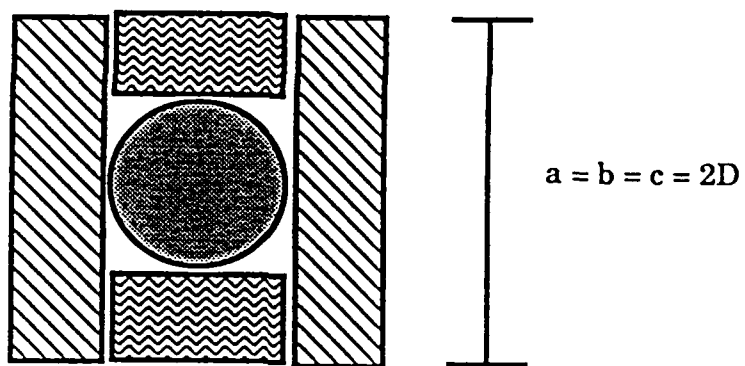
$$V_f = \frac{3(2D)(\pi D^2/4)}{8D^3} = 0.59 \quad (4-3)$$

XXYZ Geometry

The second type of orthogonal yarn geometry, XXYZ, possesses a tetrahedral unit cell. The (100) plane of an unit cell with this fiber architecture is shown in Figure 4-7. This cell differs from the unit cell of the other orthogonal geometry by the presence of two x direction yarns in each cell. This presence causes the lattice parameter a to equal $3D$. Since

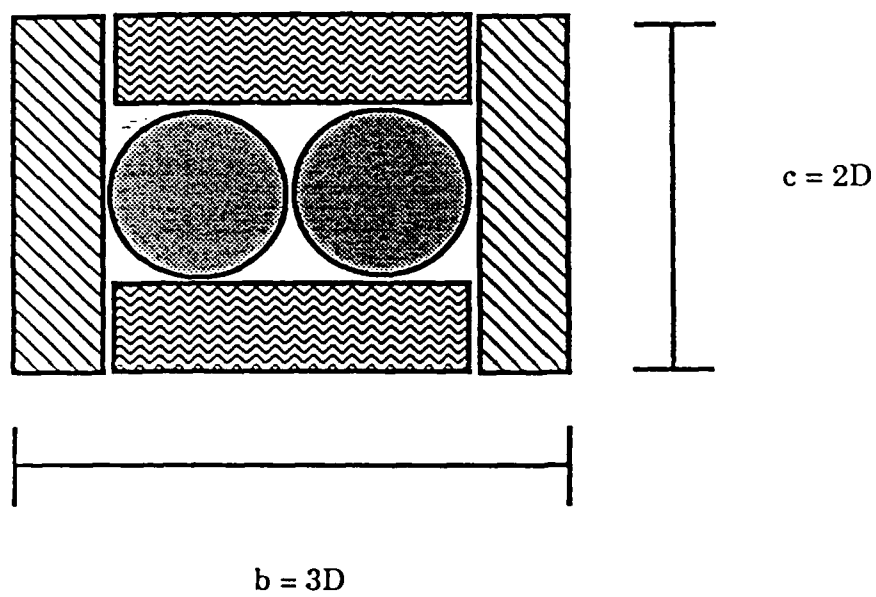


Dependence of the Fiber Volume Fraction of a Multiaxial Warp Knit
on the Relative Difference Between the Diameters of the Knitting
Yarn and the Lay-in Yarns
Figure 4-5



XYZ Geometry Unit Cell Plane

Figure 4-6



XYZ Geometry (100) Plane

Figure 4-7

the other lattice parameters are not effected by the second x yarn, they remain 2D. The fiber volume fraction for this cell is the same as with the XYZ geometry. The expression for this value is:

$$V_f = \frac{(4+3+2) \frac{\pi D^3}{4}}{12D^3} = 0.59 \quad (4-4)$$

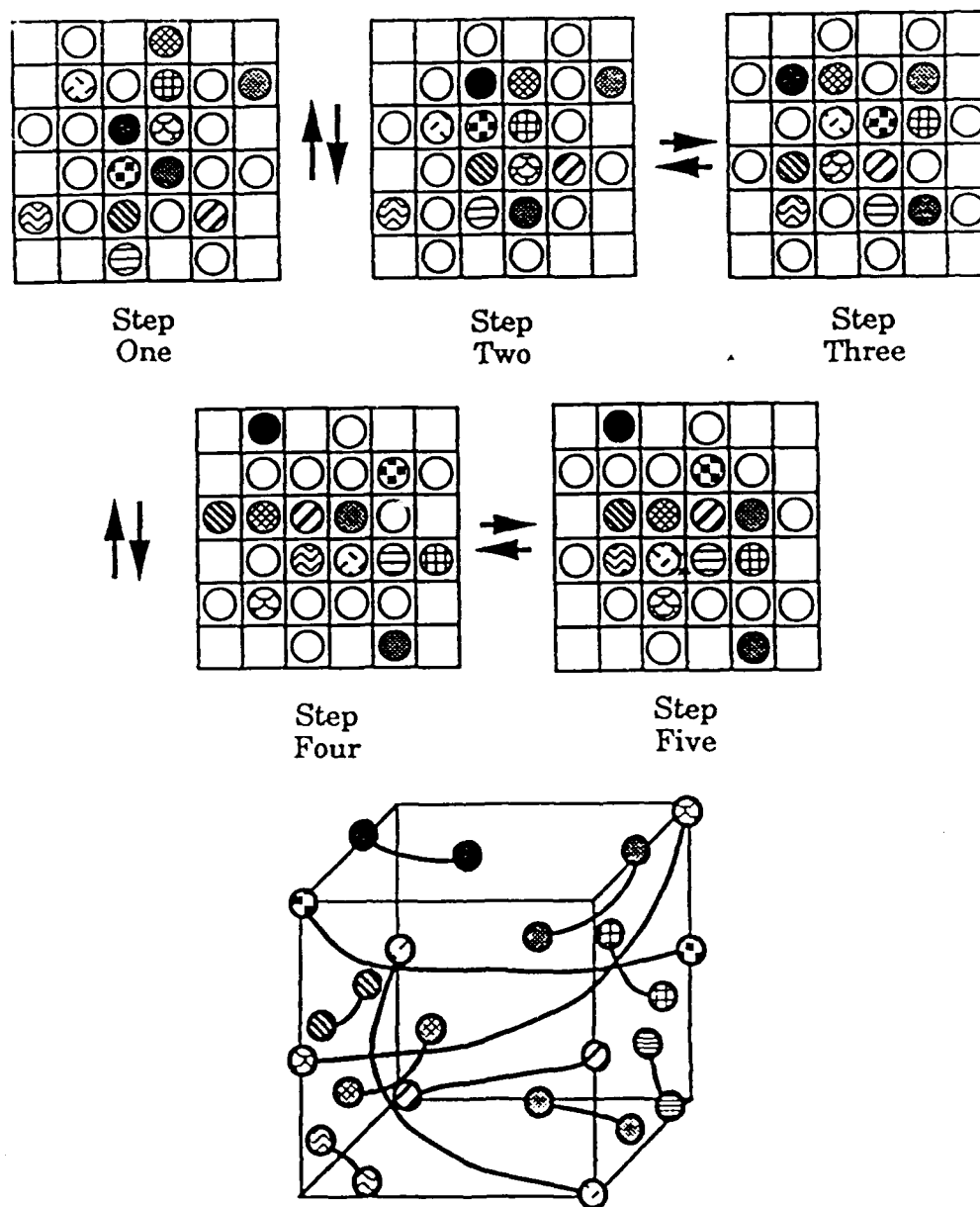
XXYYZ Geometry

The final type of orthogonal yarn geometry is XXYYZ. This geometry is similar to the XYZ geometry depicted in Figure 4-6 except here the full diameter of the x and y yarns is included in each unit cell edge. Thus $a = b = 3D$ while z remains $2D$ and there are two x and y yarns per unit cell.

$$V_f = \frac{(6+6+2) \frac{\pi D^3}{4}}{18D^3} = 0.61 \quad (4-5)$$

Body Diagonal Geometries

In this section the similar unit cells of 3D braids with 100% braiding yarns, and the 4 directional lay-in Omniweave are discussed. These unit cells are, in general, orthogonal. For the 3D braid an important consideration in determining the unit cell parameters is the process by which the braid is formed. In Figure 4-8 the unit cell of a 3D braid with a 45° braid angle is shown along with the track and column movements necessary to form this unit cell. The compacting action drastically alters this unit cell. This



Track/Column Loom motion used to Form an Euclidean Braid
and the Initial Unit Cell Produced by this Process

Figure 4-8

action compacts the bottom body diagonal pair against the top body diagonal pair, pulls the eight corner loops out of this unit cell into adjacent unit cells, and both inverses as well as reduces the amount of curvature present in the constituent yarns. The resultant unit cell is shown in Figure 4-9. The offset of the two body diagonal pairs in the xy plane is the result of subsequent track and column motions. The unit cells of the Omniweave are determined by the direction of the lay-ins. The simplified unit cells shown in Figure 4-10 will be used to describe the body diagonal geometries.

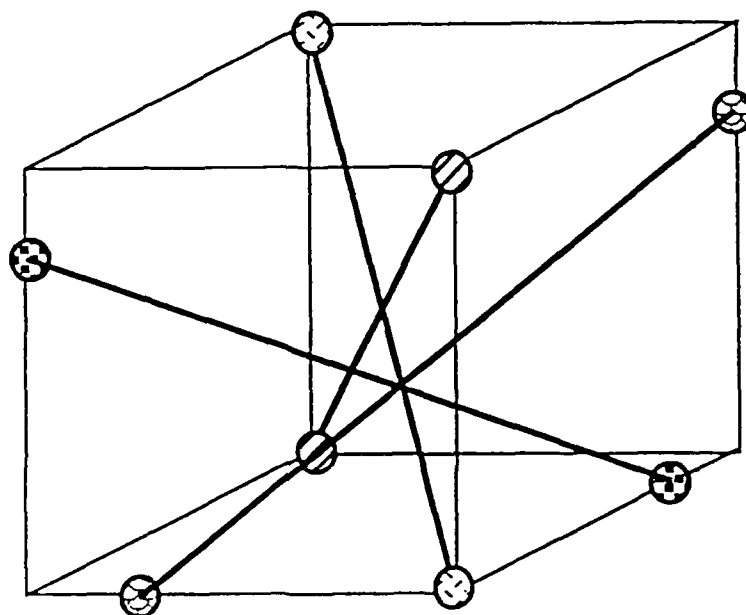
The total length of yarn in each unit cell is four times the length of the body diagonal in that cell. In this model we will also assume that the unit cell is tetragonal. This is the case when the braiding motion is an one by one track and column movement and the constituent yarns possess a circular cross-sectional area. For the tetragonal unit cell a is equal to b but is not equal to c . c can be described as

$$c = a \tan \theta \quad (4-6)$$

θ is the angle of the side face diagonal, which is equal to the complement of the braid angle.

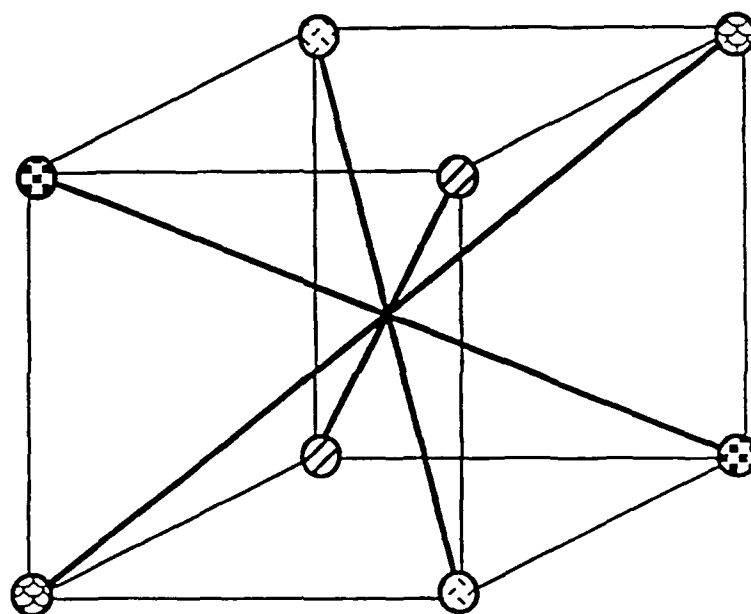
The length of a body diagonal in this unit cell is:

$$L_B = \sqrt{2a^2 + a^2 \tan^2 \theta} \quad (4-7)$$



Euclidean Braid Unit Cell After Compacting
Depicting the Effect of Subsequent Column Movement
on the Relative Position of the Two Body Diagonal Pairs

Figure 4-9



Simplified Euclidean Braid Unit Cell

Figure 4-10

The fiber volume fraction is equal to:

$$V_f = \frac{\sqrt{2 + \tan^2 \theta} \pi D^2}{a^2 \tan \theta} \quad (4-8)$$

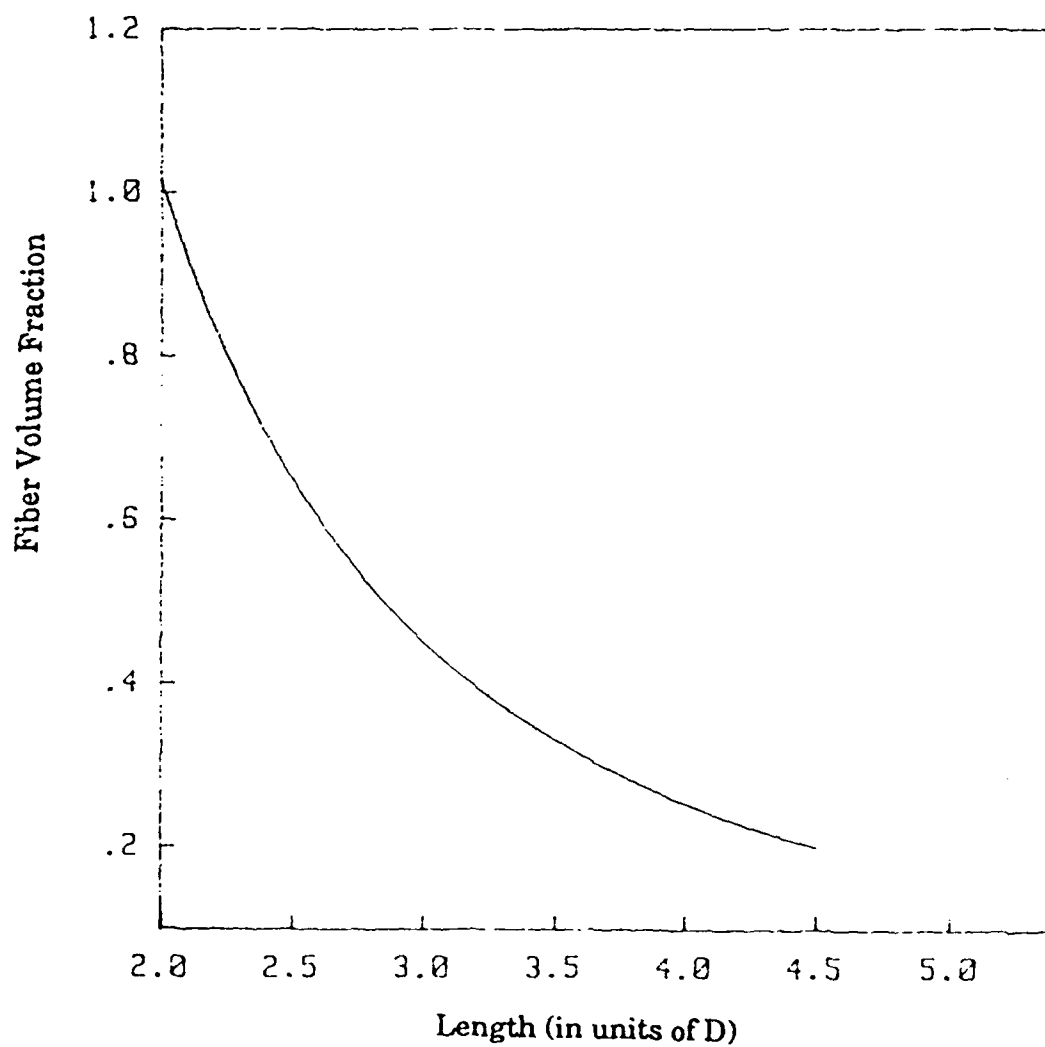
Since there is no close packed direction in this unit cell, there is no absolute relationship between the constituent yarn diameter and the lattice parameters. Figure 4-11 plots the effect of varying a in units of D on the fiber volume fraction with a braid angle of 30° . The form of this function is $V_f(a) = T/a^2$, where T is a constant. As the braid angle is increased, T increases and subsequently $V_f(a)$ increases for a specific a value.

Figure 4-12 plots the effect of varying the braid angle on the fiber volume fraction with the parameter a equal to $3D$. The fiber volume fraction steadily increases as the braid angle is increased. The increase in the value of $dV_f/d(\text{braid angle})$ above 45° results from the lattice parameter c being less than a in this region. From this plot, it is apparent that there is a minimum fiber volume fraction. This value depends on the value of a assumed. The minimum fiber volume fraction decreases as the value of a increases.

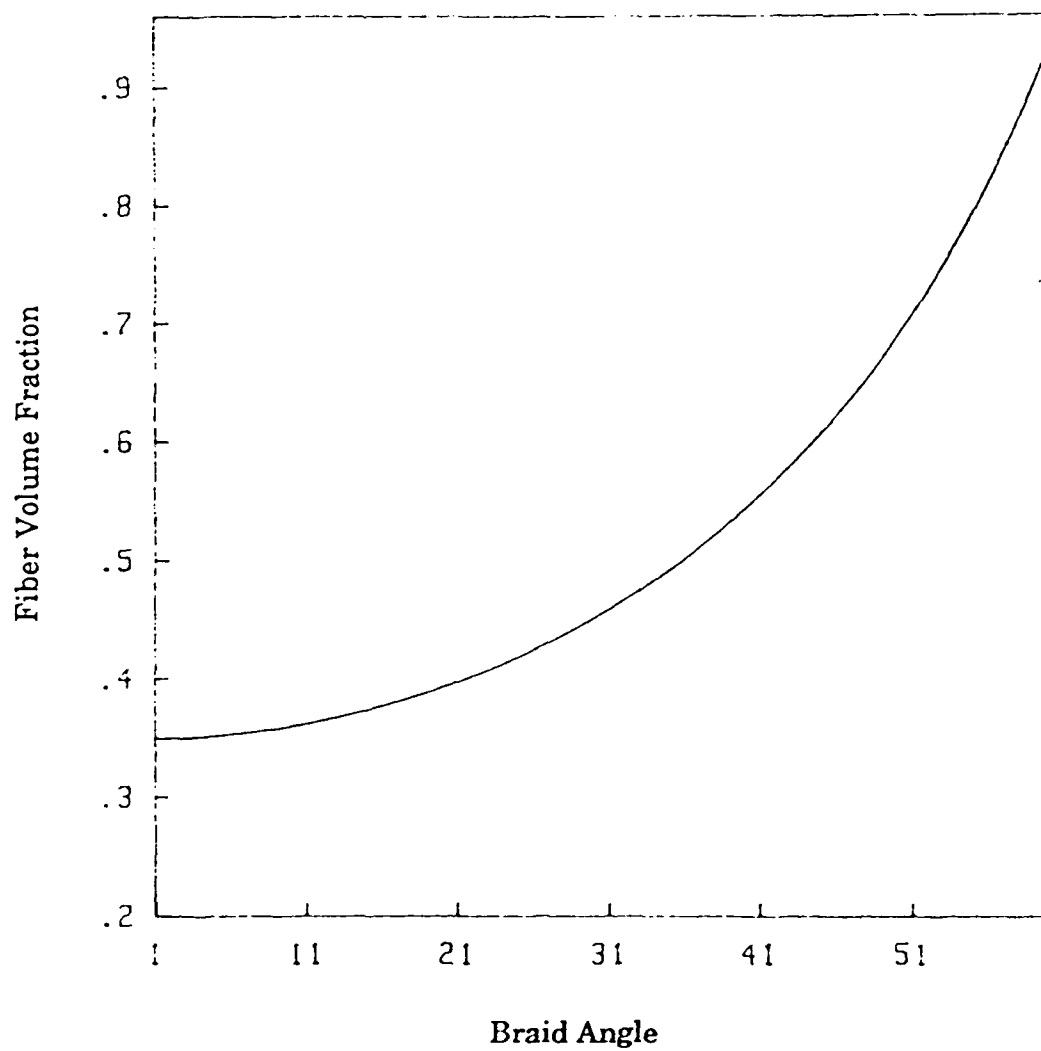
Combined Geometries

Euclidean Braid with lateral lay-ins

Combined geometries are possessed by unit cells with both orthogonal and bias direction constituent yarns. These geometries are possessed by Euclidean braids with longitudinal or lateral lay-ins, Two-Step braids, and



Dependence of the Fiber Volume Fraction of an Euclidean Braid
on the Size of the a Lattice Parameter for a Braid Angle of 45°
Figure 4-11



Dependence of the Fiber Volume Fraction of an Euclidean Braid
on the Braid Angle with $a = 3D$
Figure 4-12

Crawford's nonwovens. In the case of the Euclidean braid with lateral lay-ins, the presence of lateral lay-ins alters the fiber volume fraction equation 4-8 in the manner shown below.

$$V_f = \frac{(4\sqrt{2+\tan^2\theta}+n)\pi D^2}{4a^2 \tan\theta} \quad (4-9)$$

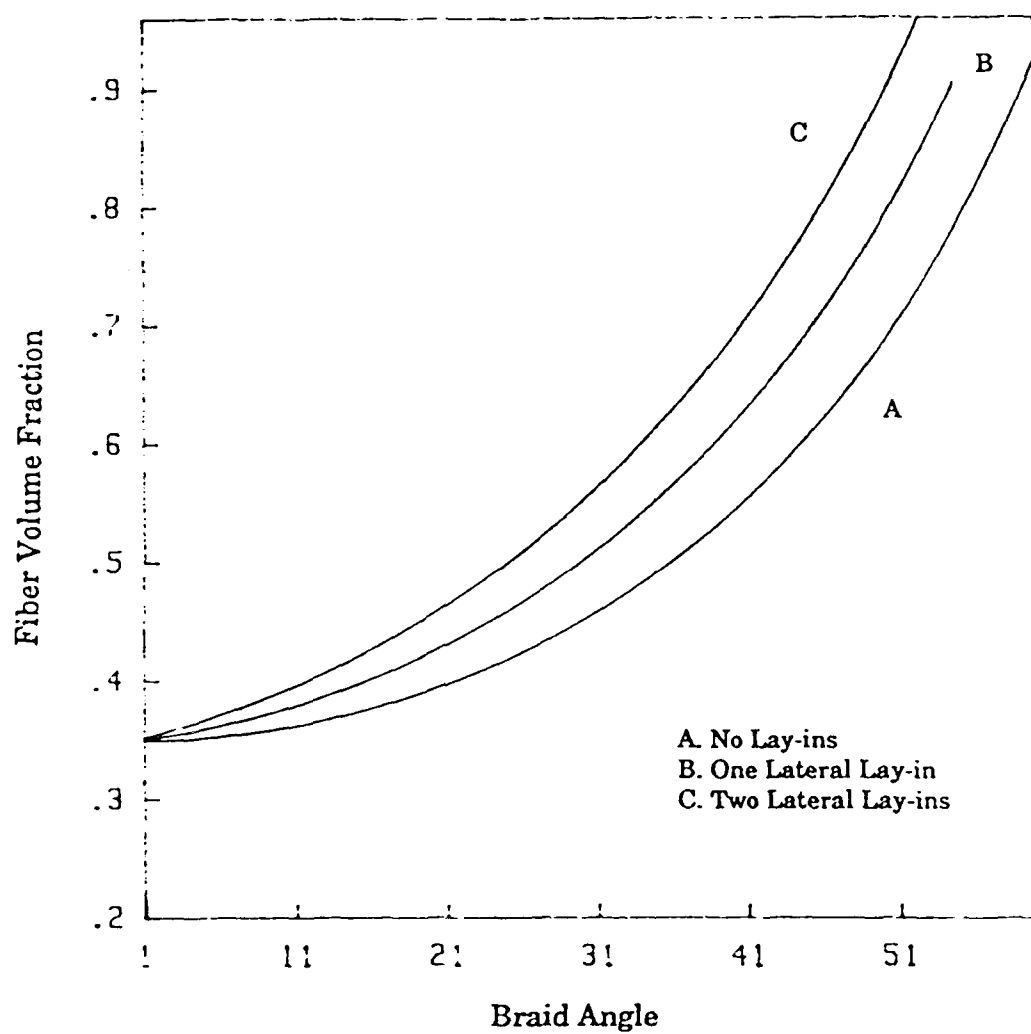
In this equation, n represents the number of lateral lay-ins. A lateral lay-in in either the x or y directions possesses length a (assuming a tetrahedral unit cell). The presence of the lateral lay-ins increases the T value of $V_f(a)$ for a specific a , as compared to a braid with 100% braiding yarns. The fiber volume fraction as a function of the braid angle for 100% braiding yarns, one lateral lay-in, and two lateral lay-ins is plotted in Figure 4-13. The effect of the lay-ins on the fiber volume fraction increases as the braid angle increases. This occurrence is attributed to the decrease in the relative length of c/a as the braid angle increases.

Euclidean Braid with Longitudinal Lay-ins

The addition of longitudinal yarns alters equation 4-8 to:

$$V_f = \frac{(4\sqrt{2+\tan^2\theta}+\tan\theta)\pi D^2}{4a^2 \tan\theta} \quad (4-10)$$

The additional $\tan\theta$ term accounts for, c , the length of the longitudinal yarn in the unit cell (the a is factored out in 4-8). The presence of the lateral lay-ins creates a T value of $V_f(a)$, for a specific a , larger than that of



A Comparison of the Dependence of the Fiber Volume Fraction on the Braid Angle for a Euclidean Braid with No, One and Two Lateral Lay-in Yarns
Figure 4-13

a braid with one lateral lay-in, but smaller than with two lateral lay-ins. The fiber volume fraction as a function of the braid angle for 100% braiding yarns and for a braid with longitudinal lay-ins is plotted in Figure 4-14. The effect of the lay-ins on the fiber volume fraction decreases as the braid angle increases. This occurs since the relative length of c/a decreases as the braid angle increases.

Two-Step Braid

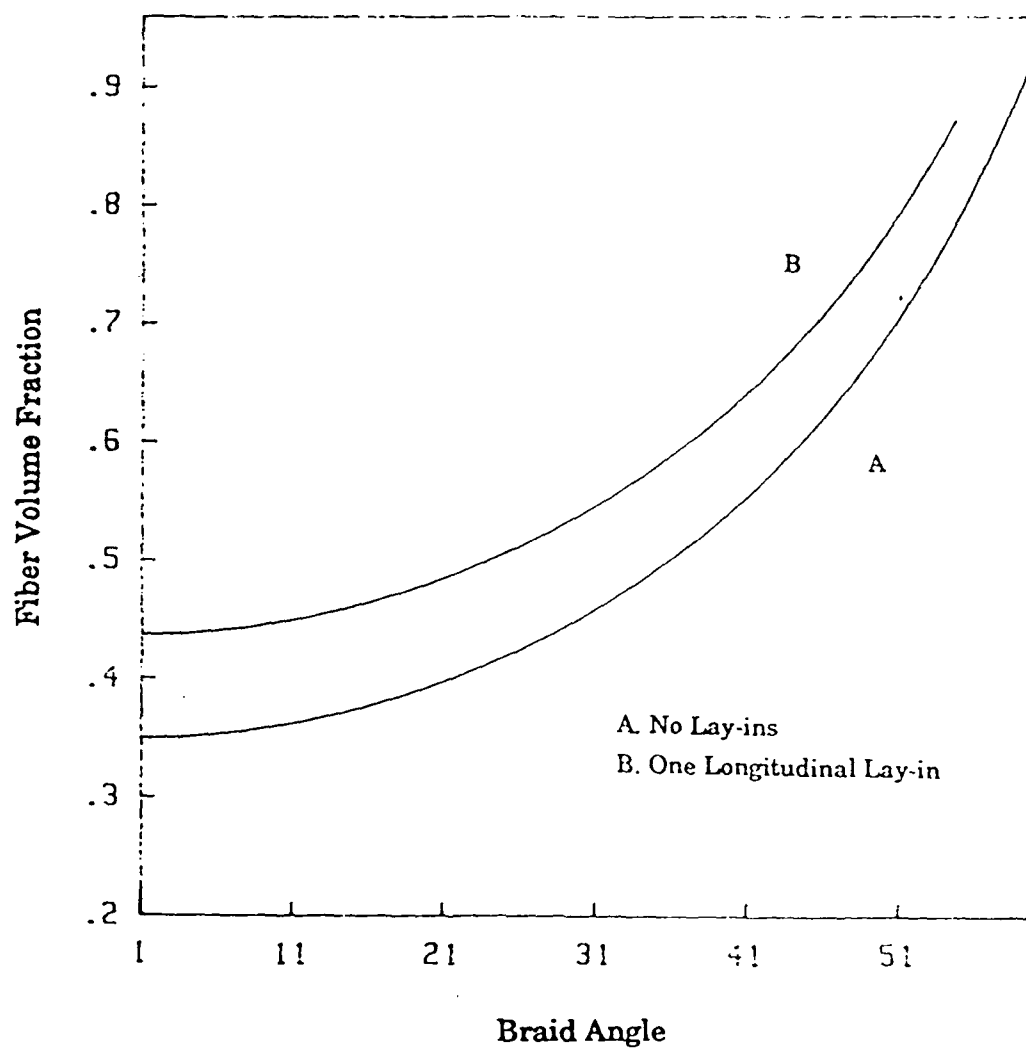
While the two step braiding process possesses a similar geometry to the Euclidean braid with longitudinal lay-ins, they are not identical. The difference in these two unit cells arises from the two different loom designs. The different loom designs are shown in Figure 4-15. The ratio of longitudinal yarns to braiding yarns is different in both processes. For the two step braid the ratio must be:

$$\frac{L}{B} = \frac{RC}{R+C} > 1 \quad (4-11)$$

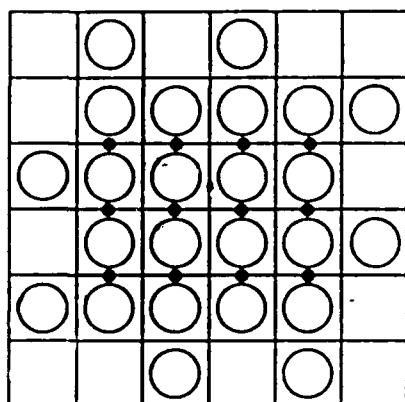
where L is the number of longitudinal yarns, B is the number of braiding yarns, R is the number of rows, C is the number of columns. In the 3D braid the number of longitudinal yarns can vary from zero upto the number of braiding yarns.

$$\frac{L}{B} \leq 1 \quad (4-12)$$

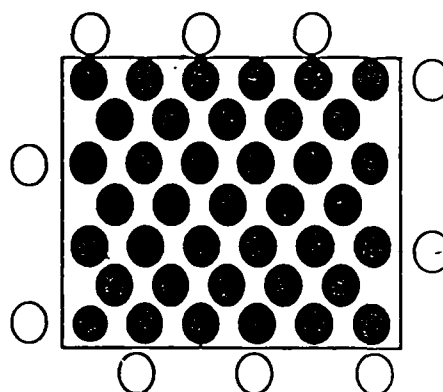
The projection of the component yarns on the (001) planes for the 3D braid with longitudinal lay-ins and the two step braid are shown in Figure 4-16.



A Comparison of the Dependence of the Fiber Volume Fraction on the Braid Angle for a Euclidean Braid with No Lay-ins and with One Longitudinal Lay-in Yarn
Figure 4-14



Euclidean Braid Loom Design with
Longitudinal Lay-ins



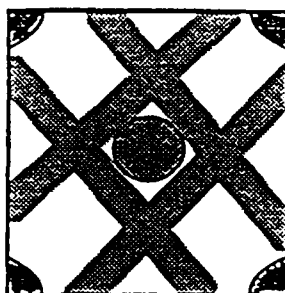
2-Step Loom Design

Key:

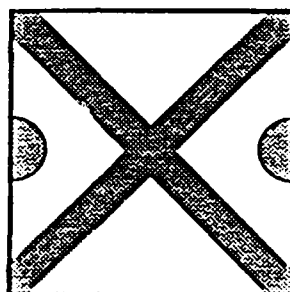
○ Braiding Yarns

● Longitudinal Yarns

A Schematic of the Different Loom Designs for the
Euclidean and the Two-Step Braid
Figure 4-15



Two-Step Braid.



Euclidean Braid with a
Longitudinal Lay-in

Projection of the Component Yarns
on the (001) Plane

Figure 4-16

The labels T and B on the two-step braid figure represent the top and bottom plane of a unit cell. The length of each bias yarn is:

$$L_B = \sqrt{2 \left(a - \frac{D}{2}\right)^2 + c^2} = \sqrt{2 \left(a - \frac{D}{2}\right)^2 + a^2 \tan^2 \theta} \quad (4-13)$$

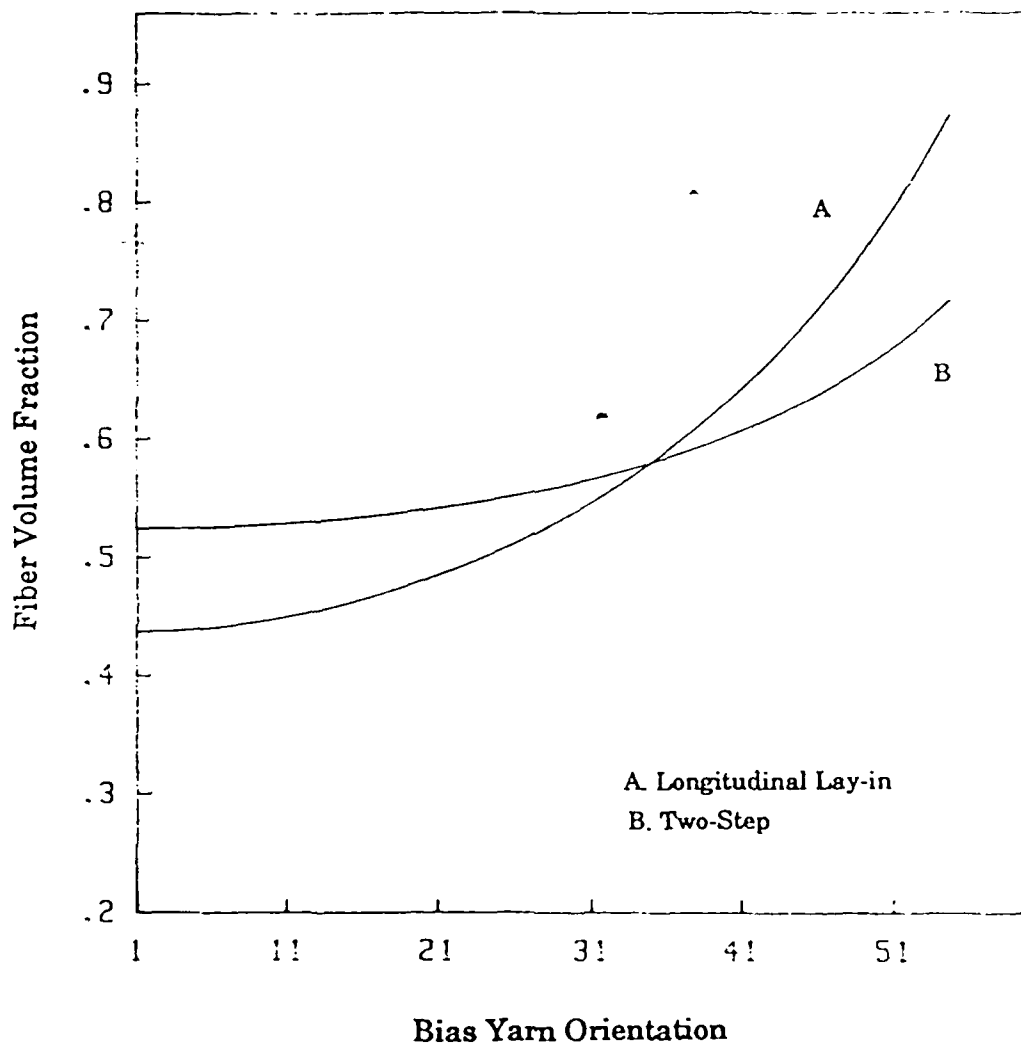
Where θ is the angle relating a and c . The expression for the fiber volume fraction for this geometry is:

$$V_f = \frac{4 \sqrt{2 \left(a - \frac{D}{2}\right)^2 + a^2 \tan^2 \theta} + 2a \tan \theta \pi D^2}{4a^3 \tan \theta} \quad (4-14)$$

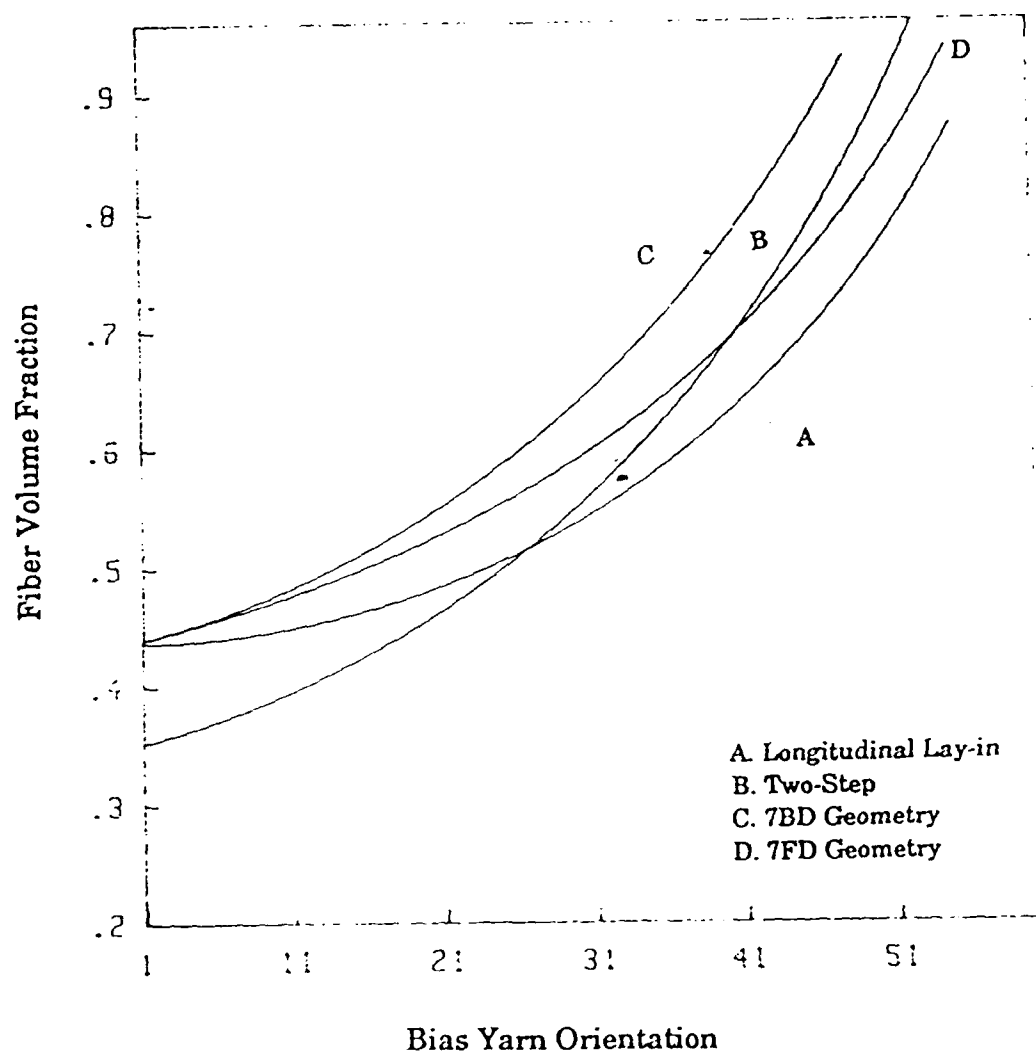
The fiber volume fraction as a function of braid angle is plotted for the Two-Step braid and the Euclidean braid with a longitudinal lay-in in Figure 4-17. The Two-Step braid possesses a higher minimum fiber volume fraction since there is a higher percentage of longitudinal yarns in this fiber architecture. Since a higher percentage of the fiber volume fraction in the Two-Step braid arises from the longitudinal yarns it is less dependent on θ .

Crawford's Nonwovens

Crawford's 7D and 11D nonwovens are combinations of orthogonal and diagonal yarn geometries. These geometries behave in a similar manner to the above mentioned combined geometries. Figure 4-18 plots the fiber volume fraction as a function of the bias yarn orientation for Euclidean braids with longitudinal and lateral inserts as well as the 7D body diagonal geometries. The fiber volume fraction function for the 7D body diagonal geometry can be expressed as:



A Comparison of the Dependence of the Fiber Volume Fraction on the Bias Yarn Orientation Angle for the Euclidean Braid with a Longitudinal Lay-in and the Two-Step Braid with $a = 3D$
Figure 4-17



A Comparison of the Dependence of the Fiber Volume Fraction on the Bias Yarn Orientation Angle for the Combined Geometries with $\alpha = 30^\circ$
Figure 4-18

$$V_f = \frac{(4\sqrt{2+\tan^2\theta} + 2 + \tan\theta)\pi D^2}{4a^2 \tan\theta} \quad (4-15)$$

In this relationship, it is assumed that $a = b$.

For the face diagonal 7D geometry the length of each face diagonal equals:

$$L_F = \sqrt{a^2 + c^2} \quad (4-16)$$

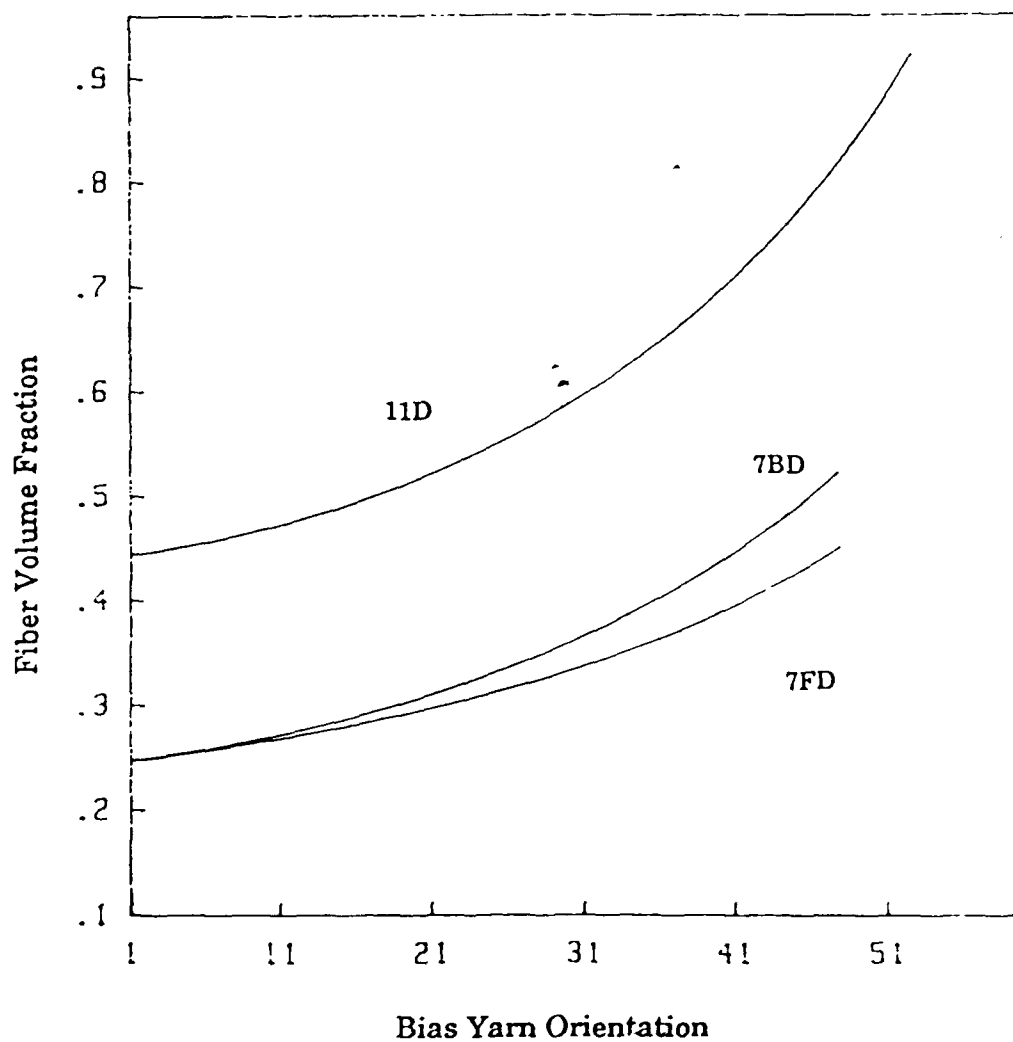
Using this relationship, the fiber volume fraction for the face diagonal 7D geometry is expressed as:

$$V_f = \frac{(4\sqrt{1+\tan^2\theta} + 2 + \tan\theta)\pi D^2}{4a^2 \tan\theta} \quad (4-17)$$

The fiber volume fraction for the 11D geometry can be determined in a similar fashion.

$$V_f = \frac{(4\sqrt{2+\tan^2\theta} + 4\sqrt{1+\tan^2\theta} + 2 + \tan\theta)\pi D^2}{4a^2 \tan\theta} \quad (4-18)$$

Figure 4-19 plots the fiber volume fraction as a function of the face diagonal angle with the lattice parameter a equal to $4D$ for the three Crawford geometries. The minimum fiber volume fraction of the 11D geometry is very high. The assumption that all the constituent yarns intersect at the center of the unit cell is partially responsible for this value. There doesn't appear to be much difference between the behavior of the 7BD and the 7FD



A Comparison of the Dependence of the Fiber Volume Fraction on the Bias Yarn Orientation Angle for the Crawford Geometries with $a = 4D$
Figure 4-19

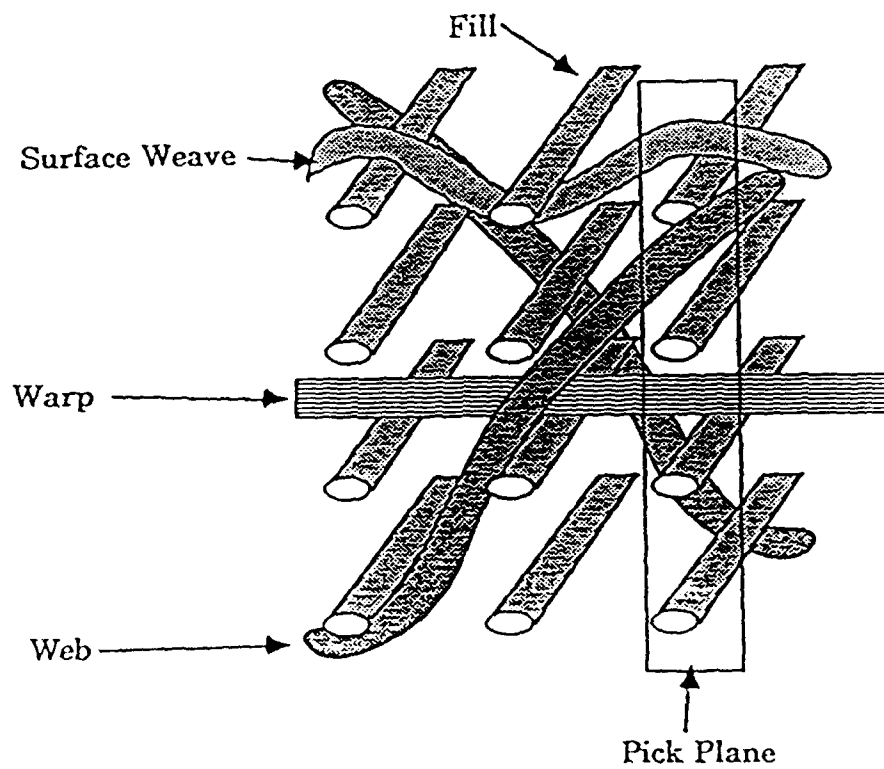
geometries as a function of orientation angle. The 11D geometry is translated vertically from these curves but appears to possess the same rate of volume fraction increase.

Three Dimensional Weaves

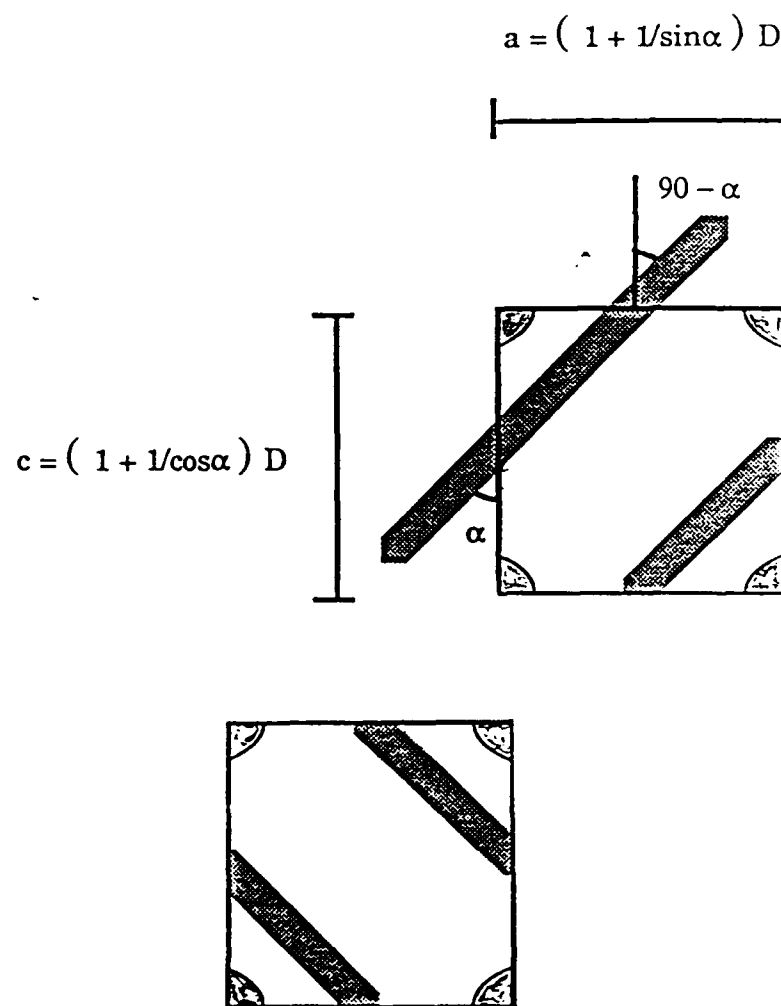
The possibilities of unit cell geometries with three dimensional weaves is numerous. For this model, weaves with a plain weave geometry in the xy plane are studied. The effect of crimp on the fiber volume fraction is assumed to be small enough that the plain weave can be modeled as a x/y lay-in geometry.

Figure 4-20 is a schematic of the xz plane of a three dimensional weave. The through thickness warp yarn is known as the web yarn. The surface yarns form a traditional plain weave on the surface of the fabric. Since the presence of the surface yarn is optional and does not effect the geometry of the interior unit cells, it will be ignored in this model. The geometry of these weaves is described by a series of unit cells. These unit cells vary by the number of web yarns in them and the orientation of these yarns. The number of web yarns can vary from zero to two in each unit cell. The two possible orientations of the web yarns is shown in Figure 4-21.

A final assumption that is made is that the lattice parameters of all unit cells are the same. This assumption is sound when there are many cells with web yarns, since these cells then tend to support the cells without web yarns. The lattice parameters in the xz plane, a and c, are equal to the sum of one fill yarn diameter plus a bias yarn diameter. The bias yarn



A Schematic of the XZ Plane of a 3D Weave
Figure 4-20



XZ Plane of Two 3D Weave Unit Cells Depicting Possible
Web Yarn Orientations and the Unit Cell Lattice Parameters

Figure 4-21

diameter depends on the web angle. The relationship of this angle to the lattice parameter is shown in Figure 4-21. Thus a and c are equal to:

$$a = (1 + \frac{1}{\sin \alpha}) D \quad (4-19)$$

$$c = (1 + \frac{1}{\cos \alpha}) D \quad (4-20)$$

Where α is defined as the web angle. Since the presence of the web yarn has no effect on the b dimension, $b = 2D$, as in a XYZ geometry. When $\alpha = 0^\circ$, the thick weave geometry is XYZ orthogonal with $a = b = c = 2D$ and $V_f = 0.59$.

The fiber volume fraction of a unit cell with no web yarn is:

$$V_f = \frac{(4 + \frac{1}{\cos \alpha} + \frac{1}{\sin \alpha}) \pi}{8 (1 + \frac{1}{\sin \alpha}) (1 + \frac{1}{\cos \alpha})} \quad (4-21)$$

The assumption is made that the web yarn enters the cell at $a/2$ and exits at $c/2$. The length of a web yarn in a unit cell is equal to:

$$L_w = \sqrt{(\frac{a}{2})^2 + (\frac{c}{2})^2} \quad (4-22)$$

Correspondingly the fiber volume fraction of a unit cell with one or two web yarns is:

$$V_f = \frac{(4 + \frac{1}{\cos\alpha} + \frac{1}{\sin\alpha} + nL_w) \pi}{8(1 + \frac{1}{\sin\alpha})(1 + \frac{1}{\cos\alpha})} \quad (4-23)$$

where n is defined as the number of web yarns per unit cell.

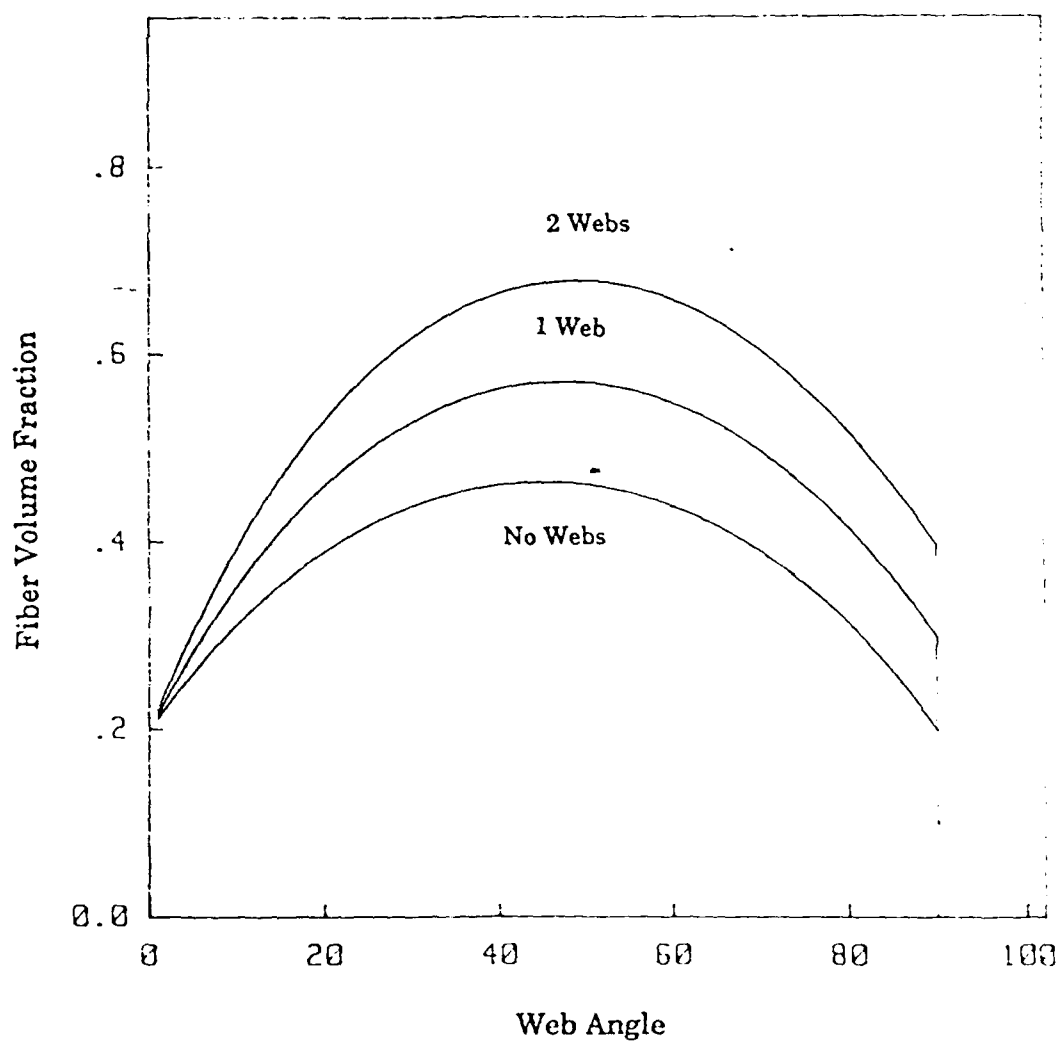
Figure 4-22 plots the fiber volume fraction as a function of α for a unit cell with one, two or no web yarns. There is a maximum fiber volume fraction at 45° for all unit cells. The sharp drop in V_f in the limit of 90° is attributed to $\cos\alpha$ going to 0 in this region. Figure 4-23 plots the effect of varying the relative proportion of cells with and without web yarns when α equals 45° by using the following function:

$$V_f(P) = P V_{f(n=0)} + (1-P) V_{f(n=2)} \quad (4-24)$$

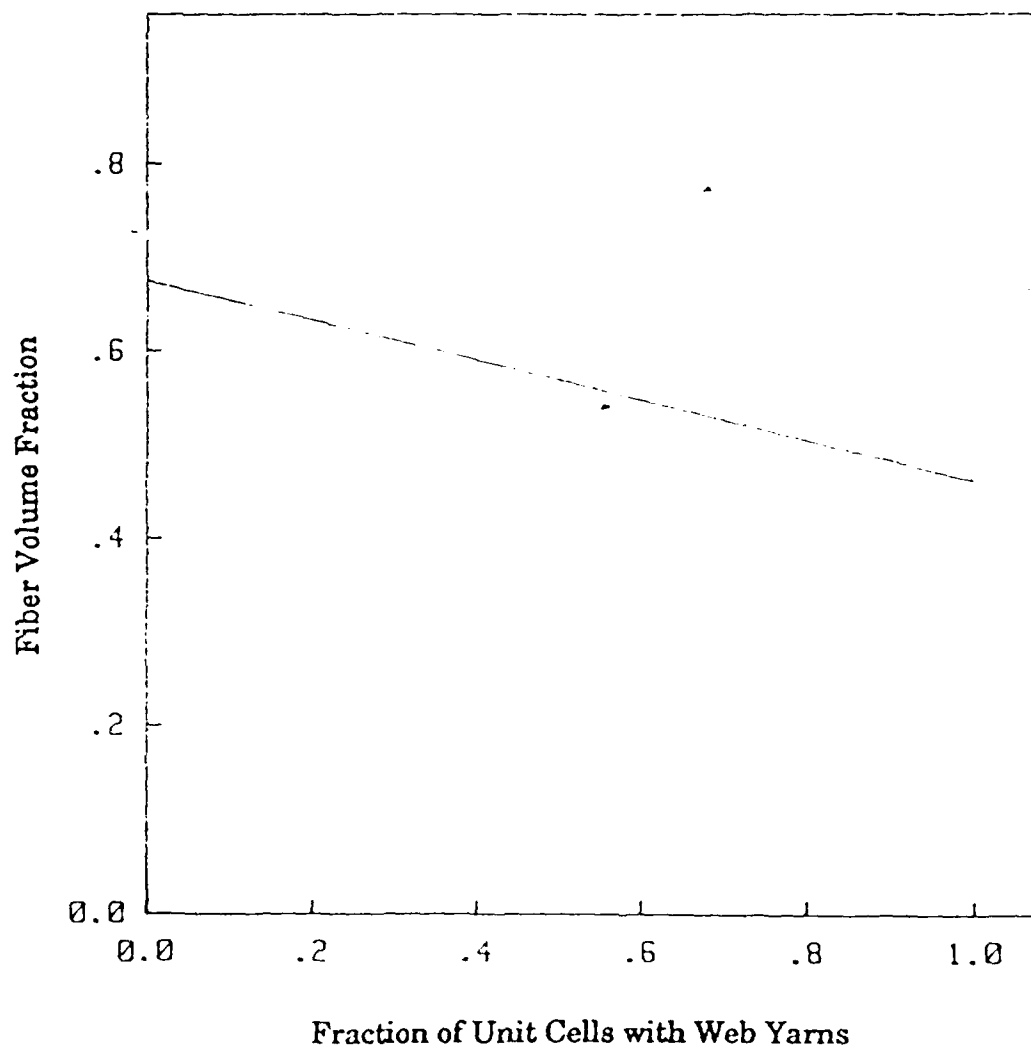
n is the number of web yarns per unit cell

Geometric Isotropy

A fiber architecture is considered to possess geometric isotropy if the variation in effective fiber volume fraction directly contributing to a loading direction is constant for any arbitrary angle. The effective fiber volume fraction of a fabric is defined as the fraction of fibers aligned in the proper direction in order for the applied load to be transferred to the fibers. For this model of geometric isotropy, the load bearing capacity of a fiber in the transverse direction is assumed to be zero. This capacity is assumed to be one in the longitudinal direction. These assumptions can be applied since



The Effect of the Number of Web Yarns Per Unit Cell on the
Fiber Volume Fraction as a Function of the Web Angle
Figure 4-22



The Range of Fiber Volume Fractions Possible by Varying the Number of Web Yarns Per Unit Cell When the Web Yarn Angle is 45
Figure 4-23

the load bearing capacity of a yarn in the transverse direction is many orders of magnitude lower than that in the longitudinal direction.

The geometric isotropy of the various fiber architectures is described by plotting the effective fiber volume fraction at any arbitrary angle in the xy , xz , and yz planes. The angle γ is defined as the projection of the arbitrary angle onto the plane being analyzed. ϕ is defined as the angle a yarn orientation makes with the axis normal to the plane in question. θ is the angle the projection of a yarn orientation makes with a given plane.

The geometric isotropy in the three orthogonal planes is plotted as a function of the arbitrary angle in the three orthogonal planes. In each plot of the geometric isotropy in an ij plane, i corresponds to the horizontal axis and j represents the vertical axis. For a totally isotropic material, the geometric isotropy plots would possess a circular shape. The greater the eccentricity of the plot, the higher the degree of anisotropy present. Geometric isotropy plots are made of the different fabric geometries described in this chapter.

Multiaxial Warp Knits

Since the contribution of the knitting yarn to the total fiber volume fraction is typically 1%, the presence of the knitting yarn is ignored when calculating the geometric isotropy. There are four yarn orientation directions of the lay-in yarns comprising a MWK. These directions and the fractional contribution they make to the total fiber volume fraction is expressed as:

$$V_f = V_x + V_y + V_{+\theta} + V_{-\theta} = 2V_n \left(1 + \frac{1}{\cos\theta}\right) \quad (4-25)$$

$$\text{since } V_x = V_y, V_{-\theta} = V_{+\theta} \text{ and } V_{+\theta} = \frac{V_x}{\cos\theta}$$

For an arbitrary angle, γ , the percent volume fraction in the xy plane is:

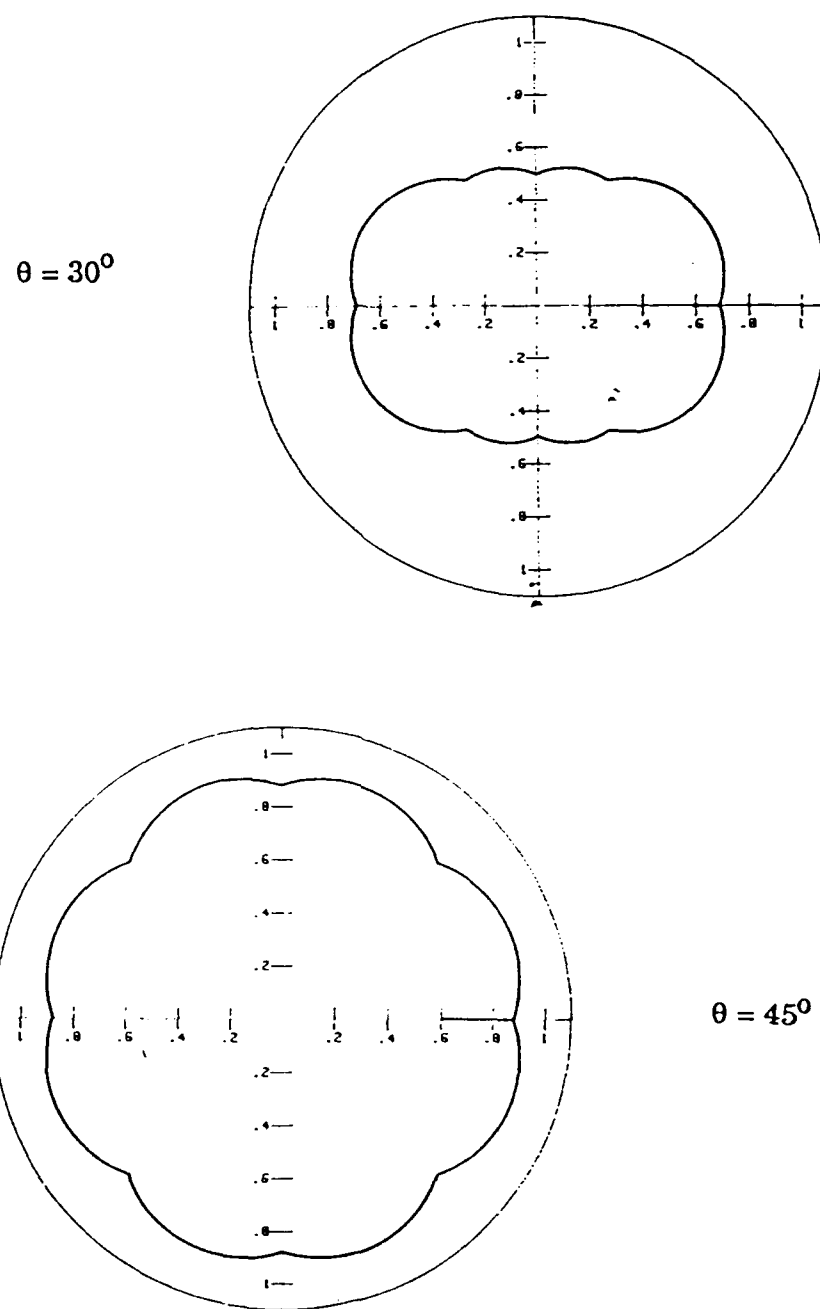
$$V(\gamma) = V_n \left(|\cos\gamma| + |\sin\gamma| + \left| \frac{\cos(\theta-\gamma)}{\cos\theta} \right| + \left| \frac{\cos(\theta+\gamma)}{\cos\theta} \right| \right) \quad (4-26)$$

Each term of 4-25 represents V_x , V_y , $V_{-\theta}$, and $V_{+\theta}$ respectively. In Figure 4-24 the geometric isotropy in the xy plane is plotted for theta is equal to 45 and 30 degrees. There is a local minimum orthogonal to every principal yarn orientation direction in the plane. This minima is greater for the $\pm 45^\circ$ direction than for the $\pm 30^\circ$ direction. In the $\pm 45^\circ$ case the bias yarns are orthogonal to each other and do not supply any effective load carrying capacity to each other.

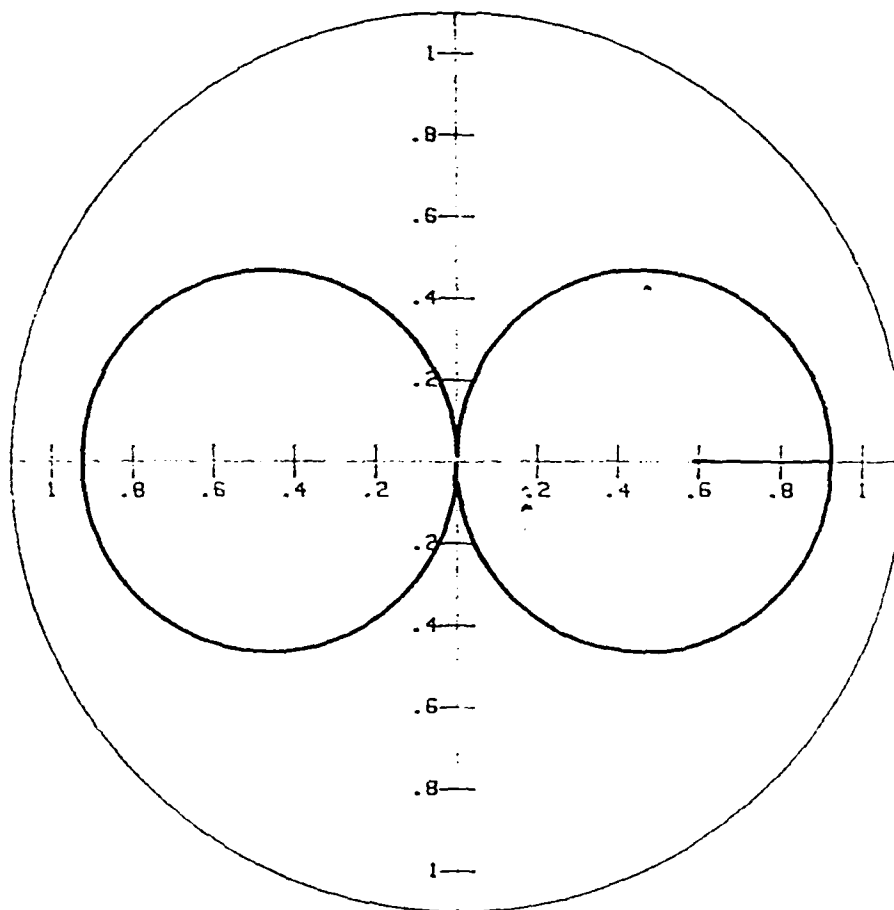
The geometric isotropy in the xz and the yz planes is similar. The effective fiber volume fraction as a function of ϕ in these planes is described by:

$$V(\phi) = V(\gamma) |\cos\phi| \quad (4-27)$$

The geometric isotropy of these planes is shown in Figure 4-25. The effect of the knitting yarn on the geometric isotropy in the xz and the yz planes was determined for a fiber volume fraction of 1% knitting yarn. This presence



The Geometric Isotropy of a MWK in the xy Plane
Figure 4-24



The Geometric Isotropy of a MWK in the xz or the yz plane
Figure 4-25

had a small effect on the geometric isotropy in the regions of $\gamma = -45^\circ$ to 45° , and 135° to 225° . In the other regions there was no significant effect.

XYZ Geometry

The distribution of the constituent yarn orientation of the XYZ orthogonal geometry is similar for all three yarn directions. This distribution is given below:

$$0.33V_f = V_x = V_y = V_z = V_n \quad (4-28)$$

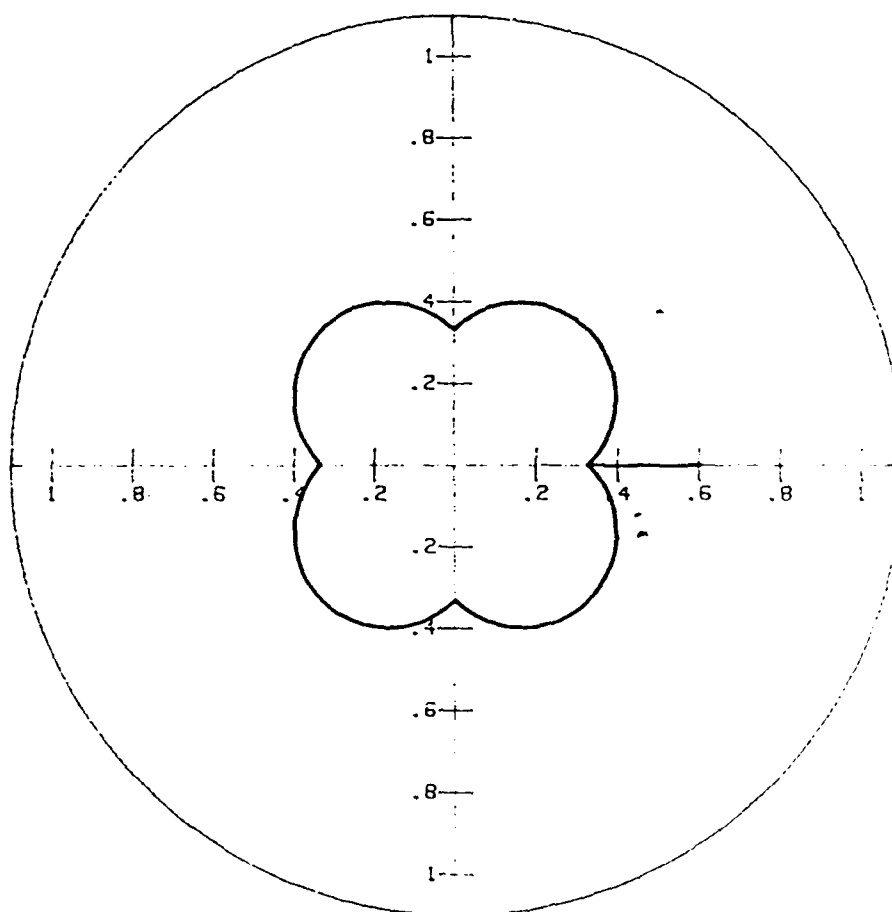
The geometric isotropy of the type one orthogonal geometry is similar for all three orthogonal planes. This relationship can be expressed as:

$$V(\gamma) = V_n (|\cos \gamma| + |\sin \gamma|) \quad (4-29)$$

The geometric isotropy of XYZ architecture is plotted in Figure 4-26. Local minima occur when constituent yarns are orthogonal to each other. In the XYZ geometry yarns are orthogonal to each other on the principal axes.

XXYZ Geometry

Because of the relative orthogonality of the constituent yarns in a XXYZ and a XXYYZ geometry, the geometric isotropic curves for these geometries possesses the same orientation angle for local minima as the XYZ geometry. The percent fiber volume fraction of each unique yarn orientation is dissimilar for these geometries. The geometric isotropy curves differ by



The Geometric Isotropy of the XYZ Fiber Architecture for all Planes
Figure 2-26

the magnitude of the effective fiber volume fraction in each plane. The fiber volume fraction distribution of the XXXYZ geometry is:

$$V_f = V_x + V_y + V_z = 4V_n + 3V_n + 2V_n = 9V_n \quad (4-30)$$

The geometric isotropy of the xy plane can be expressed as:

$$V(\gamma) = V_n (4|\cos\gamma| + 3|\sin\gamma|) \quad (4-31)$$

The geometric isotropy of the xz plane can be expressed as:

$$V(\gamma) = V_n (4|\cos\gamma| + 2|\sin\gamma|) \quad (4-32)$$

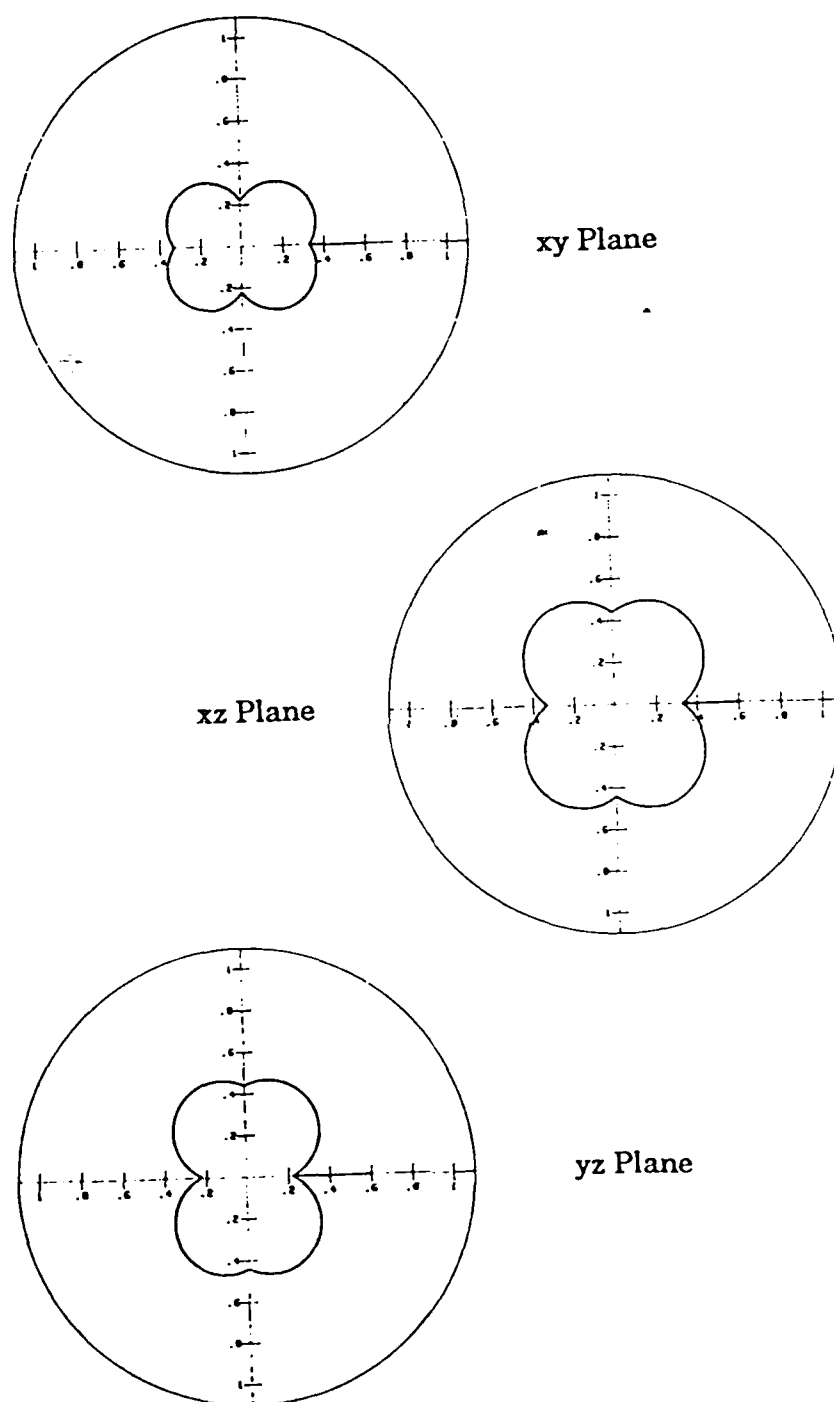
The geometric isotropy of the yz plane can be expressed as:

$$V(\gamma) = V_n (3|\cos\gamma| + 2|\sin\gamma|) \quad (4-33)$$

XXYYZ Geometry

The geometric isotropy of these three planes is plotted in Figure 4-27. The geometric isotropy of the XXYYZ geometry is described in a similar manner. The fiber volume fraction distribution of the XXYYZ geometry is:

$$V_f = V_x + V_y + V_z = 3V_n + 3V_n + 2V_n = 8V_n \quad (4-34)$$



The Geometric Isotropy of a XXYZ Fiber Architecture
Figure 4-27

The geometric isotropy of the xy plane can be expressed as:

$$V(\gamma) = V_n (3|\cos\gamma| + 2|\sin\gamma|) \quad (4-35)$$

The geometric isotropy of the xz and the yz planes can be expressed as:

$$V(\gamma) = V_n (3|\cos\gamma| + 2|\sin\gamma|) \quad (4-36)$$

Body Diagonal Geometry

The fiber volume fraction distribution of a body diagonal fabric geometry is equally divided by the four yarn orientations of this geometry. When this geometry is present in an cubic unit cell, the geometric isotropy is equivalent in all orthogonal planes. The geometric isotropy can be expressed as:

$$V(\gamma) = 0.5 |\sin(54.74)| (|\cos(45-\gamma)| + |\cos(45+\gamma)|) \quad (4-37)$$

By the symmetry of the fiber architecture, the angle made with the axis normal to the plane, 35.26°, is the same for all yarn orientations. The projection of the four yarn orientations reduces to two individual orientations in a specific plane. The two cosine terms reflect these orientations.

The geometric isotropy of the body diagonal geometry with a tetrahedral unit cell in the xy plane is described by the general form of the above equation, which is given below.

$$V(\gamma) = 0.5 |\sin\phi| (|\cos(\theta-\gamma)| + |\cos(\theta+\gamma)|) \quad (4-38)$$

$$\phi = \tan^{-1} \left(\frac{\sqrt{2}}{\tan\theta} \right) \quad (4-39)$$

The isotropy of the xz and yz planes differs from that of the xy plane through possession of a different value for θ . The geometric isotropy for the body diagonal geometry with a angle of 45° in the xy plane and 60° in the xz and yz planes is shown in Figure 4-28. There is a significant increase in the anisotropy with an angle of 60° , since c is then significantly greater than a. When $\theta = 60^\circ$ local minima occur at 30° , 150° , 210° , and 330° degrees. These angles are orthogonal to the two yarn orientations in the plane.

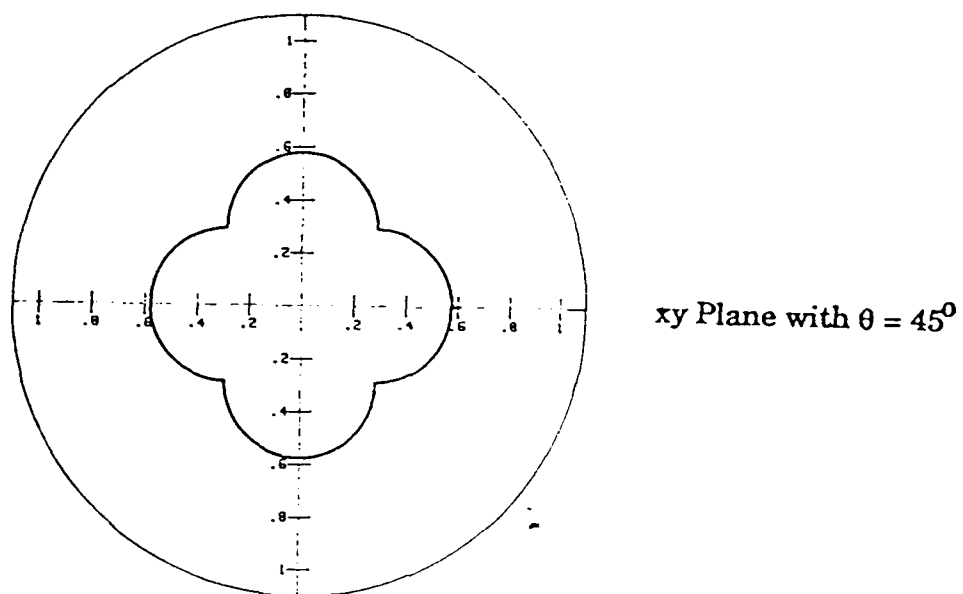
Euclidean Braid with Lateral Lay-ins

The presence of lateral lay-ins only effects the xy plane isotropy of an Euclidean braid. The geometric isotropy of this braid with two orthogonal lateral lay-ins can be expressed as:

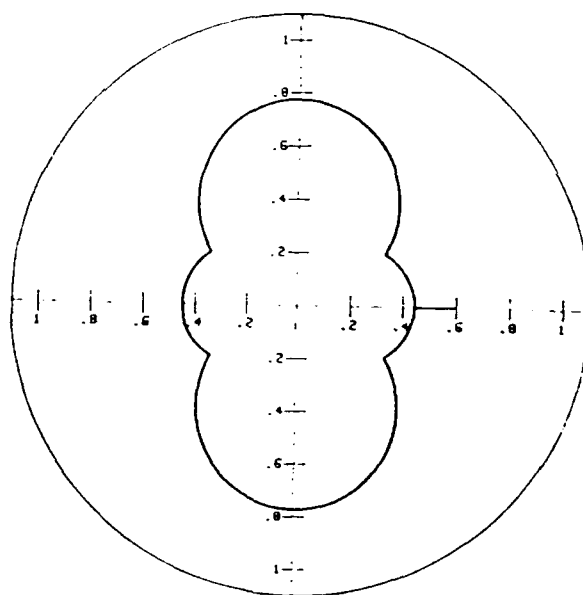
$$V(\gamma) = \frac{V_B}{2} |\sin\phi| (|\cos(\theta-\gamma)| + |\cos(\theta+\gamma)|) + \frac{V_{Lat}}{2} (|\cos\gamma| + |\sin\gamma|) \quad (4-40)$$

$$\text{where } V_f = V_B + V_{Lat}$$

The exact value of V_B can be determined with the following equation:



xz = yz Plane
 $\theta = 60^\circ$



The Geometric Isotropy of the Body Diagonal Geometry
Figure 4-28

$$V_B = 1 - \frac{2}{\sqrt{2 + \tan^2 \theta} + 2} \quad (4-41)$$

Figure 4-29 plots this geometric isotropy. The presence of the lateral yarns decreases the curvature of the plot in each segment and creates an inflection point on the axes.

Euclidean Braid with a Longitudinal Lay-in

The presence of longitudinal lay-ins effects the xz and yz plane isotropy for an Euclidean braid. The geometric isotropy of this fabric can be expressed as:

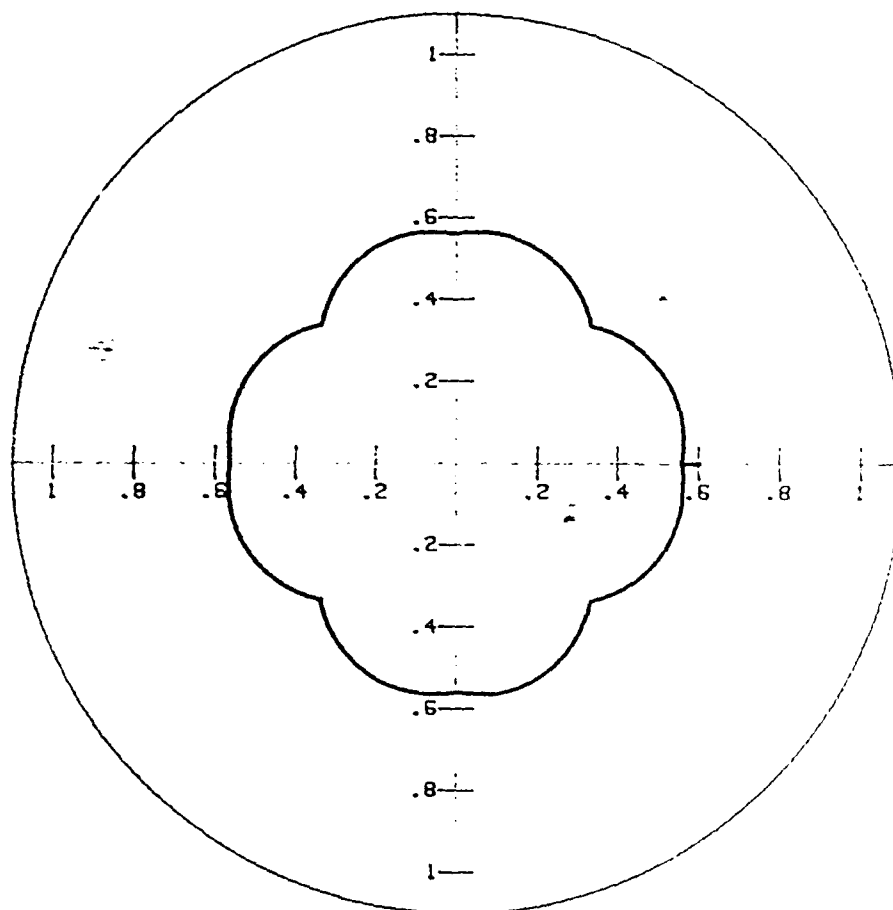
$$\begin{aligned} V(\gamma) &= \frac{V_B}{2} |\sin \phi| (|\cos(\theta - \gamma)| + |\cos(\theta + \gamma)|) \\ &\quad + V_{Long} |\sin \gamma| \end{aligned} \quad (4-42)$$

where $V_f = V_B + V_{Long}$

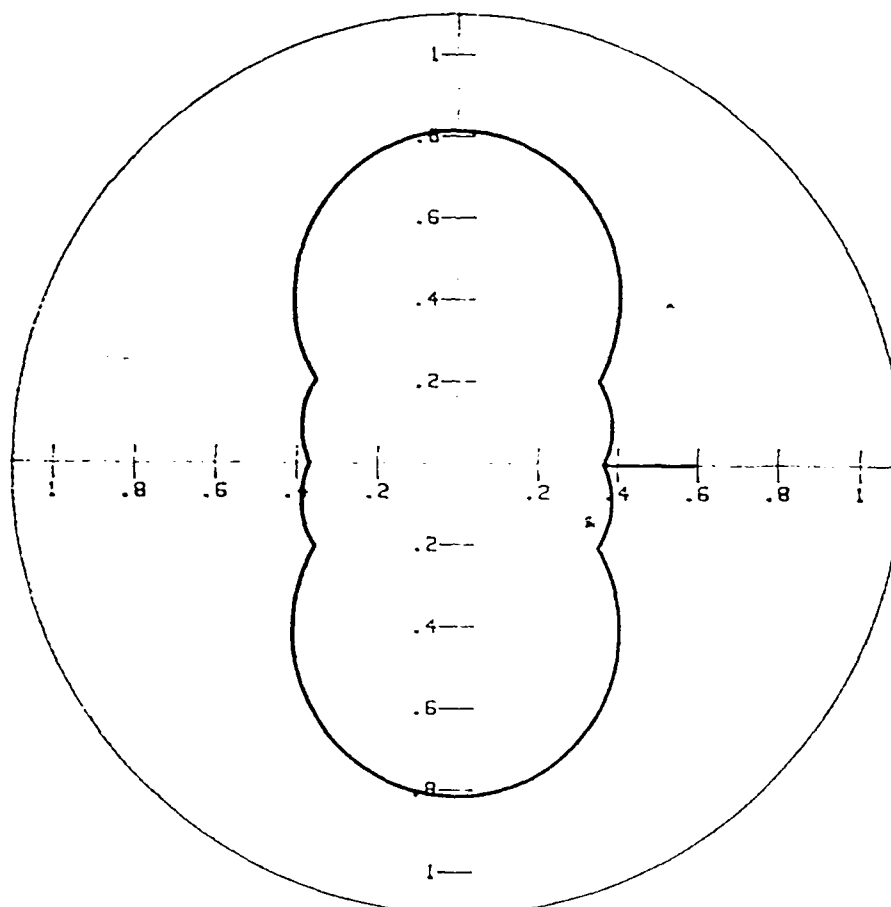
The exact value of V_B can be determined with the following equation:

$$V_B = 1 - \frac{\tan \theta}{\sqrt{2 + \tan^2 \theta} + \tan \theta} \quad (4-43)$$

Figure 4-30 plots this geometric isotropy for a theta of 60° in the xz plane. The presence of the longitudinal lay-in in the z direction creates additional local minima on the x axis.



The Geometric Isotropy of the Euclidean Braid with Two Lateral
Lay-ins in the xy Plane with $\theta = 45^\circ$
Figure 4-29



The Geometric Isotropy of the Euclidean Braid with a Longitudinal
Lay-in in the xz Plane with $\theta = 60$
Figure 4-30

Two-Step Braid

The relative value of this minima is greater in the two step braid as a result of the larger proportion of longitudinal lay-ins. The geometric isotropy of the xz plane of the two-step braid is shown in Figure 4-31. The isotropy in this plane is similar to that in the yz. The geometric isotropy is modelled using:

$$V(\gamma) = \frac{V_{\text{Bias}}}{2} |\sin\phi| (|\cos(\theta-\gamma)| + |\cos(\theta+\gamma)|) + V_{\text{Long}} |\sin\gamma| \quad (4-44)$$

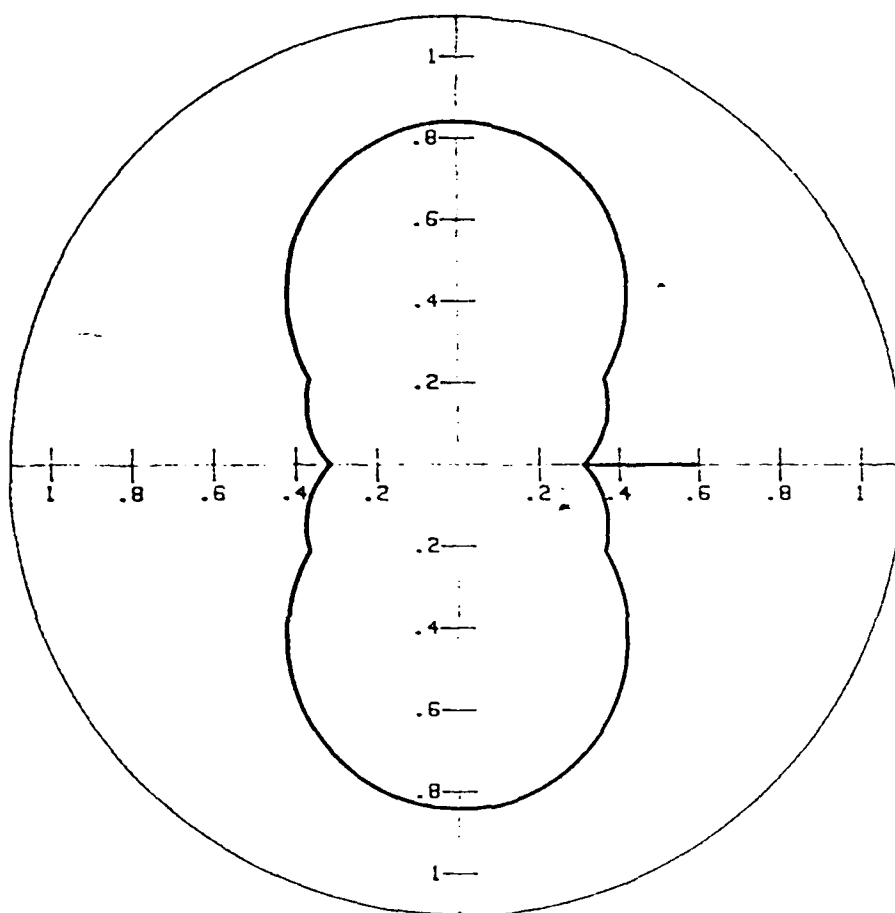
$$\phi = \tan^{-1} \left(\frac{a \tan\theta}{\sqrt{2(a - \frac{D}{2})^2}} \right) \quad (4-45)$$

$$V_f = V_{\text{Bias}} + V_{\text{Long}} \quad (4-46)$$

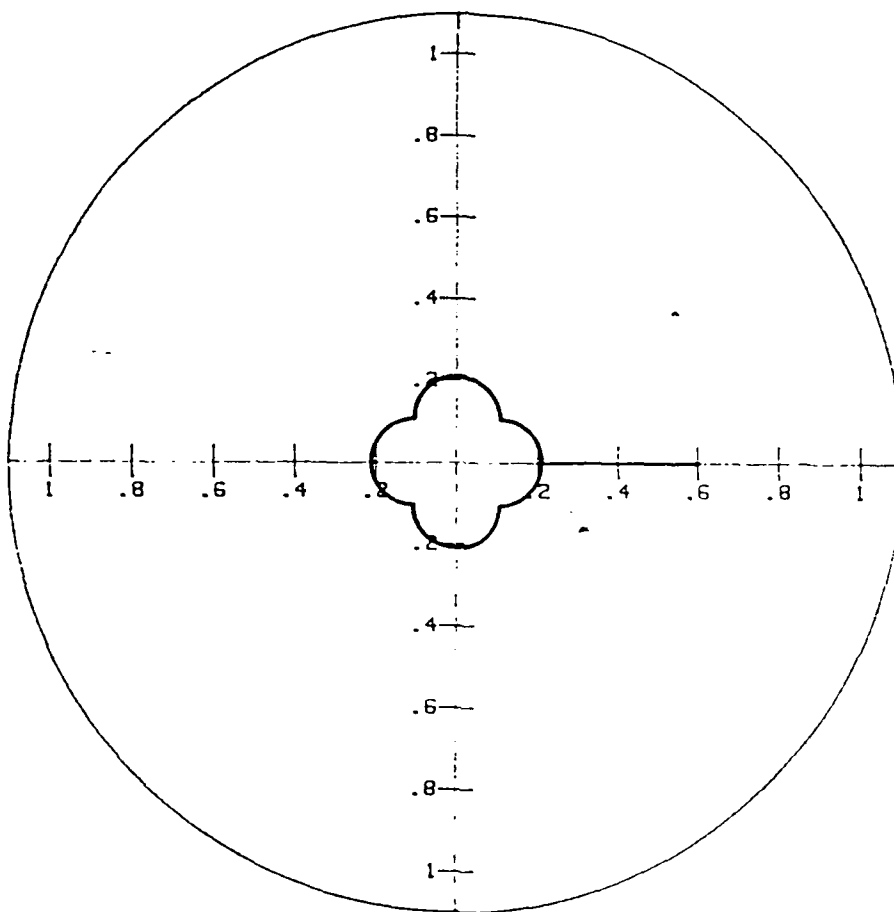
$$V_{\text{Bias}} = 1 - \frac{2a \tan\theta}{2a \tan\theta + \sqrt{2(a - \frac{D}{2})^2 + a^2 \tan^2 2\theta}} \quad (4-47)$$

θ is defined as the braid angle, a is a lattice parameter, and D is the yarn diameter used to calculate the geometry of this cell in 4-13.

The xy plane geometric isotropy of the two-step braid is shown in Figure 4-32. This plot is generated with the following function, when a tetrahedral unit cell is assumed:



The Geometric Isotropy of the xz Plane of the Two-Step Braid
with $\theta = 60^\circ$
Figure 4-31



The Geometric Isotropy of the xy Plane of a Two-Step
Braid
Figure 4-32

$$V(\gamma) = \frac{V_{\text{Bias}}}{2} |\sin\phi| (|\cos(\theta-\gamma)| + |\cos(\theta+\gamma)|) \quad (4-48)$$

$$\text{where } \phi = \tan^{-1}\left(\frac{\sqrt{2(a - \frac{D}{2})^2}}{a \tan\theta}\right)$$

Since the a and b lattice parameters are equal in this plane, θ equals 45 degrees. This function possesses the same form as equation 4-33, for the geometric isotropy of the Euclidean braid with 100% braiding yarns in the xy plane.

Crawford's 7D Body Diagonal Geometry

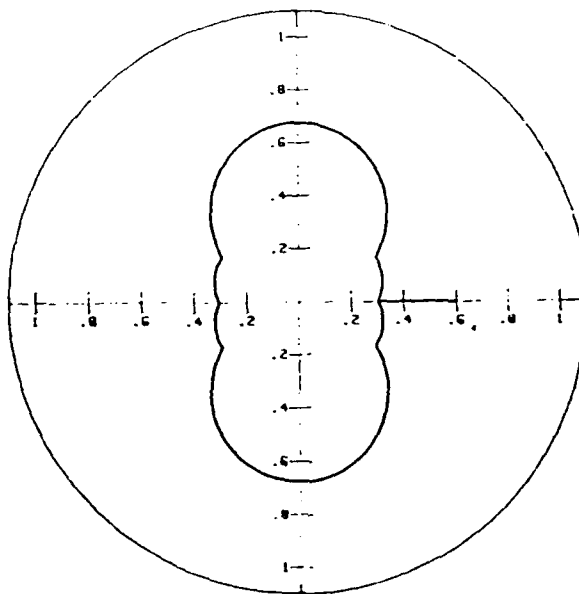
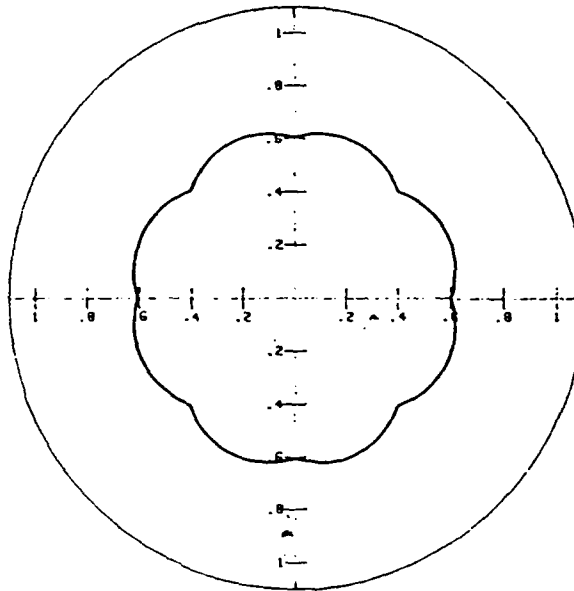
Crawford's 7D body-diagonal geometry, plotted in figure 4-33, possesses a similar geometric isotropy to the braid with lateral lay-ins in the xy plane and to the braid with longitudinal lay-ins in the xz and the yz planes. The geometric isotropy of this fiber architecture can be generated by utilizing equations 4-40 and 4-42 for the respective planes. The determination of the fiber volume fraction coefficient is made using the following relations.

$$V_f = V_B + V_{\text{Long}} + V_{\text{Lat}} \quad (4-49)$$

$$V_{\text{Lat}} = \frac{2}{4\sqrt{2+\tan^2\theta} + 2 + \tan\theta} \quad (4-50)$$

$$V_{\text{Long}} = \frac{a \tan\theta}{4\sqrt{2+\tan^2\theta} + 2 + \tan\theta} \quad (4-51)$$

xy Plane
with $\theta = 45^\circ$



xz = yz Plane
with $\theta = 60^\circ$

The Geometric Isotropy of Crawford's 7D Body Diagonal Geometry
Figure 4-33

$$V_B = 1 - V_{Long} - V_{Lat} \quad (4-52)$$

Crawford's 7D Face Diagonal Geometry

The geometric isotropy of Crawford's 7D face diagonal geometry in the xy plane when the lattice parameter $a = b$, possesses no local minima at 45° . This phenomena occurs since the projection of the face diagonal yarns into the orthogonal planes is parallel either to one of the orthogonal axes. The function used to plot the geometric isotropy in the xy plane is:

$$V(\gamma) = V_x |\cos\gamma| + V_y |\sin\gamma| + \frac{V_F}{2} \cos\theta (|\sin\gamma| + |\cos\gamma|) \quad (4-53)$$

$$V_f = V_x + V_y + V_z + V_F \quad (4-54)$$

$$V_x = V_y = \frac{1}{2 + \tan\theta + \sqrt{1 + \tan^2\theta}} \quad (4-55)$$

$$V_z = \frac{\tan\theta}{2 + \tan\theta + \sqrt{1 + \tan^2\theta}} \quad (4-56)$$

$$V_F = 1 - V_x - V_y - V_z \quad (4-57)$$

Corresponding the geometric isotropy of the xz plane is:

$$V(\gamma) = V_x |\cos\gamma| + V_z |\sin\gamma| + \frac{V_F}{4} (|\cos(\theta+\gamma)| + |\cos(\theta-\gamma)|) \quad (4-58)$$

The geometric isotropy of the yz plane is:

$$V(\gamma) = V_y |\cos\gamma| + V_z |\sin\gamma| + \frac{V_F}{4} (|\cos(\theta+\gamma)| + |\cos(\theta-\gamma)|) \quad (4-59)$$

The geometric isotropy of the xz and the yz planes are equivalent if $a = b$. The factor that is divided into V_F differs from that of the xy plane since only one-half of the face diagonals are projected into either the xz or the yz planes. The different isotropy plots for this fiber architecture are shown in Figure. 4-34

Crawford's 11D Geometry

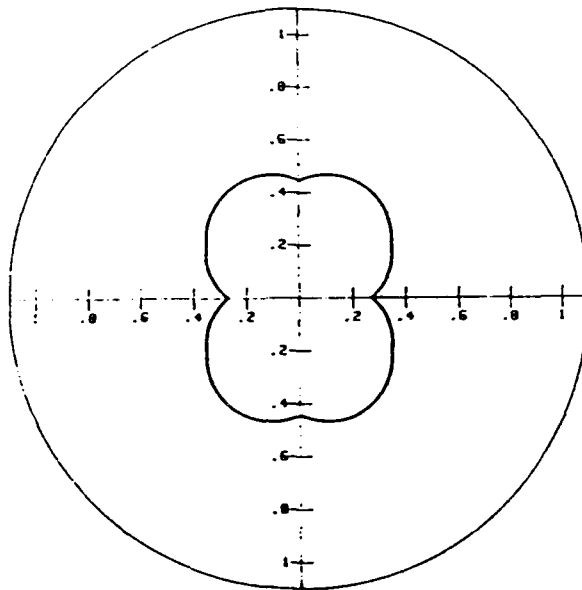
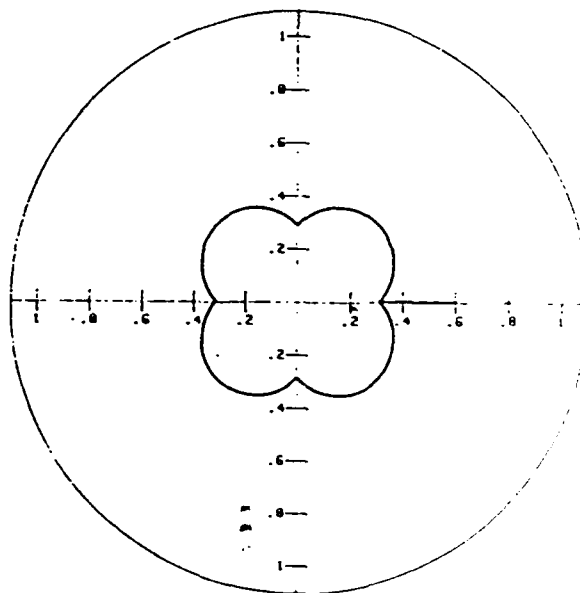
The xy plane isotropy of Crawford's 11D geometry possesses many local minima as a result presence of the body diagonal, face diagonal, and orthogonal yarns. Figure 4-35 plots the isotropy of this geometry for the xy and xz planes. Since a tetrahedral unit cell is assumed, the xz and the yz planes are equivalent. The function used to produce the xy geometric isotropy plot is:

$$\begin{aligned} V(\gamma) = & V_x |\cos\gamma| + V_y |\sin\gamma| + \frac{V_F}{2} \cos\theta (|\sin\gamma| + |\cos\gamma|) \\ & + \frac{V_B}{2} |\sin\phi| (|\cos(\theta-\gamma)| + |\cos(\theta+\gamma)|) \end{aligned} \quad (4-60)$$

with $\phi = \tan^{-1} \left(\frac{\sqrt{2}}{\tan\theta} \right)$

In the xz and the yz planes (the 12 planes):

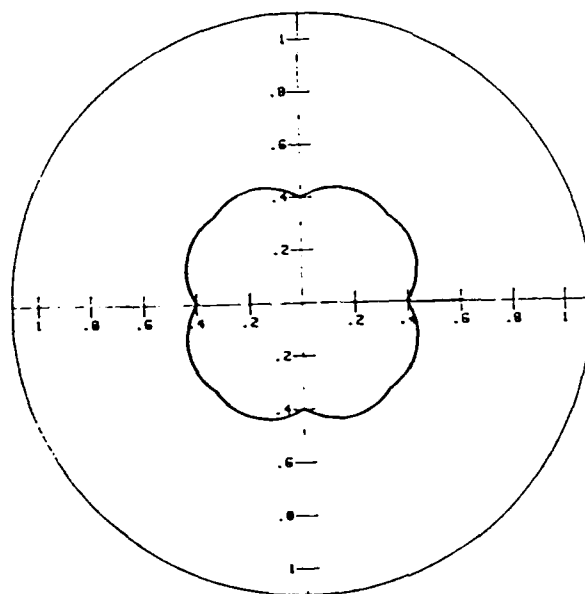
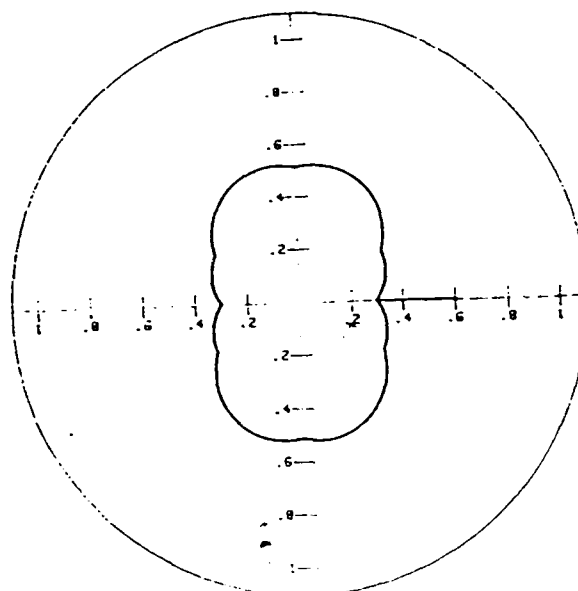
xy Plane
with $\theta = 45^\circ$



xz = yz Plane
with $\theta = 60^\circ$

The Geometric Isotropy of Crawford's 7D Face Diagonal Geometry
Figure 4-34

xz = yz Plane
with $\theta = 60^\circ$



xy Plane
with $\theta = 45^\circ$

The Geometric Isotropy of Crawford's 11D Geometry
Figure 4-35

$$V(\gamma) = V_1 |\cos \gamma| + V_2 |\sin \gamma| + \left(\frac{V_F}{4} + \frac{V_B}{2} |\sin \phi| \right) (|\cos(\theta - \gamma)| + |\cos(\theta + \gamma)|) \quad (4-61)$$

with $\phi = \tan^{-1} \left(\frac{\tan \theta}{\sqrt{2}} \right)$

The principal fiber orientation directions comprise the fiber volume fraction in the following manner:

$$V_f = V_x + V_y + V_z + V_F + V_B \quad (4-62)$$

$$V_x = V_y = \frac{1}{2 + \tan \theta + \sqrt{1 + \tan^2 \theta} + \sqrt{2 + \tan^2 \theta}} \quad (4-63)$$

$$V_z = \frac{\tan \theta}{2 + \tan \theta + \sqrt{1 + \tan^2 \theta} + \sqrt{2 + \tan^2 \theta}} \quad (4-64)$$

$$V_F = \frac{\sqrt{1 + \tan^2 \theta}}{2 + \tan \theta + \sqrt{1 + \tan^2 \theta} + \sqrt{2 + \tan^2 \theta}} \quad (4-65)$$

$$V_B = 1 - V_x - V_y - V_z - V_F \quad (4-66)$$

3D Weaves

The presence of the web yarns in the three dimensional weave geometry has the same effect on the geometric isotropy as the face diagonal yarns of the combined geometries. Each plane in this fiber architecture possesses a different geometric isotropy. The functions to generate these different

isotropies for a thick weave with two web yarns per unit cell are given below.

In the xy plane:

$$V(\gamma) = V_x |\cos \gamma| + V_y |\sin \gamma| + V_w |\cos \phi \cos \gamma| \quad (4-67)$$

In the xz plane:

$$V(\gamma) = V_x |\cos \gamma| + \frac{V}{2} (|\cos(\alpha + \gamma)| + |\cos(\alpha - \gamma)|) \quad (4-68)$$

In the yz plane:

$$V(\gamma) = V_y |\cos \gamma| \quad (4-69)$$

where:

$$\phi = \tan^{-1} \left(\frac{a}{c} \right) \quad (4-70)$$

a is defined in equation 4-18 and c is defined in 4-19.

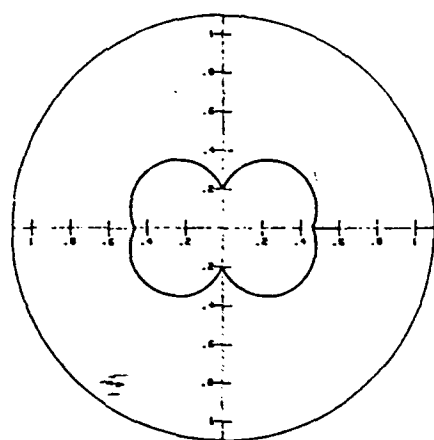
$$V_f = V_x + V_y + V_w \quad (4-71)$$

$$V_x = \frac{1 + \frac{1}{\sin \alpha}}{2 + \frac{1}{\sin \alpha} + \frac{1}{\cos \alpha} + 2L_w} \quad (4-72)$$

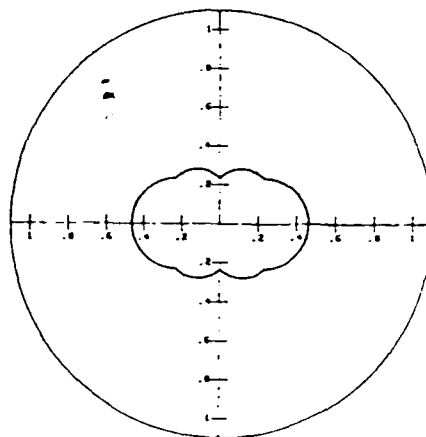
$$V_w = \frac{2L_w}{2 + \frac{1}{\sin \alpha} + \frac{1}{\cos \alpha} + 2L_w} \quad (4-73)$$

$$V_Y = 1 - V_x - V_w \quad (4-74)$$

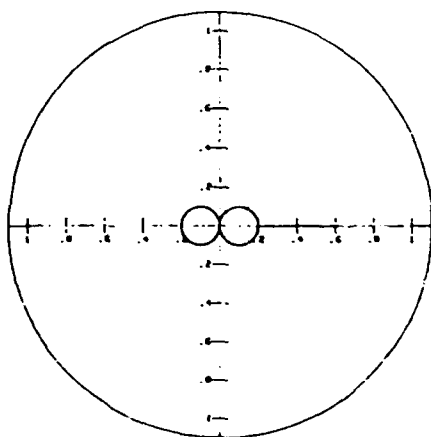
Figure 4-36 plots the geometric isotropy of these three planes. The yz plane possess an isotropy similar to that of the MWK in this plane. The xy and the xz planes possess minima at intervals of 45° as a result of the presence of the web yarns.



xy Plane



xz Plane



yz Plane

The Geometric Isotropy of a Three Dimensional Weave
Figure 4-36

CHAPTER FIVE

MECHANICAL MODELLING

The 3-D fibrous composite can be regarded as an assemblage of a finite number of individual structural cells. Each individual cell is the smallest representative volume taken from the fiber architectural system. It is then treated as a space structure with the endowed representative architecture, rather than a material with a set of effective continuum properties. The basic idea is to identify the unit cell's nodal supports, similar to the nodal points of a conventional finite element. By the introduction of the principle of virtual work in solid mechanics and structural analysis, the matrix $[k]$, the stiffness of the cell can be derived to relate nodal displacement vector to nodal forces for a cell.

Therefore, the key step in the formulation of the problem is the identification of the unit cell's nodal points. In this model, the yarns which pass by a node are considered as intersected each other and hence, can be treated as either pin-jointed two-force truss members or rigid connected frame members. With this postulate, the interaction at the yarn interlacing is not considered in this modelling. Thus, for instance, by

treating a unit cell specifically as a pin-jointed space truss , a 3-D truss finite element technique may be employed for the mechanistic analysis.

As for the matrix in a composite, it is usually used as load transfer medium. In order to include the effect of matrix, which is subjected to tension or compression under the deformation of yarns, the matrix is assumed to act as rod members. Each rod member connects the two ends of a given set of corresponding yarns in the unit cell. Hence, the matrix plays a role in restricting the free rotation and deformation of yarns.

The methodology of the finite element modelling is presented in the following. First of all, let a_{ij} represent the value of member deformation q_i caused by a unit nodal displacement r_j . The total value of each member deformation caused by all the nodal displacements may be written in the following matrix form:

$$\{q\} = [a] \{r\} \quad (5-1)$$

where $[a]$ is called the displacement transformation matrix which relates the member deformations to the nodal displacements. In other words, it represents the compatibility of displacements of a unit cell.

The next step is to establish the force-displacement relationship within the unit cell. The member force-deformation relationship can be written as:

$$[Q] = [K'] \{q\} \quad (5-2)$$

where $[K']$ is the stiffness matrix of a member

The principle of virtual work states that the work done on a system by the external forces equals the increase in strain energy stored in the system. Here, the nodal forces can be considered as the external forces of the unit cell. Therefore, if $\{R\}$ represents the nodal force vector, it follows that

$$\{\delta r\}^T \{R\} = \{\delta q\}^T \{Q\} \quad (5-3)$$

where $\{\delta r\}$ and $\{\delta q\}$ are virtual displacement and deformation, respectively. From Equations (5-1) and (5-2), the following equations can be derived through matrix manipulation:

$$\{R\} = [K] \{r\} \quad (5-4)$$

where: $\{R\}$ = nodal forces

$[K] = [a]^T [K'] [a]$ = stiffness matrix of the unit cell

$\{r\}$ = nodal displacements

Using Equation (5-4), the nodal force and the nodal displacements of a unit cell are related by the stiffness matrix of the unit cell.

In the above mentioned methodology, the stiffness matrix of a unit cell was formalized by use of the compatibility matrix $[A]$ and the concept of principle of virtual work. With this approach, the entire stiffness matrix $[K]$ was assembled by the triple matrix multiplication given as Eq.(5-4). For truss structure or simple fiber architecture of a unit cell, the compatibility matrix can be obtained without rigorous calculations. However, when the fiber architecture becomes complicated or a frame unit cell is being analyzed, it involves a large compatibility matrix where many of the elements are not easy to be evaluated correctly. From the computer programming points of view, neither the generation of this matrix $[A]$ nor the multiplication process for $[K]$ matrix assembly would be suitable to be explicitly laid out. A better methodology which combines the ideal of previously mentioned approaches and computer-oriented techniques is presented in the following, which is known as the *Direct Stiffness Method*.

In this method, the end displacements of each member are treated with respect to structural (global) coordinates. In this way all of the geometric transformation will be handled locally, and the stiffness matrix can be assembled by direct addition instead of by matrix multiplication. Thus, the assembly of the joint stiffness matrix may be stated as

$$K = \sum_{i=1}^n K_i \quad (5-5)$$

where n is total number of the members, K_i is the i -th member stiffness matrix with end-forces and displacements in the directions of structural coordinate. Therefore, the member stiffness matrix should firstly be obtained with respect to the member axes, and then transformed in reference to the structural coordinates.

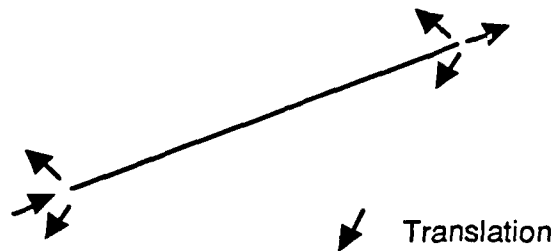
The member stiffness matrix is obtained by a unit displacement method. The unit displacements are considered to be induced one at a time while all other end displacements are retained at zero. The unknown displacements at each joint of a truss consists of three components, namely, the x , y and z components of the joint translations. The unknown displacements at each joint of a frame consists of six components, namely, the x , y and z components of the joint translations and the x , y and z components of the joint rotations.

The member stiffness matrices of the space truss and space frame in member coordinates are given in Figure 5-1 and Figure 5-2, respectively. The elements of the j th column in the matrices represent the forces required to hold the unit displacement in the j th direction, or, each column in the matrix represents the forces caused by one of the unit displacements.

The present modelling will consider the high symmetry composites as frame structures. In this sense, the axial, flexural and torsional stresses and deformations of a member may be induced under tensile load. In other words, the modelling takes into consideration of axial, bending and torsion of yarns. In general case, if the member axes are not coincident with structural axes, a rotation transformation matrix should be performed to obtain the member stiffness in structural coordinates.

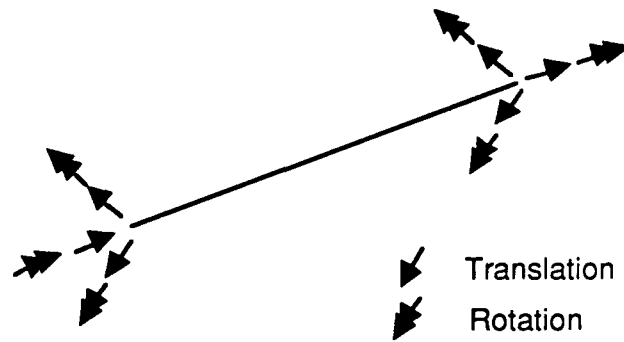
Let the spatial coordinate system of a prismatic member be given in Figure 5-3. The direction cosines r_i , s_i and t_i relate the structure axes (X_s, Y_s, Z_s) to the member axes (X_m, Y_m, Z_m). The coordinate transformation between X_m, Y_m, Z_m and X_s, Y_s, Z_s may be written as

$$\begin{Bmatrix} X_m \\ Y_m \\ Z_m \end{Bmatrix} = \begin{bmatrix} r_1 & s_1 & t_1 \\ r_2 & s_2 & t_2 \\ r_3 & s_3 & t_3 \end{bmatrix} \begin{Bmatrix} X_s \\ Y_s \\ Z_s \end{Bmatrix}$$



$$[K_m] = \begin{bmatrix} EA/L & 0 & 0 & -EA/L & 0 & 0 \\ 0 & 0 & 0 & 0 & 0 & 0 \\ 0 & 0 & 0 & 0 & 0 & 0 \\ -EA/L & 0 & 0 & EA/L & 0 & 0 \\ 0 & 0 & 0 & 0 & 0 & 0 \\ 0 & 0 & 0 & 0 & 0 & 0 \end{bmatrix}$$

Figure 5-1. Stiffness Matrix of a 3-D Truss Member
in Member Coordinates.



$ \begin{bmatrix} KP & & & & & & & & & & & \\ 0 & KS & & & & & & & & & & \\ 0 & 0 & KS & & & & & & & & & \\ 0 & 0 & 0 & KG & & & & & & & & \\ 0 & 0 & -KF & 0 & 2KM & & & & & & & \\ 0 & KF & 0 & 0 & 0 & 2KM & & & & & & \\ -KP & 0 & 0 & 0 & 0 & 0 & KP & & & & & \\ 0 & -KS & 0 & 0 & 0 & -KF & 0 & KS & & & & \\ 0 & 0 & -KS & 0 & KF & 0 & 0 & 0 & KS & & & \\ 0 & 0 & 0 & -KG & 0 & 0 & 0 & 0 & 0 & KG & & \\ 0 & 0 & -KF & 0 & KM & 0 & 0 & 0 & KF & 0 & 2KM & \\ 0 & KF & 0 & 0 & 0 & KM & 0 & -KF & 0 & 0 & 0 & 2KM \end{bmatrix} $											
SYMMETRY											

$$KP = EA/L ; KS = 12EI/L^3 ; KF = 6EI/L^2 ; KM = 2EI/L ; KG = GJ/L$$

Figure 5-2. Stiffness Matrix of a Member in a Unit Cell in Member Coordinates.

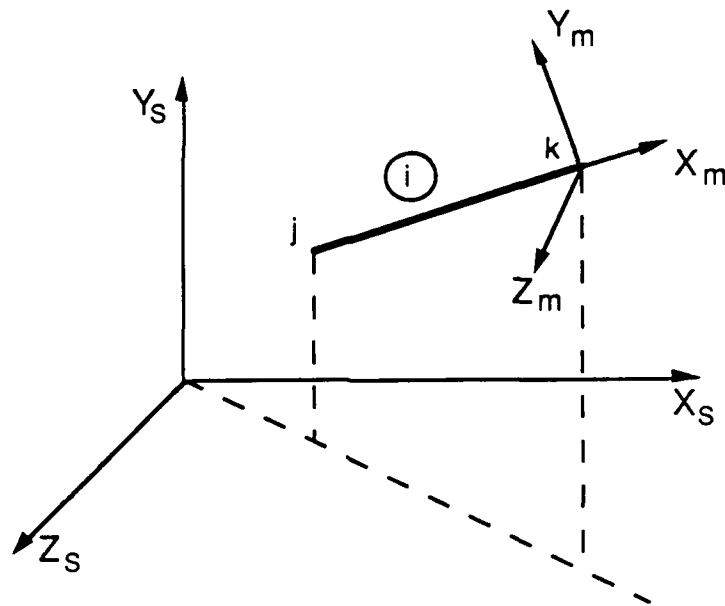


Figure 5-3. A Prismatic Member in the Spatial Coordinate.

or in the concise matrix from:

$$\{ \underline{X}_m \} = [T] \{ \underline{X}_s \} \quad (5-6)$$

The first row of matrix $[T]$ relates the structure axes to the X_m axis, and can be written as:

$$r_1 = \cos (X_m, X_s)$$

$$s_1 = \cos (X_m, Y_s)$$

$$t_1 = \cos (X_m, Z_s)$$

Similar formulations are derived for r_2, s_2, t_2 and r_3, s_3, t_3 .

If the displacements or forces are expressed in two different coordinate systems, the coordinate transformation is used as the transformation matrix between the two coordinates. For displacements, the relation is as following:

$$\{ D_m \} = [R_T] \{ D_s \} \quad (5-7)$$

and for forces

$$\{ F_m \} = [R_T] \{ F_s \} \quad (5-8)$$

where $\{ D_m \}$ and $\{ F_m \}$ represent the properties in member axes and $\{ D_s \}$ and $\{ F_s \}$ stand for the properties in structural axes. The transformation matrix $[R_T]$ is orthogonal, which consists of directional cosine matrix $[T]$ in diagonal terms. For a truss, the transformation matrix $[R_T]$ is

$$[R_T] = \begin{bmatrix} T & O \\ O & T \end{bmatrix}$$

and for a frame , the transformation matrix $[R_T]$ is

$$[R_T] = \begin{bmatrix} T & O & O & O \\ O & T & O & O \\ O & O & T & O \\ O & O & O & T \end{bmatrix}$$

Let $[K_m]$ and $[K_s]$ be the stiffness matrix in member axes and structural axes, respectively. Then the forces-displacements relationships take the following forms:

$$\{F_m\} = [K_m] \{D_m\} \quad (5-9)$$

and

$$\{F_s\} = [K_s] \{D_s\} \quad (5-10)$$

Substituting Equ.(5-7) and Equ.(5-8) into Equ.(5-9), it yields

$$\{F_s\} = [R_T]^T [K_m] [R_T] \{D_s\} \quad (5-11)$$

Compare equ(5-10) and equ(5-11), we have

$$[K_s] = [R_T]^T [K_m] [R_T] \quad (5-12)$$

Consider a typical space member i with two ends j and k , shown in Figure 5-4 with axes X_s , Y_s and Z_s being parallel to the structural axes.

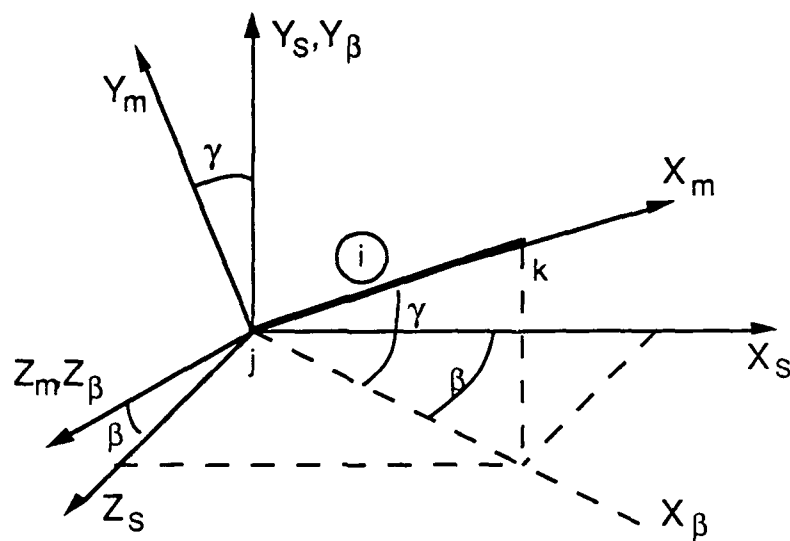


Figure 5-4. Rotation of Axes of a Space Member.

The X_m is taken as the longitudinal axis of the member while the Y_m and Z_m directions remain to be determined. Many ways can be selected for determining the directions of the Y_m and Z_m axes. A convenient way is to take the Z_m axes as being lying in the X_s - Z_s plane, as shown in the Figure 5-4. Once the X_m and Z_m axes are determined, the Y_m axis is located automatically by right-handed rule.

When the member axes are determined in the above described manner, there is no confusion about their orientations except in the case of vertical member. In this case, the position of Z_m axis in the horizontal plane is not uniquely defined. The additional restriction will be made so that the Z_m axis is always taken to be the Z_s axis. Two possibilities for this case are shown in Figure 5-5, concerning vector from initial end to final end.

The transformation from the structure axes to the member axes may be considered to take two rotation steps. The first rotation is X_s and Z_s axes rotate an angle β about Y_s axis. This rotation moves the X_s axis to the position denoted as X_β and moves the Z_s axis to the final position denoted as Z_β (same as Z_m). The transformation formula is written as follows:

$$\{ \underline{X}_\beta \} = [T_\beta] \{ \underline{X}_s \} \quad (5-13)$$

where

$$[T_\beta] = \begin{bmatrix} \cos\beta & 0 & \sin\beta \\ 0 & 1 & 0 \\ -\sin\beta & 0 & \cos\beta \end{bmatrix}$$

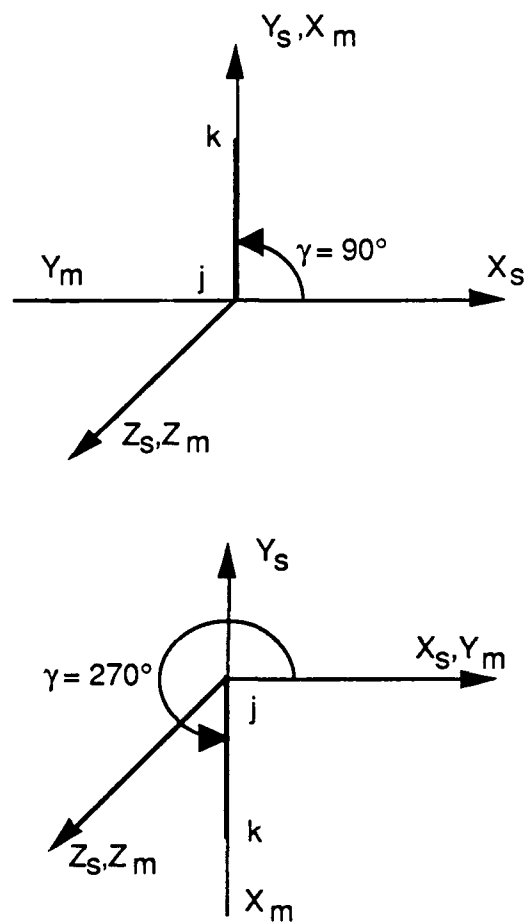


Figure 5-5. Two Possibilities of the Vertical Member.

For the second rotation, X_β and Y_β rotate an angle γ about Z_β axis. This rotation moves the X_β and Y_β axes to the final positions X_m and Y_m . The transformation is expressed as:

$$\{ \underline{X}_m \} = [T_\gamma] \{ \underline{X}_\beta \} \quad (5-14)$$

where

$$[T_\gamma] = \begin{bmatrix} \cos\gamma & \sin\gamma & 0 \\ -\sin\gamma & \cos\gamma & 0 \\ 0 & 0 & 1 \end{bmatrix}$$

Substituting Equ.(5-13) into Equ.(5-14) yields

$$\{ \underline{X}_m \} = [T_\gamma] [T_\beta] \{ \underline{X}_s \} \quad (5-15)$$

Comparing above equation with Equ(5-6), we have the rotation matrix

$$[T] = [T_\gamma] [T_\beta] \quad (5-16)$$

Let (X_j, Y_j, Z_j) and (X_k, Y_k, Z_k) be the coordinates of initial end and terminal end of the member, respectively. Then the directional cosines that relate this structure axes to X_m axis is obvious as follows:

$$r_1 = r = \frac{X_k - X_j}{L}$$

$$s_1 = s = \frac{Y_k - Y_j}{L}$$

$$t_1 = t = \frac{Z_k - Z_j}{L}$$

where L is the length of member, can be obtained from the coordinates of two ends. Let q be equal to $(r^2 + t^2)^{1/2}$, and the rotation matrix in equation (5-13) and (5-14) can be expressed as follows:

$$[T_B] = \begin{bmatrix} \frac{r}{q} & 0 & \frac{t}{q} \\ 0 & 1 & 0 \\ -\frac{t}{q} & 0 & \frac{r}{q} \end{bmatrix}$$

and

$$[T_\gamma] = \begin{bmatrix} q & s & 0 \\ -s & q & 0 \\ 0 & 0 & 1 \end{bmatrix}$$

Thus, the rotation matrix for transformation between the member axes and the structure axes takes the following form:

$$[T] = [T_\gamma][T_B] = \begin{bmatrix} \frac{r}{q} & s & \frac{t}{q} \\ -\frac{r \cdot s}{q} & q & -\frac{s \cdot t}{q} \\ -\frac{t}{q} & 0 & \frac{r}{q} \end{bmatrix} \quad (5-17)$$

The above rotation matrix $[T]$ is valid for all positions of the member except when the member is vertical. In the case of a vertical member, the directional cosines of the member axes with respect to the structure axes can be determined by inspection. Thus the rotation matrix is seen to be

$$[T_{\text{vert}}] = \begin{bmatrix} 0 & s & 0 \\ -s & 0 & 0 \\ 0 & 0 & 1 \end{bmatrix} \quad (5-18)$$

Taking the appropriate rotation matrix ,either Equ(5-17) or Equ(5-18), to acquire the desired rotation transformation matrix $[R_T]$, the member stiffness matrix in the structure axes is obtained. Then, assembly of the contributions from each member to a joint, or, a node in finite element procedure, yields the stiffness matrix of a unit cell as expressed in equ(5-5).

With the stiffness matrix of a unit cell being known, for a structural shape which consists of a large number of unit cells, a system of equations for the total structural shape can be assembled using the individual cell relations following the finite element methodology. From the solution of the equations, the stress distribution and deformation of the entire structure under applied load can be calculated and analyzed.

NUMERICAL SIMULATIONS

The FCM was implemented by the use of computer simulation. With basic parameters in a unit cell, such as yarn elastic modulus, fiber volume fraction, yarn orientation and unit cell dimension fully characterized, the applicability of the FCM to predict the structural response of composites will be demonstrated experimentally.

Finite Element Implementation of FCM

The Finite Cell Model just described has been implemented into finite element program. The basic ideas of the Finite Cell Model are laid out as a flow chart as shown in Figure 5-6. Figure 5-7 shows the more detailed computational flow of forming stiffness matrix of a unit cell. By entering the basic parameters for a unit cell and fiber/matrix properties to the program, the load-deformation and elastic properties such as elastic modulus and Poisson's ratio of the composite can be determined.

In addition, the results of structural analysis from separate studies show that the truss unit cell is not a stable structure. Therefore, the frame model is carried out in this numerical analysis.

The high symmetry composite material was proposed for structures with high compression capability. The primary idea is to put high modulus spheres into fiber reinforced materials. The fiber architecture discussed in this report will be a X-Y-Z type of structure. The spheres are in contact with each other and are confined by reinforced fibers. Ceramic material will be used as matrix for high temperature environment. The unit cell of the high symmetry composite is illustrated in Figure 5-8. From the arrangement of fibers and spheres in this figure, the unit cell dimension can be determined as the diameter of each individual sphere.

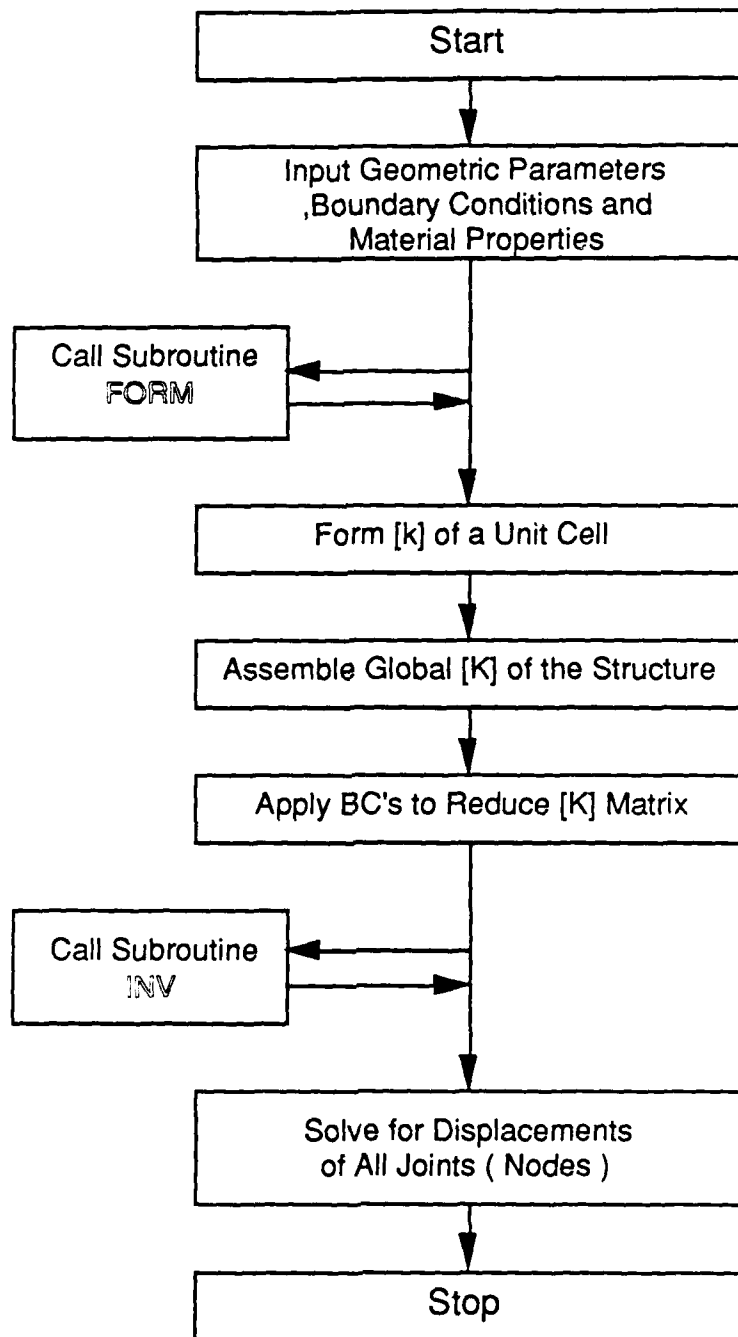


Figure 5-6. The Flowchart of FCM Finite Element Program.

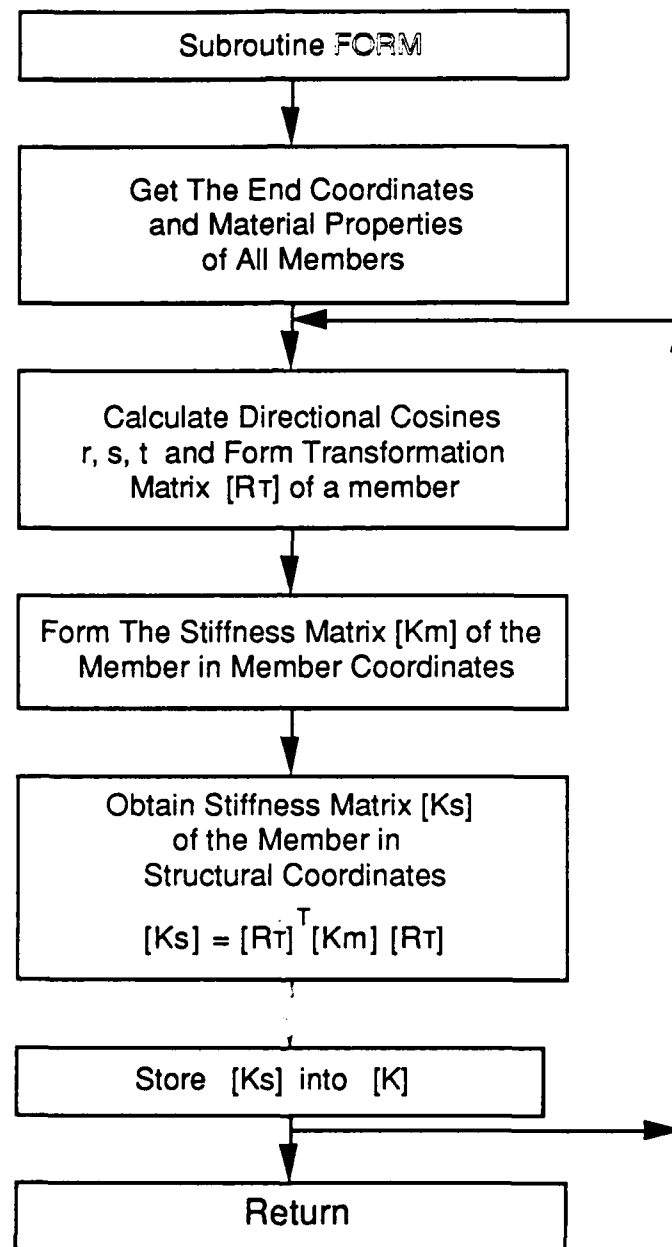


Figure 5-7. The Flowchart of Stiffness Matrix Formulation

In order to apply the finite cell modelling to the unit cell of high symmetry composites, the representation of the three constituents of the composites, i.e., matrix, fiber and spheres, need to be discussed. Consider a composite with the volume fraction of matrix, fibers and spheres being V_m , V_f and V_s , respectively. The unit cell dimension is $H \times W \times T$. Since the dimensions of a unit cell are considered to be the center lines of members of the unit cell, part of each bar lies outside the unit cell in real case. An averaging method for the determination of the cross-section areas of the bars was used. Assuming that each type of bars have the same cross-sectional area. To simplify the analysis, assume that the yarns travelling in each direction can be combined into four yarns in that direction. The four yarns are assumed to travel along four corners in that direction. In this sense, the cross-sectional area of the fiber-bars is obtained by the following formula:

$$A_f = V_f HWT / 4(H+W+T)$$

For the representation of the sphere in a unit cell, the effective sphere-bar with certain cross-section area will be assumed. The modulus of the sphere-bar is the same as the modulus of the sphere. The cross-sectional area of the sphere-bar is assumed to take the following form:

$$A_s = V_s HWT / 4(H+W+T)$$

As for the matrix, which is used to transfer load, it can be represented as bars along the three orthogonal axes. The cross-sectional area of the matrix-bars is calculated by use of the following formula:

$$A_m = V_m HWT / 4(H+W+T)$$

In the present case, the unit cell can be treated as a cube. Hence,

$$H = W = T$$

, or, the length of each bar is the same in present study. The cross-sectional area of fiber-bars, sphere-bars and matrix-bars can be rewritten as the following form:

$$A_i = V_i H^3 / 12H = V_i H^2 / 12$$

where i could be a fiber-bar, sphere-bar or matrix-bar.

From the above discussions, the cross-sectional area and length of each bar, including the matrix-bar, fiber-bar and sphere-bar, are formulated. The matrix-bar, fiber-bar and sphere-bar are modelled to travel along each edge of a cubic unit cell. For the analysis purpose, the three bars need to be combined into a composite bar with individual contribution of the three bars. The resultant properties of the composite bar is obtained rule of mixture among the three bars. For the cross-sectional area of the composite bar, A_c , it should be the sum of the cross-sectional areas of the three bars, or,

$$A_c = A_f + A_m + A_s$$

For the modulus of the composite bar, E_c , it can be obtained in the following formula:

$$A_c E_c = E_f A_f + E_m A_m + E_s A_s$$

and the shear modulus of the composite bar is

$$1/G_c = V_f/G_f + V_m/G_m + V_s/G_s$$

For a sphere in a X-Y-Z architected unit cell, the volume of the sphere is obtained by the following formula:

$$D_s = (4/3)\pi(H/2)^3$$

Thus, regardless of the dimension of the unit cell, the volume fraction of the sphere in a unit cell is:

$$V_s = D_s / H^3 = \pi/6 = 52.3\%$$

Therefore, if the fiber volume fraction is 20%, the volume fraction of matrix is 27.7%.

The spheres used for reinforcing the high symmetry composites are made of alumina with modulus being 56 Msi(386 GPa). The fibers selected for this study are Nicalon and FP-5 fibers, while the matrices are SiC, alumina and LAS-III. The modulus of the materials are listed in the following table:

<u>FIBER</u>		<u>MATRIX</u>		
FP-5	Nicalon	SiC	LAS-III	Alumina
23.3 Msi	28.5 Msi	12.3 Msi	56 Msi	42 Msi
(161 GPa)	(197 GPa)	(84.8 GPa)	(386 GPa)	(290 GPa)

In a unit cell with dimension of .2"x.2"x.2", the cross-sectional areas of the fiber, matrix, sphere and composite bars are listed in the following table:

Vf	Fiber	Matrix	Sphere	Composite
(%)	(in ²)	(in ²)	(in ²)	(in ²)
20	.000667	.000923	.001743	.003333

By inputting the above moduli, cross-sectional areas and unit cell dimension to the Finite Cell program, the response of the unit cell structure under compression can be found. Figure 5-9 shows the loading condition and boundary conditions of a specimen. The applied load was divided into several steps on account of the possible nonlinear load-deformation behavior due to geometrical conformation. In order to examine the effect of matrix reinforced with alumina spheres, the predictions of the composites without spheres are performed as well. The comparison of the stress-strain curves between various combinations of fibers, matrices and spheres are shown in Figure 5-10 to 5-13. From the figures, the high symmetry composites with sphere reinforcements have higher Young's modulus.

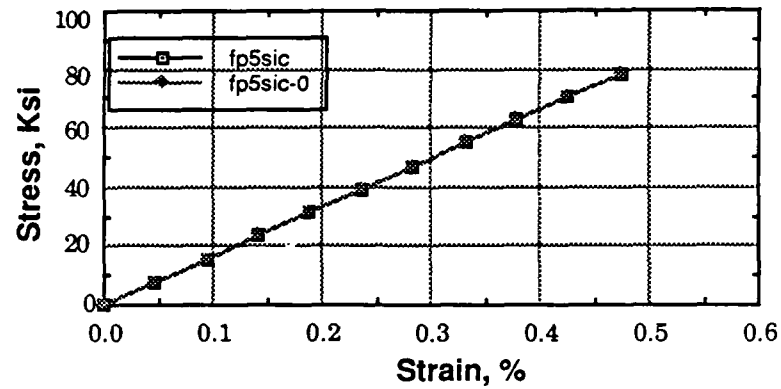


Figure 5-10. Compressive Stress-Strain Relationship of FP/SiC Composites with/without Sphere Reinforcement.

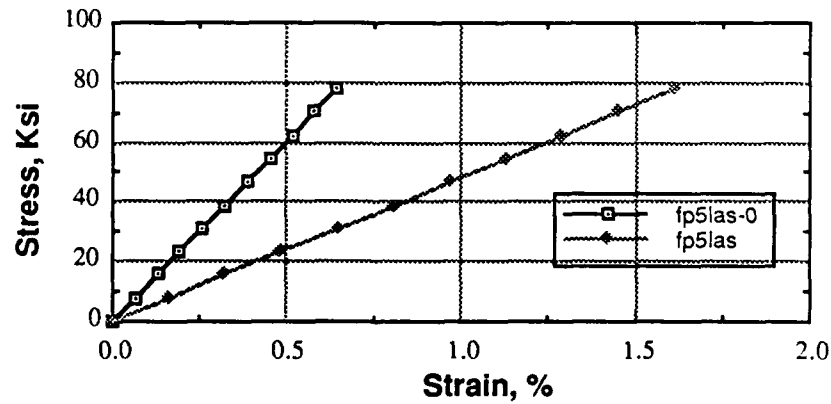


Figure 5-11. Compressive Stress-Strain Relationship of FP/LAS Composites with/without Sphere Reinforcement.

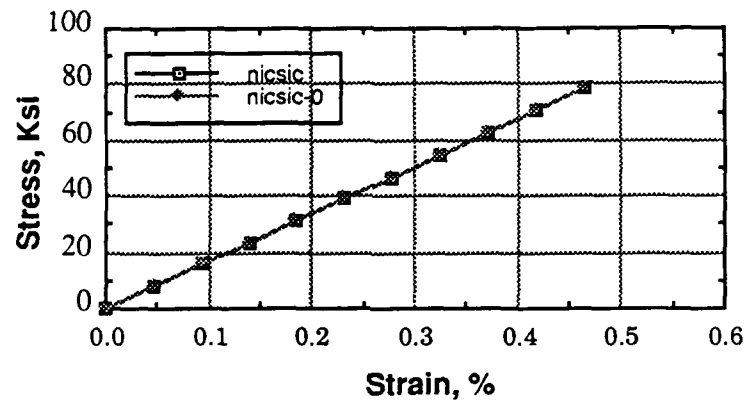


Figure 5-12. Compressive Stress-Strain Relationship of Nic/SiC Composites with/without Sphere Reinforcement.

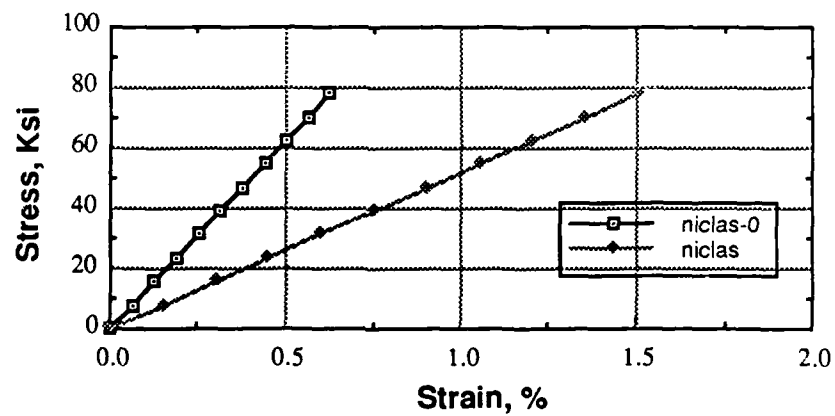


Figure 5-13. Compressive Stress-Strain Relationship of Nic/LAS Composites with/without Sphere Reinforcement.

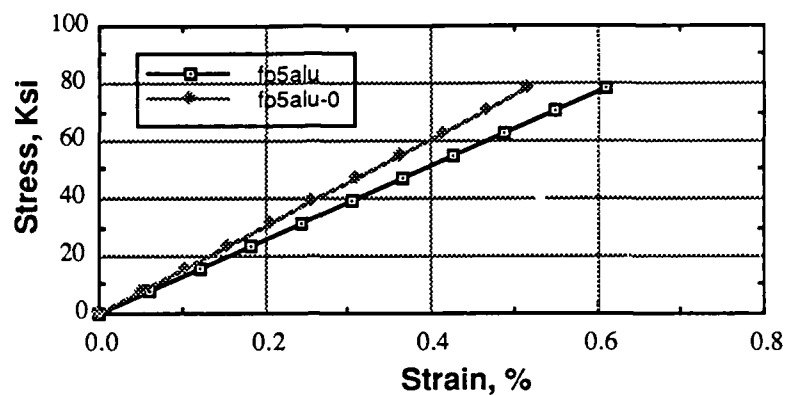


Figure 5-14. Compressive Stress-Strain Relationship of FP/Alu Composites with/without Sphere Reinforcement.

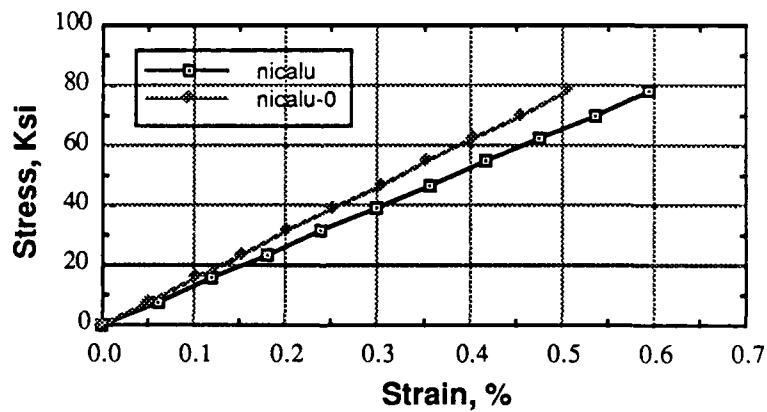


Figure 5-15. Compressive Stress-Strain Relationship of Nic/Alu Composites with/without Sphere Reinforcement.

To summarize from Figure 5-10 through Figure 5-15, the stiffness of the LAS- and Alumina-matrix composites with sphere reinforcement showed a higher value than the LAS and Alumina -matrix composites without sphere reinforcement. However, in the case of the SiC-matrix composites, no significant improvement of stiffness was shown. The reason is that the modulus of embedded sphere is the same as that of the matrix SiC. Therefore, the reinforcing effect is not seen. Hence, the addition of high modulus spheres into softer matrix composites shows improved modulus.

The other method to account for the effect of spheres in the matrix is to treat the matrix as particulate-filled system. Thus, the effective properties of the matrix can be described by Kerner's equation, which takes the following form for shear modulus:

$$G_{me} = G_m \left[\frac{\frac{V_s G_s}{(7-5v_m)G_m + (8-10v_m)G_s} + \frac{V_m}{15(1-v_m)}}{\frac{V_s G_m}{(7-5v_m)G_m + (8-10v_m)G_s} + \frac{V_m}{15(1-v_m)}} \right]$$

where V represents volume fraction, and subscripts m and s represent matrix and sphere phases, respectively. Conversion of shear to tensile modulus may be made by using the isotropic relation

$$E_{me} = 2G_{me}(1+v)$$

where the Poisson's ratio, ν , is given by a rule-of-mixture expression

$$\nu = \nu_m V_m + \nu_s V_s$$

With this consideration, the cross-sectional area of the fiber-bars is calculated by the previous formula:

$$A_f = V_f HWT / 4(H+W+T)$$

As for the sphere-filled matrix, the cross-sectional area of the effective matrix-bars is calculated by use of the following formula:

$$A_{me} = (V_m + V_s)HWT / 4(H+W+T)$$

The resultant properties of the composite bar is obtained by rule of mixture among the two bars. For the cross-sectional area of the composite bar, A_c , it should be the sum of the cross-sectional areas of the three bars, or,

$$A_c = A_f + A_{me}$$

For the modulus of the composite bar, E_c , it can be obtained in the following formula:

$$A_c E_c = E_f A_f + E_{me} A_{me}$$

and the shear modulus of the composite bar is

$$1/G_c = V_f/G_f + (V_s + V_m)/G_{me}$$

By inputting the effective moduli, cross-sectional areas and unit cell dimension to the Finite Cell program, the response of the unit cell structure under compression can be found.

Figure 5-16 and Figure 5-17 show the effect of sphere volume fraction and fiber volume fraction, respectively.

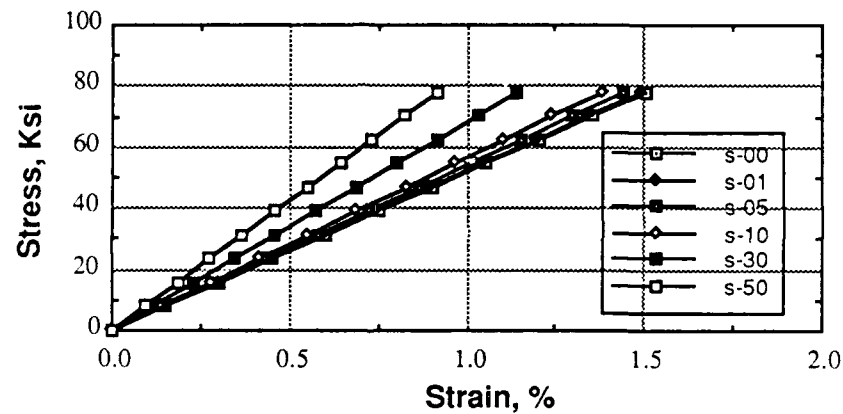


Figure 5-16. The effect of sphere volume fraction on Compressive Stress-Strain Relationship of Nic/LAS Composites.

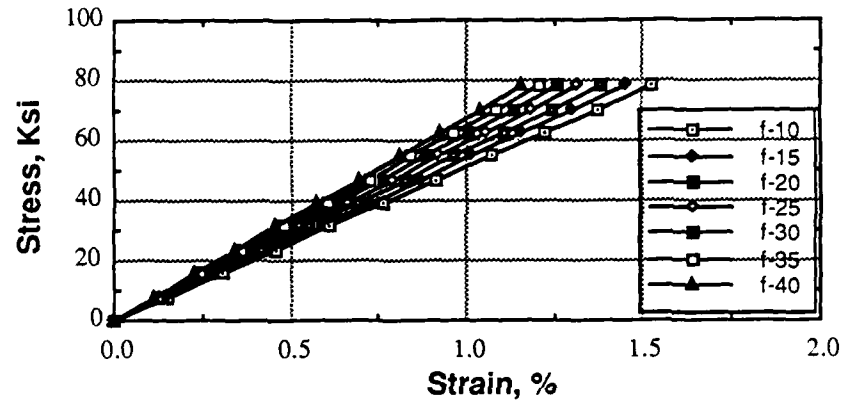


Figure 5-17. The effect of sphere volume fraction on Compressive Stress-Strain Relationship of Nic/LAS Composites.

In Finite Cell Modelling, the basic assumption on material-bar representations simplifies the analysis of high symmetry composites. The treatment of composite bar by use of the rule-of-mixture stems from the complexity of the interaction between fiber, sphere and matrix. The actual composite behavior around sphere surface and sphere-fiber contact points is very complicated. In addition to compressive stress, the shear stress, which transfers the load from sphere and fiber to matrix, takes place. The neglect of the shear stress may result in an inaccurate prediction of elastic behavior. But, the degree of inaccuracy is not under consideration in Finite Cell Modelling. The predictions should be evaluated by experimental results. Further studies on this model to investigate the interaction between fiber and matrix have to be conducted. The load transfer mechanism between fibers, spheres and matrix as well as the effect of fiber architecture in a unit cell needs to be explored. This may lead to a 3-D solid element modelling on the unit cell of a high symmetry composite.

A 3-D finite element code for analyzing the deformation of hollow spheres was developed and is discussed in the following section. This program can be integrated with finite cell modelling to further investigate the the effect of fiber/sphere interaction.

CHAPTER SIX

FABRICATION OF HIGH SYMMETRY COMPOSITES

In order to implement the concept of high symmetry structures, a method for the creation of a 3-D fiber network and the placement of the sphere was developed.

The hexagonal braiding machine (HBM) consists of the following components:

- * motion motor array (MMA)
- * locating system (LS)
- * sphere feeding mechanism (SFM)
- * hexagonal drivers (HD)
- * sphere tank (ST)
- * carriers (C)
- * take down mechanism (TDM)

As illustrated in Figure 6-1, the MMA consists of step motors and control units connected directly to a computer which offers precise control of

independent motion for each yarn carrier. Figure 6-1a is a schematic illustration of the hexagonal braiding machine (HBM). The motion motor array (MMA) is the principal driver which propels the carriers in a hexagonal pattern to create various fibrous networks that can range from orthogonal to the close-to-cubic 3-D quadraxial structure. The locating system along with sphere feeding mechanism meter the spheres into the fibrous network after each braiding operation. These operations are followed by a take-down motion which collects the 3-D fiber/sphere assembly into a storage package for composite fabrication.

To facilitate the fabrication process and assure reproducibility and numerical control system is organized and implemented through a computer. The control logic and data flow are shown in Figure 6-2. The resulting structures which can be created by the HBM are illustrated in Figure 6-3. In Figure 6-4 a model of the high symmetry system is shown.

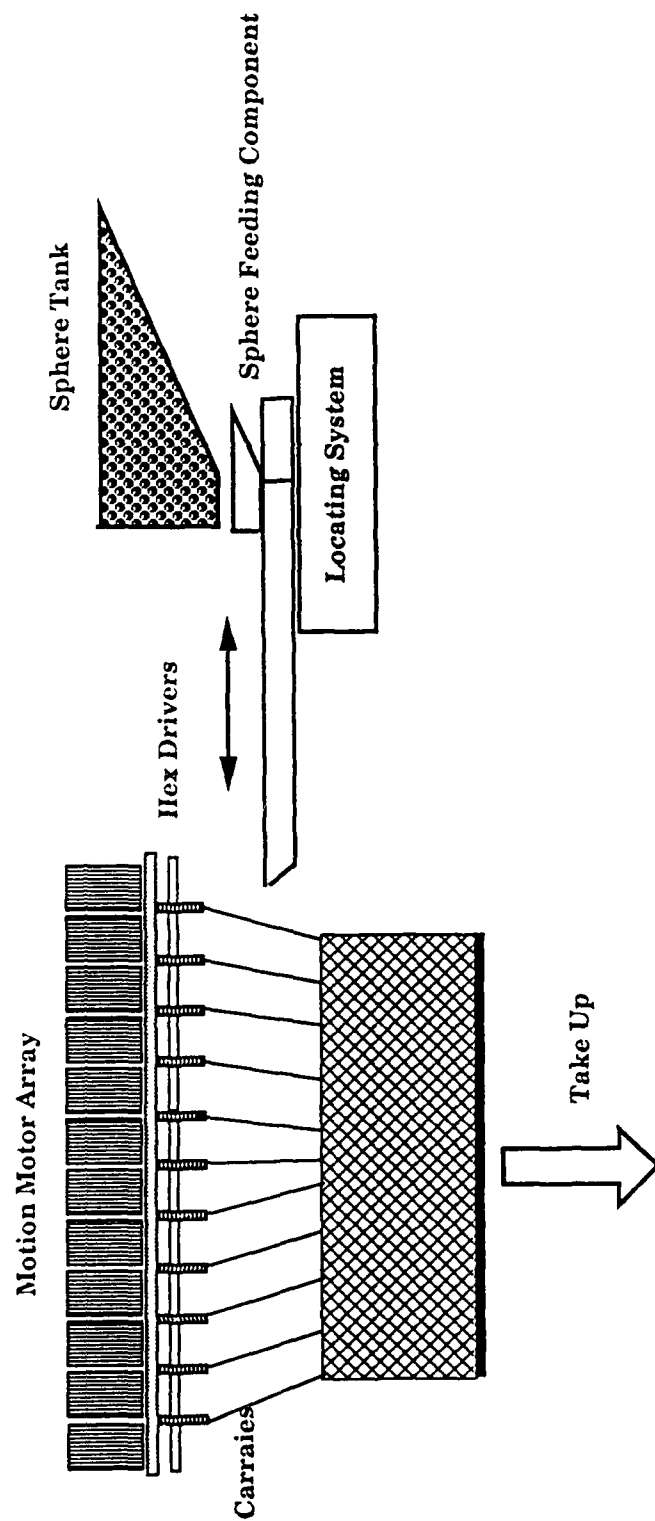


Figure 6-1a Schematic Illustration of the Hexagonal Braiding Machine.

Basic Cellular Loom Module

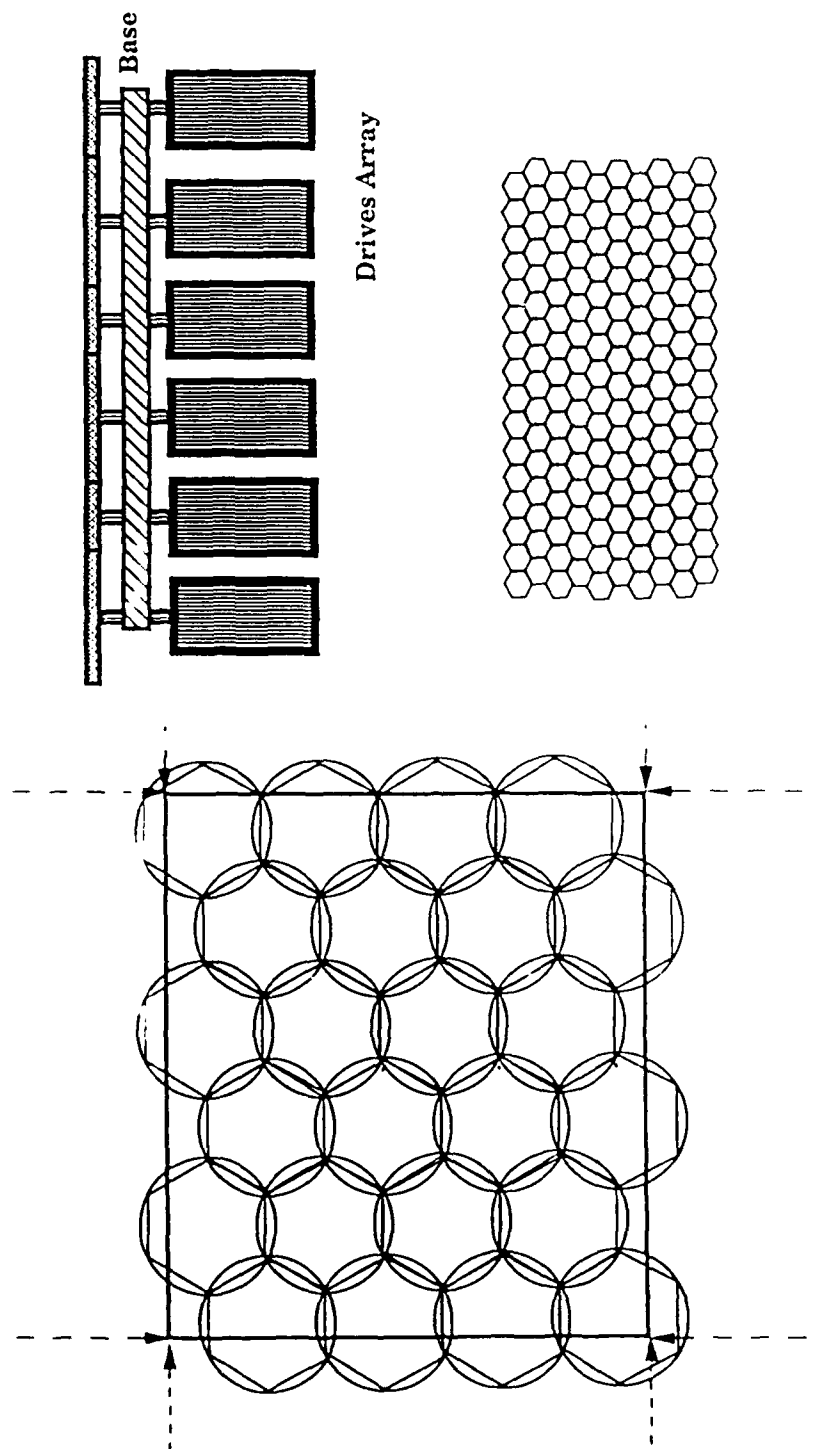
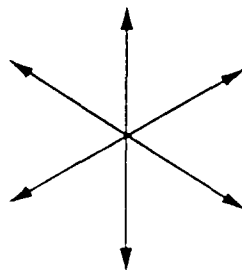
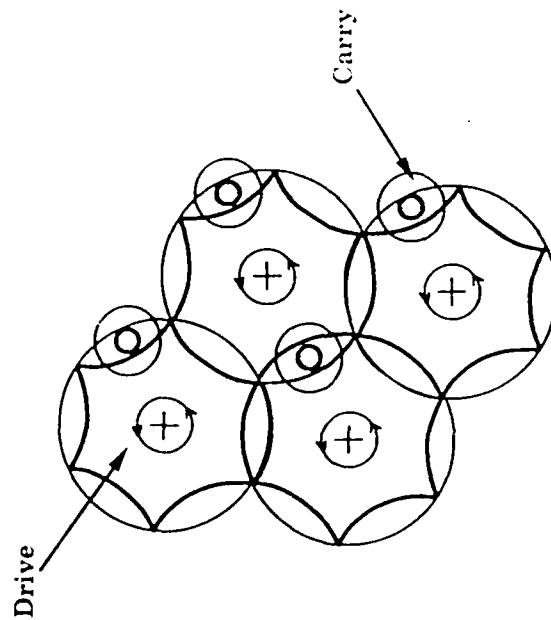


Figure 6-1b

Hexagonal Drive



- Individual Control
- Six Possible Structure/Braiding Orientations

Figure 6-1c

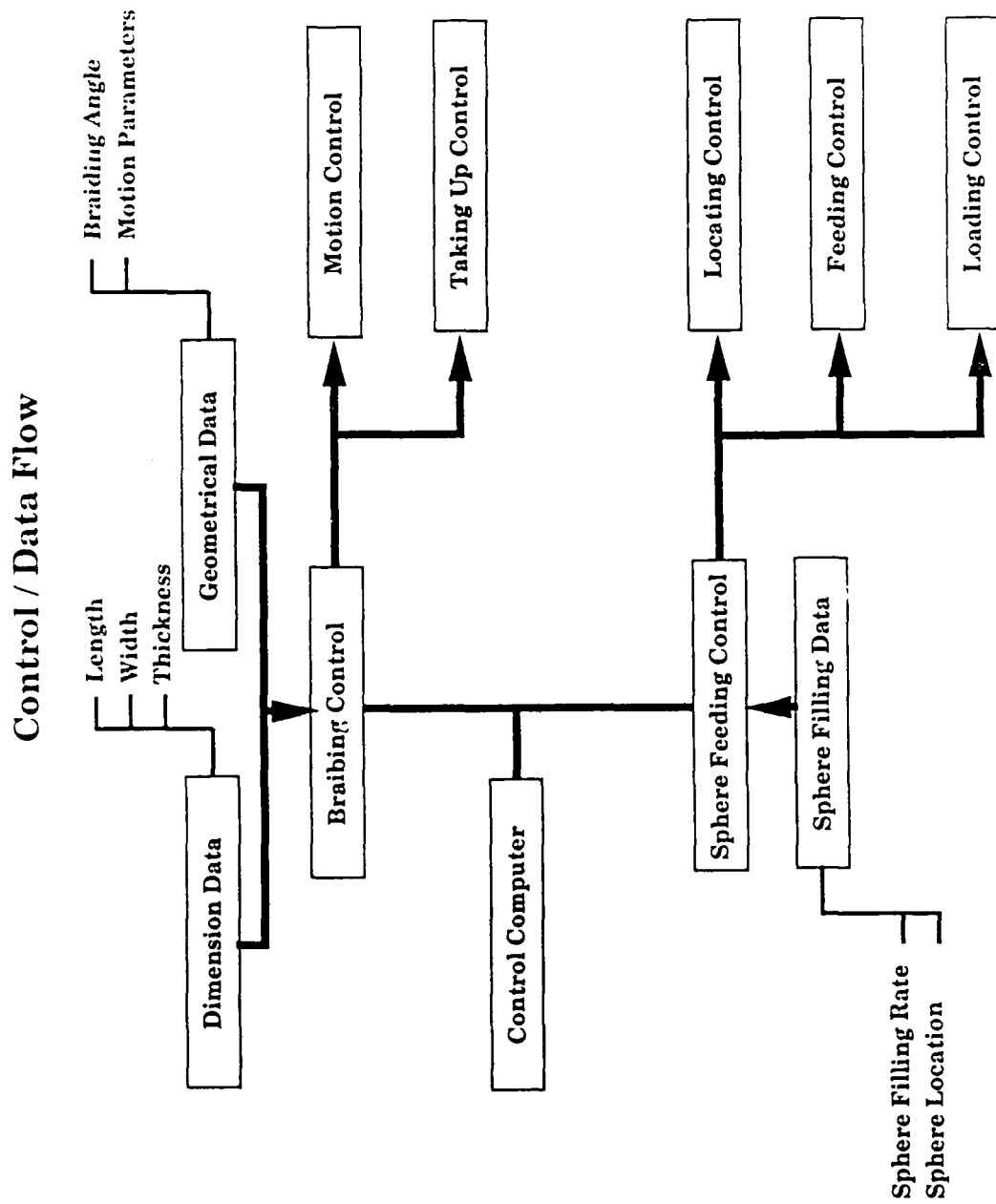
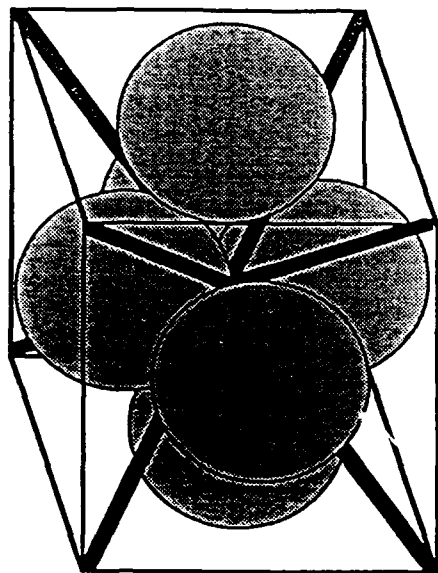
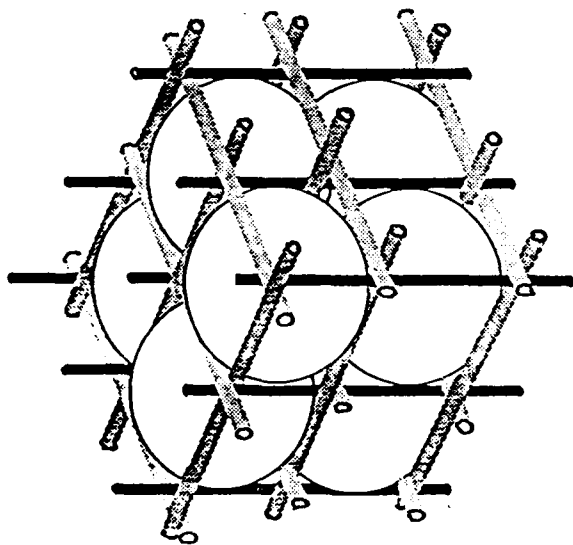


Figure 6-2 Control Logic and Data Flow of Hexagonal Braiding Machine.

- Demonstration of design concept and modelling of high-symmetry composites



High Symmetry Composites by Close Packing of
Spheres in a 3-D Fiber Network

Figure 6-3

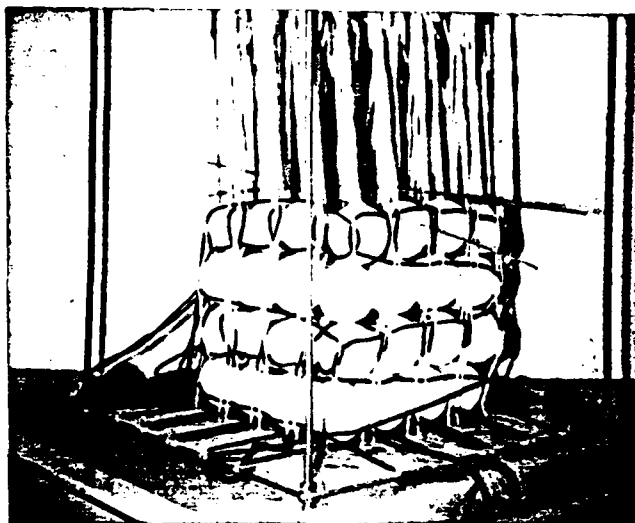


Figure 6-4 A Model of High Symmetry System.

CHAPTER SEVEN

CONCLUSIONS AND RECOMMENDATIONS

In the interest of developing toughened and hardened composite systems, the concept of structural symmetry by the placement of spheres in a 3-D fiber network was examined. By employing a 3-D fiber architecture, the composite system is anticipated to be toughened by the 3-D fiber network through complex interaction of toughening mechanism. The spheres, when strategically placed in a prearranged fiber network, will contribute to the hardening of the composite.

To demonstrate this concept of High Symmetry Composite (HSC), a systematic study was carried out and organized into three parts:

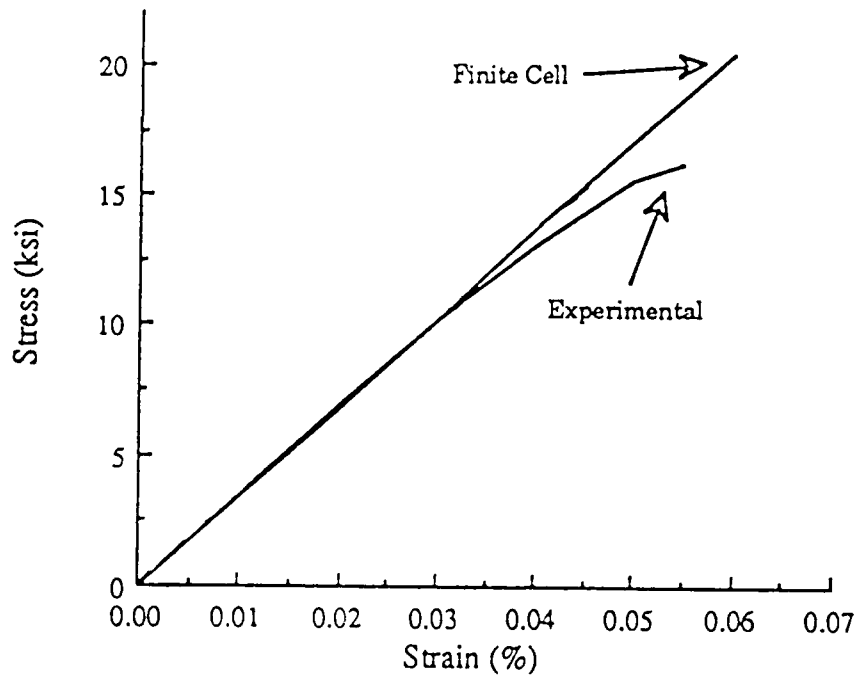
Part I. Classification of 3-D Fiber Architecture

Part II. Modelling of High Symmetry Systems

Part III. Demonstration of Concept

In Part I of this study, 3-D fiber architectures were classified according to the method of manufacture, symmetry and geometric isotropy. It was concluded that a classification scheme based on geometric isotropy provides the most efficient and useful method for the modelling of the 3-D composite system.

The modelling effort in Part II of the study consists of the development of a finite element code for the sphere; a finite cell model (FCM) for the 3-D fiber network. The sphere routine is capable of handling elastic and elastoplastic materials for laminated shell of isotropic and/or orthotropic layers under radial and tangential surface forces, as well as internal pressure loading. The finite cell code, on the other hand, was developed based on the idealization of the unit cell geometry in terms of truss systems. According to the principle of virtual work, the nodal forces within the cell structure are related to the nodal displacement by a stiffness matrix $[K]$. This finite cell code has been employed to predict the tensile stress-strain relationship of chemical vapor infiltrated (CVI) 3-D braided Nicalon SiC/SiC composites. With a volume fraction of 0.4 and using a 1 x 1 braiding pattern for the Nicalon yarn, the theoretical prediction of the tensile stress-strain relationship agrees reasonably well with the experimental results as shown in Figure 7-1.



**Tensile Stress-Strain
Relationship of 3-D Braided
SiC/SiC Composite**

Figure 7-1

Using the FCM, parametric studies were carried out for various ceramic matrix composite systems. As expected, the inclusion of the sphere reinforcement does improve the compressive stiffness.

In order to transform the high symmetry composite concept to reality, there is a need for a mechanism to create the structure. Part III of this study is dedicated to this effort. Unfortunately, due to the shortage of funding for the third year, only the manufacturing methodology was explored. The proposed method is based on a hexagonal braiding process which incorporates a sphere feeding mechanism. This manufacturing system was designed with full support of computer logic flow. Accordingly, when the prototype machine is built, a numerically controlled, reproducible preforming system will be available for the manufacturing of high symmetry composites.

Finally, it must be concluded that although the concept of high symmetry composites has been theoretically and conceptually demonstrated which simulated results and preforming mechanism. a considerable amount of work remains to be done in the verification of the model and design concepts. It is recommended polymer and ceramic matrix composites with 3-D fiber/sphere reinforcements to be fabricated, first manually and then on the hexagonal braiding machine (when it is available). Tensile and compressive tests will be performed on these composites. The failure modes will be characterized by fractography. It is further recommended

that further work be carried out to link the sphere code to the finite cell code such that the interaction of the 3-D fiber network with the sphere be fully explored.

LIST OF REFERENCES

1. Banos, J., et. al., "Three-Dimensional Woven Articles", U.S. Patent 4,346,741 granted 1982.
2. Banos, J., et. al, "Method and Machine for Three-Dimensional Weaving for Obtaining Woven Hollow Reinforcements of Revolution", U.S. Patent 4,183,232 granted 1980.
3. Bluck, R.M., "High Speed Bias Weaving and Braiding", U.S. Patent ,426,804 granted 1969.
4. Brazil, J.P., "Advanced Hardened Antenna Window Materials Study", AMMRC CTR 72-1, 1972.
5. Brown, R.T., "Braiding Apparatus", U.S. Patent 4,753,150 granted 1988.
6. Brown, R.T., "Method of Sequenced Braider Motion for Multi-Ply Braiding Apparatus", U.S. Patent 4,621,560 granted 1986.
7. Bruno, P.S., Keith, D.O., and Vicario Jr., A.A., "Automatically Woven Three-Directional Composite Structures", SAMPE Quarterly, Vol. 17, No. 4, July 1986, pp 10-17.
8. Cahuzac, G.J.J., "Hollow Reinforcements of Revolution Made By Three-Dimensional Weaving Method and Machine for Fabricating Such Reinforcements", U.S. Patent 4,492,096, granted 1985.
9. Crawford, J.A., "Multifilament Composites", U.S. Patent 3,949, 126 granted 1976.

10. Edwards, M.W., "Weaving Advanced Composite Materials", Aerospace Eng., June 1988, pp33-34.
11. Emerson, P.A., et. al, "Circular Weaving Apparatus Product and Process", U.S. Patent 3,719,210 granted 1973.
12. Encyclopedia Brittanica, Textile Industry 1988.
13. Florentine, R.A., "Apparatus for Weaving a Three-Dimensional Article", U.S. Patent 4,312,261 granted 1982.
14. Fukuta, K., "Three-Dimensional Fabric, and Method and Loom Construction for the Production Thereof", U.S. Patent 3,834,424 granted 1974.
15. Geoghegan Jr., P.J., "DuPont Ceramic Composites", Presented June 2, 1988 at the 3RD Textile Stuctural Composites Symposium, Phila., PA.
16. Kallmeyer, A.W., "Yarn Inserting and Packing Machine", U.S. Patent, 4,095,619 granted 1978.
17. Kelly, A., and Groves, G.W., Crystallography and Crystal Defects, Addison Wesley, Reading MA 1970.
18. King, R.W., "Three-Dimensional Fabric Material", U.S. Patent 4,001,478 granted 1977.
19. Ko, F.K., "Braiding", Engineered Materials Handbook, pp519-528, 1988.
20. Ko, F.K., "Recent Advances in Textile Structure Composites", Advanced Composites Conference, Dearborn Michigan, December 2-4 1985.

21. Ko, F.K., Fang, P., and Pastore, C., "Multilayer Multidirectional Warp Knit Fabrics for Industrial Applications", *J. Ind. Fab.*, Vol. 4, No. 2, 1985.
22. Ko, F.K., and Pastore, C.M., "Structure and Properties of an Integrated 3-D Fabric for Structural Composites", *Recent Advances in Composites in the United States and Japan*, ASTM STP 864, J.R., Vinson and M. Taya, Eds., ASTM, Phila. PA 1985, pp 428-439.
23. Ko., F.K., "Three-Dimensional Fabrics for Composites - An Introduction to the Magnaweave Structure", Progress in Science and Engineering of Composites, T. Hayashi, K. Kawata, and S., Umekawa, eds., Proceedings of the ICCM-IV, Tokyo, Japan, 1982.
24. Ko, F.K., Bruner, J., Pastore, A., and Scardino, F., "Development of Multi-Bar Weft-Insert Warp Knit Glass Fabrics for Industrial Applications", *J. Eng. Ind.*, Vol. 102, 1980, pp333-341.
25. Li, W. and Shiekh, A.E., "The Effect of Processes and Processing Parameters on 3D Braided Preforms for Composites", *SAMPE Quarterly*, Vol. 19, No. 4, July 1988, pp 22-28.
26. Love, A.E.H., A Treatise on the Mathematical Theory of Elasticity, Fourth Edition, Dover Publications, New York, 1944.
27. Maistre, M.A., "Construction of a Three Dimensional Structure", F.R.D. Patent P2301696.8, 1973.
28. McAllister, L.E., and Lachman, W.L., "Multidirectional Carbon-Carbon Composites", Handbook of Composites Vol. 4, edited by A. Kelly and S.T. Mileiko, 1983, pp 109-175.
29. McConnell, R.F., and Popper, P., "Complex Shaped Braided Structures", U.S. Patent 4,719,837 granted 1988.
30. Paustenbaugh, J.T., "Capability in 3-D Woven Composites Using the Aerospace Process, Presented June 2, 1988 at the 3RD Textile Structural Composites Symposium, Phila., PA.

31. Pastore, C.M., A Processing Science Model for Three Dimensional Braiding, PhD Thesis, Drexel University, 1988.
32. Pastore, C.M., and Ko, F., "Near Net Shape Manufacturing of Composite Engine Components By 3-D Fiber Architecture",
33. Pastore, C.M., Whyte, D.W., Soebruto, H. and Ko, F., "Design and Analysis of Multiaxial Warp Knit Fabrics for Composites", J. Ind. Fab., Vol. 5, No. 1, 1986, pp 4-17.
34. Rheume, W.A., "Thick Fabrics", U.S. Patent 3,749,138 granted 1973.
35. Rolincik, P.G., "Autoweave", Avco Specialty Materials Technical Information, Lowell, MA 01851.
36. Scardino, F., Presented June 2, 1987 at the 2RD Textile Structural Composites Symposium, Phila., PA.
37. Wagner, J.R., "Nonwovens: the State of the Art," Tappi J. April 1988, pp 115-121.
38. Whyte, D.W., On the Structure and Properties of 3D Braid Reinforced Composites", PhD Thesis, Drexel University, June 1986.
39. Williams, D., "New Knitting Methods Offer Continuous Structures", Engineering, Vol. 227, No. 6, 1987, pp 12-13.

APPENDIX A

LISTING OF FINITE CELL MODELLING PROGRAM

```

C --- THIS PROGRAM IS DESIGNED TO DEMONSTRATE THE CONCEPT AND FORMULATIONS
C --- OF FINITE-CELL MODELLING for X-Y-Z fiber reinforced composites.
C --- The maximum number of unit cells of this program is 5.

```

```

IMPLICIT DOUBLE PRECISION (A-H,O-Z)
COMMON /ARR/ DISP(72),FORCE(72),FORCE1(72),DISP1(72)
COMMON /ARR1/ FORCE2(72),CORD(72),COORD(72)
CHARACTER*20 INFILE,OUTFIL
COMMON /PARAM/ E(4),G(4),A(4),DIA(4),FR,EA(4),EAL(4)
COMMON /REDUCT/ IRN,IRDOF,IR2,IRR2,IR1,IR5,IK6,IRR6
COMMON /NUMBER/ NCELL, NOD,NDOF,NBC,NFORCE,NSTEP,ITER
COMMON /INDEX/ IND(72),IBC(72),KL(72),IREDUCE(72),IDELE(6,8)
COMMON /STIF1/ STIFF(72,72)
COMMON /STIF/ STIFF1(48,48),COR(24,3)
COMMON /MCONN/ MCN(6,16,2)
COMMON /MATRIX/ B(72,72)
COMMON /VALUE/ RATIO1,RATIO2,RATIO,TDIS
CHARACTER*1 ANS

```

```

--- OPEN INPUT DATA FILE

```

```

OPEN (UNIT=10,FILE='INFILE',STATUS='OLD')

```

```

--- READ THE NUMBER OF UNIT CELLS

```

```

READ(10,*) NCELL

```

```

--- READ THE COORDINATES OF EACH NODE

```

```

READ(10,*) NOD
NDOF=6*NOD
DO 20 I=1,NOD
  READ(10,2001) COR(I,1),COR(I,2),COR(I,3)
20 CONTINUE

```

```

--- STORE THE CELL CONNECTION

```

```

DO 25 I=1,NCELL
  READ(10,*) (IDELE(I,J), J=1,8)

```

```

--- STORE THE UNIT CELL MEMBER CONNECTION

```

```

DO 27 I = 1,NCELL
  READ(10,*) (MCN(I,J,1),J=1,12)
  READ(10,*) (MCN(I,J,2),J=1,12)
27 CONTINUE

```

```

--- ENTRY OF BOUNDARY CONDITIONS FOR DISPLACEMENTS

```

```

DO 30 I=1,NDOF
  IND(I)=1
  READ(10,*) NBC

```

```

--- IND = 0 (FIXED SUPPORT), IND = 1 (FREE SUPPORT)

```

```

DO 35 I=1,NBC
  READ(10,*) IBC(I)
  IBC1=6*(IBC(I))-5
  IBC2=6*(IBC(I))-4
  IBC3=6*(IBC(I))-3
  IBC4=6*(IBC(I))-2
  IBC5=6*(IBC(I))-1
  IBC6=6*(IBC(I))
35 READ(10,*) IND(IBC1),IND(IBC2),IND(IBC3),IND(IBC4),IND(IBC5),

```

```

& IND(IBC6)
C
C --- ENTRY OF BOUNDARY CONDITIONS FOR FORCES
C
DO 40 I=1,NDOF
FORCE(I)=0.0
FORCE1(1)=0.0
DISP(I)=0.0
DISP1(I)=0.0
40 CONTINUE
READ(10,*) NFORCE
DO 43 I=1,NFORCE
READ(10,*) IFORC
IFORC1=6*IFORC-5
IFORC2=6*IFORC-4
IFORC3=6*IFORC-3
IFORC4=6*IFORC-2
IFORC5=6*IFORC-1
IFORC6=6*IFORC
READ(10,*) FORCE(IFORC1),FORCE(IFORC2),FORCE(IFORC3),
& FORCE(IFORC4),FORCE(IFORC5),FORCE(IFORC6)
43 CONTINUE
C
C --- MATERIAL PROPERTIES
C
READ(10,2001) VF,VFB,VM
READ(10,2002) EF,PF,EM,PM,EBALL
READ(10,2001) HEIGHT,WIDTH,THICK
READ(10,*) NX,NY,NZ
HL=HEIGHT
WL=WIDTH
TL=THICK
ABALL=VFB*HL*WL*TL/(4.*(HL+WL+TL))
AF = VF*HL*WL*TL/(4.*(HL+WL+TL))
AM = VM*HL*WL*TL/(4.*(HL+WL+TL))
AC = AF + AM + ABALL
print *, af,am,aball,ac
EBALLX = (EBALL/ABALL)*HL
eballx = eball
EBALLY = EBALLX
EBALLZ = EBALLX
GF = EF/(2.+2.*PF)
GM = EM/(2.+2.*PM)
GB = EBALL/(2.+2.*.3)
A(1) = AC
A(2) = AC
A(3) = AC
ac1=af/ac
ac2=am/ac
ac3=aball/ac
print *, ac1,ac2,ac3
E(1)=(AF*EF+AM*EM+EBALLX*ABALL)/A(1)
E(2)=(AF*EF+AM*EM+EBALLY*ABALL)/A(2)
E(3)=(AF*EF+AM*EM+EBALLZ*ABALL)/A(3)
if(vfb.eq.0.) then
GC = 1./(PF/GF+PM/GM+.3/GB)
endif
gc = 1./(pf/gf+pm/gm)
G(1) = GC
G(2) = GC
G(3) = GC
DIA(1)=DSQRT(4.*A(1)/3.14159)
DIA(2)=DSQRT(4.*A(2)/3.14159)
DIA(3)=DSQRT(4.*A(3)/3.14159)

```

```

EA(1)=E(1)*A(1)
EA(2)=E(2)*A(2)
EA(3)=E(3)*A(3)
EAL(1)=EA(1)/HL
EAL(2)=EA(2)/WL
EAL(3)=EA(3)/TL
2001 FORMAT(3F10.0)
2002 FORMAT(5F10.0)
C
CLOSE(UNIT=10)
C
DO 55 I=1,NDOF
55 COOR(I)=0.
DO 60 I = 1,NOD
I1 = 6*I-5
I2 = 6*I-4
I3 = 6*I-3
COOR(I1) = COR(I,1)
COOR(I2) = COR(I,2)
COOR(I3) = COR(I,3)
60 CONTINUE
C
PRINT *, '      HOW MANY STEPS ?      '
READ(5,*) NSTEP
C
PRINT *, '      ENTER LOAD INCREMENT      '
READ(5,*) DLOAD
C
PRINT *, '      ENTER THE RATIO OF FRAME JOINT      '
READ(5,*) FR
C
PRINT *, '      ENTER ULTIMATE STRENGTH ( KSI )      '
READ(5,*) UTS
C
C --- INCREMENTAL LOAD LOOP STARTS HERE
C
OPEN(UNIT=50,FILE='OUTFIL',STATUS='UNKNOWN')
WRITE(50,*) '      NSTEP ', '      DLOAD ', '      FR ', '      UTS '
WRITE(50,1007) NSTEP,DLOAD,FR,UTS
WRITE(50,*)
WRITE(50,*)
WRITE(50,*) ' EX      ', 'EY      ', 'EZ      ', 'EB      '
WRITE(50,1008) E
WRITE(50,*)
WRITE(50,*) ' AX      ', 'AY      ', 'AZ      ', 'AB      '
WRITE(50,1008) A
WRITE(50,*)
WRITE(50,*) ' DX      ', 'DY      ', 'DZ      ', 'DB      '
WRITE(50,1008) DIA
WRITE(50,*)
WRITE(50,*) ' PX      '
WRITE(50,1008) PX
WRITE(50,*)
WRITE(50,*) ' HL      ', 'WL      ', 'TL      '
WRITE(50,1008) HEIGHT,WIDTH,THICK
WRITE(50,*)
WRITE(50,*) '      NX', '      NY', '      NZ'
WRITE(50,1010) NX,NY,NZ
WRITE(50,*)
WRITE(50,*) ' EAX      ', 'EAY      ', 'EAZ      ', 'EAB      '
WRITE(50,1008) EA
WRITE(50,*)
WRITE(50,*) ' EAX/L      ', 'EAY/L      ', 'EAZ/L      ', 'EAB/L      '
WRITE(50,1008) EAL

```

```

WRITE(50,*)
WRITE(50,*)
WRITE(50,*) 'DATA OF 3-NODE '
WRITE(50,*)
WRITE(50,*) ' FORCE      ' STRESS      ' STRAIN      '
&Exx      ' Vxy      '
C
DO 1000 ILOOP=1,NSTEP
RATIO1=4.*ILOOP*DLOAD/(WIDTH*THICK)
RATIO=DLOAD*(ILOOP)
C
C --- ITERATION OF ONE STEP LOAD STARTS HERE -----
C
DO 999 ITER=1,10
C
C --- FORM STIFFNESS MATRIX -----
C
DO 99 I=1,NDOF
DO 99 J=1,NDOF
99 STIFF(I,J)=0.
DO 98 I=1,48
DO 98 J=1,48
98 STIFF1(I,J)=0.
DO 100 KK=1,NCELL
C
C --- OPERATION ON LOCAL ELEMENT -----
C
DO 110 L=1,8
LI=IDELE(KK,L)
C
L1=6*L-5
L2=6*L-4
L3=6*L-3
L4=6*L-2
L5=6*L-1
L6=6*L
KL(L1)=6*LI-5
KL(L2)=6*LI-4
KL(L3)=6*LI-3
KL(L4)=6*LI-2
KL(L5)=6*LI-1
KL(L6)=6*LI
C
110 CONTINUE
C
CALL FORM(48, KK)
C
C --- STORE LOCAL [K] TO GLOBAL [K]
C
DO 120 I=1,48
DO 120 J=1,48
IX=KL(I)
IY=KL(J)
STIFF(IX,IY)=STIFF(IX,IY)+STIFF1(I,J)
120 CONTINUE
100 CONTINUE
IF(ITER.EQ.1) THEN
GOTO 170
ENDIF
C
C ---- CALCULATE BIASED LOAD FOR ITERATION -----

```

```

C      DO 150 I=1,NDOF
      FORCE2(I)=0.
      DO 150 J=1,NDOF
      FORCE2(I)=STIFF(I,J)*DISP1(J)+FORCE2(I)
150  CONTINUE
C
      RATIO2=RATIO-FORCE2(1)
      IF(RATIO2.LT.0.001) THEN
      GOTO 400
      ENDIF
C
C --- APPLY BOUNDARY CONDITIONS TO REDUCE THE SIZE OF GLOBAL [K] -----
C
170  J=0
      DO 200 I=1,NDOF
      IF(IND(I).EQ.0) THEN
      J=J+1
      IREDUCE(J)=I
      ENDIF
200  CONTINUE
      IRN=J
C
C --- COLUMN REDUCTION
C
      IR2=1
      DO 210 IR1=1,NDOF
      IF(IR2.GT.IRN) THEN
      GOTO 215
      ENDIF
      IF(IR1.EQ. IREDUCE(IR2)) THEN
      IR2=IR2+1
      GOTO 210
      ENDIF
215  IRR2=IR1-IR2+1
      FORCE1(IRR2)=FORCE(IR1)
      DO 216 IR3=1,NDOF
216  STIFF(IRR2,IR3)=STIFF(IR1,IR3)
210  CONTINUE
      IRDOF=IRR2
C
C --- ROW REDUCTION -----
C
      IR6=1
      DO 250 IR5=1,NDOF
      IF(IR6.GT.IRN) THEN
      GOTO 255
      ENDIF
      IF(IR5.EQ. IREDUCE(IR6)) THEN
      IR6=IR6+1
      GOTO 250
      ENDIF
255  IRR6=IR5-IR6+1
      DO 256 IR7=1,IRDOF
256  STIFF(IRR6,IRR7)=STIFF(IR5,IRR7)
250  CONTINUE
C
C --- CALCULATE INVERSE OF REDUCED [K] -----
C
      DO 260 I=1,IRDOF
      DO 260 J=1,IRDOF
260  B(I,J)=STIFF(I,J)
C
      CALL INV(IRDOF)

```

```

C
275 DO 300 I=1,IRDOF
    DISP(I)=0.
    DO 300 J=1,IRDOF
300 DISP(I)=B(I,J)*FORCE1(J)*RATIO+DISP(I)
C
C --- RESTORE THE DISPLACEMENTS -----
C
    IR8=1
    DO 350 I=1,NDOF
    IF (IREDUCE(IR8).EQ.I) THEN
    IR8=IR8+1
    GOTO 350
    ENDIF
    IR9=I-IR8+1
    DISP1(I)=DISP(IR9)
350 CONTINUE
C
C --- CALCULATE THE DISPLACED COORDINATES -----
C
    DO 380 I=1,NDOF
380 CORD(I)=COOR(I)+DISP1(I)
    DO 390 I=1,NOD
    I1 = 6*I-5
    I2 = 6*I-4
    I3 = 6*I-3
    COR(I,1) = CORD(I1)
    COR(I,2) = CORD(I2)
    COR(I,3) = CORD(I3)
390 CONTINUE
999 CONTINUE
C
C --- PRINT OUT THE RESULTS
C
400 TDIS=CORD(13)-COOR(13)
    YDIS=CORD(14)-COOR(14)
    ZDIS=CORD(15)-COOR(15)
    STRAIN=TDIS/HEIGHT
    SY = YDIS/WIDTH
    SZ = ZDIS/THICK
    Exx = RATIO1/STRAIN
    Vxy = -SY/STRAIN
    Vxz = -SZ/STRAIN
    WRITE(50,1006) RATIO,RATIO1,STRAIN,Exx,Vxy
C
C --- THE END OF THE LOOP -----
C
    UTS1 = 1000.*UTS
    IF(RATIO1.GT.UTS1) THEN
    GOTO 500
    ENDIF
1000 CONTINUE
500 WRITE(50,*)
    WRITE(50,*)
    WRITE(50,*) 'FINAL DISPLACEMENT OF ALL NODES '
    WRITE(50,*)
    WRITE(50,*) ' X ' Y ' Z '
    & NO. '
    DO 501 I=1,NOD
    J1=6*I-5
    J2=6*I-4
    J3=6*I-3
    WRITE(50,*)
501 WRITE(50,1009) DISP1(J1),DISP1(J2),DISP1(J3),I

```

```

WRITE(50,*)
WRITE(50,*) 'FINAL ROTATION '
DO 505 I=1,NOD
J1=6*I-2
J2=6*I-1
J3=6*I
WRITE(50,*)
505 WRITE(50,1009) DISP1(J1),DISP1(J2),DISP1(J3),I
CLOSE(UNIT=50)
C
1001 FORMAT(/'REDUCED [K] ', ' ILOOP = ',I3,' ITER = ',I3)
1002 FORMAT(/2E16.6)
1003 FORMAT(/'INVERSE [K] ', ' ILOOP = ',I3,' ITER = ',I3)
1004 FORMAT(/12E10.3)
1005 FORMAT(/4E16.7)
1006 FORMAT(/5E14.5)
1007 FORMAT(/I10,3F12.2)
1008 FORMAT(4E12.4)
1009 FORMAT(3E14.5,I6)
1010 FORMAT(2X,3I5)
C
511 STOP
END
CCCCCCCC-----
C
C --- THIS SUBROUTINE IS TO FORM THE CELL STIFFNESS MATRIX
C
SUBROUTINE FORM(IQAZ, KK)
C
IMPLICIT DOUBLE PRECISION (A-H,O-Z)
COMMON /STIF/ STIFF1(48,48),COR(24,3)
COMMON /MCONN/ MCN(6,16,2)
COMMON /PARAM/ E(4),G(4),A(4),DIA(4),FR
DIMENSION SM(12,12),SR(12,12),SK(12,12),GK(48,48)
DIMENSION RM(3,3),RTM(12,12)
INTEGER IQAZ
C
DO 100 I = 1,IQAZ
DO 100 J = 1,IQAZ
100 STIFF1(I,J)=0.0
C
C--- FORM THE COORDINATE TRANSFER MATRIX [R]
C
DO 600 M = 1,12
II = MCN(KK,M,1)
JJ = MCN(KK,M,2)
X = COR(JJ,1)-COR(II,1)
Y = COR(JJ,2)-COR(II,2)
Z = COR(JJ,3)-COR(II,3)
SL = DSQRT(X*X+Y*Y+Z*Z)
R = X/SL
S = Y/SL
T = Z/SL
RT = DSQRT(R*R+T*T)
C
601 FORMAT(/8E15.5)
C
C --- [R] FOR MEMBERS THAT ARE IN THE DIRECTION OF Y-AXIS
C
IF(RT.LT.0.001) THEN
RM(1,1)=0.
RM(1,2)=S
RM(1,3)=0.
RM(2,1)=-S

```



```

      RM(2,2)=0.
      RM(2,3)=0.
      RM(3,1)=0.
      RM(3,2)=0.
      RM(3,3)=1.
    ELSE
C
C --- [R] FOR OTHER MEMBERS
C
      RM(1,1)=R
      RM(1,2)=S
      RM(1,3)=T
      RM(2,1)=-R*S/RT
      RM(2,2)=RT
      RM(2,3)=-S*T/RT
      RM(3,1)=-T/RT
      RM(3,2)=0.
      RM(3,3)=R/RT
    ENDIF
    DO 102 I=1,12
    DO 102 J=1,12
102  RTM(I,J)=0.
    DO 105 I=1,3
    DO 105 J=1,3
      RTM(I,J)=RM(I,J)
      RTM(I+3,J+3)=RM(I,J)
      RTM(I+6,J+6)=RM(I,J)
      RTM(I+9,J+9)=RM(I,J)
105  CONTINUE
C
C --- GET MATERIAL PROPERTIES FOR EACH MEMBER
C
      IF (M-4) 110,110,115
110  N = 1
      GO TO 150
115  IF (M-8) 120,120,125
120  N = 2
      GO TO 150
125  IF (M-12) 130,130,130
130  N = 3
C
150  H = 3.14159*DIA(N)**4./64.
      Q = E(N)*A(N)/SL
      F = (12.*E(N)*H/SL**3.)*FR
      B = (6.*E(N)*H/SL**2.)*FR
      C = (2.*E(N)*H/SL)*FR
      D = (2.*G(N)*H/SL)*FR
C
C --- FORM MEMBER STIFFNESS MATRIX [SM]
C
155  DO 160 I = 1,12
    DO 160 J = 1,12
160  SM(I,J) = 0.
      SM(1,1) = Q
      SM(1,7) = -Q
      SM(2,2) = F
      SM(2,6) = B
      SM(2,8) = -F
      SM(2,12) = B
      SM(3,3) = F
      SM(3,5) = -B
      SM(3,9) = -F
      SM(3,11) = -B
      SM(4,4) = D

```

```

SM(4,10) = -D
SM(5,5) = 2.*C
SM(5,9) = B
SM(5,11) = C
SM(6,6) = 2.*C
SM(6,8) = -B
SM(6,12) = C
SM(7,7) = Q
SM(8,8) = F
SM(8,12) = -B
SM(9,9) = F
SM(9,11) = B
SM(10,10) = D
SM(11,11) = 2.*C
SM(12,12) = 2.*C

C
C --- APPLIED SYMERTIC CONDITION
C
DO 170 I = 1,11
DO 170 J = I+1,12
170 SM(J,I) = SM(I,J)

C --- FORM [SM][R]
C
DO 175 I = 1,12
DO 175 J = 1,12
SR(I,J) = 0.
DO 175 K = 1,12
175 SR(I,J) = SR(I,J)+SM(I,K)*RTM(K,J)

C --- FORM [RT][SM][R]
C
DO 185 I = 1,12
DO 185 J = 1,12
SK(I,J) = 0.
DO 185 K = 1,12
185 SK(I,J) = SK(I,J)+RTM(K,I)*SR(K,J)

C --- STORE MEMBER STIFFNESS [SK] IN TO UNIT CELL STIFFNESS MATRIX
C
DO 195 I = 1,48
DO 195 J = 1,48
195 GK(I,J) = 0.
II=MCN(1,M,1)
JJ=MCN(1,M,2)
DO 200 I2 = 1,12
IF (I2.LT.7) THEN
I3 = (II-1)*6+I2
ELSE
I3 = (JJ-1)*6+I2-6
ENDIF
DO 200 J2 = 1,12
IF (J2.LT.7) THEN
J3 = (II-1)*6+J2
ELSE
J3 = (JJ-1)*6+J2-6
ENDIF
GK(I3,J3) = SK(I2,J2)
200 CONTINUE
DO 210 I = 1,48
DO 210 J = 1,48
210 STIFF1(I,J) = STIFF1(I,J)+GK(I,J)
600 CONTINUE
RETURN

```

END

C
C
C
C
C

----- SUBROUTINE FOR MATRIX INVERSION

SUBROUTINE INV(N)

C

IMPLICIT DOUBLE PRECISION (A-H,O-Z)

COMMON /MATRIX/ B(72,72)

DIMENSION A(72,144)

C

EPS=1.E-18

DO 100 I=1,N

DO 100 J=1,N

100 A(I,J)=B(I,J)

L=N+1

M=2*N

DO 200 I=1,N

DO 200 J=L,M

A(I,J)=0.

IF(I+N-J) 200,210,200

210 A(I,J)=1.

200 CONTINUE

DO 300 I=1,N

K=I

IF(I-N) 10,40,10

10 IF(A(I,I)-EPS) 20,30,40

20 IF(-A(I,I)-EPS) 30,30,40

30 K=K+1

DO 35 J=1,M

35 A(I,J)=A(I,J)+A(K,J)

GO TO 10

40 DIV=A(I,I)

DO 50 J=1,M

50 A(I,J)=A(I,J)/DIV

DO 300 K=1,N

DELT=A(K,I)

IF(DABS(DELT)-EPS) 300,300,60

60 IF(K-I) 70,300,70

70 DO 80 J=1,M

80 A(K,J)=A(K,J)-A(I,J)*DELT

300 CONTINUE

DO 400 I=1,N

DO 400 J=L,M

K=J-N

B(I,K)=A(I,J)

400 CONTINUE

RETURN

END

APPENDIX B

A FINITE ELEMENT CODE FOR HOLLOW SPHERES

FINITE ELEMENT CODE FOR HOLLOW SPHERES

INTRODUCTION

The hollow sphere is a major component in the high symmetry ceramic matrix composite which is studied in this research. Fig. 1 illustrates the conceptual unit cell of the composite in which closely packed spheres are embedded in the 3-D fiber network. To describe the load-deformation response of the total unit cell and the internal stresses in the constituent components of the unit cell, the response of the individual spheres must be described first and then incorporated in the total UNIT CELL model.

Since the UNIT CELL model has been described elsewhere in this report, this section present only the results stemming from our efforts in developing a finite element code for a single sphere which is subjected to surface forces, internal pressure and/or thermal loading.

GENERAL CHARACTERISTICS OF THE FINITE ELEMENT CODE

The finite element code is developed based on the so-called degenerated quadratic plate/shell element formulation found in the outlines of Hinton and Owen [1]. In essence, the usual assumptions made in the simple plate/shell theories continue to be valid in the formulation of the code. These include the assumptions of simple bending: the omission of deformation in the thickness direction and any deformation caused by transverse shear. Thus, there are only 5 degree-of-freedom at each node; namely, three displacements and two rotations.

The so-called degenerated isoparametric elements include three

different configurations: the 8-node Serendipity, the 9-node Lagrangian and 9-node Heterosis. The Serendipity is the simplest, requiring a normal rule of integration such as the 3x3 Gauss quadrature approach. This type of element, however, has been shown to yield stiff solutions if the shell is thin (as compared to its radius). To improve the accuracy of the computed stresses, a reduced integration technique such as suggested in Hinton and Owen [1] may be followed for shells of thin thicknesses. The 9-node Lagrangian is basically the 8-node serendipity with an additional middle node in the center of the quadrilateral element. Usually, a full integration technique must be followed, though the reduced integration method can also be used. However, problems of reduced rank (or rank deficiency) may sometimes arise in the stiffness matrix if the reduced integration technique is used. While the additional node helps to improve the computed results, it nevertheless causes increased degree-of-freedom of the element and requires a different set of the nodal shape functions. The Heterosis is a mix of the Serendipity and the Lagrangian in that the element employs serendipity shape functions for the transverse displacement w and the Lagrangian shape function for the rotations. This allows selective integration techniques to be used. Choice of these different element shapes is a matter of decision to be made for the specific problem which is to be analyzed [1].

The code can analyze structures constructed using shell elements, such the hollow sphere. The material of the sphere may be elastic and/or elasto-plastic; the sphere may be concentrically layered with isotropic and/or orthotropic materials; the applied load may be surface forces (radial and tangential, concentrated or distributed), internal pressure and/or temperature changes.

The code uses the FRONTAL solver for the finite element solution. A flow chart showing the block structure and the computational flow of the program is provided in Fig. 2.

A brief version of the user's instruction is provided at the end of this section.

A listing of the code PLASTOSHELL is provided in the appendix.

REFERENCE

- [1] "Finite Element Software for Plates and Shells" Hinton and Owen, Pineridge Press, Swansea, 1984.

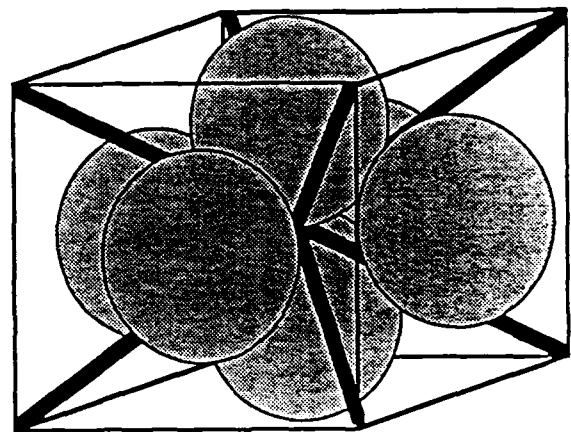
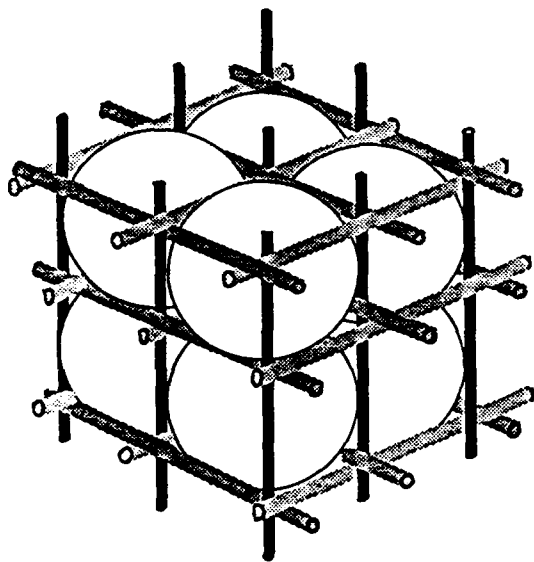


Fig. 1 Close Packing of Spheres in A 3-D Fiber Network

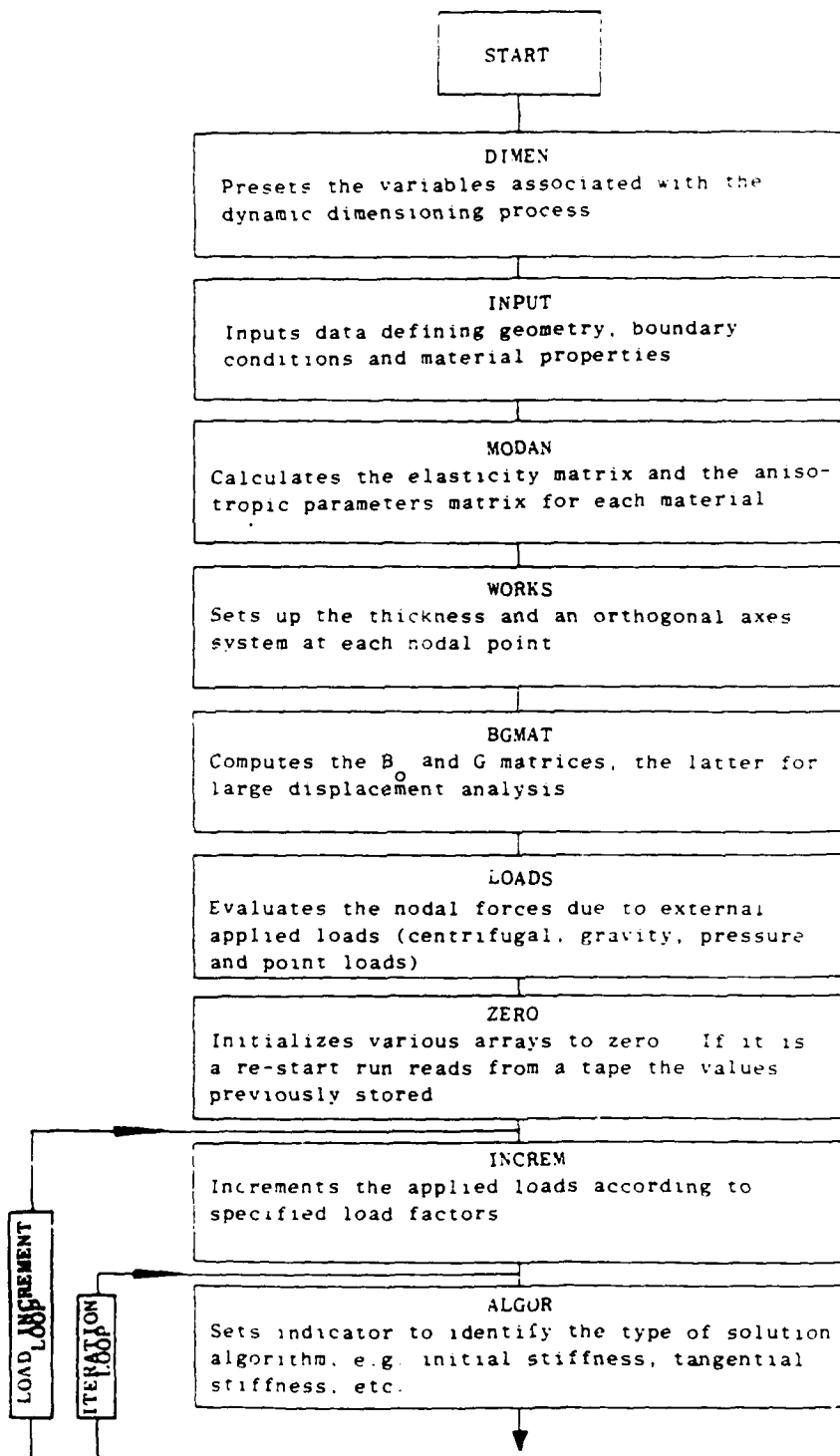
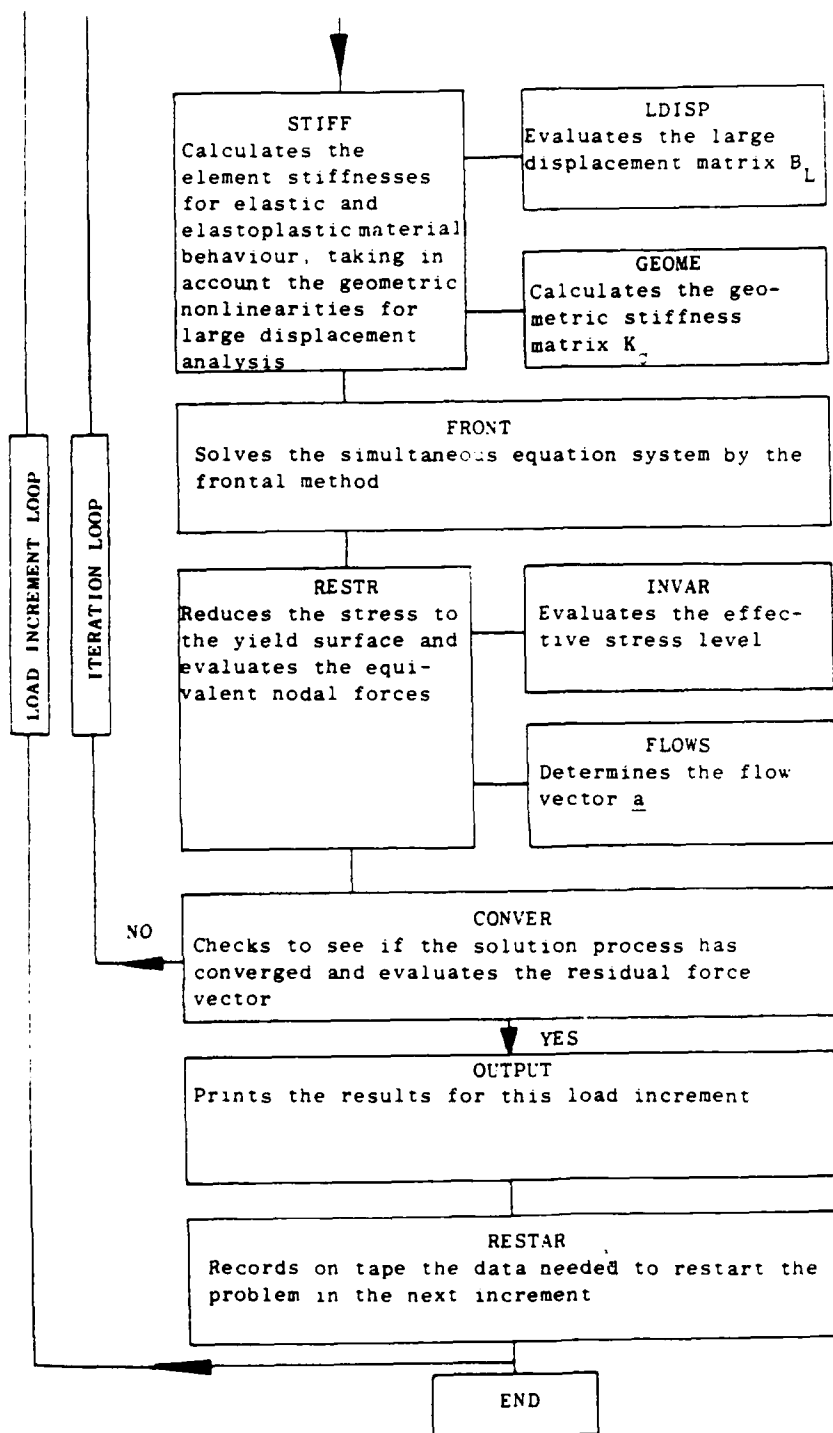


Fig. 2 Flow Chart for the PLASTOSHELL Code (continued on next page)



USER INSTRUCTION FOR PREPARING THE INPUT DATA

The program undertakes elastic or ultimate load analysis (if material is elasto-plastic) of thin, thick and layered plates and/or shells, including the full sphere. To execute a specific problem, element mesh must be generated first. This code assumes that the element mesh has already been generated and that the coordinates of each node are all known. Thus, the required input data format described below does not include mesh generation.

The general order of the input data is as follows:

- characterization of elements
- specification of material(s) and shell thickness structure
- nodal coordinate connections
- specification of boundary conditions
- specification of loading
- output instruction

Card Set 1 - Title Card (12A6) one card

Card Set 2 - Control Card (12I5) One card

Cols.	1-5	NPOIN	Total number of nodal points
	6-10	NELEM	Total number of element
	11-15	NVFIX	Total number of points where one or more degrees of freedom are prescribed
	16-20	NNODE	Number of nodes per element 8 - for 8 node Serendipity 9 - for Heterosis and 9 node Lagrangian
	21-25	NMATS	Total number of different materials
	26-30	NGAUS	Number of Gauss points per element

31-35	NGAUZ	Number of Gauss points per element (Shear)
		NGAUS=3, NGAUZ=3 - Normal integration rule
		NGAUS=3, NGAUZ=2 - Selective integration rule
		NGAUS=2, NGAUZ=2 - Reduced integration rule
36-40	NCOLA	Set the constraints for the Lagrangian 9 node element:
		=0 9 node Lagrangian element (no constraints)
		=1 Heterosis - constrain the 9th node displacements (u,v,w)
41-45	NALGO	Nonlinear solution process indicator:
		=1 initial stiffness method is used
		=2 tangential stiffness method is used
		=3 stiffness matrix is recalculated in the first iteration of each increment
		=4 stiffness matrix is recalculated in the second iteration of each increment and also when there are one or more unloaded integration points in the previous iteration
46-50	NINCS	Total number of load increments
51-55	NLAYR	(i) Total number of layers through the thickness (PLASTOSHELL)
		(ii) Total number of layer patterns in the structure (CONSHELL)
56-60	LARGE	Large deformation parameter
		=0 Geometrically linear analysis
		=1 Geometrically nonlinear analysis
61-65	NREST	Restart facility parameter
		=0 to start the analysis
		=1 to restart the analysis from the last previously converged load increment

CARD SET 3 (5F10.5) One Card

Cols. 1-10 GRAVI(1) Gravitational acceleration in the
x-direction
11-20 GRAVI(2) Gravitational acceleration in the
y-direction
21-30 GRAVI(3) Gravitational acceleration in the
z-direction
31-40 ANVEL Angular velocity (referred to the z axis)

(i) PLASTOSHELL

CARD SET 4 - ELEMENT CARDS (16I5,/,5X,15I5) One or two Cards
for each element

Cols. 1-5 NUMEL Element number
6-10 MATNO(NUMEL) Material property number for each
layer, ILAYR from Bottom to Top
56-60 MATNO(NUMEL, (case of NLAYR = 10)
NLAYR)
61-65 LNODS(NUMEL, Element node numbers (anticlockwise)
INODE)
106-110 LNODS(NUMEL, (Case of NNODE = 9)
NNODE)

(ii) CONSHELL

CARD SET 4 - ELEMENT CARDS (11I5) One Card for each element

Cols. 1-5 NUMEL Element number
6-10 MATNO(NUMEL) Element layer pattern number
11-15 LNODS(NUMEL,1)
16-20 LNODS(NUMEL,2) Element node number (anticlockwise)
46-50 LNODS(NUMEL,8)
51-55 LNODS(NUMEL,9) (Case of NNODE = 9)

CARD SET 5 NODAL COORDINATE CARDS (I5,4F15.10/5X,4F15.10)

Two Cards for each node whose coordinates must be
input - finishing with the last node. (Coordinates
of the central 9th node and also mid-side nodes
whose coordinates are obtained by a linear inter-
polation of the corresponding corner nodes need not
be input).

First Card

Cols. 1-5 IPOIN Node number
6-20 COORD(IPOIN,1) Top x coordinate
21-35 COORD(IPOIN,2) Top y coordinate
36-50 COORD(IPOIN,3) Top z coordinate
51-65 COORD(IPOIN,4) Top pressure

Second Card

Cols. 6-20 COORD(IPOIN,5) Bottom x coordinate
21-35 COORD(IPOIN,6) Bottom y coordinate
36-50 COORD(IPOIN,7) Bottom z coordinate
51-65 COORD(IPOIN,8) Bottom pressure

CARD SET 6 RESTRAINED NODE CARDS (15,5X,15,5X,5F10.6) One
Card for each restrained node. (Total of NVFIX
Cards)

Cols. 1-5 NOFIX Restrained node number
11-15 IFPRE Condition of the degree of freedom:
restrained (=1)
otherwise (=0)
position 11 - u displacement (x-direction)
12 - v displacement (y-direction)
13 - w displacement (z-direction)
14 - β_1 rotation
15 - β_2 rotation
21-30 PRESC(IVFIX,1) - The prescribed value of the nodal
31-40 : variables (u,v,w, β_1 and β_2
41-50 : respectively)
51-60 :
61-70 PRESC(IVFIX,5)

(1) PLASTOSHELL

CARD SET 7 MATERIAL CARDS Four Cards for each different
material (Total number of cards = 4*NMATS)

First card (15)

Cols. 1-5 NUMAT Material identification number

Second card (7F10.5)

Cols. 1-10 PROPS(NUMAT,1) E_1 Young's modulus in 1 direction

Cols. 11-20 PROPS(NUMAT,2) ν_{12} Poisson's ratio ($\nu_{12}/E_1 = \nu_{21}/E_2$)³⁹³
 21-30 PROPS(NUMAT,3) t_ζ Layer thickness expressed in the
 normalised ζ coordinate
 31-40 PROPS(NUMAT,4) ρ Material density
 41-50 PROPS(NUMAT,5) α Coefficient of thermal expansion
 51-60 PROPS(NUMAT,6) σ_{01} Uniaxial yield stress (1 direction)
 61-70 PROPS(NUMAT,7) H' Hardening parameter (1 direction)

Third card (7F10.5)

Cols. 1-10 PROPS(NUMAT,8) E_2 Young's modulus in 2-direction
 11-20 PROPS(NUMAT,9) G_{12} Shear modulus in $\overline{12}$ plane
 21-30 PROPS(NUMAT,10) G_{13} Shear modulus in $\overline{13}$ plane
 31-40 PROPS(NUMAT,11) G_{23} Shear modulus in $\overline{23}$ plane
 41-50 PROPS(NUMAT,12) σ_{02} Uniaxial yield stress (2 direction)
 51-60 PROPS(NUMAT,13) σ_{03} Uniaxial yield stress (3 direction)
 or σ_θ Uniaxial yield stress (At 45° to
 1 direction)
 61-70 PROPS(NUMAT,14) τ_{012} Shear yield stress ($\overline{12}$ plane)

Fourth card (7F10.5)

Cols. 1-10 PROPS(NUMAT,15) τ_{013} Shear yield stress ($\overline{13}$ plane)
 11-20 PROPS(NUMAT,16) τ_{023} Shear yield stress ($\overline{23}$ plane)
 21-30 PROPS(NUMAT,17) θ Angle between the reference
 system and the material system
 in the layer plane (anticlock-
 wise - in radians)

NOTE: The 1,2,3 axes are the principal material axes, with 1,2
 being in the plane of the layer.

(11) CONSHELL

CARD SET 7-A CONCRETE AND STEEL DISCRETIZATION PATTERN Two
 Cards for each layer pattern

First card (16I5)

Cols. 1-5 NCLAY(ILAYR) Number of concrete layers
 6-10 NSLAY(ILAYR) Number of steel layers (ILAYR - Layer
 pattern identification number)

Second card (16I5)

Cols. 1-5 MACON(ILAYR,ICONL)
 ICONL - Material identification

number for each concrete layer from
bottom to top

MASTE(ILAYR,ISTEL)

ISTEL - Material identification

number for each steel layer

CARD SET 7-B MATERIAL CARDS - Three Cards for each different
material

First card (I5)

Cols. 1-5 NUMAT Material identification number

Second card (7F10.5) FOR CONCRETE MATERIAL ONLY

Cols. 1-10 PROPS(NUMAT,1) E_c Young's Modulus
11-20 PROPS(NUMAT,2) ν Poisson's ratio
21-30 PROPS(NUMAT,3) t_z Layer thickness expressed in the
normalized ξ coordinate
31-40 PROPS(NUMAT,4) ρ Material density
41-50 PROPS(NUMAT,5) f'_t Concrete ultimate tensile strength
51-60 PROPS(NUMAT,6) f'_c Concrete ultimate compression
strength
61-70 PROPS(NUMAT,7) ϵ_u Concrete ultimate compressive
strain

Second card (7F10.5) - FOR STEEL MATERIAL ONLY

Cols. 1-10 PROPS(NUMAT,1) E_s Young's Modulus
11-20 PROPS(NUMAT,2) E'_s Elasto-plastic Young's Modulus
21-30 PROPS(NUMAT,3) t_z Layer thickness expressed in
terms of the normalized ξ
coordinate
31-40 PROPS(NUMAT,4) ρ Material density
41-50 PROPS(NUMAT,5) f_y Steel yield stress
51-60 PROPS(NUMAT,6) ξ_s Layer position in terms of the
normalized ξ coordinate
61-70 PROPS(NUMAT,7) θ Angle between the reinforcement
and the x' -axis (measured anti-
clockwise in radians with
 $-\pi/2 < \theta \leq \pi/2$)

Third card (7F10.5) - FOR CONCRETE MATERIAL ONLY

Cols. 1-10 PROPS(NUMAT,8) ϵ_m Tension stiffening parameter ϵ_m

11-20 PROPS(NUMAT,9) α Tension stiffening parameter α

Third card (7F10.5) - FOR STEEL MATERIAL ONLY

Blank card

CARD SET 8 LOAD CARDS At least one card for each element

First card (3I5)

Cols. 1-5 NPRES Distributed load indicator
=0 no distributed loads on this element
=1 distributed loads to be input
6-10 NUCLO Number of concentrated loads on this
element (=0, no concentrated loads)
11-15 NBODY Body load indicator (gravity and/or centri-
fugal
=0 no body loads on this element
=1 body loads to be input

Second card (I5,F5.1,2F15.5) [Only exists if NPRES=1]

Cols. 1-5 KPRES Distributed load type indicator
=0 Uniformly distributed load
=1 Hydrostatic load
=2 Load specified as nodal values (See
Card Set 5)
6-10 CFACE = + 1.0 Pressure is on top surface
= - 1.0 Pressure is on bottom surface
11-25 PREVA Uniformly distributed load if KPRES = 0
Maximum value of hydrostatic load if
KPRES = 1
26-40 SURFA z coordinate of zero pressure if KPRES = 1

Third set cards (2I5,F10.5) [Only exists if NUCLO > 0]

Number of cards to be input equals NUCLO

Cols. 1-5 LPOIN Local node number (in the range 1-8) at
which the load is applied
6-10 LDOFN Nodal variable number corresponding to the
applied load
=1 - x displacement
=2 - y displacement

=3 - z displacement

=4 - \hat{e}_1 rotation

=5 - \hat{e}_2 rotation

11-20 CARGA Concentrated load value

CARD SET 9 LOAD INCREMENT CONTROL CARDS (2F10.5,3I5) One Card
for each load increment (total of NINCS cards)

Cols. 1-10 FACTO Applied load factor for the current
increment

11-20 TOLER Convergence tolerance factor

21-25 MITER Maximum number of iterations allowed

26-30 NOUPT(1) Control output parameter of the unconverged
results after the first iteration

=1 - Print the displacements only

=2 - Print displacements and nodal
reactions

=3 - Print displacements, reactions and
stresses

31-35 NOUPT(2) Control output parameter of the converged
results

=1 Print the final displacements only

=2 Print displacements and nodal reactions

=3 Print displacements, reactions and
stresses.

LISTING OF PLASTOSHELL

A PROGRAM FOR ANALYSIS OF SHELLS BY THE FINITE ELEMENT METHOD

THIS PROGRAM HAS BEEN EXTRACTED FROM THE BOOK
FINITE ELEMENT PROGRAMMING FOR PLATES AND SHELLS
BY HINTON AND OWEN

SURESH N.

JULY 1989

SUBROUTINE ALGOR(FIXED, KITER, IITER, KRESL, MTOTV, NALCO,
NTOTV, KUNLO, KINCS)

-----THIS SUBROUTINE SETS EQUATION RESOLUTION INDEX, KRESL

DIMENSION FIXED(MTOTV)

KRESL = 2

IF(NALGO.EQ.1.AND.KITER.EQ.2) KRESL = 1

IF(NALGO.EQ.2) KRESL=1

IF(NALGO.EQ.3.AND.IITER.EQ.1) KRESL = 1

IF(NALGO.EQ.4.AND.KITER.EQ.2) KRESL = 1

IF(NALGO.EQ.4.AND.IITER.EQ.2) KRESL = 1

IF(NALGO.EQ.4.AND.KUNLO.GT.0) KRESL = 1

IF(KITER.EQ.(KINCS+1+1)) KRESL = 1

IF(IITER.EQ.1) RETURN

DO 100 ITOTV = 1, NTOTV

FIXED(ITOTV) = 0.0

CONTINUE

RETURN

END

SUBROUTINE BGMAT, FORMS THE [Bo] MATRIX AND THE [G] MATRIX

SUBROUTINE BGMAT(COORD, DICOS, LNODS, MATNO, MELEM,
MLAYR, MMATS, MPOIN, M3POI, NELEM,
NEVAB, NGAUS, NGAUZ, NLAYR, NNODE, NPROP,
POSGP, PROPS, THICK, WEIGP)

THIS SUBROUTINE COMPUTES BMATX AND GMATX (THE LATTER FOR LARGE
DISPLACEMENT ANALYSIS). THESE MATRICES ARE STORED ON TAPE 8 FOR
LATER SELECCTIVE INTEGRATION(TRANSVERSE SHEAR TERMS)CAN BE
ACCOUNTED FOR).

COMMON WORMX(3,24), GVALU, DJACB
DIMENSION BMATX(5,45), BDUMY(8,45), COORD(MPOIN,8), DICOS(3,M3POI),
FUNCT(4), GMATX(2,45), LNODS(MELEM,9), MATNO(MELEM,MLAYR),
POSGP(5), PROPS(MMATS,NPROP), THICK(MPOIN), SHAPE(3,9),
WEIGP(5)

REWIND 8

LGAUS = NGAUS - NGAUZ

LGAUS = 0 FOR NORMAL OR REDUCED INTEGRATION RULE,

LGAUS = 1 FOR SELECTIVE INTEGRATION RULE

WRITE(5,*) 'NELEM IN BGMAT=', NELEM

DO 100 IELEM = 1, NELEM

WRITE(5,*)

WRITE(5,*) 'IELEM=', IELEM

WRITE(5,*)

IF(LGAUS.EQ.0) GO TO 25

NBORP = 0

REDUCED INTEGRATION IS USED TO SET UP THE TRANSVERSE SHEAR TERMS OF
THE [B] MATRIX, FIRSTLY THESE TERMS ARE STORED IN BDUMY MATRIX

CONS1 = 1.0/POSGP(4)

CONS2 = -CONS1

ZETSP = 0.0

KGAUZ = -1

DO 20 IGAUZ = 1, NGAUZ

```

DO 15 IEVAB =1,NEVAB
DO 15 IPOSI = 1,2
JPOSI = 2*KGAUZ+IPOSI
BDUMY(JPOSI,IEVAB) = GMATX(IPOSI,IEVAB)
CONTINUE

```

```

      NBORP = 1
      DO 50 IGAUS =1, NGAUS
      DO 50 JGAUS =1, NGAUS
         WRITE(5,*) 'IGAUS.....JGAUS...', IGAUS, JGAUS
      EXISP = POSGP(IGAUS)
      ETASP = POSGP(JGAUS)
         WRITE(20,*) 'POSGP"S IN BGMAT'
         WRITE(20,*) POSGP(IGAUS), POSGP(JGAUS)
      CALL      SFR1(SHAPE, EXISP, ETASP)
         WRITE(20,*) 'COMES OUT OF SHAPE IN BGMAT'
         WRITE(20,777)((SHAPE(III, JJJ), JJJ=1,9), III=1,3)
         FORMAT(1X, 3F14.7)

```

```

      ZETSP = -1.0
      DO 45 ILAYR = 1,NLAYR
      LPROP = MATNO(IELEM,ILAYR)
      DZETA = PROPS(LPROP,3)
      ZETSP = ZETSP+DZETA/2.0
      CALL FUNC(BMATX, SHAPE, THICK, NBORP, NNODE, ZETSP, MELEM,
               COORD, DICOS, LNODS, IELEM, MPOIN, M3POI, GMATX)
      WRITE(5,*) '***** F U N C E N D S *****', LGAUS
      PAUSE
      DVOLU = DJACB*WEIGP(IGAUS)*WEIGP(JGAUS)*DZETA
      IF(LGAUS.EQ.0) GO TO 40

```

```

FUNCT(1) = 0.25*(1.0+CONS1*EXISP)*(1.0+CONS1*ETASP)
FUNCT(2) = 0.25*(1.0+CONS1*EXISP)*(1.0+CONS2*ETASP)
FUNCT(3) = 0.25*(1.0+CONS2*EXISP)*(1.0+CONS1*ETASP)
FUNCT(4) = 0.25*(1.0+CONS2*EXISP)*(1.0+CONS2*ETASP)

```

```

      INTERPOLATE THE TRANSVERSE SHEAR TERM OF BMATX FROM 4 TO 9 G.P
      DO 30 IEVAB = 1,NEVAB
      DO 30 IDOFN = 4,5
      BMATX(IDOFN,IEVAB) = 0.0
      DO 30 INTPO =1,4
      IGASH = 2*INTPO+IDOFN-5
      BMATX(IDOFN,IEVAB) = BMATX(IDOFN,IEVAB)+FUNCT(INTPO)*
      BDUMY(IGASH,IEVAB)

```

```
CONTINUE
WRITE(8) BMATX, GMATX, DVOLU
ZETSP = ZETSP + DZETA/2.0
CONTINUE
CONTINUE
```

```
WRITE(30,*) 'IELEM =', IELEM  
WRITE(30,666) ((BMATX(I,J), J=1,45), I=1,5)  
FORMAT(1X, 5E14, 7/1X, 5E14, 7/1X, 5E14, 7/1X, 5E14, 7/  
       /1X, 5E14, 7, /1X, 5E14, 7, /1X, 5E14, 7/1X, 5E14, 7)
```

CONTINUE
RETURN
END

```

SUBROUTINE CHECK1, THIS CHECKS THE MAIN CONTROL DATA

```

SUBROUTINE CHECK1(NDOFN, NELEM, NGAUS, NMATS, NNODE, NPOIN,
MMATS, NVFIX, NGAUZ, NLAYR)

```

DIMENSION NEROR(20)
DO 10 IEROR = 1,4
  NEROR(IEROR) = 0

```

CREATE THE DIAGNOSTIC MESSAGES

```

IF(NPOIN.LE.0) NEROR(1) =1
IF(NELEM*NNODE.LT.NPOIN) NEROR(2) = 1
IF(NVFIX.LT.2.OR.NVFIX.GT.NPOIN) NEROR(3) =1
IF(NNODE.LT.8.OR.NNODE.GT.9) NEROR(4) =1
IF(NDOFN.NE.5.OR.NLAYR.GT.10) NEROR(5) =1
IF(NMATS.LT.1.OR.NMATS.GT.MMATS) NEROR(6) =1
IF(NGAUS.LT.2.OR.NGAUS.GT.3) NEROR(7) =1
IF(NGAUZ.LT.2.OR.NGAUZ.GT.3) NEROR(8) =1

```

EITHER RETURN, OR ELSE PRINT THE ERROR DIAGNOSIS

```

KEROR = 0
DO 20 IEROR = 1,8
  IF(NEROR(IEROR).EQ.0) GO TO 20
  KEROR = 1
  WRITE(6,900) IEROR
    FORMAT(/31H,***DIAGNOSIS BY CHECK1, ERROR, I3)
    FORMAT(25HDIAGNOSIS BY CHECK1 ERROR, I3)
  CONTINUE
  IF(KEROR.EQ.0) RETURN
  OTHERWISE ECHO ALL THE REMAINING DATA WITHOUT FURTHER COMMENT

CALL ECHO
END

```

```

-----
SUBROUTINE CHECK2(COORD, IFFIX, LNODS, MATNO, MELEM, MFRON, MPOIN,
  MTOTV, MVFIX, NDFRO, NDOFN, NELEM, NMATS, NNODE, NOFIX,
  NPOIN, NVFIX, NLAYR)
-----

```

THIS SUBROUTINE CHECKS THE REMAINDER OF THE INPUT DATA

```

DIMENSION COORD(MPOIN,8), IFFIX(MTOTV), LNODS(MELEM,12),
  MATNO(MELEM,NLAYR), NDFRO(MELEM), NEROR(20), NOFIX(MVFIX)

```

CHECK AGAINST TWO IDENTICAL NONZERO NODAL DISPLACEMENTS

```

DO 5 IEROR = 9,20
  NEROR(IEROR) = 0
DO 10 IELEM = 1,NELEM
  NDFRO(IELEM) = 0
DO 50 IPOIN = 2,NPOIN
  KPOIN = IPOIN-1
DO 30 JPOIN = 1,KPOIN
DO 20 IDIME=1,3
  IF(COORD(IPOIN, IDIME).NE.COORD(JPOIN, IDIME)) GO TO 30
  CONTINUE
  NEROR(9) = NEROR(9)+1
  CONTINUE
CONTINUE

```

CHECK THE LIST OF ELEMENT PROPERTY NUMBERS

```

DO 50 IELEM = 1,NELEM
DO 50 ILAYR = 1,NLAYR
  IF(MATNO(IELEM, ILAYR).GT.NMATS) NEROR(10) = NEROR(10)+1

```

CHECK FOR IMPOSSIBLE NODE NUMBERS

```

DO 70 IELEM = 1,NELEM
DO 60 INODE = 1,NNODE
  IF(LNODS(IELEM, INODE).EQ.0) NEROR(11) = NEROR(11) + 1
  IF(LNODS(IELEM, INODE).LT.0.OR.LNODS(IELEM, INODE).GT.NPOIN)
    NEROR(12) = NEROR(12) + 1
  CONTINUE

```

CHECK FOR ANY REPETITION OF A NODE NUMBER WITHIN AN ELEMENT

```

DO 140 IPOIN = 1, NPOIN
KSTAR = 0
DO 100 IELEM = 1, NELEM
KZERO = 0
DO 90 INODE = 1, NNODE
IF(LNODS(IELEM, INODE).NE. IPOIN) GO TO 90
KZERO = KZERO + 1
IF(KZERO.GT.1) NEROR(13) = NEROR(13) +1

    SEEK FIRST, LAST AND INTERMEDIATE APPEARANCES OF NODE IPOIN

IF(KSTAR.NE.0) GO TO 80
KSTAR = IELEM

    CALCULATE INCREASE OR DECREASE IN FRONTWIDTH AT EACH ELEMENT STAGE
NDFRO(IELEM) = NDFRO(IELEM) + NDOFN
CONTINUE

    AND CHANGE THE SIGN OF THE LAST APPEARANCE OF EACH NODE
KLAST = IELEM
NLAST = INODE
CONTINUE
CONTINUE
IF(KSTAR.EQ.0) GO TO 110
IF(KLAST.LT.NELEM) NDFRO(KLAST+1) = NDFRO(KLAST+1) - NDOFN
LNODS(KLAST, NLAST) = -IPOIN
GO TO 140

    CHECK THAT CO-ORDINATES FOR AN UNUSED NODE HAVE NOT BEEN SPECIFIED
WRITE(6,900) IPOIN
FORMAT(/15HCHECK WHY NODE, I4, 14H NEVER APPEARS)
FORMAT(/14HCHECK WHY NODE, I4, 14H NEVER APPEARS)
NEROR(14) = NEROR(14) +1
SIGMA = 0.0
DO 120 IDIME = 1, 3
    SIGMA = SIGMA + ABS(COORD(IPOIN, IDIME))
IF(SIGMA.NE.0.0) NEROR(15) = NEROR(15) +1

    CHECK THAT AN UNUSED NODE NUMBER IS NOT A RESTRAINED NODE
DO 130 IVFIX = 1, NVFIX
    IF(NOFIX(IVFIX).EQ. IPOIN) NEROR(16) = NEROR(16) +1
CONTINUE

    CALCULATE THE LARGEST FRONTWIDTH'
NFRON = 0
KFRON = 0
DO 150 IELEM = 1, NELEM
NFRON = NFRON + NDFRO(IELEM)
    IF (NFRON.GT.KFRON) KFRON = NFRON
WRITE(6,905) KFRON
FORMAT(/33H MAXIMUM FRONTWIDTH ENCOUNTERED =, I5/)
IF(KFRON.GT.MFRON) NEROR(17) =1

    CONTINUE CHECKING DATA FOR THE FIXED VALUES
DO 170 IVFIX = 1, NVFIX
IF(NOFIX(IVFIX).LE.0.OR.NOFIX(IVFIX).GT.NPOIN) NEROR(18)
=NEROR(18)+1
8)+1

KOUNT = 0
NLOCA = (NOFIX(IVFIX)-1)*NDOFN
DO 160 IDOFN = 1, NDOFN
NLOCA = NLOCA +1
    IF(IVFIX(NLOCA).GT.0) KOUNT =1
IF(KOUNT.EQ.0) NEROR(19) = NEROR(19) +1
KVFIX = IVFIX -1
DO 170 JVFIX = 1, KVFIX
    IF((IVFIX.NE.1).AND.(NOFIX(IVFIX).EQ.NOFIX(JVFIX)))
        NEROR(20) = NEROR(20) + 1
KEROR = 0
DO 180 IEROR = 9, 20

```

```
IF(NEROR(IEROR).EQ.0) GO TO 180
```

```
KEROR = 1
```

```
WRITE(6,910) IEROR,NEROR(IEROR)
```

```
FORMAT(//25HDIAGNOSIS BY CHECK2 ERROR,I3,6X,9HASSTD NO.,I5)
```

```
CONTINUE
```

```
IF(KEROR.NE.0) GO TO 200
```

```
RETURN ALL NODAL CONNECTION NUMBERS TO POSITIVE VALUES
```

```
DO 190 IELEM = 1,NELEM
```

```
DO 190 INODE = 1,NNODE
```

```
LNODS(IELEM,INODE) = IABS(LNODS(IELEM,INODE))
```

```
RETURN
```

```
CALL ECHO
```

```
END
```

```
SUBROUTINE CONVER
```

```
SUBROUTINE CONVER(ELOAD,IITER,LNODS,MELEM,MEVAB,MTOTV,NCHEK,  
NDOFN,NELEM,NEVAB,NNODE,NTOTV,STFOR,  
TLOAD,TOFOR,TOLER)
```

```
THIS SUBROUTINE CHECKS FOR CONVERGENCE OF THE ITERATION PROCESS
```

```
DIMENSION ELOAD(MELEM,MEVAB),LNODS(MELEM,12),STFOR(MTOTV),  
TOFOR(MTOTV),TLOAD(MELEM,MEVAB)
```

```
NCHEK = 0
```

```
RESID = 0.0
```

```
RETOT = 0.0
```

```
REMAX = 0.0
```

```
DO 5 ITOTV = 1,NTOTV
```

```
STFOR(ITOTV) = 0.0
```

```
TOFOR(ITOTV) = 0.0
```

```
CONTINUE
```

```
DO 40 IELEM = 1,NELEM
```

```
KEVAB = 0
```

```
DO 40 INODE = 1,NNODE
```

```
LOCNO = IABS(LNODS(IELEM,INODE))
```

```
DO 40 IDOFN = 1,NDOFN
```

```
KEVAB = KEVAB + 1
```

```
NPOSI = (LOCNO-1)*NDOFN+IDOFN
```

```
STFOR(NPOSI) = STFOR(NPOSI) + ELOAD(IELEM,KEVAB)
```

```
TOFOR(NPOSI) = TOFOR(NPOSI) + TLOAD(IELEM,KEVAB)
```

```
DO 50 ITOTV = 1,NTOTV
```

```
REFOR = TOFOR(ITOTV) - STFOR(ITOTV)
```

```
RESID = RESID + REFOR*REFOR
```

```
RETOT = RETOT + TOFOR(ITOTV) * TOFOR(ITOTV)
```

```
AGASH = ABS(REFOR)
```

```
IF(AGASH.GT.REMAX) REMAX = AGASH
```

```
DO 10 IELEM = 1,NELEM
```

```
DO 10 IEVAB = 1,NEVAB
```

```
ELOAD(IELEM,IEVAB) = TLOAD(IELEM,IEVAB) - ELOAD(IELEM,IEVAB)
```

```
RESID = SQRT(RESID)
```

```
RETOT = SQRT(RETOT)
```

```
RATIO = 100.0*RESID/RETOT
```

```
IF(RATIO.GT.TOLER) NCHEK = 1
```

```
IF(IITER.EQ.1) GO TO 20
```

```
IF(RATIO.GT.PVALU) NCHEK = 999
```

```
PVALU = RATIO
```

```
WRITE(6,30) NCHEK,RATIO,REMAX
```

```
FORMAT(1H0,3X,17HCONVERGENCE CODE=,I4,3X,29HNORM OF RESIDUAL SUM M
```

```
RATIO =,E14.6,3X,18HMAXIMUM RESIDUAL =,E14.6)
```

```
RETURN
```

```
END
```

```
-----  
SUBROUTINE DIMEN(MBUFA,MELEM,MEVAB,MFRON,MMATS,MPOIN,MSTIF,MTOTG,  
MTOTV,MVFIX,NDOFN,NPROP,NSTRE,M3POI,MLAYR)  
-----
```

```
THIS SUBROUTINE PRESETS VARIABLES ASSOCIATED WITH DYNAMIC  
DIMENSIONING  
-----
```

```
MBUFA = 10
```

```
MELEM = 20
```

```
MFRON = 75
```

```
MLAYR = 10
```



```

MMATS = 5
MPOIN = 100
M3POI = 3*MPOIN
NDOFN = 5
NSTRE = 5
MEVAB = NDOFN*9
MSTIF = (MFRON+1)*MFRON/2
MTOTG = MELEM*MLAYR*9
MTOTV = MPOIN*NDOFN
MVFIX = 36
NPROP = 17
WRITE(5,*) 'SOME DATA IN DIMENSION'
WRITE(5,*) MFRON, MLAYR, MMATS, MPOIN, M3POI, NDOFN, NSTRE, MEVAB,
MSTIF, MTOTG, MVFIX
RETURN

```

```
END
```

```

-----
SUBROUTINE ECHO
SUBROUTINE ECHO
-----

```

```

IF DATA ERRORS HAVE BEEN DETECTED BY SUBROUTINES CHECK1 OR
CHECK2, THIS ROUTINE READS AND WRITES THE REMAINING DATA CARDS
-----

```

```

DIMENSION NTITL(80)
WRITE(6,900)
FORMAT(/50H NOW FOLLOWS A LISTING OF POST-DISASTER DATA CARDS) /)
READ(15,905) NTITL
FORMAT(80A1)
WRITE(6,910) NTITL
FORMAT(20X,80A1)
GO TO 10
END

```

```

-----
SUBROUTINE FLOWS(ABETA, AVECT, DVECT, LPROP, MMATS, NPROP, PROPS,
SG, A, DMATT)
-----

```

```

THIS SUBROUTINE CALCULATES THE FLOW VECTOR -AVECT- AND COMPUTES
-DVECT- AND -ABETA-
-----

```

```

DIMENSION AVECT(5), DMATT(5,5,MMATS), DVECT(5),
PROPS(MMATS,NPROP), SG(5), A(9,MMATS)

```

```
SET UP MATERIAL PROPERTIES
```

```
HARDS = PROPS(LPROP,7)
```

```
COMPUTES THE VECTOR AVECT
```

```

L = LPROP
AFUNC = (A(1,L)*SG(1)+2.0*A(2,L)*SG(1)*SG(2)+2.0*A(3,L)*
SG(1)*SG(3)+A(4,L)*SG(2)*SG(2)+2.0*A(5,L)*SG(2)*SG(3)+
A(6,L)*SG(3)*SG(3)+A(7,L)*SG(4)*SG(4)+2.0*A(8,L)*SG(4)*
SG(5)+A(9,L)*SG(5)*SG(5))*0.5
AVECT(1) = (A(1,L)*SG(1)+A(2,L)*SG(2)+A(3,L)*SG(3))/AFUNC
AVECT(2) = (A(2,L)*SG(1)+A(4,L)*SG(2)+A(5,L)*SG(3))/AFUNC
AVECT(3) = (A(3,L)*SG(1)+A(5,L)*SG(2)+A(6,L)*SG(3))/AFUNC
AVECT(4) = (A(7,L)*SG(4)+A(8,L)*SG(5))/AFUNC
AVECT(5) = (A(8,L)*SG(4)+A(9,L)*SG(5))/AFUNC
WRITE(6,910) AVECT
FORMAT(8H AVECT =, 5E15.6)

```

```
COMPUTE DVECT = DMATX*AVECT
```

```

DO 10 I = 1,5
DVECT(I) = 0.0
DO 10 J = 1,5
DVECT(I) = DVECT(I) + DMATT(I,J,LPROP)*AVECT(J)
WRITE(6,920) DVECT
FORMAT(8H DVECT =, 5E15.6)

```

```

DENOM = HARDS
DO 20 ISTR = 1,5
DENOM = DENOM + AVECT(ISTR)*DVECT(ISTR)
ABETA = 1.0/DENOM
WRITE(6,930) ABETA

```

```

930      FORMAT(8H ABETA =, E15.6)
      RETURN
      END
-----
      SUBROUTINE FRAME(N1,N2,N3,NOPN)

      *****
      MULTIPLE VECTOR AND/OR MATRIX MANIPULATIONS
      *****

      NOPN = 1, CREATE UNIQUE ORTHOGONAL AXES IN MATRIX N1 INCLUDING VEC
      NOPN = 2, SCISSORS ON OTHER TWO VECTORS IN N1, THEN N2 MADE ORTHO
      NOPN = 3, BEST ORTHOGONAL APPROXIMATION TO GIVEN NON-CARTESIAN FRA
      NOPN = 4, N2 BECOMES N1*N2*N1 USING N3 = GASH
      NOPN = 5, N2 BECOMES N1*N2*N1T USING N3 = GASH
      *****

      COMMON NORMX(3,24), QVALU, DJACOB
      WRITE(5,*) 'ENTERING FRAME WITH N1,N2,N3,NOPN AS'
      WRITE(5,*) N1,N2,N3,NOPN
      M3 = N1 +2
      I2 = N2 -1
      WRITE(5,*) 'M3,I2 IN FRAME.....',M3,I2
      IF(I2.GE.N1) GO TO 10
      I2 = I2 +3
      I1 = N1 + N1+N1 + 3 -N2 -I2
      WRITE(5,*) 'SINCE I2.GE.N1, I1=', I1,N1,N2,I2
      GO TO (1,2,3,4,5),NOPN
      WORMX(1,I1) = WORMX(3,N2)
      WRITE(5,*) '-----I1', I1
      WORMX(2,I1) = 0.0
      WORMX(3,I1) = -WORMX(1,N2)
      IF(WORMX(1,I1).EQ.0.0.AND.WORMX(3,I1).EQ.0.0)
        WORMX(1,I1) = -WORMX(2,N2)
      CALL VECT(N2,I1,I2,4)
      GO TO 14
      CALL MATM(I1,I2,0,7)
      CALL VECT(I1,I2,N2,4)
      WRITE(5,*) 'CALL.....ING MATM'
      CALL MATM(N1,N1,0,6)
      RETURN
      I1 = N1 +1
      I2 =M3
      DO 11 I =1,50
      DO 11 N =N1,M3
      CALL MATM(I1,I2,0,7)
      I1=I2
      I2=N
      RETURN
      CALL MATM(N1,N2,N3,2)
      NLPN =3
      CALL MATM(N3,N1,N2,NLPN)
      RETURN
      CALL MATM(N1,N2,N3,3)
      CALL SINGOP(N3,3)
      CALL MATM(N1,N3,N2,3)
      RETURN
      END
      SUBROUTINE FRONT
      SUBROUTINE FRONT(ASDIS,ELOAD,EGRHS,EQUAT,ESTIF,FIXED,
        GLOAD,GSTIF,IFFIX,IINCS,ITER,KRESL,
        LOCEL,LNODS,MBUFA,MELEM,MEVAB,MFRON,
        MSTIF,MTOTV,MVFIX,NACVA,NAMEV,NDEST,
        NDOFN,NELEM,NEVAB,NNODE,NOFIX,NPIVO,
        NPOIN,NTOTV,TDISP,TLOAD,TREAC,VECRV)
      *****
      THIS SUBROUTINE UNDERTAKES EQUATION SOLUTION BY THE
      FRONTAL METHOD.
      *****

      DIMENSION ASDIS(MTOTV),ELOAD(MELEM,MEVAB),EGRHS(MBUFA),
        EQUAT(MFRON,MBUFA),ESTIF(MEVAB,MEVAB),FIXED(MTOTV),
        GLOAD(MFRON),GSTIF(MSTIF),IFFIX(MTOTV),
        LNODS(MELEM,9),LOCEL(MEVAB),NACVA(MFRON),NAMEV(MBUFA),
        NDEST(MEVAB),NOFIX(MVFIX),NPIVO(MBUFA),TDISP(MTOTV),
        TLOAD(MELEM,MEVAB),TREAC(MVFIX,NDOFN),VECRV(MFRON)

```

```

NFUNC(I,J) = (J*J-J)/2+I
WRITE(5,*)'VALUE OF KRESL AT BEGINING',KRESL
WRITE(5,*)'VALUE OF NDOFN,NPOIN IN BEGIN OF FRONT',NDOFN,NPOIN
WRITE(5,*)'VALUE OF NTOTV AT BEGINIG OF FRONT',NTOTV
IIRSL = KRESL
WRITE(5,*)'VALUE OF IIRSL AT BEGINING',IIRSL

WRITE(5,*)'VALUE OF NELEM,NEVAB',NELEM,NEVAB
WRITE(5,*)'VALUE OF ELOAD IN FRONT BEGINING'
WRITE(5,*)((ELOAD(I,J),J=1,NEVAB),I=1,NELEM)
CHANGE THE SIGN OF THE LAST APPEARANCE OF EACH NODE

```

```

WRITE(5,*)'CHANGE THE SIGN OF THE LAST APPEARANCE OF EACH NODE'
IF(IINCS.GT.1.OR.IITER.GT.1) GO TO 455
DO 140 IPOIN = 1,NPOIN
KLAST = 0
DO 130 IELEM = 1,NELEM
DO 120 INODE = 1,NNODE
IF(LNODS(IELEM,INODE).NE.IPOIN) GO TO 120
KLAST = IELEM
NLASt = INODE
CONTINUE
CONTINUE
IF(KLAST.NE.0) LNODS(KLAST,NLAST) = -IPOIN
CONTINUE
CONTINUE

```

START BY INITIALIZING EVERYTHING THAT MATTERS TO ZERO

```

WRITE(5,*)'START BY INITIALIZING EVERYTHING THAT MATTERS TO ZERO'
WRITE(5,*)'***MBUFA, MSTIF,KRESL***',MBUFA,MSTIF,KRESL,IIRSL
DO 145 IBUFA = 1,MBUFA
EGRHS(IBUFA) = 0.0
KKRSL = KRESL
WRITE(5,*)'KRESL, IIRSL, KKRSL, AFTER EGRHS = 0.0',IIRSL,KRESL,KKRSL
DO 150 ISTIF = 1,MSTIF
GSTIF(ISTIF) = 0.0
WRITE(5,*)'****AFTER GSTIF = 0.0*****'
DO 160 IFRON = 1,MFRON
GLOAD(IFRON) = 0.0
VECRV(IFRON) = 0.0
NACVA(IFRON) = 0
DO 160 IBUFA = 1,MBUFA
EQUAT(IFRON,IBUFA) = 0.0
WRITE(5,*)'IIRSL, KKRSL, KRESL AFTER 160 CON',IIRSL,KKRSL,KRESL

```

AND PREPARE FOR DISC READING AND WRITING OPERATIONS

```

WRITE(5,*)'AND PREPARE FOR DISC READING AND WRITING OPERATIONS'
NBUFA = 0
WRITE(5,*)'VALUES OF KRESL AFTER DISC...',KRESL,IIRSL,KKRSL
IF(KRESL.GT.1) NBUFA = MBUFA
REWIND 1
REWIND 2
REWIND 4
REWIND 7
WRITE(5,*)'AFTER RWINDING II, KK, KR',IIRSL,KKRSL,KRESL

```

ENTER MAIN ELEMENT ASSEMBLY-REDUCTION LOOP

```

WRITE(5,*)'ENTER MAIN ELEMENT ASSEMBLY-REDUCTION LOOP'
NFRON = 0
KELVA = 0
IIRSL = KRESL
WRITE(5,*)'+++++VALUE OF IIRSL,KRESL+++++',IIRSL,KRESL
DO 320 IELEM = 1,NELEM
WRITE(5,*)'IELEM, IIRSL',IELEM,IIRSL
WRITE(25,*)'IELEM, IIRSL',IELEM,IIRSL
IF(IIRSL.GT.1) GO TO 400
KEVAB = 0
READ(1) ESTIF
DO 170 INODE = 1,NNODE
DO 170 IDOFN = 1,NDOFN
NPOSI = (INODE-1)*NDOFN+IDOFN
LOCNO = LNODS(IELEM,INODE)
IF(LOCNO.GT.0) LOCEL(NPOSI) = (LOCNO-1)*NDOFN+IDOFN
IF(LOCNO.LT.0) LOCEL(NPOSI) = (LOCNO+1)*NDOFN-IDOFN

```

CONTINUE

START AT LOOKING FOR EXISTING DESTINATIONS

```

WRITE(5,*) 'START BY LOOKING FOR EXISTING DESTINATIONS'
DO 210 IEVAB =1, NEVAB
  NIKNO = IABS(LOC(IEVAB))
  KEXIS = 0
  WRITE(25,*) 'NIKNO AT AFTER KEXIS =0.0', NIKNO, IABS(LOC(IEVAB))
  WRITE(5,*) 'NFRON=', NFRON
  DO 180 IFRON =1, NFRON
    WRITE(25,*) 'IFRON, NIKNO, NACVA IN 180', IFRON, NIKNO, NACVA(IFRON)
    IF(NIKNO.NE.NACVA(IFRON)) GO TO 180
    KEVAB = KEVAB + 1
    KEXIS = 1
    NDEST(KEVAB) = IFRON
  CONTINUE
  IF(KEXIS.NE.0) GO TO 210

```

WE NOW SEEK NEW EMPTY PLACES FOR DESTINATION VECTOR

```

DO 190 IFRON =1, MFRON
  WRITE(25,*) 'NACVA AT 190 FIRST', NACVA(IFRON)
  IF(NACVA(IFRON).NE.0) GO TO 190
  NACVA(IFRON) = NIKNO
  WRITE(25,*) 'NACVA, NIKNO IN 190 SECOND', NACVA(IFRON), NIKNO
  KEVAB = KEVAB+1
  NDEST(KEVAB) = IFRON
GO TO 200
CONTINUE

```

THE NEW PLACES MAY DEMAND AN INCREASE IN CURRENT FRONTWIDTH

```

IF(NDEST(KEVAB).GT.NFRON) NFRON = NDEST(KEVAB)
CONTINUE
WRITE(5,*) 'COMES OUT OF, WE NOW SEEK EMPTY PLACES.....'
WRITE(7) LOC, NDEST, NACVA, NFRON
WRITE(5,*) 'WRITES ON TO UNIT 7'
WRITE(5,*) LOC, NDEST, NACVA, NFRON
GO TO 400
IF(IIRSL.GT.1) READ(7) LOC, NDEST, NACVA, NFRON

```

```

WRITE(5,*) 'START ASSEMBLING ELEMENT LOADS'
ASSEMBLE ELEMENT LOADS
WRITE(5,*) 'ELEMENT STIFFNESSES BUT NOT IN RESOLUTION'
WRITE(5,*) 'ELEMENT NO.=', IELEM
WRITE(20,*) 'ELEMENT NO.=', IELEM
WRITE(5,*) '(ESTIF(IF, JF), JF=IF, IF), IF=1, 45)

```

```

WRITE(45,*) 'ELEMENT NO.=', IELEM
DO 220 IEVAB =1, NEVAB
  IDEST = NDEST(IEVAB)
  GLOAD(IDEST) = GLOAD(IDEST) + ELOAD(IELEM, IEVAB)
  WRITE(50,*) 'NEVAB, IEVAB, IDEST, GLOAD, ELOAD'
WRITE(50,*) NEVAB, IEVAB, IDEST, GLOAD(IDEST), ELOAD(IELEM, IEVAB)

```

ASSEMBLE THE ELEMENT STIFFNESSES BUT NOT IN RESOLUTION

```

IF(IIRSL.GT.1) GO TO 402
DO 222 JEVAB =1, IEVAB
  WRITE(45,*) 'NEVAB, IEVAB, JEVAB, NDEST(IEVAB), NDEST(JEVAB)'
  WRITE(45,*) NEVAB, IEVAB, JEVAB, NDEST(IEVAB), NDEST(JEVAB)
  JDEST = NDEST(JEVAB)
  NGASH = NFUNC(IDEST, JDEST)
  NGISH = NFUNC(JDEST, IDEST)
  IF(JDEST.GE.IDEST) GSTIF(NGASH)=GSTIF(NGASH)+ESTIF(IEVAB, JEVAB)
  IF(JDEST.LT.IDEST) GSTIF(NGISH)=GSTIF(NGISH)+ESTIF(IEVAB, JEVAB)
  WRITE(45,*) 'VALUEOF NGASH, NGISH, GSTIF, IDEST, JDEST, ESTIF, VBS'
  WRITE(45,*) NGASH, NGISH, GSTIF(NGASH), GSTIF(NGISH), IDEST, JDEST,
    ESTIF(IEVAB, JEVAB), IEVAB, JEVAB
  CONTINUE
CONTINUE
CONTINUE

```

RE-EXAMINE EACH ELEMENT NODE, TO ENQUIRE WHICH CAN BE ELIMINATED

```

WRITE(5,*) 'RE-EXAMINE ELEMENT NODE.....'
WRITE(5,*) '..... IIRSL,KRESL.....', IIRSL, KRESL
WRITE(5,*) 'VALUE OF NEVAB =', NEVAB
WRITE(50,*) 'ELEMENT NO. =', IELEM
WRITE(50,*) 'VALUE OF GSTIF(406) INITIAL', GSTIF(406)
DO 310 IEVAB = 1, NEVAB
WRITE(5,*) 'VALUE OF IEVAB AT 310', IEVAB
NIKNO = -LOC(IEVAB)
WRITE(5,*) 'NIKNO= AT 310', NIKNO
IF(NIKNO.LE.0) GO TO 310

```

FIND POSITIONS OF VARIABLES READY FOR ELEIMINATION

```

WRITE(5,*) 'NFRON', NFRON
DO 300 IFRON = 1, NFRON
WRITE(5,*) '+++++IFRON =+++++', IFRON
WRITE(5,*) 'VALUE OF NACVA(IFRON), NIKNO', NACVA(IFRON), NIKNO
IF(NACVA(IFRON).NE.NIKNO) GO TO 300
NBUFA = NBUFA + 1
WRITE(50,*) 'IFRON=', IFRON, 'NBUFA=', NBUFA

```

WRITE EQUATIONS TO DISC OR TO TAPE

```

WRITE(5,*) 'WRITE EQUATIONS TO DISC OR TO TAPE'
WRITE(5,*) 'NBUFA, MBUFA', NBUFA, MBUFA
IF(NBUFA.LE.MBUFA) GO TO 406
NBUFA = 1
WRITE(5,*) 'VALUE OF NBUFA IF NBUFA GT MBUFA', NBUFA, IIRSL
IF(IIRSL.GT.1) GO TO 408
WRITE(2) EQUAT, EQRHS, NPIVO, NAMEV
GO TO 406
WRITE(4) EQRHS
READ(2) EQUAT, EQRHS, NPIVO, NAMEV
CONTINUE

```

EXTRACT THE CO-EFFICIENTS OF THE NEW EQUATION FOR ELEIMINATION

```

WRITE(5,*) 'EXTRACT THE CO-EFFICIENTS OF THE NEW EQUATION'
WRITE(5,*) '++++VALUE OF KRESL+++ ', IIRSL, KRESL
IF(IIRSL.GT.1) GO TO 404
IF(KRESL.GT.1) GO TO 404
WRITE(5,*) '..... MFRON=', MFRON, IFRON
WRITE(50,*) 'VALUE OF GSTIF(406) AFTER 406 CONT', GSTIF(406)
DO 230 JFRON = 1, MFRON
IF(IFRON.LT.JFRON) NLOCA = NFUNC(IFRON, JFRON)
IF(IFRON.GE.JFRON) NLOCA = NFUNC(JFRON, IFRON)
EQUAT(JFRON, NBUFA) = GSTIF(NLOCA)
GSTIF(NLOCA) = 0.0
CONTINUE

```

AND EXTRACT THE CORRESPONDING RIGHT HAND SIDES

```

WRITE(5,*) 'EXTRACT CORRESPONDING RHS'
EQRHS(NBUFA) = GLOAD(IFRON)
GLOAD(IFRON) = 0.0
KELVA = KELVA + 1
NAMEV(NBUFA) = NIKNO
NPIVO(NBUFA) = IFRON

```

DEAL WITH PIVOT

```

WRITE(5,*) 'NOW START DEALING WITH PIVOT'
WRITE(5,*) 'EQUAT(IFRON, NBUFA), IFRON, NBUFA', EQUAT(IFRON, NBUFA),
IFRON, NBUFA
EQUAT(3,3) = 1.0
PIVOT = EQUAT(IFRON, NBUFA)
WRITE(50,*) 'IFRON, NBUFA, PIVOT'
WRITE(50,*) IFRON, NBUFA, PIVOT
WRITE(5,*) 'NIKNO, PIVOT', NIKNO, PIVOT
IF(PIVOT.GT.0) GO TO 235
WRITE(6,900) NIKNO, PIVOT
FORMAT(1H0,3X,51HNEGATIVE OR ZERO PIVOT ENCOUNTERED FOR VARIABLE LE N
0, 14, 10H OF VALUE ,E17.6)
STOP
CONTINUE
EQUAT(IFRON, NBUFA) = 0.0

```

ENQUIRE WHETHER PRESENT VARIABLE IS FREE OR PRESCRIBED

IF (IFFIX(NIKNO).EQ.0) GO TO 250

DEAL WITH A PRESCRIBED DEFLECTION

DO 240 JFRON = 1, NFRON
 GLOAD(JFRON) = GLOAD(JFRON) - FIXED(NIKNO)*EQUAT(JFRON, NBUFA)
 GO TO 280

ELIMINATE A FREE VARIABLE - DEAL WITH THE RIGHT HAND SIDE FIRST

DO 270 JFRON = 1, NFRON
 GLOAD(JFRON) = GLOAD(JFRON) - EQUAT(JFRON, NBUFA)*EQRHS(NBUFA)/PIVOT

NOW DEAL WITH THE CO-EFFICIENTS IN CORE

IF (IIRSL.GT.1) GO TO 418
 IF (EQUAT(JFRON, NBUFA).EQ.0.0) GO TO 270
 NLOCA = NFUNC(0, JFRON)
 CUREQ = EQUAT(JFRON, NBUFA)
 DO 260 LFRON = 1, JFRON
 NGASH = LFRON + NLOCA
 GSTIF(NGASH) = GSTIF(NGASH) - CUREQ*EQUAT(LFRON, NBUFA)/PIVOT
 CONTINUE
 CONTINUE
 EQUAT(JFRON, NBUFA) = PIVOT

RECORD THE NEW VACANT SPACE, AND REDUCE FRONTWIDTH IF POSSIBLE

NACVA(IFRON) = 0
 GO TO 290

COMPLETE THE ELEMENT LOOP IN THE FORWARD ELIMINATION

CONTINUE
 IF (NACVA(NFRON).NE.0) GO TO 310
 NFRON = NFRON - 1
 IF (NFRON.GT.0) GO TO 290
 CONTINUE
 CONTINUE
 EQUAT(3,3) = 1.0
 IF (IIRSL.EQ.1) WRITE(2) EQUAT, EQRHS, NPIVO, NAMEV
 BACKSPACE 2

WRITE(5,4) 'ENTERS BACK-SUBSTITUTION PHASE...'
 ENTER BACK-SUBSTITUTION PHASE, LOOP BACKWARDS THROUGH VARIABLES

WRITE(50,4) 'KELVA=', KELVA, NBUFA
 DO 340 IELVA = 1, KELVA

READ A NEW BLOCK OF EQUATIONS - IF NEEDED

IF (NBUFA.NE.0) GO TO 412
 BACKSPACE 2
 READ(2) EQUAT, EQRHS, NPIVO, NAMEV
 BACKSPACE 2
 NBUFA = MBUFA
 IF (IIRSL.EQ.1) GO TO 412
 BACKSPACE 4
 READ(4) EQRHS
 BACKSPACE 4
 CONTINUE

PREPARE TO BACK-SUBSTITUTE FROM THE CURRENT EQUATION

IFRON = NPIVO(NBUFA)
 NIKNO = NAMEV(NBUFA)
 PIVOT = EQUAT(IFRON, NBUFA)
 IF (IFFIX(NIKNO).NE.0) VECRV(IFRON) = FIXED(NIKNO)
 IF (IFFIX(NIKNO).EQ.0) EQUAT(IFRON, NBUFA) = 0.0
 WRITE(50,*) 'IFRON, NIKNO, PIVOT, VECRV(IFRON), FIXED(NIKNO)'
 WRITE(50,*) IFRON, NIKNO, PIVOT, VECRV(IFRON), FIXED(NIKNO)

BACK-SUBSTITUTE IN THE CURRENT EQUATION

```

DO 330 JFRON = 1, MFRON
  EQRHS(NBUFA) = EQRHS(NBUFA) - VECRV(JFRON)*EQUAT(JFRON, NBUFA)

```

```

  PUT THE FINAL VALUES WHERE THEY BELONG

```

```

IF(IFFIX(NIKNO).EQ.0) VECRV(IFRON) = EQRHS(NBUFA)/PIVOT
IF(IFFIX(NIKNO).NE.0) FIXED(NIKNO) = -EQRHS(NBUFA)
NBUFA = NBUFA - 1
ASDIS(NIKNO) = VECRV(IFRON)
CONTINUE

```

```

WRITE(5,*) 'ADD DISPLACEMENTS.....'
ADD DISPLACEMENTS TO PREVIOUS TOTAL VALUES
WRITE(50,*) 'NTOTV=', NTOTV
DO 345 ITOTV = 1, NTOTV
  TDISP(ITOTV) = TDISP(ITOTV) + ASDIS(ITOTV)

```

```

WRITE(50,*) 'NTOTV, TDISP, ASDIS'
WRITE(50,*) 'NTOTV, (TDISP(ITD)), ITD=1, NTOTV'
WRITE(50,*) 'ASDIS(ITA), ITA=1, NTOTV'

```

```

STORE REACTIONS FOR PRINTING LATER

```

```

KBOUN = 1
DO 370 IPOIN = 1, NPOIN
  NLOCA = (IPOIN-1)*NDOFN
  DO 350 IDOFN = 1, NDOFN
    NGUSH = NLOCA + IDOFN
    IF(IFFIX(NGUSH).GT.0) GO TO 360

```

```

    CONTINUE

```

```

  GO TO 370

```

```

  DO 510 IDOFN = 1, NDOFN

```

```

  NGASH = NLOCA + IDOFN

```

```

    TREAC(KBOUN, IDOFN) = TREAC(KBOUN, IDOFN) + FIXED(NGASH)

```

```

    WRITE(5,*) 'IDOFN, KBOUN, TREAC(KBOUN, IDOFN), FIXED, NGASH'

```

```

  WRITE(5,*) 'IDOFN, KBOUN, TREAC(KBOUN, IDOFN), NGASH, FIXED(NGASH)'

```

```

  KBOUN = KBOUN + 1

```

```

CONTINUE

```

```

ADD REACTIONS INTO THE TOTAL LOAD ARRAY

```

```

WRITE(5,*) 'ADD REACTIONS'

```

```

DO 700 IPOIN = 1, NPOIN
DO 710 IELEM = 1, NELEM
DO 710 INODE = 1, NNODE
  NLOCA = IABS(LNODS(IELEM, INODE))

```

```

  IF(IPOIN.EQ.NLOCA) GO TO 720

```

```

  DO 730 IDOFN = 1, NDOFN

```

```

  NGASH = (INODE-1)*NDOFN + IDOFN

```

```

  MGASH = (IPOIN-1)*NDOFN + IDOFN

```

```

  WRITE(50,*) 'TLOAD(IELEM, NGASH), IELEM, NGASH'

```

```

  WRITE(50,*) 'TLOAD(IELEM, NGASH), IELEM, NGASH'

```

```

  TLOAD(IELEM, NGASH) = TLOAD(IELEM, NGASH) + FIXED(MGASH)

```

```

  CONTINUE

```

```

  WRITE(5,*) 'START RETURNING FROM FRONT'

```

```

  GO TO 333

```

```

RETURN

```

```

END

```

```

-----
SUBROUTINE FUNC

```

```

SUBROUTINE FUNC(BMATX, SHAPE, THICK, NBORP, NNODE, ZETA, MELEM,
  COORD, DICOS, LNODS, IELEM, MPOIN, M3POI, GMATX)

```

```

*****
SETS UP THE [B] MATRIX AND JACOBIAN, BEING THE MOST CHARECTERISTIC
SUBROUTINE OF THIS ELEMENT
*****

```

```

COMMON WORMX(3, 24), GVALU, DJACB
DIMENSION BMATX(5, 45), SHAPE(3, 9), THICK(MPOIN), GMATX(2, 45),
  COORD(MPOIN, 8), DICOS(3, M3POI), LNODS(MELEM, 9)

```

```

THIS CREATES X, Y, Z IN COLUMN 1 AND J-TRANSPOSE IN COLUMN 2-4

```

```

DO 20 I = 1, 3
DO 20 J = 1, 4

```

```

10      WORMX(I,J) = 0.0

      WRITE(20,*) 'SHAPE IN FUNC'
      WRITE(20,888) ((SHAPE(I,J), J=1,9), I=1,3)
888      FORMAT(1X,3F14.7)
      THE ELEMENT GEOMETRY IS DEFINED BY THE 8-NODE SERENDIPITY
      PPN = 8
      DO 24 INODE = 1,PPN
      IPOIN = IABS(LNODS(IELEM, INODE))
      WRITE(5,*) '####IPOIN IN FUNC####', IPOIN, IELEM, INODE
      DO 24 K = 1,3
      GTOP = COORD(IPOIN,K)
      GBOT = COORD(IPOIN,K+4)
      GOSH = ((1.0+ZETA)*GTOP + (1.0-ZETA)*GBOT)/2.0
      WRITE(5,*) 'GTOP, GBOT, GOSH...', GTOP, GBOT, GOSH
      DO 22 J = 1,3
      WRITE(20,*) 'WORMX(K,J)', WORMX(K,J), 'K=', K, 'J=', J
      WORMX(K,J) = WORMX(K,J) + GOSH*SHAPE(J, INODE)
      WORMX(K,4) = WORMX(K,4) + SHAPE(1, INODE)*(GTOP-GBOT)/2.0
      THIS CREATES J INVERSE IN COLUMNS 5-7 OF WORMX
      CALL MATM(2,5,0,1)
      DJACB = 1.0/QVALU
      EXIT FOR A CASE WHEN J, J-INVERSE AND DET-J ONLY ARE REQUIRED
      IF(NBORP.EQ.2) GO TO 50
      THIS CREATES DIRECTION ZETA NORMAL TO XI AND ETA
      CALL VECT(2,3,10,4)
      THIS CREATES A LOCAL CARTESIAN SET
      NFR = 8
      CALL FRAME(NFR,10,0,1)
      IF(NBORP.EQ.4) GO TO 50

      CREATES THE TERMS OF STRAIN/DISPLACEMENT MATRIX

      DO 40 INODE = 1,NNODE
      DO 40 INODE = 1,1
      DO 40 J = 1,5
      ***      5 SHAPE FUNCTIONS CREATED AT A NORMAL
      NSHAP = 5*(INODE-1) + J
      WRITE(20,*) 'INODE, J, NSHAP', INODE, J, NSHAP
      DO 26 I = 11,17
      DO 26 K = 1,3
      WORMX(K,I) = 0.0
      IF(J.GE.4) GO TO 30
      DO 29 K = 1,3
      ***      SHAPE AND XI AND ETA DERIVATIVES
      WORMX(K,K+10) = SHAPE(K, INODE)
      WRITE(20,*) 'WORMX(J,K+10) =', WORMX(J,K+10)
      GO TO 25
      JPOSI = J-2
      **      JPOSI IS 1,2 FOR LOCAL X,Y DEFLECTIONS OF ENDS OF NORMA
      DO 35 M = 1,3
      X,Y,Z COMPONENTS OF LOCAL X,Y DEFLECTIONS
      IPOIN = IABS(LNODS(IELEM, INODE))
      IPOSI = (IPOIN-1)*3
      GASH = EIGENM(IPOSI+JPOSI)
      IF(JPOSI.NE.2) GO TO 32
      GASH = -GASH
      DO 34 K = 1,4
      **      SHAPE AND ITS XT, ETA DERIVATIVES - K-4 GIVES SPECIAL ZETA DRIVATIVES
      IF(K.EQ.4) GO TO 31
      WORMX(M,K+10) = ZETA*SHAPE(K, INODE)*GASH*(THICK(IPOIN)/2.0)
      U,V,W ARE NOW IN COL 11
      GO TO 24
      WORMX(M,K+10) = SHAPE(1, INODE)*GASH*(THICK(IPOIN)/2.)
      CONTINUE
      CONTINUE
      THIS TRANSPOSES XI,ETA AND ZETA DERIVATIVES OF U,V,W
      CALL SINGOP(12,3)
      WRITE(5,*) 'COMES OUT OF SINGOP, J =', J
      MULTIPLIES BY J-INVERSE TO FORM X-Y-Z DERIVATIVES OF U,V,W
      CALL MATM(5,12,15,3)
      TRANSFERS X,Y,Z DERIVATIVES OF U,V,W FROM COL 15 TO COL 18
      WRITE(5,*) 'ENTERS MATM WITH NPN = 8'
      NPN = 8
      CALL MATM(15,18,0,NPN)
      WRITE(5,*) 'COMES OUT OF MATM WITH NOPN =3'

```



```

WRITE(5,*) 'COMES OUT OF MATM WITH NPON = 8'
WRITE(20,*) 'VALUE OF WORMX IN FUNC'
WRITE(20,1191) ((WORMX(IKI,JKJ)),JKJ=1,24),IKI=1,3)
191  FORMAT(1X,SE14.7)
THIS CONVERTS TO LOCAL AXES AT INTEGRATING POINT
INN = 8
JNN = 18
KNN = 31
CALL FRAME (INN,JNN,KNN,4)
WRITE(5,*)
WRITE(5,*) 'COMES OUT OF FRAME IN FUNC'
WRITE(20,*) 'VALUE OF WORMX IN FUNC'
1191 WRITE(20,1191) ((WORMX(IKI,JKJ)),JKJ=1,24),IKI=1,3)
FORMAT(1X,SE14.7)

```

```

SETS UP THE STRAIN MATRIX TERMS
IF(NBDRP.EQ.0) GO TO 39
BMTX(1,NSHAP) = WORMX(1,18)
BMTX(2,NSHAP) = WORMX(2,19)
BMTX(3,NSHAP) = WORMX(2,18) + WORMX(1,19)
BMTX(4,NSHAP) = WORMX(1,20) + WORMX(3,18)
BMTX(5,NSHAP) = WORMX(2,20) + WORMX(3,19)
WRITE(20,*) 'COMPONENTS OF BMTX'
WRITE(20,*) (BMTX(IK,NSHAP)),IK=1,5)
*   LOCAL STRAINS GO IN BMTX IN THE ORDER X,Y,XY,XZ,YZ
GMATX(1,NSHAP) = WORMX(1,20)
4** GMATX(2,NSHAP) = WORMX(2,20)
LOCAL DERIVATIVES GO IN -GMATX- IN THE ORDER DW/DX, DW/DY
GO TO 40
CONTINUE
*   TRANSVERSE SHEAR TERMS FOR SELECTIVE INTEGRATION
GMATX(1,NSHAP) = WORMX(1,20)+WORMX(3,18)
GMATX(2,NSHAP) = WORMX(2,20)+WORMX(3,19)
CONTINUE
WRITE(5,*) 'COMES OUT OF 40'
PAUSE
GO TO 50
50  WRITE(5,*) 'RETURNING BACK TO BGMAT'
RETURN
END

```

```

SUBROUTINE GAUSSG
SUBROUTINE GAUSSG(NGAUS,POSGP,WEIGP)
*****
THIS SUBROUTINE SETS UP THE GAUSS-LEGENDRE INTEGRATION CONSTANTS
*****
DIMENSION POSGP(5),WEIGP(5)
DO 2 IGASH = 1,5
POSGP(IGASH) = 0.0
WEIGP(IGASH) = 0.0
IF(NGAUS GT 2) GO TO 4
POSGP(1) = -0.577350269189626
WEIGP(1) = 1.0
GO TO 8
POSGP(1) = -0.774596669241483
POSGP(2) = 0.0
WEIGP(1) = 0.5555555555555556
WEIGP(2) = 0.8888888888888889
3  KGAUS = NGAUS/2
DO 10 IGASH = 1,KGAUS
JGASH = NGAUS + 1 - IGASH
POSGP(JGASH) = -POSGP(IGASH)
WEIGP(JGASH) = WEIGP(IGASH)
CONTINUE

```

```

EXTRA POSITION FOR TWO GAUSS POINT RULE(SELECTIVE INTEGRATION)
POSGP(4) = -0.57735026918926
WEIGP(4) = 1.0
POSGP(5) = -POSGP(4)
WEIGP(5) = WEIGP(4)
RETURN
END

```

```

SUBROUTINE GEOME(ESTIF,GMATX,STRSG,MEVAB,NEVAB,MTOTG,KGAUS,DVOLL)
*****

```

THIS SUBROUTINE CALCULATES THE GEOMETRIC MATRIX -GEMTX-

```

DIMENSION ESTIF(MEVAB,MEVAB), GMATX(2,45), STRSG(5,MTOTG),      45),
          GEMTX(45,45), GDUMM(2,45), STDUM(2,2)
DO 5 IEVAB =1,NEVAB
DO 5 JEVAB =1,NEVAB
  GEMTX(IEVAB,JEVAB) = 0.0

```

SET UP -STUDM- MATRIX WITH THE ACTUAL IN-PLANE STRESSES

```

STDUM(1,1) = STRSG(1,KGAUS)
STDUM(1,2) = STRSG(3,KGAUS)
STDUM(2,1) = STRSG(3,KGAUS)
STDUM(2,2) = STRSG(2,KGAUS)
EVALUATE THE PRODUCT OF STUDM*GMATX
DO 10 I =1,2
DO 10 IEVAB = 1,NEVAB
  GDUMM(I,IEVAB) = 0.0
DO 10 J =1,2
  GDUMM(I,IEVAB)=GDUMM(I,IEVAB)+STDUM(I,J)*GMATX(J,IEVAB)
CALCULATE THE GEOMETRIC MATRIX
DO 20 IEVAB =1,NEVAB
DO 20 JEVAB = IEVAB,NEVAB
DO 20 I =1,2
  GEMTX(IEVAB,JEVAB)=GEMTX(IEVAB,JEVAB)+GMATX(I,IEVAB)*
                    GDUMM(I,JEVAB)*DVOLU
EVALUATE THE NEW STIFFNESS MATRIX ADDING -GEMTX-
DO 30 IEVAB =1,NEVAB
DO 30 JEVAB =IEVAB,NEVAB
  ESTIF(IEVAB,JEVAB)=ESTIF(IEVAB,JEVAB)+GEMTX(IEVAB,JEVAB)
RETURN
END

```

SUBROUTINE INCREMENT

```

SUBROUTINE INCREMENT(ELoad, FIXED, IINCS, MELEM, MEVAB, MITER,
                    MTOTV, MVFIX, NDOFN, NELEM, NEVAB, NOUTP,
                    NOFIX, NTOTV, NVFIX, PRESC, RLOAD, TFACT,
                    TLOAD, TOLER, UNODS, IFFIX, NNODE, NCOLA,
                    NREST, KINCS)
*****
THIS SUBROUTINE INCREMENTS THE APPLIED LOADING
*****
DIMENSION ELOAD(MELEM,MEVAB), FIXED(MTOTV), NOUTP(2), NOFIX(MVFIX),
          PRESC(MVFIX, NDOFN), RLOAD(MELEM, MEVAB), TLOAD(MELEM, MEVAB),
          UNODS(MELEM, 7), IFFIX(MTOTV)
WRITE(50,*) (NREST, IINCS, KINCS, NEVAB)
WRITE(50,*) NREST, IINCS, KINCS
IF(NREST EQ 0) GO TO 20
IF(IINCS GT KINCS) GO TO 20
DO 10 IINCS = 1,KINCS
  READ(15,950) FACTO
  WRITE(5,900) IINCS
  FORMAT(///,5X,22H### INCREMENT NUMBER ,I5)
  READ(15,950) FACTO, TOLER, MITER, NOUTP(1), NOUTP(2)
  FORMAT(2F10.5,3I5)
  TFACT = TFACT + FACTO
  WRITE(6,960) TFACT, TOLER, MITER, NOUTP(1), NOUTP(2)
  FORMAT(1H0,5X,13HLOAD FACTOR =,F10.5,5X,
    24H CONVERGENCE TOLERANCE =,F10.5,5X,23HMAX. NO. OF ITERATIONS=,,
    15,7/32H INITIAL OUTPUT PARAMETER =,I5,5X,26HFINAL OUTPUT PA
    ARAMETER =,I5)
  WRITE(50,*) 'FACTO=', FACTO
DO 80 IELEM =1,NELEM
DO 80 IEVAB =1,NEVAB
  ELOAD(IELEM,IEVAB)=ELOAD(IELEM,IEVAB)+RLOAD(IELEM,IEVAB)*FACTO
  TLOAD(IELEM,IEVAB)=TLOAD(IELEM,IEVAB)+RLOAD(IELEM,IEVAB)*FACTO
  WRITE(50,*) 'ELOAD IN 80', ELOAD(IELEM,IEVAB), IELEM, IEVAB, RLOAD(
    IELEM,IEVAB)

  WRITE(50,*) 'SOME OUTPUTS FROM INCREMEN'
  WRITE(50,*) 'FACTO=', FACTO
  WRITE(50,*) 'RLOAD'
  WRITE(50,*) ((RLOAD(IL, JL), JL=1, NEVAB), IL=1, NELEM)
  WRITE(50,*) 'ELOAD'
  WRITE(50,*) ((ELOAD(IL, JL), JL=1, NEVAB), IL=1, NELEM)

```

```

WRITE(50,*)('TLOAD')
WRITE(50,*)('TLOAD(IL,UL),UL=1,NEVAB),IL=1,NELEM)
INTERPRET FIXITY DATA IN VECTOR FORM

```

```

DO 100 ITOTV = 1,NTOTV
  FIXED(ITOTV) = 0.0
  WRITE(50,*)('NVFIX',NVFIX)
DO 110 IVFIX = 1,NVFIX
  NLOCA = (NDFIX(IVFIX)-1)*NDOFN
DO 110 IDOFN = 1,NDOFN
  NGASH = NLOCA+IDOFN
  FIXED(NGASH) = PRESQ(IVFIX,IDOFN)*FACTO
  WRITE(50,*)('NGASH',FIXED(NGASH),PRESQ(IVFIX,IDOFN),FACTO)
  WRITE(50,*)('NGASH',FIXED(NGASH),PRESQ(IVFIX,IDOFN),FACTO)
CONTINUE

```

```

ADDITIONAL CONSTRAINTS FOR THE HETEROSIS ELEMENT
IF(NNODE EQ 8 OR NCOLA NE 1) GO TO 130
DO 120 IELEM = 1,NELEM
  LNOD9 = LNODS(IELEM,9)
  NLOCA = (LNOD9-1)*NDOFN
  IDOFN=3
DO 120 IDOFN = 1,3
  NGASH = NLOCA+IDOFN
  IFFIX(NGASH) = -1
CONTINUE
RETURN
END

```

SUBROUTINE INPUT

```

SUBROUTINE INPUT(ANVEL,COORD,GRAVI,IFFIX,LNODS,
  MATNO,MFRON,MELEM,MMATS,MPOIN,
  MTOTV,MVFIX,NDFRO,NDOFN,NELEM,NCOLA,
  NEVAB,NGAUS,NGAUZ,NMATS,NNODE,MLAYR,
  NDFIX,NPOIN,NPROP,NTOTG,NLAYR,NREST,
  NTOTV,NVFIX,POSGP,PRESQ,PROPS,WEIGP,
  NALGO,NINCS,LARGE)

```

```

*****
THIS SUBROUTINE ACCEPTS MOST OF THE INPUT DATA
*****

```

```

DIMENSION COORD(MPOIN,8),IFFIX(MTOTV),LNODS(MELEM,9),
  MATNO(MELEM,MLAYR),NDFRO(MELEM),GRAVI(3),
  NDFIX(MVFIX),POSGP(5),PRESQ(MVFIX,NDOFN),
  PROPS(MMATS,NPROP),TITLE(12),WEIGP(5)

```

```

READ(15,920) TITLE
WRITE(6,920) TITLE
FORMAT(12A6)

```

READ THE FIRST DATA CARD, AND ECHO IT IMMEDIATELY

```

READ(15,900) NPOIN,NELEM,NVFIX,NNODE,NMATS,NGAUS,NGAUZ,NCOLA,
  NALGO,NINCS,NLAYR,LARGE,NREST
FORMAT(16I5,75X,15I5)

```

```

WRITE(5,900) NPOIN,NELEM,NVFIX,NNODE,NMATS,NGAUS,NGAUZ,NCOLA,
  NALGO,NINCS,NLAYR,LARGE,NREST

```

```

NEVAB = NDOFN*NNODE
NTOTV = NPOIN*NDOFN
NGAU2 = NGAUS*NGAUS
NTOTG = NELEM*NGAU2*NLAYR

```

```

WRITE(5,*)('NEVAB,NDOFN,NNODE,NPOIN,NGAUS,NGAU2,NLAYR,NTOTV',
  WRITE(5,*)('NEVAB,NDOFN,NNODE,NPOIN,NGAUS,NGAU2,NLAYR,NTOTV',
WRITE(6,901) NPOIN,NELEM,NVFIX,NNODE,NMATS,NGAUS,NGAUZ,NEVAB,
  NCOLA,NALGO,NINCS,NLAYR,LARGE,NREST

```

```

FORMAT(77,5X,8H NPOIN =,15,75X,8H NELEM =,15/5X,8H NVFIX =,15, /
  75X,8H NNODE =,15/5X,8H NMATS =,15/5X,8H NGAUS =,15/
  5X,8H NGAUZ =,15/5X,8H NEVAB =,15/5X,8H NCOLA =,15/5X,
  8H NALGO =,15/5X,8H NINCS =,15, /,
  5X,8H NLAYR =,15/5X,8H LARGE =,15/5X,8H NREST =,15)

```

```

WRITE(6,912)

```

```

READ(15,913) GRAVI(1),GRAVI(2),GRAVI(3),ANVEL

```

```

WRITE(6,913) GRAVI(1),GRAVI(2),GRAVI(3),ANVEL
FORMAT(7741H X-GRAVITY Y-GRAVITY Z-GRAVITY ANG VEL /)
FORMAT(4F10,5)

```

```
CALL CHECK1(NDOFN, NELEM, NGAUS, NMATS, NNODE, NPOIN,
            NMATS, NVFIX, NGAUZ, NLAYR)
```

```
READ THE ELEMENT NODAL CONNECTIONS, AND THE PROPERTY NUMBERS
```

```
WRITE(6,902)
  2  FORMAT(/8H ELEMENT, 5X, 15H PROPERTY/LAYER, 35X, 12HNODE NUMBERS)
DO 2 IELEM = 1, NELEM
  READ(15,999) NUMEL, (MATNO(NUMEL, ILAYR), ILAYR=1, NLAYR)
  READ(15,999) (LNODS(NUMEL, INODE), INODE=1, NNODE)
  WRITE(6,903) NUMEL, (MATNO(NUMEL, ILAYR), ILAYR=1, NLAYR)
  WRITE(5,903) NUMEL, (MATNO(NUMEL, ILAYR), ILAYR=1, NLAYR)
  WRITE(6,9401) (LNODS(NUMEL, INODE), INODE=1, NNODE)
  903 WRITE(5,9401) (LNODS(NUMEL, INODE), INODE=1, NNODE)
  01  FORMAT(1X, 15, 4X, 10I5)
  9  FORMAT(12I5)
  FORMAT(11I5)
```

```
ZERO ALL THE NODAL COORDINATES, PRIOR TO READING SOME OF THEM
```

```
DO 4 IPOIN = 1, NPOIN
DO 4 IDIME = 1, 8
  COORD(IPOIN, IDIME) = 0.0
```

```
D10 READ SOME NODAL CO-ORDINATES, FINISHING WITH LAST NODE OF ALL
```

```
WRITE(6,904)
  904  FORMAT(/5H NODE, 8X, 1HX, 14X, 1HY, 14X, 1HZ, 13X, 5HPRESS)
  READ(15,905) IPOIN, (COORD(IPOIN, IDIME), IDIME=1, 8)
  WRITE(5,905) IPOIN, (COORD(IPOIN, IDIME), IDIME=1, 8)
  905  FORMAT(15, 4F15. 10/5X, 4F15. 10)
  IF(IPOIN.NE.NPOIN) GO TO 6
```

```
INTERPOLATE CO-ORDINATES OF MID-SIDE NODES
```

```
CALL NODEX(COORD, LNODS, MELEM, MPOIN, NELEM, NNODE)
DO 10 IPOIN = 1, NPOIN
  10  WRITE(6,906) IPOIN, (COORD(IPOIN, IDIME), IDIME=1, 8)
  WRITE(5,906) IPOIN, (COORD(IPOIN, IDIME), IDIME=1, 8)
  5  FORMAT(15, 4F15. 10/5X, 4F15. 10)
```

```
READ THE FIXED VALUES
```

```
WRITE(6,907)
  907  FORMAT(/5H NODE, 6X, 4HCODE, 15X, 12HFIXED VALUES)
DO 8 IVFIX = 1, NVFIX
  READ(15,908) NOFIX(IVFIX), IFPRE, (PRESG(IVFIX, IDOFN), IDOFN=1, NDOFN)
  WRITE(6,908) NOFIX(IVFIX), IFPRE, (PRESG(IVFIX, IDOFN), IDOFN=1, NDOFN)
  NLOCA = (NOFIX(IVFIX)-1)*NDOFN
  IFDOF = 10*(NDOFN-1)
  DO 8 IDOFN = 1, NDOFN
    NGASH = NLOCA+IDOFN
    IF(IFPRE.LT.IDOFN) GO TO 8
    IFFIX(NGASH) = 1
    IFPRE = IFPRE - IFDOF
    IFDOF = IFDOF/10
  8  FORMAT(1X, 14, 5X, 15, 5X, 5F10. 6)
```

```
READ THE AVAILABLE SELECTION OF ELEMENT PROPERTIES
```

```
WRITE(6,910)
  910  FORMAT(/6H NUMAT, 10X, 18HELEMENT PROPERTIES)
DO 18 IMATS = 1, NMATS
  READ(15,9002) NUMAT
  902  FORMAT(15)
  READ(15,930) (PROPS(NUMAT, IPROP), IPROP=1, NPROP)
  910  FORMAT(7F10. 5/7F10. 5/3F10. 5)
  18  WRITE(6,911) NUMAT, (PROPS(NUMAT, IPROP), IPROP=1, NPROP)
  18  WRITE(5,*) NUMAT, PROPS, .....
  WRITE(6,9002) NUMAT
  WRITE(6,9003) (PROPS(NUMAT, IPROP), IPROP=1, 7)
  WRITE(6,9003) (PROPS(NUMAT, IPROP), IPROP=8, 14)
  WRITE(6,9004) (PROPS(NUMAT, IPROP), IPROP=15, 17)
  911  FORMAT(7E12. 5)
  911  FORMAT(3E15. 5)
  WRITE(5,*) NUMAT, (PROPS(NUMAT, IPROP), IPROP=1, NPROP)
  FORMAT(1X, 14, 3X, 7E15. 5/, 8X, 7E15. 5/, 8X, 3E15. 5)
```

```

      SET UP THE GAUSSIAN INTEGRATION CONSTANTS
      CALL GAUSSQ(NGAUS, POSGP, WEIGP)
      CALL CHECK2(COORD, IFFIX, LNODS, MATNO, MELEM, MFRON, MPOIN, MTOTV,
      MVFIX, NDFRO, NDOFN, NELEM, NMATS, NNODE, NOFIX, NPOIN,
      NVEIX, NLAYR)

```

RETURN
END

```

SUBROUTINE INVAR
SUBROUTINE INVAR(A, ST, LPROP, MMATS, YIELD)
*****
THIS SUBROUTINE EVALUATES THE CURRENT VALUE OF THE YIELD FUNCTION
*****
DIMENSION ST(5), A(9, MMATS)
L=LPROP
GASH = A(1,L)*ST(1)+2.0*A(2,L)*ST(1)+2.0*A(3,L)*ST(1)*ST(3)+
      A(4,L)*ST(2)*ST(2)+2.0*A(5,L)*ST(2)*ST(3)+A(6,L)*ST(3)*ST(3)
      +A(7,L)*ST(4)*ST(4)+A(8,L)*ST(4)*ST(5)+A(9,L)*ST(5)*ST(5)
YIELD = SQRT(GASH)
RETURN
END

```

```

SUBROUTINE LDISP
SUBROUTINE LDISP(BMATX,GMATX,ETDIS,NEVAB)
*****
THIS SUBROUTINE EVALUATES THE INITIAL DISPLACEMENT MATRIX -BLARG-
AND ADDS IT UP TO BMATX
*****
DIMENSION BMATX(5,45),GMATX(2,45),ETDIS(45),ADUMM(3,2),
        BLARG(3,45)
CALCULATE THE ACTUAL -X- AND -Y- DERIVATIVES OF -W- DISPLACEMENT
DWDXX = 0.0
DWDYY = 0.0
DO 10 IEVAB =1,NEVAB
DWDXX = DWDXX+GMATX(1,IEVAB)*ETDIS(IEVAB)
DWDYY = DWDYY+GMATX(2,IEVAB)*ETDIS(IEVAB)

SET UP THE -ADUMM- MATRIX
ADUMM(1,1) = DWDXX
ADUMM(1,2) = 0.0
ADUMM(2,1) = 0.0
ADUMM(2,2) = DWDYY
ADUMM(3,1) = DWDYY
ADUMM(3,2) = DWDXX
NOW CALCULATE THE -BLARG- MATRIX
DO 20 IEVAB =1,NEVAB
DO 20 I=1,3
BLARG(I,IEVAB) = 0.0
DO 20 J=1,2
        BLARG(I,IEVAB)= BLARG(I,IEVAB)+ADUMM(I,J)*GMATX(J,IEVAB)
THE NEW -BMATX- IS EQUAL TO -BMATX+BLARG
DO 30 IEVAB =1,NEVAB
DO 30 I=1,3
        BMATX(I,IEVAB) = BMATX(I,IEVAB)+BLARG(I,IEVAB)
RETURN
END

```

```

SUBROUTINE LOADS
SUBROUTINE LOADS(ANVEL,COORD,ELOAD,GRAVI,LNODS,
MATNO,MELEM,MEVAB,MMATS,MPOIN,DICOS,
MELEM,MEVAB,NGAUS,THICK,
NNODE,NPROP,NSTRE,POSGP,M3POI,
PROPS,WEIGP,MLAYR,NLAYR)
*****
THIS SUBROUTINE EVALUATES THE NODAL FORCES DUE TO EXTERNAL
APPLIED LOADS(CENTRIFUGAL, GRAVITY, PRESSURE AND POINT LOADS)
*****
COMMON WORMX(3,24),GVALU,DJACB
DIMENSION BMATX(5,45),COORD(MPOIN,8),
ELOAD(MELEM,MEVAB),GRAVI(3),LNODS(MELEM,9),
MATNO(MELEM,MLAYR),POSGP(5),DICOS(3,M3POI),
PROPS(MMATS,NPROP),SHAPE(3,9),STREN(5),
THICK(MPOIN),WEIGP(5),GMATX(2,45)

```

REWIND 8

LOOP OVER EACH ELEMENT
DO 150 IELEM = 1, NELEM

READ THE CHARACTERISTICS OF THE APPLIED LOADS

WRITE(60,*) 'ELEMENT =', IELEM

READ(15,900) NPRES, NUCLO, NBDY
WRITE(60,901) NPRES, NUCLO, NBDY
WRITE(6,901) NPRES, NUCLO, NBDY

FORMAT(5I5)

FORMAT(8H NPRES =, I5, 5X, 8H NUCLO =, 5X, 8H NBDY =, I5)

IF(NPRES.EQ.0) GO TO 3

READ(15,902) KPRES, CFACE, PREVA, SURFA
WRITE(6,902) KPRES, CFACE, PREVA, SURFA

FORMAT(I5, F5.1, 2F15.5)

CFACE IS +1.0 OR -1.0, ACCORDING AS PRESSURE IS ON TOP OR
BOTTOM SURFACE

CONTINUE

INITIALIZE THE LOAD MATRIX ELOAD ONE COLUMN AT EACH TIME

DO 4 IEVAB = 1, NEVAB
ELOAD(IELEM, IEVAB) = 0.0

ENTER THE LOOPS OVER GAUSS POINTS FOR NUMERICAL INTEGRATION

DO 145 IGAUS = 1, NGAUS

DO 145 JGAUS = 1, NGAUS

EXISP = POSGP(IGAUS)

ETASP = POSGP(JGAUS)

WRITE(60,*) 'EXISP, ETASP, POSGP(IGAUS), POSGP(JGAUS)'

WRITE(60,*) EXISP, ETASP, POSGP(IGAUS), POSGP(JGAUS)

CALL SFR1(SHAPE, EXISP, ETASP)

IF(NBDY.EQ.0) GO TO 141

ZETSP = -1.0

DO 140 ILAYR = 1, NLAYR

LPROP = MATNO(IELEM, ILAYR)

DZETA = PROPS(LPROP, 3)

ZETSP = ZETSP + DZETA/2.0

READ(8) BMATX, GMATX, DVOLU

CALCULATE THE CENTRIFUGAL, GRAVITATIONAL PRESSURE AND POINT LOADS

CENTRIFUGAL FORCE

IF(ANVEL.EQ.0.0) GO TO 70

NPROP = 2

CALL FUNC(BMATX, SHAPE, THICK, NBORP, NNODE, ZETSP, MELEM, COORD, DICOS,
LNODS, IELEM, MPOIN, M3POI, GMATX)

GASH = PROPS(LPROP, 4)*ANVEL*ANVEL*DVOLU

DO 45 IS=1,2

STREN(IS) = GASH*WORMX(IS, 1)

CONTINUE

STREN(3) = 0.0

DO 65 INODE = 1, NNODE

FIND THE POSITION OF THE V-1 AND V-2 VECTORS

IPOIN = IABS(LNODS(IELEM, INODE))

JPOSI = (IPOIN-1)*3

DO 65 ISTR = 1, NSTRE

IEVAB = (INODE-1)*5+ISTR

IF(ISTR.GT.3) GO TO 50

ELOAD(IELEM, IEVAB) = ELOAD(IELEM, IEVAB) + STREN(ISTR)*SHAPE(1, INODE)

GO TO 65

JPOSI = JPOSI + 1

GASH = SHAPE(1, INODE)*(THICK(IPOIN)/2.0)*ZETSP

IF(ISTR.NE.5) GO TO 55

GASH = -GASH

DO 60 ILL=1,2

ELOAD(IELEM, IEVAB) = ELOAD(IELEM, IEVAB) + STREN(ILL)*
DICOS(ILL, JPOSI)*GASH

CONTINUE

CONTINUE

```

GRAVITY
GASH = PROPS(LPROP, 4)*DVOLU
DO 75 IMM=1, 3
  STREN(IMM) = GRAVI(IMM)*GASH
DO 95 INODE=1, NNODE
  IPOIN = IABS(LNODS(IELEM, INODE))
  JPOSI=(IPOIN-1)*3
DO 95 ISTR=1, NSTRE
  IEVAB=(INODE-1)*5+ISTR
  IF(ISTR GT. 3) GO TO 80
  ELOAD(IELEM, IEVAB)=ELOAD(IELEM, IEVAB)+STREN(ISTR)*
    SHAPE(1, INODE)
GO TO 95
JPOSI = JPOSI+1
GASH = SHAPE(1, INODE)*(THICK(IPOIN)/2.0)*ZETSP
IF(ISTR NE. 5) GO TO 85
GASH = -GASH
DO 90 IKK=1, 3
  ELOAD(IELEM, IEVAB)=ELOAD(IELEM, IEVAB)+STREN(IKK)*
    DICOS(IKK, JPOSI)*GASH
CONTINUE
ZETSP = ZETSP+DZETA/2.0
CONTINUE

CALCULATE THE NODAL LOADS DUE TO PRESSURE

IF(NPRES EQ. 0) GO TO 142
CALL PRES(BMATX, COORD, ELOAD, LNODS, POSGP, SHAPE, THICK,
  WEIGP, IELEM, IGAUS, JGAUS, MELEM, MPOIN, NNODE,
  NEVAB, KPRES, CFACE, PREVA, SURFA, DICOS, M3POI)
CONTINUE
CONTINUE

POINT LOADS
IF(NUCLO EQ. 0) GO TO 150

IS THE PRESENT ELEMENT A LOADED ELEMENT. IF IT IS
READ AND ACCUMULATE THE LOADS IN ELOAD
WRITE(60,*) 'NUCLO=', NUCLO
DO 120 IGASP=1, NUCLO
  READ(15, 950) LPOIN, LDOFN, CARGA
  WRITE(60, 960) LPOIN, LDOFN, CARGA
  WRITE(6, 960) LPOIN, LDOFN, CARGA
  WRITE(5,*) 'HERE ARE SOME VALUES READ'
  WRITE(5, 960) LPOIN, LDOFN, CARGA
  IEVAB = (LPOIN-1)*5+LDOFN
  WRITE(60,*) 'IEVAB, LDOFN', IEVAB, LDOFN
  ELOAD(IELEM, IEVAB)=ELOAD(IELEM, IEVAB)+CARGA
  WRITE(60,*) 'ELOAD...', ELOAD(IELEM, IEVAB)
CONTINUE
  WRITE(60,*) 'ELOAD', ((ELOAD(I, J), J=1, IEVAB), I=1, NELEM)
  FORMAT(2I5, F10.5)
  FORMAT(/8H LPOIN =, I5, 8H LDOFN =, I5, 7H LOAD =, F16.8/)
RETURN
END

SUBROUTINE MATM
SUBROUTINE MATM(N1, N2, N3, NOPN)
*****
MATRIX MANIPULATIONS
NOPN = 1, TRANSPOSE-INVERT N1 INTO N2, DJACB = 1/GVALU
NOPN = 2, TRANSPOSE-MULT., A(K, I)*B(K, J) = C(I, J)
(I.E. A IS TRANSPOSED)
NOPN = 3, TRUE MULTIPLY, A(I, K)*B(K, J) = C(I, J)
NOPN = 4, MATRIX (TRANSPOSED)*VECTOR
NOPN = 5, TRANSPOSE MATRIX N1 INTO N2
NOPN = 6, NORMALIZE N1 INTO N2, IN COLUMNS
NOPN = 7, N1 AND N2 OPEN SCISSORS-FAXHION TO BE ORTHOGONAL
NOPN = 8, TRANSFER MATRIX N1 INTO N2
NOPN = 9, MATRIX N1*VECTOR N2 = VECTOR N3
*****
COMMON WORMX(3, 24), GVALU, DJACOB
WRITE(5,*) '..... E N T E R I N G M A T M'
WRITE(5,*) '..... NOPN IN MATM', NOPN
FORMAT(/1X, 3E14.7)
GO TO (1, 2, 3, 4, 5, 6, 7, 8, 9), NOPN
K = 2

```

```

DO 10 I =1,3
J = 4 - I -K
M1 = N1 + J
M2 = N1 + K
M3 = N2 + I -1
M4 = N1 + I -1
WRITE(5,*) 'GVALU IN MATM FIRST BEFORE CALLING VECT', GVALU
WRITE(5,*) '++++++I, J, K, M1, M2, M3, M4+++++', I, J, K, M1, M2, M3, M4
CALL VECT(M1, M2, M3, 4)
WRITE(5,*) 'GVALUE ONCE', GVALU
CALL VECT(M4, M3, 0, 1)
WRITE(5,*) 'GVALU NEXT', GVALU
WRITE(5,*) 'GVALU IN MATM AFTER CALLING VECT'
WRITE(5,*) '!!!!!!GVGLU!!!!', GVALU
IF (GVALU.NE.0.0) GO TO 22
WRITE(6,21)
FORMAT(17H ZERO DETERMINANT)
STOP
EXECUTION IS TERMINATED WHEN THE DETERMINANT IS ZERO
GVALU = 1.0/GVALU
CALL VECT(M3, M3, 0, 3)
K = I -1
RETURN
DO 11 I =1,3
N1 = N1 + I -1
DO 11 J =1,3
M2 = N2 + J -1
M3 = N3 + J -1
CALL VECT(M1, M2, 0, 1)
WORMX(I, M3) = GVALU
RETURN
DO 13 I = 1,3
DO 13 K = 1,3
M2 = N2 + K -1
M3 = N3 + K -1
GASH = 0.0
DO 12 L =1,3
M1 = N1 + L -1
GASH = GASH + WORMX(I, M1)*WORMX(L, M2)
WORMX(I, M3) = GASH
RETURN
DO 14 I = 1,3
M1 = N1+I-1
CALL VECT(M1, N2, 0, 1)
WORMX(I, N3) = GVALU
RETURN
DO 15 I =1,3
N1I = N1 + I -1
N2I = N2 + I -1
DO 15 J =I,3
N1J = N1 + J -1
N2J = N2 + J -1
GASH = WORMX(J, N1I)
WORMX(J, N2I) = WORMX(I, N1J)
WORMX(J, N2J) = GASH
RETURN
DO 16 I=1,3
I1 = N1 + I -1
I2 = N2 + I -1
CALL VECT(I1, I2, 0, 2)
RETURN
CALL SINGOP(N1, 2)
CALL SINGOP(N2, 2)
CALL VECT(N1, N2, 0, 1)
GASH = -GVALU/(1.0+SQRT(1.0-GVALU*GVALU))
DO 17 I =1,3
GISH = WORMX(I, N1)
GOSH = WORMX(I, N2)
WORMX(I, N1) = GISH+GASH*GOSH
WORMX(I, N2) = GOSH + GASH*GISH
RETURN
DO 18 J =1,3
N1J = N1+J-1
N2J = N2 +J -1
DO 18 I =1,3
WORMX(I, N2J) = WORMX(I, N1J)

```



```

RETURN
DO 20 I = 1, 3
  GASH = 0.0
DO 19 J = 1, 3
  N1J = N1 + J - 1
  GASH = GASH + WORMX(I, N1J)*WORMX(J, N2)
  WORMX(I, N3) = GASH
RETURN
END

```

```

-----
SUBROUTINE MODAN
SUBROUTINE MODAN(AMATX, DMATT, NMATS, NPROP, PROPS, MMATS,
  MATNO, MELEM, MLAYR, NELEM, NLAYR)
*****
CALCULATES THE MATRIX OF ELASTICITY -D- AND THE MATRIX OF
ANISOTROPIC PARAMETERS -AMATX- FOR EACH MATERIAL
*****
DIMENSION AMATX(9, MMATS), DMATT(5, 5, MMATS), PROPS(MMATS, NPROP),
  APARA(5, 5), TRANS(5, 5), GASHM(5, 5), MATNO(MELEM, MLAYR),
  COEFE(2)
DO 15 IMATS = 1, NMATS

  SETS UP THE MATRIX OF THE ANISOTROPIC PARAMETERS
  UNIAX = PROPS(IMATS, 6)
DO 5 I = 1, 9
  AMATX(I, IMATS) = 0.0
AMATX(1, IMATS) = 1.0
  WRITE(5, *) '..... PROPS(IMATS, 12) = ..... ', PROPS(IMATS, 12)
AMATX(4, IMATS) = (UNIAX/PROPS(IMATS, 12))*2.0
A3Z = (UNIAX/PROPS(IMATS, 13))*2.0
AMATX(6, IMATS) = (UNIAX/PROPS(IMATS, 14))*2.0
AMATX(2, IMATS) = 2.0*A3Z - 0.5*(1.0+AMATX(4, IMATS)+AMATX(6, IMATS))
AMATX(7, IMATS) = (UNIAX/PROPS(IMATS, 15))*2.0
AMATX(9, IMATS) = (UNIAX/PROPS(IMATS, 16))*2.0

  SETS UP THE ELASTICITY MATRIX -D-
  GASH = 1.0 - PROPS(IMATS, 2)*2.0*PROPS(IMATS, 8)/PROPS(IMATS, 1)
DO 10 I = 1, 5
DO 10 J = 1, 5
  DMATT(I, J, IMATS) = 0.0
DMATT(1, 1, IMATS) = PROPS(IMATS, 1)/GASH
DMATT(2, 2, IMATS) = PROPS(IMATS, 8)/GASH
DMATT(1, 2, IMATS) = PROPS(IMATS, 2)*DMATT(2, 2, IMATS)
DMATT(2, 1, IMATS) = DMATT(1, 2, IMATS)
DMATT(3, 3, IMATS) = PROPS(IMATS, 9)
DMATT(4, 4, IMATS) = PROPS(IMATS, 10)
DMATT(5, 5, IMATS) = PROPS(IMATS, 11)
  CONTINUE

  CALCULATE THE SHEAR CORRECTION FACTOR
  IF (NMATS.NE.1) GO TO 25
DO 20 I = 1, 2
  COEFE(I) = 5.0/6.0
GO TO 27
DO 26 IELEM = 1, NELEM
  KOUNT = 0
DO 26 ILAYR = 1, NLAYR
  IF (MATNO(IELEM, ILAYR).EQ. MATNO(IELEM, ILAYR-1)) GO TO 26
  KOUNT = KOUNT + 1
  CONTINUE
  IF (KOUNT.EQ.0) GO TO 19
  CALL SHEARC(MATNO, MELEM, MLAYR, PROPS, MMATS, NPROP,
    COEFE, NLAYR, DMATT)
DO 28 IMATS = 1, NMATS
  DMATT(4, 4, IMATS) = DMATT(4, 4, IMATS)*COEFE(1)
  DMATT(5, 5, IMATS) = DMATT(5, 5, IMATS)*COEFE(2)
WRITE(6, 900) (COEFE(I), I=1, 2)
  FORMAT(/' COEFE(1) =', E15.4, 5X, 'COEFE(2) =', E15.8/)
DO 80 IMATS = 1, NMATS
  IF THE REFERENTIAL SYSTEM OF AXES COINCIDES WITH THE
  PRINCIPAL AXES OF MATERIAL - GO TO 80

  THETA = PROPS(IMATS, 17)
  IF (ABS(THETA).LT.0.001) GO TO 80

```

SETS UP THE TRANSFORMATION MATRIX -TRANS-

```

DO 30 I =1,5
DO 30 J =1,5
  TRANS(I,J) = 0.0
C = COS(THETA)
S = SIN(THETA)
TRANS(1,1) = C*C
TRANS(1,2) = S*S
TRANS(2,1) = TRANS(1,2)
TRANS(2,2) = TRANS(1,1)
TRANS(1,3) = C*S
TRANS(3,1) = -2.0*TRANS(1,3)
TRANS(2,3) = -TRANS(1,3)
TRANS(3,2) = -TRANS(3,1)
TRANS(3,3) = TRANS(1,1)-TRANS(1,2)
TRANS(4,4) = C
TRANS(4,5) = S
TRANS(5,4) = -S
TRANS(5,5) = C

```

CALCULATE THE PRODUCT OF D MATRIX BY T MATRIX

```

DO 35 I =1,5
DO 35 J =1,5
  GASHM(I,J) = 0.0
DO 35 K =1,5
  GASHM(I,J) = GASHM(I,J) + DMATT(I,K,IMATS)* TRANS(K,J)

```

CALCULATED THE TRANSPOSED D MATRIX

```

DO 40 I =1,5
DO 40 J =1,5
  DMATT(I,J,IMATS) = 0.0
DO 40 K =1,5
  DMATT(I,J,IMATS) = DMATT(I,J,IMATS) +TRANS(K,I)*GASHM(K,J)
DO 45 I =1,5
DO 45 J =1,5
  DMATT(J,I,IMATS) = DMATT(I,J,IMATS)

```

SET UP THE MATRIX OF THE ANISOTROPIC PARAMETERS FOR THE MATERIAL

```

DO 50 I=1,5
DO 50 J =1,5
  APARA(I,J) = 0.0
APARA(1,1) = AMATX(1,IMATS)
APARA(1,2) = AMATX(2,IMATS)
APARA(2,1) = APARA(1,2)
APARA(2,2) = AMATX(4,IMATS)
APARA(3,3) = AMATX(6,IMATS)
AMATX(4,4) = AMATX(7,IMATS)
AMATX(5,5) = AMATX(9,IMATS)

```

SET UP THE NEW TRANSFORMATION MATRIX

```

TRANS(3,1) = -C*S
TRANS(2,3) = 2.0*TRANS(3,1)
TRANS(3,2) = -TRANS(3,1)
TRANS(1,3) = -TRANS(2,3)

```

CALCULATE THE PRODUCT OF A MATRIX BY T MATRIX

```

DO 55 I =1,5
DO 55 J =1,5
  GASHM(I,J) = 0.0
DO 55 K=1,5
  GASHM(I,J) = GASHM(I,J)+APARA(I,K)*TRANS(K,J)

```

CALCULATE THE NEW ANISOTROPIC PARAMETERS

```

DO 60 I =1,5
DO 60 J =1,5
  APARA(I,J) = 0.0
DO 60 K=1,5
  APARA(I,J) = APARA(I,J)+TRANS(K,I)*GASHM(K,J)
AMATX(1,IMATS) = APARA(1,1)
AMATX(2,IMATS) = APARA(1,2)
AMATX(3,IMATS) = APARA(1,3)
AMATX(4,IMATS) = APARA(2,2)
AMATX(5,IMATS) = APARA(2,3)

```

```

AMATX(6, IMATS) = APARA(3,3)
AMATX(7, IMATS) = APARA(4,4)
AMATX(8, IMATS) = APARA(4,5)
AMATX(9, IMATS) = APARA(5,5)

```

```

CONTINUE
WRITE(5,*) '.....GETING OUT OF SUB MODAN ..... '
RETURN
END

```

```

-----
SUBROUTINE NODES
SUBROUTINE NODEX(COORD, LNODS, MELEM, MPOIN, NELEM, NNODE)
*****
THIS SUBROUTINE INTERPOLATES THE MID SIDE NODES OF STRAIGHT
SIDES OF TH ELEMENTS
*****
DIMENSION COORD(MPOIN,8), LNODS(MELEM,9), ELCOR(8,8)

```

```

LOOP OVER EACH ELEMENT
NNOD1 = 7
DO 20 INODE = 1, NNOD1, 2

```

```

    COMPUTE THE NODE NUMBER OF THE FIRST NODE

```

```

    NODST = LNODS(IELEM, INODE)
    IGASH = INODE*2
    IF(IGASH.GT.8) IGASH = 1

```

```

    COMPUTE THE NODE NUMBER OF THE LAST NODE

```

```

    NODFN = LNODS(IELEM, IGASH)
    MIDPT = INODE + 1

```

```

    COMPUTE THE NODE NUMBER OF THE INTERMEDIATE NODE
    NODMD = LNODS(IELEM, MIDPT)
    TOTAL=ABS(COORD(NODMD,1))+ABS(COORD(NODMD,2))+ABS(COORD(NODMD,3)))

```

```

    IF THE COEFFICIENTS OF THE INTERMEDIATE NODE ARE ALL ZERO
    INTERPOLATE BY A STRAIGHT LINE
    IF(TOTAL.GT.0.0) GO TO 20
    KOUNT = 1

```

```

    COORD(NODMD, KOUNT) = (COORD(NODST, KOUNT)+COORD(NODFN, KOUNT))/2.0
    KOUNT = KOUNT + 1
    IF(KOUNT.LE.8) GO TO 10
    CONTINUE
    IF(NNODE.EQ.8) GO TO 60

```

```

    SET UP THE CENTRAL POINT COORDINATES
    NODCE = LNODS(IELEM, 9)

```

```

    DO 30 INODES = 1, 8
    NODEB = LNODS(IELEM, INODE)
    DO 30 IDIME = 1, 8
    ELCOR(IDIME, INODE) = COORD(NODEB, IDIME)
    DO 50 IDIME = 1, 8
    GENCO = 0.0
    DO 35 INODE = 1, 7, 2
    GENCO = GENCO + ELCOR(IDIME, INODE)
    GENCO = GENCO*(-0.5)
    DO 40 INODE = 2, 8, 2
    GENCO = GENCO + ELCOR(IDIME, INODE)
    GENCO = GENCO * 0.5
    COORD(NODCE, IDIME) = GENCO
    CONTINUE

```

```

RETURN
END

```

```

-----
SUBROUTINE OUTPUT
SUBROUTINE OUTPUT(IITER, MTOTG, MTOTV, MVFIX, NCHECK, NELEM, NGAUS,
NOFIX, NOUTP, NPOIN, NSTRE,
NVFIX, STRSG, TDISP, TREAC, EPSTN, POSGP,
EFFST, MATNO, MMATS, PROPS, NPROP, MELEM, THICK,
MPOIN, LNODS, MLAYR, NLAYR)

```

```

*****
THIS SUBROUTINE OUTPUTS DISPLACEMENTS, REACTIONS AND STRESSES
*****
DIMENSION NOFIX(MVFIX), NOUTP(2), STRSG(3, MTOTG), STRES(6),
TDISP(MTOTV), TREAC(MVFIX, 5), EPSTN(MTOTG),

```

```

      POSGP(5), SHAPE(3,9), EFFST(MTOTG),
      THICK(MPOIN), LNODS(MELEM,9),
      FORCE(8), MATNO(MELEM,MLAYR),
      PROPS(MMATS,NPROP)
KOUTP = NOUTP(1)
IF(IITER.GT.1) KOUTP = NOUTP(2)
IF(IITER.EQ.1.AND.NCHECK.EQ.0) KOUTP = NOUTP(2)

      OUTPUT DISPLACEMENTS
      IF(KOUTP.LT.1) GO TO 10
      WRITE(6,900)
      FORMAT(1H0,5X,13HDISPLACEMENTS)
      WRITE(6,905)
      FORMAT(1H0,6X,4HNODE,4X,6HX-DISP,8X,6HY-DISP,8X,6HZ-DISP,
      8X,6HAF-ROT,8X,6HBT-ROT)
      DO 20 IPOIN = 1, NPOIN
      NGASH = IPOIN*5
      NGISH = NGASH - 4
      WRITE(6,910) IPOIN, (TDISP(IGASH), IGASH = NGISH, NGASH)
      FORMAT(1H0,5E14.6)
      CONTINUE

      OUTPUT REACTIONS
      IF(KOUTP.LT.2) GO TO 30
      WRITE(6,920)
      FORMAT(1H0,5X,9HREACTIONS)
      WRITE(6,925)
      FORMAT(1H0,6X,4HNODE,4X,6HX-REAC,8X,6HY-REAC,8X,6HZ-REAC,
      8X,6HAF-MOM,8X,6HBT-MOM)
      DO 40 IVFIX = 1, NVFIX
      WRITE(6,910) NOFIX(IVFIX), (TREAC(IVFIX, IDOFN), IDOFN=1,5)
      CONTINUE

      OUTPUT STRESSES
      IF(KOUTP.LT.3) GO TO 120
      WRITE(6,927)
      FORMAT(1H0,5X,8HSTRESSES)
      WRITE(6,926)
      FORMAT(1H0,1X,5HKLAYR,5X,6HXX-STR,8X,6HYY-STR,8X,6HXY-STR,
      8X,6HXZ-STR,8X,6HYZ-STR,6X,10HEFF-STRESS,3X,
      13HEFF.PL.STRAIN)
      KGAUS = 0
      DO 110 IELEM = 1, NELEM
      KELGS = 0
      WRITE(6,940) IELEM
      FORMAT(1H0,18H ELEMENT NO., =, I5, /)
      DO 105 IGAUS = 1, NGAUS
      DO 105 JGAUS = 1, NGAUS
      EXISP = POSGP(IGAUS)
      ETASP = POSGP(JGAUS)
      SET TO ZERO THE STRESS RESULTANT VECTOR
      DO 70 JFORC = 1,8
      FORCE(JFORC) = 0.0
      KGASP = 0
      KELGS = KELGS + 1
      WRITE(6,945) KELGS
      FORMAT(11H G.P. NO. =, I5)
      CALL SFR1(SHAPE, EXISP, ETASP)

      COMPUTE GAUSS POINT THICKNESS
      THIGP = 0.0
      DO 65 INODE = 1,8
      IPOIN = IABS(LNODS(IELEM, INODE))
      THIGP = THIGP + SHAPE(1, INODE)*THICK(IPOIN)
      ZETSP = -1.0
      DO 100 ILAYR = 1, NLAYR
      LPROP = MATNO(IELEM, ILAYR)
      DZETA = PROPS(LPROP, 3)
      ZETSP = ZETSP + DZETA/2.0
      KGAUS = KGAUS + 1
      KGASP = KGASP + 1

      THE FIVE LOCAL STRESSES IN THE ORDER XX, YY, XY, XZ, YZ
      DO 50 ISTRE = 1, NSTRE

```

```

10 STRES(ISTRE) = STRSG(ISTRE,KGAUS)
WRITE(6,950) KGASP,(STRES(ISTRE),ISTRE=1,NSTRE),
      EFFST(KGAUS),EPSTN(KGAUS)

SET UP THE STRESS RESULTANTS IN THE ORDER NX,NY,NXY,MX,MY,GX,GY

DO 75 ISTRE = 1,3
FORCE(ISTRE) = FORCE(ISTRE)+STRES(ISTRE)*THIGP/2.0*DZETA
FORCE(ISTRE+3) = FORCE(ISTRE+3)-STRES(ISTRE)*THIGP*THIGP*
      ZETSP*DZETA/4.0
DO 80 ISTRE=4,5
FORCE(ISTRE+3) = FORCE(ISTRE+3)+STRES(ISTRE)*THIGP/2.0*DZETA
FORMAT(I5,2X,8E14.6)
ZETSP = ZETSP*DZETA/2.0
CONTINUE
WRITE(6,960) FORCE(1),FORCE(4),FORCE(2),FORCE(5),FORCE(3),
      FORCE(6),FORCE(7),FORCE(8)
FORMAT(/,22H STRESS RESULTANTS = ,6HN-XX =,E12.5,5X,
      6HM-XX =,E12.5/22X,6HN-YY =,E12.5,5X,6HM-YY =,
      E12.5/22X,6HN-YY =,E12.5,6HM-XY =,E12.5/,
      22X,6HQ-XZ =,E12.5,5X,6HQ-YZ =,E12.5)
5 CONTINUE
10 CONTINUE
20 CONTINUE
RETURN
END

-----
SUBROUTINE PRES
SUBROUTINE PRES(BMATX,COORD,ELOAD,LNODS,POSGP,SHAPE,THICK,
      WEIGP,IELEM,IGAUS,JGAUS,MELEM,MPOIN,NNODE,
      NEVAB,KPRES,CFACE,PREVA,SURFA,DICOS,M3POI)
*****
THIS SUBROUTINE EVALUATES THE NODAL LOADS DUE TO PRESSURE
*****
COMMON WORMX(3,24),GVALU,DJACB
DIMENSION BMATX(5,45),COORD(MPOIN,8),ELOAD(MELEM,NEVAB),
      LNODS(MELEM,9),POSGP(5),PREMX(2,9),SHAPE(3,9),
      THICK(MPOIN),WEIGP(5),DICOS(3,M3POI),GMATX(2,45)
ZETA = CFACE
NBORP = 2
CALL FUNC(BMATX,SHAPE,THICK,NBORP,NNODE,ZETA,MELEM,
      COORD,DICOS,LNODS,IELEM,MPOIN,M3POI,GMATX)

EVALUATE THE PRESSURE AT SAMPLING POINTS KPRES = 0,1 OR 2
ACCORDING AS PRESSURE IS U.D, HYDROSTATIC, OR SPECIFIED AS NODAL
COORDINATES
IF(KPRES.EQ.0) GO TO 20
IF(KPRES.EQ.2) GO TO 10
WORMX(3,1) = WORMX(3,1) - SURFA
PRESS = PREVA*WORMX(3,1)
IF(PRESS.GE.0.0) GO TO 25
PRESS = 0.0
GO TO 25
PREVA = 0.0
DO 15 INODE =1,8
NGASH = IABS(LNODS(IELEM,INODE))

SET UP ARRAY OF NODAL PRESSURE; ROW 1 TOP, ROW 2 BOTTOM

PREMX(1,INODE) = COORD(NGASH,4)
PREMX(2,INODE) = COORD(NGASH,8)
GISH = ((1.0-ZETA)*PREMX(1,INODE)+(1.0-ZETA)*PREMX(2,INODE))/2.0
PREVA = PREVA+GISH*SHAPE(1,INODE)
PRESS = PREVA
GMULT = WEIGP(IGAUS)*WEIGP(JGAUS)*CFACE*PRESS

CALCULATE CONSISTENT NODAL LOADS

DO 45 INODE =1,NNODE
IPOIN = IABS(LNODS(IELEM,INODE))
GVALU = -GMULT*SHAPE(1,INODE)*DJACB
CALL VECT(7,21,0,3)
DO 30 I =1,3
IPOS1 = (INODE-1)*5+I
ELOAD(IELEM,IPOS1)=ELOAD(IELEM,IPOS1)+WORMX(I,21)
GVALU = ZETA*THICK(IPOIN)/2.0

```

```

CALL SINGOP(21,1)
NPOSI = (IPOIN-1)*3
DO 40 I = 1,2
  JPOSI = (INODE-1)*5+(I+3)
  NPOSI = NPOSI+1
DO 32 K = 1,3
  WORMX(K,24) = DICOS(K,NPOSI)
CALL VECT(21,24,0,1)
IF(I.EQ.2) GO TO 35
  QVALU = -QVALU
  ELOAD(IELEM,JPOSI) = ELOAD(IELEM,JPOSI) + QVALU
  CONTINUE
CONTINUE
RETURN
END

```

```

-----
SUBROUTINE RESTR
SUBROUTINE RESTR(ASDIS, EFFST, ELOAD, LNODS,
  MATNO, MELEM, MMATS, MPOIN, MTOTG, MTOTV,
  NDOFN, NELEM, NEVAB, NGAUS, NNODE,
  NPROP, NSTRE, POSGP, PROPS, STRSG,
  TDISP, WEIGP, EPSTN, KUNLO, AMATX, DMATT,
  THICK, MLAYR, NLAYR, LARGE)
*****
THIS SUBROUTINE REDUCES THE STRESSES TO THE YIELD SURFACE AND
EVALUATES THE EQUIVALENT NODAL FORCES
*****
DIMENSION ASDIS(MTOTV), AVECT(5), BMATX(5,45),
  DMATT(5,5,MMATS), DVECT(5), EFFST(MTOTG), ELDIS(45),
  ELOAD(MELEM,NEVAB), GVECT(5), LNODS(MELEM,9),
  MATNO(MELEM,MLAYR), POSGP(5), PROPS(MMATS,NPROP),
  DESIG(5), SIGMA(5), SGTOT(5), ETDIS(45),
  STRES(5), EPSTN(MTOTG), TDISP(MTOTV), THICK(MPOIN),
  STRSG(5,MTOTG), WEIGP(5),
  AMATX(9,MMATS), GMATX(2,45)
REWIND 8
DO 5 IELEM = 1,NELEM
DO 5 IEVAB = 1,NEVAB
  ELOAD(IELEM,IEVAB) = 0.0
  KUNLO = 0
  KGAUS = 0

```

```

  WRITE(5,*) 'STARTS PROCESS IN RESTR'
  LOOP OVER EACH ELEMENT

```

```

DO 210 IELEM = 1,NELEM

```

```

  IDENTIFY THE DISPLACEMENTS OF THE ELEMENT NODAL POINTS

```

```

  JPOSI = 0
DO 10 INODE = 1,NNODE
  LNODE = IABS(LNODS(IELEM,INODE))
  NPOSN = (LNODE-1)*NDOFN
  DO 10 IDOFN = 1,NDOFN
    NPOSN = NPOSN + 1
  JPOSI = JPOSI + 1
  ELDIS(JPOSI) = ASDIS(NPOSN)
  ETDIS(JPOSI) = TDISP(NPOSN)
  CONTINUE
  KELGS = 0

```

```

  ENTER LOOPS OVER EACH SAMPLING POINTS

```

```

  WRITE(6,*)
  WRITE(6,*)
  WRITE(6,*)
  WRITE(6,*) 'DOF', 'SIGX', 'SIGY', 'SIGZ'
  'TOUXY', 'TOUYZ'
DO 205 IGAUS = 1,NGAUS
DO 205 JGAUS = 1,NGAUS
DO 200 ILAYR = 1,NLAYR
  LPROP = MATNO(IELEM,ILAYR)
  UNIAX = PROPS(LPROP,6)
  HARDS = PROPS(LPROP,7)
  KGAUS = KGAUS + 1
  KELGS = KELGS + 1

```

```

EPSTN(KGAUS) = ABS(EPSTN(KGAUS))
READ(8) BMATX, GMATX, DVOLU

```

```

CALL SUBROUTINE WHICH SETS UP -BMATX- TAKING INTO ACCOUNT
THE GEOMETRIC NON-LINEARITY

```

```

IF(LARGE.EQ.1) CALL LDISP(BMATX, GMATX, ETDIS, NEVAB)

```

```

NOW PROCEED TO CALCULATE STRESSES FROM STRESS = DMATX*BMATX*ELDIS
FIRST STORE IN GASH VECTOR GVECT THE PRODUCT BMATX*ELDIS

```

```

DO 30 IDOFN = 1, NDOFN

```

```

GASH = 0.0

```

```

DO 25 IEVAB = 1, NEVAB

```

```

GASH = GASH + BMATX(IDOFN, IEVAB)*ELDIS(IEVAB)

```

```

GVECT(IDOFN) = GASH

```

```

CALCULATE THE FIVE LOCAL STRESSES IN THE ORDER XX, YY, XY, XZ, YZ

```

```

DO 50 ISTRE = 1, NSTRE

```

```

GASH = 0.0

```

```

DO 45 JSTRE = 1, NSTRE

```

```

GASH = GASH + DMATX(ISTRE, JSTRE, LPROP)*GVECT(JSTRE)

```

```

STRES(ISTRE) = GASH

```

```

FORMAT(/1X, I3, 1X, 5E14, 7)

```

```

WRITE(6, I3) ISTRE, STRES(1), STRES(2), STRES(3), STRES(4), STRES(5)

```

```

CONTINUE

```

```

CONTINUE

```

```

CONTINUE

```

```

WRITE(5, *) '***IN RESTR COMES UP TO REDUCE STRESSES'

```

```

RETURN

```

```

GO TO 11101

```

```

REDUCE STRESSES TO THE YIELD SURFACE FOR YIELDED GAUSS POINTS

```

```

PREYS = UNIAX + EPSTN(KGAUS)*HARDS

```

```

DO 150 ISTR1 = 1, NSTRE

```

```

DESIG(ISTR1) = STRES(ISTR1)

```

```

SIGMA(ISTR1) = STRSG(ISTR1, KGAUS) + STRES(ISTR1)

```

```

CALL INVAR(AMATX, SIGMA, LPROP, MMATS, YIELD)

```

```

ESPRE = EFFST(KGAUS) - PREYS

```

```

IF(ESPRE.GE.0) GO TO 55

```

```

ESCUR = YIELD - PREYS

```

```

IF(ESCUR.LE.0.0) GO TO 60

```

```

RFACT = ESCUR/(YIELD-EFFST(KGAUS))

```

```

GO TO 70

```

```

ESCUR = YIELD - EFFST(KGAUS)

```

```

IF(ESCUR.LE.0.0) GO TO 60

```

```

RFACT = 1.0

```

```

MSTEP = ESCUR*8.0/UNIAX + 1.0

```

```

ASTEP = MSTEP

```

```

REDUC = 1.0 - RFACT

```

```

DO 80 ISTR1 = 1, NSTRE

```

```

SGTOT(ISTR1) = STRSG(ISTR1, KGAUS) + REDUC*STRES(ISTR1)

```

```

STRES(ISTR1) = RFACT*STRES(ISTR1)/ASTEP

```

```

DO 90 ISTEP = 1, MSTEP

```

```

CALL INVAR(AMATX, SGTOT, LPROP, MMATS, YIELD)

```

```

CALL FLOWS(ABETA, AVECT, DVECT, LPROP, MMATS, NPROP, PROPS,
SGTOT, AMATX, DMATX)

```

```

AGASH = 0.0

```

```

DO 100 ISTR1 = 1, NSTRE

```

```

AGASH = AGASH + AVECT(ISTR1)*STRES(ISTR1)

```

```

DLAMD = AGASH*ABETA

```

```

IF(DLAMD.LT.0.0) DLAMD = 0.0

```

```

BGASH = 0.0

```

```

DO 110 ISTR1 = 1, NSTRE

```

```

BGASH = BGASH + AVECT(ISTR1)*SGTOT(ISTR1)

```

```

SGTOT(ISTR1) = SGTOT(ISTR1) + STRES(ISTR1) - DLAMD*DVECT(ISTR1)

```

```

EPSTN(KGAUS) = EPSTN(KGAUS) + DLAMD*BGASH/YIELD

```

```

CONTINUE

```

```

CALL INVAR(AMATX, SGTOT, LPROP, MMATS, YIELD)

```

```

CURYS = UNIAX + EPSTN(KGAUS)*HARDS

```

```

BRING = 1.0

```

```

IF(YIELD.GT.CURYS) BRING = CURYS/YIELD

```

```

DO 130 ISTR1 = 1, NSTRE

```

```

STRSG(ISTR1, KGAUS) = BRING*SGTOT(ISTR1)

```

```

EFFST(KGAUS) = BRING*YIELD

```

ALTERNATIVE LOCATION OF STRESS REDUCTION LOOP TERMINATION CARD
CONTINUE

GO TO 190

DO 180 ISTR1 = 1, NSTRE
STRSG(ISTR1, KGAUS) = STRSG(ISTR1, KGAUS) + DESIG(ISTR1)
EFFST(KGAUS) = YIELD
IF(EPSTN(KGAUS).EQ.0.0.OR.ESCUR.EQ.0.0) GO TO 190
EPSTN(KGAUS) = -EPSTN(KGAUS)
KUNLO = KUNLO + 1

CONTINUE
CALCULATE THE EQUIVALENT NODAL FORCES AND ASSOCIATE WITH THE
ELEMENT NODES

MGASH = 0

DO 140 INODE = 1, NNODE

DO 140 IDOFN = 1, NDOFN

MGASH = MGASH + 1

DO 140 ISTR = 1, NSTRE

ELOAD(IELEM, MGASH) = ELOAD(IELEM, MGASH) + BMATX(ISTR, MGASH) *

STRSG(ISTR, KGAUS) * DVOLU

CONTINUE

CONTINUE

CONTINUE

RETURN

END

SUBROUTINE SFR1
SUBROUTINE SFR1(W, G, H)

PARABOLIC SHAPE FUNCTIONS AND THEIR FIRST DERIVATIVES FOR
8-NODE ELEMENT PLUS THE CENTRAL HIERARCHIAL FUNCTION
G AND H DENOTE THE XI AND ETA VALUES AT THE POINT CONSIDERED

DIMENSION W(3,9)

GG = G*G

GH = G*H

HH = H*H

GGH = GG*H

GHH = G*HH

G2 = G*2

H2 = H*2

GH2 = GH*2

W(1,1) = (-1. +GH+GG+HH-GGH-GHH)/4.

W(1,2) = (1. -H-GG+GGH)/2.

W(1,3) = (-1. -GH+GG+HH-GGH+GHH)/4.

W(1,4) = (1. +G-HH-GHH)/2.

W(1,5) = (-1. +GH+GG+HH+GGH+GHH)/4.

W(1,6) = (1. +H-GG-GGH)/2.

W(1,7) = (-1. -GH+GG+HH+GGH-GHH)/4.

W(1,8) = (1. -G-HH+GHH)/2.

W(1,9) = 1. 0-GG-HH+GG*HH

W(2,1) = (H+G2-GH2-HH)/4.

W(2,2) = -G+GH

W(2,3) = (-H+G2-GH2+HH)/4.

W(2,4) = (1. -HH)/2.

W(2,5) = (H+G2+GH2+HH)/4.

W(2,6) = -G-GH

W(2,7) = (-H+G2+GH2-HH)/4.

W(2,8) = (-1+HH)/2.

W(2,9) = -G2*(1. 0-HH)

W(3,1) = (G+H2-GG-GH2)/4.

W(3,2) = (-1. +GG)/2.

W(3,3) = (-G+H2-GG+GH2)/4.

W(3,4) = -H+GH

W(3,5) = (G+H2+GG+GH2)/4.

W(3,6) = (1. -GG)/2.

W(3,7) = (-G+H2+GG-GH2)/4.

W(3,8) = -H+GH

W(3,9) = -H2*(1. 0-GG)

RETURN

END

SUBROUTINE SINGOP
SUBROUTINE SINGOP(N1, NOPN)

VECTORS OR MATRIX MANIPULATIONS INCLUDING SINGLE SPACE

NOPN = 1, MULT

NOPN = 2, NORMALISE VECTOR

NOPN = 3, TRANSPOSE MATRIX

NOPN = 4, FIND VECTOR SQUARED

NOPN = 5, FORM UNIT DIAGONAL MATRIX IN N1

COMMON WORMX(3,24), GVALU, DJACB

WRITE(40,*) 'ENTERS SIGNOP AND RECEIVES THE FOLLOWING

N1, NOPN, FROM VECT'

WRITE(40,*) 'N1, NOPN= ', N1, NOPN

GO TO (1,2,3,4,5), NOPN

CALL VECT(N1, N1, 0, 3)

RETURN

CALL VECT(N1, N1, 0, 2)

RETURN

WRITE(40,*) 'NOPN = ', NOPN, 'N1= ', N1

CALL MATM(N1, N1, 0, 5)

RETURN

CALL VECT(N1, N1, 0, 1)

RETURN

N2 = N1 + 2

DO 12 J = N1, N2

DO 11 I = 1, 3

WORMX(I, J) = 0.0

II = II + 1

WORMX(II, J) = 1.0

RETURN

END

SUBROUTINE STIFF(EPSTN, ESTIF, KITER, LNODS, MATNO,
MELEM, MEVAB, MMATS, MPOIN, MTOTG, NDOFN,
NELEM, NEVAB, NGAUS, NNODE, NPROP,
NSTRE, POSGP, PROPS, STRSG, WEIGP, AMATX,
DMATT, MLAYR, NLAYR, THICK,
TDISP, MTOTV, LARGE)

THIS SUBROUTINE EVALUATES THE STIFFNESS MATRIX FOR EACH
ELEMENT IN TURN

DIMENSION BMATX(5,45), DBMAT(5,45), DMATX(5,5),
ESTIF(MEVAB, MEVAB), LNODS(MELEM, 9), MATNO(MELEM, MLAYR),
POSGP(5), PROPS(MMATS, NPROP), AMATX(9, MMATS),
STRES(5), THICK(MPOIN), WEIGP(5), EPSTN(MTOTG),
STRSG(5, MTOTG), AVECT(5), DVECT(5), DMATT(5, 5, MMATS),
TDISP(MTOTV), ETDIS(45), GMATX(2, 45)

REWIND 1

REWIND 8

KGAUS = 0

LOOP OVER EACH ELEMENT

DO 110 IELEM = 1, NELEM

SET UP THE ELEMENT DISPLACEMENT VECTOR -ETDIS-

JPOSI = 0

DO 10 INODE = 1, NNODE

LNODE = IABS(LNODS(IELEM, INODE))

NPOSN = (LNODE-1)*NDOFN

DO 10 IDOFN = 1, NDOFN

NPOSN = NPOSN + 1

JPOSI = JPOSI + 1

ETDIS(JPOSI) = TDISP(NPOSN)

DO 20 IEVAB = 1, NEVAB

DO 20 JEVAB = 1, NEVAB

ESTIF(IEVAB, JEVAB) = 0.0

KGASP = 0

INITIALIZE THE ELEMENT STIFFNESS MATRIX

DO 105 IGAUS = 1, NGAUS

DO 105 JGAUS = 1, NGAUS

DO 100 ILAYR = 1, NLAYR

LPROP = MATNO(IELEM, ILAYR)

KGASP = KGASP - 1

KGAUS = KGAUS + 1

READ(8) BMATX, GMATX, DVOLU

```

CALL SUBROUTINE WHICH SETS UP -BMATX- TAKING INTO ACCOUNT
THE LARGE DISPLACEMENTS
IF (LARGE.EQ.1.AND.KITER.GT.2)
CALL LDISP(BMATX,GMATX,ETDIS,NEVAB)
IF(KITER.EQ.2)GO TO 80
IF(EPSTN(KGAUS).LE.0.0) GO TO 80
CALCULATE THE ELASTO-PLASTIC -D- MATRIX

DO 30 ISTR = 1,NSTRE
STRS(ISTR) = STRSG(ISTR,KGAUS)
CALL FLOWS(ABETA,AVECT,DVECT,LPROP,MMATS,NPROP,PROPS,
STRS,AMATX,DMATT)
DO 70 ISTR = 1,NSTRE
DO 70 JSTR = 1,NSTRE
DMATX(ISTR,JSTR) = DMATT(ISTR,JSTR,LPROP)-ABETA*
DVECT(ISTR)*DVECT(JSTR)
WRITE(30,*) ((DMATX(IST,JST),JST=1,NSTRE),IST=1,NSTRE)
WRITE(30,*) 'VALUE OF NSTRE=',NSTRE

CALCULATE THE PRODUCT OF D MATRIX AND B MATRIX

DO 35 ISTR = 1,NSTRE
DO 35 IEVAB = 1,NEVAB
DBMAT(ISTR,IEVAB) = 0.0
DO 35 JSTR = 1,NSTRE
DBMAT(ISTR,IEVAB) = DBMAT(ISTR,IEVAB)+DMATX(ISTR,JSTR)*
BMATX(JSTR,IEVAB)
35 CONTINUE
GO TO 90
3 CONTINUE
DO 85 ISTR = 1,NSTRE
DO 85 IEVAB = 1,NEVAB
DBMAT(ISTR,IEVAB) = 0.0
DO 85 JSTR = 1,NSTRE
DBMAT(ISTR,IEVAB) = DBMAT(ISTR,IEVAB)+
DMATT(ISTR,JSTR,LPROP)*BMATX(JSTR,IEVAB)

WRITING BGMAT FOR TEST ON UNIT 30
WRITE(30,*) 'BGMAT'
WRITE(30,666) ((BMATX(I,J),J=1,45),I=1,5)
666 FORMAT(1X,5E14.7/1X,5E14.7/1X,5E14.7/1X,5E14.7/1X,5E14.7
/1X,5E14.7/1X,5E14.7/1X,5E14.7/1X,5E14.7)
WRITE D MATRX ONTO 30 FOR CHECK ONLY
WRITE(30,*) 'DMATT'
WRITE(30,777) ((DMATT(I,J,1),J=1,5),I=1,5)
777 FORMAT(1X,5E14.7)

CALCULATE THE ELEMENT STIFFNESS

DO 90 IEVAB =1,NEVAB
DO 40 JEVAB = IEVAB,NEVAB
DO 40 ISTR = 1,NSTRE
ESTIF(IEVAB,JEVAB) = ESTIF(IEVAB,JEVAB)+BMATX(ISTR,IEVAB)*
DBMAT(ISTR,JEVAB)*DVOLU

CALL SUBROUTINE WHICH CALCULATES THE GEOMETRIC MATRIX -GEMTX-
WRITE(5,*) '*****CALLIN GEOME*****'

CALL GEOME(ESTIF,GMATX,STRSG,MEVAB,NEVAB,MTOTG,KGAUS,DVOLU)

WRITE(5,*) '*****COMING OUT OF GEOME*****'
98 CONTINUE
99 CONTINUE
100 CONTINUE
101 CONTRACT THE LOWER TRIANGLE OF THE STIFFNESS MATRIX
DO 60 IEVAB = 1,NEVAB
DO 60 JEVAB = 1,NEVAB
ESTIF(JEVAB,IEVAB) = ESTIF(IEVAB,JEVAB)
CONTINUE

WRITE(20,*) 'ESTIF(22,22',ESTIF(22,22)
WRITE(20,*) 'ESTIF(27,27',ESTIF(27,27)
STORE THE STIFFNESS MATRIX FOR EACH ELEMENT ON DISC FILE
WRITE(1) ESTIF

```

```

10      CONTINUE
      DO 771 ILM1 = 1, 2
      WRITE(30,*) 'ELEMENT NO. = ', ILM, MEVAB
      WRITE(30,*) ((ESTIF(I,J), J=1, 45), I=1, 45)
771    CONTINUE
      RETURN
      END

-----
      SUBROUTINE VECT
      SUBROUTINE VECT(N1, N2, N3, NOPN)
      *****
      VECTOR MANIPULATIONS
      NOPN = 1, QVALU BECOMES SCALAR PRODUCT OF COL. N1 AND N2
      NOPN = 2, NORMALISE N1 INTO N2
      NOPN = 3, MULTIPLY N1 BY QVALU, PLACE IN N2
      NOPN = 4, N3 BECOMES VECTOR PRODUCT OF N1 AND N2
      NOPN = 5, N3 BECOMES VECTOR N1 + VECTOR N2*QVALU
      *****
      COMMON WORMX(3, 24), QVALU, DJACOB
      WRITE(5,*) '..... ENTERS VECT.....'
      WRITE(5,*) 'N1, N2, N3, NOPN', N1, N2, N3, NOPN
      DO 1101 I = 1, N1
      WRITE(5,*) '..... WORMX(I, N1)....', WORMX(I, N1)
1101    CONTINUE
      I1 = N1
      GO TO (1, 2, 3, 4, 5), NOPN
      I1 = N2
      WRITE(5,*) '-----NOPN=, I1, N1, N2', NOPN, I1, N1, N2
      WRITE(5,*) 'WORMX"X...', WORMX(1, N1), WORMX(2, N1), WORMX(3, N1)
      WRITE(5,*) 'WORMX"S. I, I1', WORMX(1, I1), WORMX(2, I1), WORMX(3, I1)
      QVALU = 0.0
      DO 10 I = 1, 3
      QVALU = QVALU + WORMX(I, N1)*WORMX(I, I1)
      GO TO (15, 16), NOPN
      IF(QVALU.NE.0.0)GO TO 18
      WRITE(6, 17)
      FORMAT(12H NULL VECTOR)
      STOP
      EXECUTINON IS TERMINATED WHEN A VECTOR IS NULL
      QVALU = 1.0/SQRT(QVALU)
      DO 12 I = 1, 3
      WORMX(I, N2) = WORMX(I, N1)*QVALU
      RETURN
      K = 3
      DO 13 I = 1, 3
      J = 6-I-K
      WRITE(5,*) ' I, J, K...', I, J, K, N1, N2, N3
      WORMX(I, N3) = WORMX(J, N1)*WORMX(K, N2)-WORMX(K, N1)*WORMX(J, N2)
      WRITE(5,*) '##### WORMX(I, N3) IN VECT &&&&', WORMX(I, N3)
      K = I
      RETURN
      DO 14 I = 1, 3
      WORMX(I, N3) = WORMX(I, N1) + QVALU*WORMX(I, N2)
      RETURN
      END

-----
      SUBROUTINE WORKS
      SUBROUTINE WORKS(COORD, DICOS, LNODS, THICK, MELEM, MPOIN, NPOIN, M3POI)
      *****
      THIS SUBROUTINE SETS UP THE THICKNESS AND ORTHOGONAL
      SYSTEM OF AXES AT EACH NODAL POINT
      *****
      DIMENSION COORD(MPOIN, 8), LNODS(MELEM, 9), THICK(MPOIN),
      DICOS(3, M3POI)
      COMMON WORMX(3, 24), QVALU, DJACB
      TOP AND BOTTOM CO-ORDINATES ARE SET UP AT COLUMNS -1- AND -2-
      DO 30 IPOIN = 1, NPOIN
      WRITE(5, 3101) IPOIN
      FORMAT(/'+', I2)
      DO 10 I = 1, 3
      WORMX(I, 1) = COORD(IPOIN, I)
      WORMX(I, 2) = COORD(IPOIN, I+4)
      NGASH = 3
      NGISH = NGASH + 2
3101

```

```

QUALU = -1.0
VECTOR V-3 IN COLUMN NGISH
CALL VECT(1,2,NGISH,5)

SETS QUALU EQUAL TO SCALAR PRODUCT OF THE VECTOR (V-3)*(V-3)

WRITE(5,*) 'START ENTERING SIGNOP.....'
CALL SINGOP(NGISH,4)
THICK(IPOIN) = SQRT(QUALU)
CREATES AND NORMALISES AT EACH NODE THE VECTORS V-1,V-2 AND V-3
CALL FRAME(NGASH,NGISH,0,1)
DO 354 I = 1,3
  WRITE(5,*) '-----WORMX-----', WORMX(I,1), WORMX(I,2)
CONTINUE

SET UP THE DIRECTION COSINE MATRIX OF THE LOCAL AXES AT EACH
POINT IN ORDER V-1,V-2,V-3

NPOSI = (IPOIN-1)*3
DO 20 I=1,3
DO 20 J =1,3
JPOSI = NPOSI + I
  DICOS(J,JPOSI) = WORMX(J,I+2)
CONTINUE
RETURN
END

```

```

-----
SUBROUTINE RESTAR
SUBROUTINE RESTAR(EFFST,ELOAD,EPSTN,MELEM,MEVAB,MTOTG,
  MTOTV,MVFIX,TDISP,TLOAD,TREAC,STRSG,
  TFACT,KINGS)
*****
THIS SUBROUTINE RECORDS ONTO TAPE 12 THE DATA NEEDED TO
RESTART THE PROBLEM
*****
DIMENSION EFFST(MTOTG),ELOAD(MELEM,MEVAB),EPSTN(MTOTG),
  TDISP(MTOTG),TLOAD(MELEM,MEVAB),TREAC(MVFIX,5),
  STRSG(5,MTOTG)
REWIND 12
WRITE(12) KINGS,TFACT,EFFST,ELOAD,EPSTN
WRITE(12) TDISP,TLOAD,TREAC,STRSG
RETURN
END

```

```

-----
SUBROUTINE ZERO
SUBROUTINE ZERO(EFFST,ELOAD,EPSTN,MELEM,MEVAB,KINGS,
  MTOTG,MTOTV,NDOFN,NELEM,NEVAB,NREST,
  NSTRE,NTOTG,NTOTV,NVFIX,MVFIX,STRSG,
  TDISP,TFACT,TLOAD,TREAC)
*****
THIS SUBROUTINE INITIALISES VARIOUS ARRAYS TO ZERO
*****
DIMENSION ELOAD(MELEM,MEVAB),STRSG(5,MTOTG),TDISP(MTOTG),
  TLOAD(MELEM,MEVAB),TREAC(MVFIX,5),EPSTN(MTOTG),
  EFFST(MTOTG)
WRITE(50,*) 'VALUE OF NEVAB WITHIN ZERO=',NEVAB
IF(NREST.EQ.1) GO TO 70
KINGS = 0
TFACT = 0.0
DO 30 IELEM = 1,NELEM
DO 30 IEVAB = 1,NEVAB
  ELOAD(IELEM,IEVAB) = 0.0
  TLOAD(IELEM,IEVAB) = 0.0
DO 40 ITOTV = 1,NTOTV
  TDISP(ITOTV) = 0.0
DO 50 IVFIX = 1,NVFIX
DO 50 IDOFN = 1,NDOFN
  TREAC(IVFIX,IDOFN) = 0.0
DO 60 ITOTG = 1,NTOTG
  EPSTN(ITOTG) = 0.0
  EFFST(ITOTG) = 0.0
DO 60 ISTR1 = 1,NSTRE
  STRSG(ISTR1,ITOTG) = 0.0
GO TO 80
REWIND 12

```

```

READ(12) KINGS, TREAT, EFFST, ELOAD, EPSTN
READ(12) TDISP, TLOAD, TREAC, STRSG
CONTINUE
RETURN
END

```

```

-----
SUBROUTINE SHEARC
SUBROUTINE SHEARC(MATNO, MELEM, MLAYR, PROPS, MMATS, NPROP,
                  COEFE, NLAYR, DMATT)

```

```

*****
CALCULATES THE SHEAR CORRECTION FACTOR FOR THE CASE OF
LAMINATED COMPOSITE STRUCTURES
*****
DIMENSION RFACT(2), TRLOW(2), UPTER(2), GBARF(2), MATNO(MELEM, MLAYR),
          COEFE(2), ZETA1(2), ZETA2(2), DINDX(2), PROPS(MMATS, NPROP),
          GINDX(2), DIFF2(2), DIFF3(2), SUMLA(2), DMATT(5, 5, MMATS),
          DIFF5(2)

```

```

INITIALISE SOME ARRAYS
DO 10 I = 1, 2
SUMLA(I) = 0.0
RFACT(I) = 0.0
GBARF(I) = 0.0
UPTER(I) = 0.0
TRLOW(I) = 0.0
COEFE(I) = 0.0

```

CALCULATE THE POSITION OF THE NEUTRAL AXIS

```

DSUMM = 0.0
DO 15 ILAYR = 1, NLAYR
LPROP = MATNO(1, ILAYR)
DZETA = PROPS(LPROP, 3)
ZHEIG = DSUMM + DZETA/2.
DO 14 I = 1, 2
DINDX(I) = DMATT(I, 1, LPROP)
UPTER(I) = UPTER(I) + DINDX(I) * ZHEIG * DZETA
TRLOW(I) = TRLOW(I) + DINDX(I) * DZETA
DSUMM = DSUMM + DZETA
DO 16 I = 1, 2
ZETA2(I) = -UPTER(I) / TRLOW(I)

```

CALCULATE THE SHEAR CORRECTION FACTOR

```

DO 20 ILAYR = 1, NLAYR
LPROP = MATNO(1, ILAYR)
DIFF1 = PROPS(LPROP, 3)
INDEX = 10
DO 20 I = 1, 2
ZETA1(I) = ZETA2(I)
ZETA2(I) = ZETA1(I) * DIFF1
DIFF2(I) = ZETA2(I) ** 2 - ZETA1(I) ** 2
DIFF3(I) = ZETA2(I) ** 3 - ZETA1(I) ** 3
DIFF5(I) = ZETA2(I) ** 5 - ZETA1(I) ** 5

DINDX(I) = DMATT(I, 1, LPROP)
GINDX(I) = PROPS(LPROP, INDEX)

RFACT(I) = RFACT(I) + DINDX(I) * DIFF3(I) / 3.
GBARF(I) = GBARF(I) + GINDX(I) * DIFF1 / 2.
TERM1 = SUMLA(I) * SUMLA(I) * DIFF1
TERM2 = DINDX(I) * (ZETA1(I) ** 4) * DIFF1 / 4.
TERM3 = DINDX(I) * DIFF5(I) / 20.
TERM4 = -DINDX(I) * ZETA1(I) * ZETA1(I) * DIFF3(I) / 6.
TERM5 = SUMLA(I) * ZETA1(I) * ZETA1(I) * DIFF1
TERM6 = -SUMLA(I) * DIFF3(I) / 3.
COEFE(I) = COEFE(I) + (TERM1 + DINDX(I) * (TERM2 +
      TERM3 + TERM4 + TERM5 + TERM6)) / GINDX(I)
INDEX = INDEX + 1
SUMLA(I) = SUMLA(I) - DINDX(I) * DIFF2(I) / 2.
CONTINUE
DO 30 I = 1, 2
COEFE(I) = RFACT(I) * RFACT(I) / (2. * GBARF(I) * COEFE(I))
RETURN
END

```

MAIN MASTER OR CONTROLLING SEGMENT

```

PROGRAM PLSHELL(.....)
PROGRAM PLSHELL
  (INPUT, OUTPUT, TAPE5=INPUT, TAPE6=OUTPUT,
    TAPE1, TAPE2, TAPE4, TAPE7, TAPE8, TAPE12)
  *****
  PROGRAM FOR ELASTO-PLASTIC ANALYSIS OF ANISOTROPIC SHELL
  STRUCTURES USING QUADRATIC DEGENERATE SHELL ELEMENTS(8-NODE
  HETEROSIS AND 9-NODE) AND A LAYERED APPROACH, ACCOUNTING FOR
  LARGE DISPLACEMENTS AND SELECTIVE INTEGRATION(TRANSVERSE
  SHEAR TERMS). THE ANISOTROPIC PARAMETERS REMAIN CONSTANT
  DURING THE FLOW RESTART FACILITIES INCLUDED
  *****
  DIMENSION ASDIS(500), COORD(100,8), ELOAD(20,45), EGRHS(10),
    EQUAT(75,10), EFFST(1800), EPSTN(1800), ESTIF(45,45),
    FIXED(500), GLOAD(75), GSTIF(2850), GRAVI(3),
    IFFIX(500), LOCEL(45), LNODS(20,9), MATNO(20,10),
    NACVA(75), NAMEV(10), NDEST(45), NDFRO(20),
    NDOFIX(36), NOUTP(2), NPIVO(10), POSGP(5), THICK(100),
    PRESC(36,5), PROPS(5,17), RLOAD(20,45), STFOR(500),
    STRSG(5,1800), TDISP(500), TLOAD(20,45), TOFOR(500),
    TREAC(36,5), VECRV(75), WEIGP(5), DICOS(3,300),
    AMATX(9,5), DMATT(5,5,5)
  OPEN(UNIT=15, FILE='/' SHELL1 INP A', STATUS = 'OLD')
  OPEN(UNIT=6, FILE='/' SHELL OUT A', STATUS = 'NEW')
  OPEN(UNIT=1, STATUS='SCRATCH')
  OPEN(UNIT=4, STATUS='SCRATCH')
  OPEN(UNIT=7, STATUS='SCRATCH')
  OPEN(UNIT=8, STATUS='SCRATCH')
  OPEN(UNIT=12, STATUS='SCRATCH')

  PRESET VARIABLES ASSOCIATED WITH DYNAMIC DIMENSIONING
  CALL DIMEN(MBUFA, MELEM, MEVAB, MFRON, MMATS, MPOIN, MSTIF,
    MTOTG, MTOTV, MVFIX, NDOFN, NPROP, NSTRE, M3POI,
    MLAYR)

  CALL THE SUBROUTINE WHICH READS MOST OF THE PROBLEM DATA
  CALL INPUT(ANVEL, COORD, GRAVI, IFFIX, LNODS,
    MATNO, MFRON, MELEM, MMATS, MPOIN,
    MTOTV, MVFIX, NDFRO, NDOFN, NELEM, NCOLA,
    NEVAB, NGAUS, NGAUZ, NMATS, NNODE, MLAYR,
    NDOFIX, NPOIN, NPROP, NTOTG, NLAYR, NREST,
    NTOTV, NVFIX, POSGP, PRESC, PROPS, WEIGP,
    NALGD, NINCS, LARGE)

  CALL SUBROUTINE WHICH COMPUTES THE ELASTICITY MATRIX -D- AND
  THE MATRIX OF THE ANISOTROPIC PARAMETERS
  CALL MODAN(AMATX, DMATT, NMATS, NPROP, PROPS, MMATS,
    MATNO, MELEM, MLAYR, NELEM, NLAYR)

  CREATE THE THICKNESS AND A LOCAL ORTHOGONAL SET AT EACH NODAL POINT
  CALL WORKS(COORD, DICOS, LNODS, THICK, MELEM, MPOIN,
    NPOIN, M3POI)
  WRITE(5,*) '+++++++C O M E S O U T O F W O R K +++++'
  PAUSE

  CALL SUBROUTINE WHICH COMPUTES BMATX AND GMATX. THESE MATRICES
  ARE STORED ON TAPE 8 FOR LATER USAGE
  CALL BGMAT(COORD, DICOS, LNODS, MATNO, MELEM,
    MLAYR, MMATS, MPOIN, M3POI, NELEM,
    NEVAB, NGAUS, NGAUZ, NLAYR, NNODE, NPROP,
    POSGP, PROPS, THICK, WEIGP)
  CALL SUBROUTINE WHICH COMPUTES THE APPLIED LOADS
  AFTER READING SOME NODAL DATA
  WRITE(5,*) 'ENTERS LOADS AFTER COMING OUT OF BGMAT'
  PAUSE
  CALL LOADS(ANVEL, COORD, RLOAD, GRAVI, LNODS,
    MATNO, MELEM, MEVAB, MMATS, MPOIN, DICOS,
    NELEM, NEVAB, NGAUS, THICK,
    NNODE, NPROP, NSTRE, POSGP, M3POI,
    PROPS, WEIGP, MLAYR, NLAYR)
  WRITE(5,*) '!!!!!!C O M E S O U T O F L O A D S'

```

```

INITIALISE CERTAIN ARRAYS
WRITE(50,*) 'VALUE OF NEVAB ENTERING ZERO=', NEVAB

CALL ZERO(EFFST, ELOAD, EPSTN, MELEM, MEVAB, KINGS,
          MTOTG, MTOTV, NDOFN, NELEM, NEVAB, NREST,
          NSTRE, NTOTG, NTOTV, NVFIX, MVFIX, STRSG,
          TDISP, TFACT, TLOAD, TREAC)

WRITE(50,*) 'VALUE OF NEVAB COMING OUT OF ZERO=', NEVAB
LOOP OVER EACH ELEMENT

WRITE(50,*) 'NINCS =', NINCS
DO 100 IINCS = 1, NINCS

  READ DATA FOR CURRENT INCREMENT

  WRITE(50,*) 'VALUE OF NEVAB ENTERING INCREM', NEVAB
  CALL INCREM(ELOAD, FIXED, IINCS, MELEM, MEVAB, MITER,
            MTOTV, MVFIX, NDOFN, NELEM, NEVAB, NOUTP,
            NOFIX, NTOTV, NVFIX, PRESC, RLOAD, TFACT,
            TLOAD, TOLER, LNODS, IFFIX, NNODE, NCOLA,
            NREST, KINGS)

  LOOP OVER EACH ITERATION
  KSTOP = 0
  KUNLO = 0
  DO 50 IITER = 1, MITER
    KITER = IINCS + IITER
    JINCS = IINCS - KINGS

    CALL SUBROUTINE WHICH SELECTS SOLUTION ALGORITHM VARIABLE KRESL

    CALL ALGOR(FIXED, KITER, IITER, KRESL, MTOTV, NALGO,
              NTOTV, KUNLO, KINGS)
    WRITE(5,*) 'COMES OUT OF ALGOR'
    WRITE(5,*) 'VALUES OF KRESL, NALGO', KRESL, NALGO

    CHECK WHETHER A NEW EVALUATION OF THE STIFFNESS MATRIX
    IS REQUIRED

    IF (KRESL.EQ.1)
      CALL STIFF(EPSTN, ESTIF, KITER, LNODS, MATNO,
                MELEM, MEVAB, MMATS, MPOIN, MTOTG, NDOFN,
                NELEM, NEVAB, NGAUS, NNODE, NPROP,
                NSTRE, POSGP, PROPS, STRSG, WEIGP, AMATX,
                DMATT, MLAYR, NLAYR, THICK,
                TDISP, MTOTV, LARGE)
    WRITE(5,*) '*****COMES OUT OF STIFF*****'

    MERGE AND SOLVE THE RESULTING EQUATIONS BY THE FRONTAL SOLVER
    WRITE(5,*) '*****CALLING FRONT*****'
    WRITE(50,*) 'KRESL, NALGO BEFORE CALLING STIFF', KRESL, NALGO

    WRITE(50,*) 'VALUE OF NTOTV BEFORE CALLING FRONT', NTOTV
    CALL FRONT(ASDIS, ELOAD, EGRHS, EQUAT, ESTIF, FIXED,
              GLOAD, GSTIF, IFFIX, JINCS, IITER, KRESL,
              LOCEL, LNODS, MBUFA, MELEM, MEVAB, MFRON,
              MSTIF, MTOTV, MVFIX, NACVA, NAMEV, NDEST,
              NDOFN, NELEM, NEVAB, NNODE, NOFIX, NPIVO,
              NPOIN, NTOTV, TDISP, TLOAD, TREAC, VECRV)

    WRITE(5,*) 'START ENTERING RESTR'
    WRITE(5,*) '*****COMES OUT OF FRONT*****'

    CALCULATE RESIDUAL FORCES

    CALL RESTR(ASDIS, EFFST, ELOAD, LNODS,
              MATNO, MELEM, MMATS, MPOIN, MTOTG, MTOTV,
              NDOFN, NELEM, NEVAB, NGAUS, NNODE,
              NPROP, NSTRE, POSGP, PROPS, STRSG,
              TDISP, WEIGP, EPSTN, KUNLO, AMATX, DMATT,
              THICK, MLAYR, NLAYR, LARGE)

    CHECK FOR CONVERGENCE
    WRITE(5,*) '*****CALLING CONVER *****'

```

```

CALL CONVER(ELOAD, IITER, LNODS, MELEM, MEVAB, MTOTV,
            NCHEK, NDOFN, NELEM, NEVAB, NNODE, NTOTV,
            STFOR, TLOAD, TOFOR, TOLER)
WRITE(5,*) '*****COMES OUT OF CONVER*****'

```

```

OUTPUT RESULTS IF REQUIRED

```

```

IF(IITER.EQ.1.AND.NOUTP(1).GT.0)
  CALL OUTPUT(IITER, MTOTG, MTOTV, MVFIX, NCHECK, NELEM,
             NGAUS, NOFIX, NOUTP, NPOIN,
             NSTRE, NVFIX, STRSG, TDISP, TREAC, EPSTN,
             POSGP, EFFST, MATNO, MMATS, PROPS,
             NPROP, MELEM, THICK,
             MPOIN, LNODS, MLAYR, NLAYR)

```

```

IF SOLUTION HAS CONVERGED STOP ITERATING AND OUTPUT RESULTS

```

```

IF(IITER.EQ.1.AND.NCHECK.EQ.0) GO TO 100
IF(NCHECK.EQ.0) GO TO 75
CONTINUE

```

```

      KSTOP =1
      CALL OUTPUT(IITER, MTOTG, MTOTV, MVFIX, NCHECK, NELEM,
                 NGAUS, NOFIX, NOUTP, NPOIN,
                 NSTRE, NVFIX, STRSG, TDISP, TREAC, EPSTN,
                 POSGP, EFFST, MATNO, MMATS, PROPS,
                 NPROP, MELEM, THICK,
                 MPOIN, LNODS, MLAYR, NLAYR)

```

```

IF(KSTOP.EQ.1) STOP

```

```

RECORD ONTO TAPE 12 THE DATA NEEDED FOR RESTART THE PROBLEM
TO NEXT INCREMENT

```

```

CALL RESTR(EFFST, ELOAD, EPSTN, MELEM, MEVAB, MTOTG,
           MTOTV, MVFIX, TDISP, TLOAD, TREAC, STRSG,
           TFACT, IINCS)

```

```

CONTINUE
STOP
END

```


APPENDIX C

LISTINGS OF PUBLICATIONS

A Finite Cell Model For 3-D Braided Composites

Charles S. C. Lei, Albert S. D. Wang and Frank K. Ko

*Presented at
Winter Meeting of ASME
Advanced Composites Processing Technology
Chicago, IL
Nov 28- Dec. 3, 1988*

ABSTRACT

The macroscopic elastic behavior of 3-D braided composites is characterized on the basis of a micromechanical analysis of a unit cell structure. Treating a 3-D braided composite as an assembly of individual unit cells idealized as a pin-jointed truss in the shape of a brick, the Finite Cell model is based on the principle of virtual work and structural truss analysis. The usefulness of the resultant model is explored via parametric study and verified using the tensile properties of carbon-carbon composites.

INTRODUCTION

The explosive growth of aerospace industry in recent years has stimulated a rapid development of innovative design and fabrication techniques for advanced structural composites. The recent progress in fabric formation technology has created new options in composite structural design. Using the fabric formation technology, various fiber geometric structures can be formed easily. In order to fully explore the potential of these new material systems, an analytical framework is needed to link fiber architecture and material properties to composite properties.

Among the large family of textile structural composites, the 3-D braided composites have received a great deal of attention owing to their improved stiffness and strength in the thickness direction, their delamination-free characteristics and their near net shape manufacturing capabilities. Several analytic models have been developed to characterize the elastic moduli and structural behavior of 3-D braided composites.

Ma, Yang and Chou [1] assumed the yarns in a unit cell of a 3-D braided composite as composite rods, which form a parallel pipe. Strain energies due to yarn axial tension, bending and lateral compression are considered and formulated within the unit cell. By Castigliano's theorem, closed form expressions for axial elastic moduli and Poisson's ratios have been derived as functions of fiber volume fractions and fiber orientations.

Ma, et.al. also developed a "Fiber Inclination Model" according to the idealized zig-zagging yarn arrangement in the braided preform.[2] They assumed an inclined lamina as a representation of one set of diagonal yarns in a unit cell. In this way, four inclined unidirectional laminae form a unit cell. Then, by the employment of classical laminate theory, the elastic moduli can be expressed in terms of the laminae properties.

From a 'preform processing science' point of view, Ko et al.[3] developed a "Fabric Geometric Model" using similar assumptions. The stiffness of a 3-D braided composite was considered to be the sum of stiffnesses of all its laminae. A maximum strain energy criterion was used to determine the failure point for each lamina by taking bending stress on yarn crossover into consideration. The stiffness matrix forms a link between applied strains and the corresponding stress responses. Throughout this analysis, the stress-strain characteristics of the composite are determined.

The results of elastic properties from the above three models can be used as input to a generalized finite element program in order to analyze more complex shaped structures. By doing so, the 3-D braided composite has to be treated as effective continuum, and the unique characteristics of each individual yarn and matrix are smeared out. With these complex fiber architecture systems, the

effective continuum concept can no longer provide accurate description. It is the objective of this paper to establish a finite cell model (FCM) which can accommodate structures with variable unit cells and provide a link between microstructural design and macro-structural analysis. In complex structural shapes such as I-beams, turbine blades, the final structure often consists of several types of fiber architecture.

THE FINITE CELL MODEL

The FCM is based on the concept of fabric unit cell structure and structural truss analysis. The fiber architecture within the composite is considered as an assemblage of a finite number of individual structural cells with brick shape. Each individual cell is the smallest representative volume from the fibrous assembly. The unit cell is then treated as a space-truss structure with the endowed representative architecture, rather than a material with a set of effective continuum properties.

The key step in the formulation of the problem is the identification of the unit cell's nodal supports, similar to the nodal points of a conventional finite element. In this model, the yarns are assumed to travel along the diagonals in a unit cell and are treated as pin-jointed two-force truss members. By treating a unit cell specifically as a 3-D space truss, a 3-D truss finite element technique may be employed for the mechanistic analysis.

A displacement method is chosen in the finite element procedure which follows the principle of virtual work. This method regards the nodal displacements as basic unknowns. Thus, a virtual displacement or a unit displacement is used in the finite element procedure. The compatibility condition is first satisfied by correlating the nodal displacements to the end deformations of the members.

The force-displacement relationship is then established between the member end forces and deformations and between the possible nodal forces and nodal displacements. Finally, using nodal equilibrium equations, the member forces and deformations of the structure are obtained. The matrix $[K]$ or the stiffness of the cell is then derived to relate nodal displacement vector to nodal forces for a cell.

In order to include the effect of matrix, which is subjected to tension or compression under the deformation of yarns, the matrix is assumed to act as truss members, connecting the two ends of a given set of yarns in the unit cell as shown in Figure 1. In the unit cell, the nodes, or the ends of yarns, are pin-jointed with three degrees of freedom in translation. Hence, the matrix plays a role in restricting the free rotation and deformation of yarns. There are a total of 24 degrees of freedom in a four diagonal yarn unit cell. For this analysis, the interaction at the yarn interlacing and bending effect of yarns are not considered.

Let q_i represent the value of member deformation caused by a unit nodal displacement r_j . The

total value of each member deformation caused by all the nodal displacements may be written in the following matrix form:

$$\{q\} = [a]\{r\} \quad (1)$$

$$\begin{Bmatrix} q_1 \\ q_2 \\ \vdots \\ q_m \end{Bmatrix} = \begin{bmatrix} a_{11} & a_{12} & \dots & a_{1n} \\ a_{21} & a_{22} & \dots & a_{2n} \\ \vdots & \vdots & \ddots & \vdots \\ a_{m1} & a_{m2} & \dots & a_{mn} \end{bmatrix} \begin{Bmatrix} r_1 \\ r_2 \\ \vdots \\ r_n \end{Bmatrix}$$

where $[a]$ is called the displacement transformation matrix which relates the member deformations to the nodal displacements. In other words, it represents the compatibility of displacements of a system.

The next step is to establish the force-displacement relationship within the unit cell. For a pin-connected truss, the member force-deformation relationship can be written as:

$$\{Q\} = [K]\{q\} \quad (2)$$

where:

$$[K] = \begin{bmatrix} AE/L & & & \\ & AE/L & & \\ & & \ddots & \\ & & & AE/L \end{bmatrix}$$

The principle of virtual work states that the work done on a system by the external forces equals the increase in strain energy stored in the system. Here, the nodal forces can be considered as the external forces of the unit cell. Therefore, if $\{R\}$ represents the nodal force vector, it follows that

$$\{r\}^T \{R\} = \{q\}^T \{Q\} \quad (3)$$

where $\{r\}$ and $\{q\}$ are virtual displacement and deformation, respectively. From Eqs.(1) and (2), the following equations can be derived:

$$\{Q\} = [K][a]\{r\} \quad (4)$$

$$\{q\}^T = \{r\}^T [a]^T \quad (5)$$

and

$$\{r\}^T \{R\} = \{r\}^T [a]^T [K] \{r\} \quad (6)$$

Or,

$$\{R\} = [K]\{r\} \quad (7)$$

where

$$\{R\} = \text{nodal forces}$$

$$[K] = [a]^T [K] [a] = \text{stiffness matrix of the unit cell}$$

$$\{r\} = \text{nodal displacements}$$

Using Equation 7, the nodal force and the nodal displacements of a unit cell are related. Thus, for a structural shape which consists of a finite number of unit cells with a specific assemblage pattern, a sys-

tem of equations for the total structural shape can be assembled using the individual cell-relations following the finite element methodology. A complete listing of the terms associated with the K matrix is given in Figure 2.

From the solution of the equations, the stress distribution and deformation of the entire structure under applied load can be calculated and analyzed. To illustrate the application of the FCM, 3-D braided composites are used for this study. With basic parameters in a unit cell, such as yarn elastic modulus, fiber volume fraction, yarn orientation and unit cell dimension fully characterized, the applicability of the FCM to predict the structural response of composites will be demonstrated through a parametric study and verified experimentally.

NUMERICAL SIMULATIONS

The FCM was implemented by the use of computer simulation. By entering the basic parameters for a unit cell and fiber/matrix properties to the program, the load-deformation and elastic properties, such as elastic moduli and Poisson's ratios, of a composite can be calculated. A few examples are employed to demonstrate the applicability of the FCM under different conditions.

To study the elastic behavior between different fiber geometries, the composites under 1x1 and 1x2 braiding processes are chosen. The basic parameters are identical except the dimensions of the two unit cells. Figure 3 shows the predicted tensile stress-strain curves, where higher stiffness of 1x1 braiding can be observed. The reason is that the 1x1 braiding has compact fiber geometry in a unit cell.

Figure 4a and 4b depict the elastic behavior of 1x1 braided composites under 1-1, 2-2 and 3-3 directional tensile loading conditions for Kevlar 49/Epon 828 and carbon/carbon composites, respectively. As shown in the figure, the modulus in 1-1 direction is the highest as expected, while the modulus in 3-3 direction is the lowest.

The effect of fiber volume fraction under the same braiding process is illustrated in Figure 5. Three volume fractions are chosen for study. Here, the dimension of a unit cell, fiber-bar area and matrix-bar area are different due to different fiber volume fraction. The results demonstrate that the composite with higher fiber volume fraction has higher modulus.

In laminated composite, it is known that for the same fiber volume fraction, the composite with higher off-axis fiber orientation has lower elastic properties. To study this phenomenon, composites of 0°, 20°, 24°, 30° and 40° of braiding angles are analyzed, as shown in Figure 6. The composite with 0° braiding angle exhibits the highest modulus, and when the braiding angle is above 20°, the elastic behavior of composite tends to be insensitive to braiding fiber orientation.

The model can be extended to analyze the 3-D braided composite with different kind of unit cells.

To do so, the positions of each unit cell should be identified and recorded like traditional finite element programming. Hence, a complex shaped structure, such as 3-d braided I-beam, rotor, etc. can be analyzed if the basic parameters of unit cells and fiber volume fraction are given.

EXPERIMENTAL VERIFICATION

To provide a preliminary verification of the model, simple rectangular coupons of the 3-D braided carbon-carbon composite were fabricated and characterized by tensile testing. When using a simple shape, as detailed in [4], the key parameter in the braiding process is the track and column displacements. These displacements determine the projected orientation of fibers in the x-y plane, as well as affecting the overall structural geometry of the fabric.

The track/column displacements chosen for this study were 1/1 and 1/2. The notation u/v indicates a track displacement of u bobbins and a column displacement of v bobbins in one motion. The smallest representative volume of these fabrics, or the unit cell, is identified by the displacement values of u/v.

Using the FCM, the structural response of the unit cell under applied load was examined. The simulated results were compared to the experimental data. The material used for this study was T-40 carbon fiber, with a fiber modulus of 40 Msi. The 1/8"x1"x10" 3-D braided preforms were consolidated with carbon; the fiber volume fraction of the composite was 35%. End tabs were adhered to the ends of the specimens, and strain gages were applied to the specimen surface. The tensile tests were carried out according to ASTM Standard.

From the experimental stress-strain curves shown in Figure 7, it can be seen that the tensile responses of the 3-D braided Carbon/Carbon composites are nearly linear to the point of failure. The possible nonlinear behavior due to geometric effect and microcracking are not evident.

For the lack of accurate measurement of fiber volume fraction of a unit cell, a theoretical value of 35% of fiber volume fraction was used for the numerical computation. The dimension of a unit cell is determined from the measurements by a digital caliper. Since the dimensions of a unit cell are considered to be the center lines of members of the unit cell, part of the bars lie outside the unit cell. Thus, an averaging method for the determination of the cross-section areas of the bars was used. For a unit cell dimension of $H \times W \times T$, the area of a fiber-bar can be obtained as $A_f = 0.35HWT / 4(H^2 + W^2 + T^2)^{1/2}$; the area of a matrix-bar can be expressed as $A_m = 0.65HWT / 4(H + W + T)$. Here, area of each fiber-bar as well as the matrix-bar are the same. Accordingly, the elastic properties used for the unit cell are:

$$E_f = 40 \text{ msi}; V_f = 0.35$$

$$E_m = 1.3 \text{ msi}; V_m = 0.65$$

for 1x2 unit cell, the dimension is 0.295"x 0.13"x 0.0864"
and $A_f = 0.000852 \text{ in}^2$ $A_m = 0.0010309 \text{ in}^2$

Since each cell has an similar geometry and boundary conditions, it is sufficient to model only one element, as shown in Figure 8. A uniform load was applied at one end of the cell. The applied load was divided into several load steps on account of the possible nonlinear load-deformation behavior due to geometrical conformation. At each load step, convergence was achieved after several iterations. Figure 9 shows both calculated and experimental stress-strain curves for 1x1 and 1x2 unit cells, respectively. The results show that variation of fiber geometry from 1x1 to 1x2 does not have much effect on the overall characteristics of the stress-strain curves.

The predicted stiffness of the composites tended towards a higher value than experimental results. This can be attributed to the use of fiber data as an input for our prediction. In order to reflect the fiber breakage and degradation during manufacturing, the use of yarn data may be more appropriate.

CONCLUDING REMARKS

A finite cell model has been developed to predict the mechanical behavior of 3-D braid composites. By appropriate choice of yarn mechanical properties and precise determination of dimension of a unit cell, the FCM has been shown to be an adequate model for any 3-D braided composite for a first approximation. Further studies on yarn properties should be conducted in order to provide a realistic basis for the application of FCM to composite mechanical properties.

In a 3-D braided composite, the yarns actually experience bending moments throughout the unit cell during the braiding process. The present model will be modified to include the bending effect and the pin-jointed truss replaced as a stiffer frame structure. It should be pointed out that the fiber geometry of a unit cell along the boundary of a specimen is slightly different from the one near the center. In order to more precisely characterize the load-deformation relationship of the whole composite, especially at the corner of a complex shape 3-D braid composite, a few different unit cell may be introduced within a analysis.

ACKNOWLEDGEMENTS

This study is supported in part by the AirForce Office of Scientific Research.

REFERENCES

1. Ma, C. L., Yang, J. M. and Chou, T. W., "Elastic Stiffness of Three-Dimensional Braided Textile Structural Composites," *Composite Materials*:

Testing and Design (Seventh Conference), ASTM STP 893, J. M. Whitney, Ed., American Society for Testing and Materials, Philadelphia, 1986, pp. 404-421.

2. Yang, J. M., Ma, C. L. and Chou, T. W., "Fiber Inclination Model of Three-Dimensional Textile Structural Composites," *J. of Composite Materials*, Vol 20, 1986, pp 472-484.
3. Ko, F. K., Pastore, C. M., Lei, C. and Whyte, D. W., "A Fabric Geometry Model for 3-D Braid Reinforced FP/AL-Li Composites," *Competitive Advancements in Metals/Metals Processing*, SAMPE Meeting, Aug. 18-20, 1987, Cherry Hill, NJ.
4. Ko, F. K. and Pastore, C. M., "Structure and Properties of an Integrated 3-D Fabric for Structural Composites," *Recent Advances in Composites in the United States and Japan*, ASTM STP 864, J. R. Vinson and M. Taya, Eds., American Society for Testing and Materials, Philadelphia, 1985, pp.428-439.

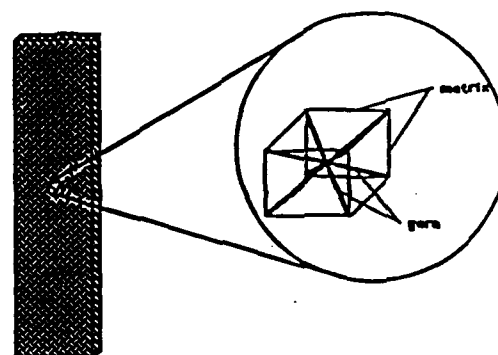
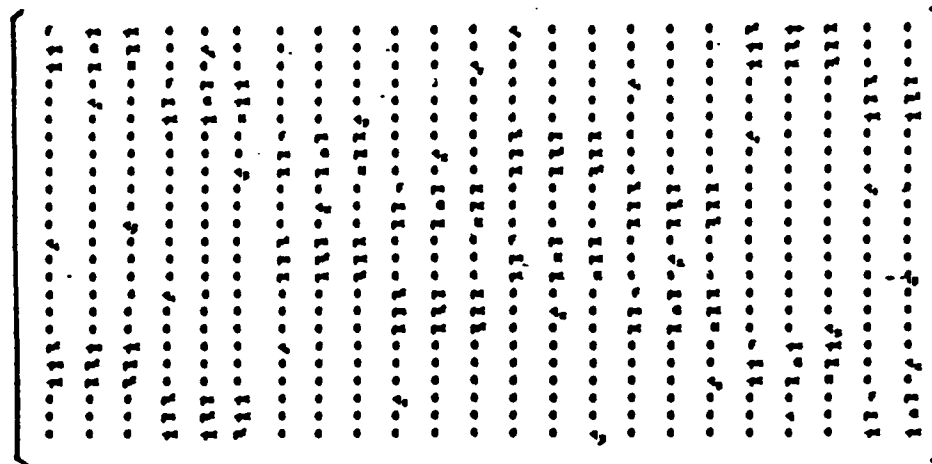


Figure 8. Schematic of a 3-D Braided Composite Unit Cell Geometry



where $p = E_1 A_f / l_f$ $r = \cos(\theta_f, 1)$ $F = p^2 + q$
 $q = E_2 A_{f2} / l_{f2}$ $s = \cos(\theta_f, 2)$ $G = p^2 + q$
 $q = E_3 A_{f3} / l_{f3}$ $t = \cos(\theta_f, 3)$ $H = p^2 + q$
 $q = E_4 A_{f4} / l_{f4}$

Figure 2. Explicit Listing of the K Matrix Formulated for the FCM Analysis.

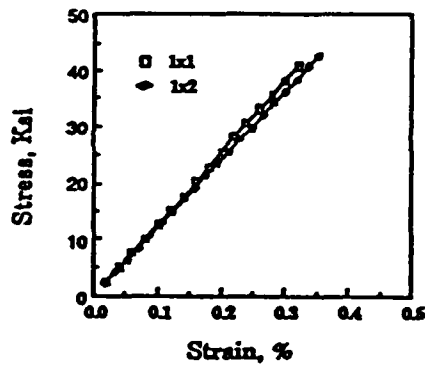


Figure 3 The Effect Of Fiber Geometry Of A Unit Cell

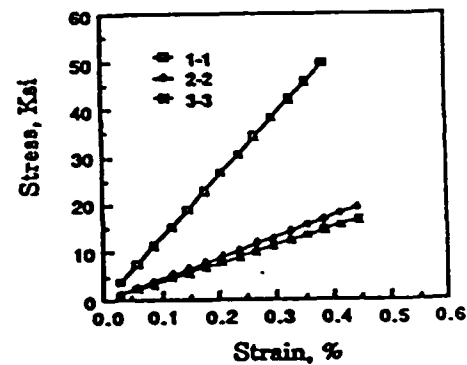


Figure 4b Elastic Behavior Along 1-1, 2-2 and 3-3 axes for Kevlar 149/Epoxy 828 Composite.

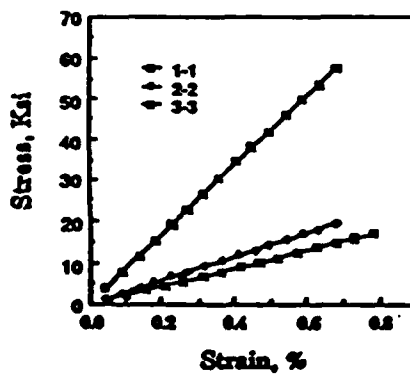


Figure 4a Elastic Behavior Along 1-1, 2-2 and 3-3 Axes for Carbon/Carbon Composite.

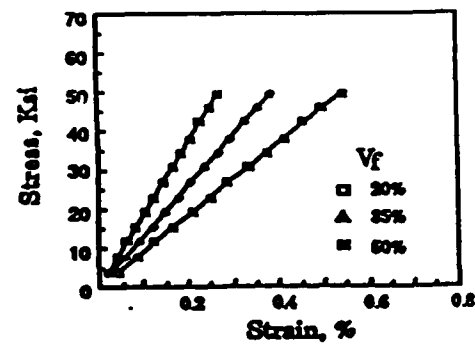


Figure 5 The Effect Of Fiber Volume Fraction On Elastic Behavior.

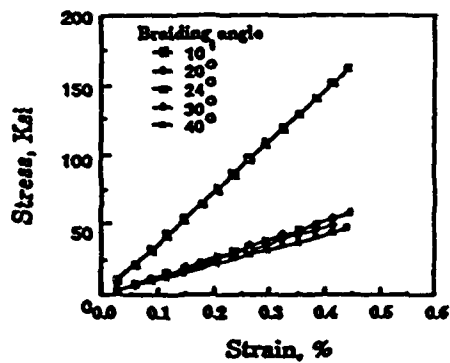


Figure 6 Effect of Braiding Angle On Elastic Properties

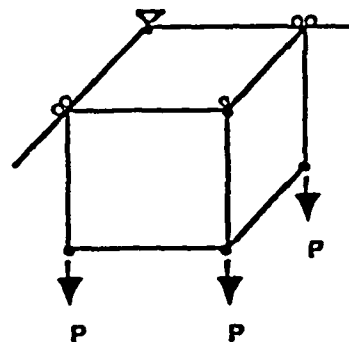


Figure 8. Boundary and Loading Conditions of a Unit Cell.

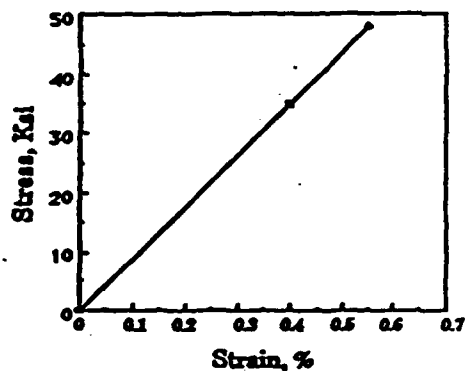


Figure 7a. Experimental Stress-Strain Curves of 1x1 Braided OC Composites.

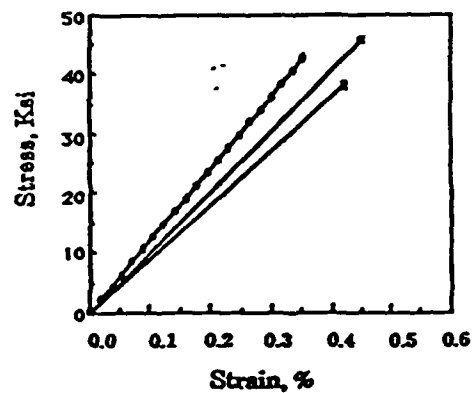


Figure 8a. Stress-Strain Curves of Experimental and Predicted 1x1 Braided Composites.

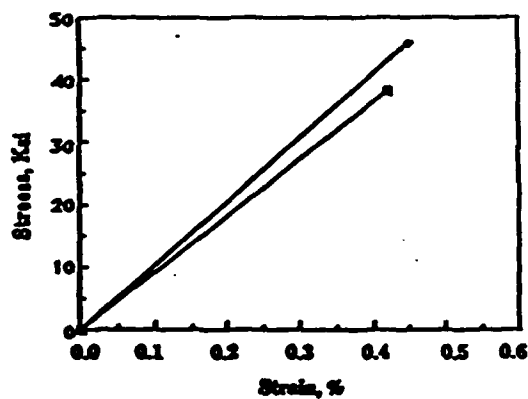


Figure 7b. Experimental Stress-Strain Curves of 1x2 Braided OC Composites

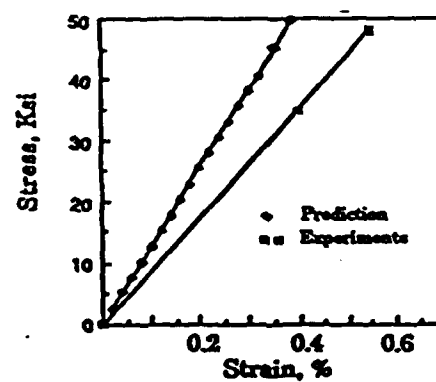


Figure 8b. Stress-Strain Curves of Experimental and Predicted 1x2 Braided Composites.

Finite Element Analysis of 3-D Braided Composites

Charles Lei, Yun-Jia Cai and Frank Ko

Fibrous Materials Research Center

Department of Materials Engineering, Drexel University

Philadelphia, PA 19104

ABSTRACT

A numerical method, which utilizes the computer aided geometric modelling (CAGM) in conjunction with finite element procedures, is presented to predict the mechanical behavior of 3-D braid composites. The CAGM, based on the computer geometric technique and textile formation process, provides the detailed information of the fiber architecture of 3-D braid composites. With the fiber architecture being defined, unit cell structures can be identified and be treated as space structures. Then, finite element procedures can be performed on each unit cell to obtain the elastic behavior of the composites. The present analysis includes the consideration of the interior and boundary elements of the entire cross-section, and consideration of bending moment of the yarns. The present model predicts a lower value of Young's modulus than that of experimental results. Modifications will be made on how to properly represent the matrix effect of a 3-D braid composite.

INTRODUCTION

In the family of advanced composites, 3-D textile composites have received great attention because of their superior structural properties such as no delamination, improved stiffness, toughness in the through-thickness direction and improved impact tolerance.[1] In developing these composites with innovated fiber architecture, an analytic model is needed in order to describe the load-deformation-failure properties of a composite on a macroscale. Such a model must be developed based on the accurate description of geometry and material interactions in the composite fiber architecture.

As reviewed in the papers of Rosen et al.[2] and Ko[3], the literature for the analysis of 3-D, or X-D fibrous reinforced composites are very limited. Most of the publications concern with the formulation and prediction of mechanical properties of the composites. For instance, Rosen et al. [2] used the concept of "constant stress state" to derive the average elastic constants and thermal coefficients of a unit cell structure. Chou et al. predicted elastic moduli of 3-D braided composites based on energy method [4] and on the modified classical laminate theory [5], respectively. Combining textile engineering methodology and averaging effective properties of a unit cell, Ko et al. [6] developed "fabric geometric model" to predict the mechanical properties and failure of 3-D composites. Following the similar considerations of volume averaging method, Byun et al. [7] predicted elastic moduli of 2-step braid composites. The elastic properties from the above models can be used as input to a generalized finite element program in order to analyze complex 3-D structures.

As far as the methodology is concerned, the conventional finite element method assumes the fibrous composite to be an effective continuum which possesses anisotropic deformation properties. Therefore, the finite element method can be used to analyze structures of complex conformation. For example, the well-known structural analysis programs based on the finite element method, such as NASTRAN, ABAQUS and ANSYS, treat the composite material structures computations in classical sense. That is, every element is given apparent homogeneous properties in terms of the type, orientation and stacking sequence of fibers and type of matrix. The stiffness matrix is calculated for the model consisting of elements with equivalent properties. Displacements, strains and internal forces of a structure are first obtained for that model and then the stresses in the structure are calculated.

With complex fiber architecture system such as 3-D braids, however, the effective continuum concept can no longer provide an accurate description. The reason is that the microstructure of such new system is much more complicated than those found in laminated composites. Recently, Lei et al. [8,9], following finite element procedure, developed a finite cell model (FCM) to analyze the elastic behavior of 3-D braid composites. The FCM takes account of the fiber architecture of a unit cell in a 3-D braid composite and performs 3-D structural analysis of the considered unit cell. Thus, the first step of the analysis is to identify the unit cells in a composite. This paper presents a methodology for the identification and classification of unit cells based on 3-D

braiding processing parameters. The identified unit cell structures form the basis for 3-D graphic illustration of the fiber architecture and for the finite element analysis of the 3-D preform as a structure. With the FCM, the elastic properties and the stress-strain relationship of 3-D braid reinforced composites are predicted and compared with experimental results.

MODELLING OF 3-D BRAID COMPOSITES

The 3-D braid composite can be regarded as an assemblage of a finite number of individual structural cells. Each individual cell is the smallest representative volume taken from the fiber architectural system. It is then treated as a space structure with the endowed representative architecture, rather than a material with a set of effective continuum properties. The basic idea is to identify the unit cell's nodal supports, similar to the nodal points of a conventional finite element. By the introduction of the principle of virtual work in solid mechanics and structural analysis, the matrix $[k]$, the stiffness of the cell can be derived to relate nodal displacement vector to nodal forces for a cell. In this section, the utilization of fiber architecture model and the finite cell modelling will be discussed.

Unit Cell Characterization by CAGM

The analysis of textile composites depends directly on fiber architecture of the composites. The fiber architecture of a textile composite can be accurately characterized by a computer aided geometric model (CAGM). The details of development of this model is given in Pastore et al.'s paper [10]. This model considers the relative motions of the tracks and columns in the braiding machine and generates a mathematical simulation of the machine process. Thus, the detailed internal geometry of a textile reinforced composite can be visualized and the unit cell of the composite can be identified. Figure 1 shows the fiber architecture of a 3-D braid with an inclined cut-out generated by CAGM. The next step is to find out what the unit cell structure is in the braid.

In the paper [9], a unit cell structure shown in Figure 2 was proposed and assumed to represent the entire structure of a braid. The unit cell structure was used to simulate the behavior of 3-D braid carbon/carbon composites. The recent development of CAGM suggests a finer and more accurate description of unit cell structure. By simulating the yarn movements across tracks and columns of a loom and taking account of braiding direction, unit cell conformation can be traced through 3-D geometric index of data. From the

data, space nodes of a braid can be defined by the interweaving, or interlock, of yarns. Once the space nodes are known, the braid is divided into small cells by connecting the space nodes with straight lines. In each cell, the fiber architecture can be identified and treated as a combination of several basic patterns. Figure 3 shows all possible patterns in a 3-D braid generated by 1x1 column/track movement. In practical case, a 3-D braid usually contains several patterns.

For instance, Figure 4 shows top view of a cross-sectional cell patterns of a 3-D braid fabricated by a loom of 4 tracks and 20 columns. Figure 4.a shows the cell patterns after a column/track movement, and Figure 4.c shows the cell patterns after next column/track movement. Figure 4.b and Figure 3.d shows the corresponding pattern numbers of each cell, respectively. From Figure 4, one can recognize the cell structures in the outer region differ from the ones in the inner region of the braid. Therefore, the CAGM can provide the information of the various element types, i.e., central and boundary elements, for finite element modelling. Figure 5 shows the space fiber structure formed by a loom of 10 tracks and 4 columns under 4 column/track movements.

Finite Cell Modelling

The FCM is based on the concept of fabric unit cell structure and structural analysis. The composite is considered as an assemblage of a finite number of individual structural cells with brick shape. Each unit cell is then treated as a space structure with the endowed representative architecture.

The key step in the formulation of the problem is the identification of the unit cell's nodal points. As mentioned in the previous section, the CAGM provides not only the detailed fiber architecture of each unit cell but also the coordinates of each node. In this model, the yarns which pass by a node are considered as intersected each other and hence, can be treated as either pin-jointed two-force truss members or rigid connected frame members. With this consideration, the interaction at the yarn interlacing is not treated in this modelling. Thus, by treating a unit cell specifically as a pin-jointed space truss, a 3-D truss finite element technique may be employed for the mechanistic analysis.

In order to include the effect of matrix, which is subjected to tension or compression under the deformation of yarns, the matrix is assumed to act as

rod members, connecting the two ends of a given set of yarns in the unit cell. Hence, the matrix plays a role in restricting the free rotation and deformation of yarns.

Let a_{ij} represent the value of member deformation q_i caused by a unit nodal displacement r_j . The total value of each member deformation caused by all the nodal displacements may be written in the following matrix form:

$$\{q\} = [a] \{r\} \quad (1)$$

where $[a]$ is called the displacement transformation matrix which relates the member deformations to the nodal displacements. In other words, it represents the compatibility of displacements of a system.

The next step is to establish the force-displacement relationship within the unit cell. The member force-deformation relationship can be written as:

$$[Q] = [K] \{q\} \quad (2)$$

The principle of virtual work states that the work done on a system by the external forces equals the increase in strain energy stored in the system. Here, the nodal forces can be considered as the external forces of the unit cell. Therefore, if $\{R\}$ represents the nodal force vector, it follows that

$$\{r\}^T \{R\} = \{q\}^T \{Q\} \quad (3)$$

where $\{r\}$ and $\{q\}$ are virtual displacement and deformation, respectively. From Equations (1) and (2), the following equations can be derived:

$$\{R\} = [K] \{r\} \quad (4)$$

where: $\{R\}$ = nodal forces

$[K] = [a]^T [K'] [a]$ = stiffness matrix of the unit cell

$\{r\}$ = nodal displacements

Using Equation (4), the nodal force and the nodal displacements of a truss unit cell are related by the stiffness matrix of the unit cell.

In present study, each unit cell is modelled to be a frame structure. Therefore, axial, flexural, and torsional deformations of the yarns are considered in the analysis. The unknown displacements at the joints consist of six components, namely, the x, y and z components of the joint translations and the x, y and z components of the joint rotations. Therefore, for a 9-node frame unit cell, there are 54 degrees of freedom in this unit cell. Suppose that a member i in a space frame will have joint number j and k at its ends. The twelve possible displacements of the joints associated with this member are also indicated in Figure 6. To obtain the stiffness matrix of a unit cell in a simple way, the stiffness matrix of a member is constructed first instead of construction of displacement compatibility matrix.

The member stiffness matrix is obtained by a unit displacement method. The unit displacements are considered to be induced one at a time while all other end displacements are retained at zero. Thus, the stiffness matrix for a member, denoted $[S_M]$, is of order 12×12 , and each column in the matrix represents the forces caused by one of the unit displacements. The layout of the 12×12 matrix is shown in Figure 7. In general case, if the member axes are not coincident with structural axes, the member stiffness should be transformed by a rotation transformation matrix. The rotation matrix $[R_T]$ for a space frame takes the following form:

$$[R_T] = \begin{bmatrix} [T] & 0 & 0 & 0 \\ 0 & [T] & 0 & 0 \\ 0 & 0 & [T] & 0 \\ 0 & 0 & 0 & [T] \end{bmatrix} \quad (5)$$

where the matrix $[T]$ for a circular member is as follows:

$$[T] = \begin{bmatrix} C_X & C_Y & C_Z \\ -C_X C_Y / C_{XZ} & C_{XZ} & -C_Y C_Z \\ -C_Z / C_{XZ} & 0 & C_X / C_{XZ} \end{bmatrix} \quad (6)$$

where $C_X = (x_k - x_j) / L$; $C_Y = (y_k - y_j) / L$; $C_Z = (z_k - z_j) / L$; $L = [(x_k - x_j)^2 + (y_k - y_j)^2 + (z_k - z_j)^2]^{1/2}$; $C_{XZ} = (C_X^2 + C_Z^2)^{1/2}$

Thus, for a member, the stiffness matrix $[S_{MD}]$ in structure axes may be expressed in the following form:

$$[S_{MD}] = [R_T]^{-1}[S_M][R_T] \quad (7)$$

Then, assembly of the contributions from each member to a joint, or a node, yields the stiffness matrix of a unit cell.

With the stiffness matrix of a unit cell being known, for a structural shape which consists of a finite number of unit cells, a system of equations for the total structural shape can be assembled using the individual cell relations following the finite element methodology. From the solution of the equations, the stress distribution and deformation of the entire structure under applied load can be calculated and analyzed.

NUMERICAL SIMULATIONS

The FCM was implemented by the use of computer simulation. With basic parameters in a unit cell, such as yarn elastic modulus, fiber volume fraction, yarn orientation and unit cell dimension fully characterized, the applicability of the FCM to predict the structural response of composites will be demonstrated experimentally.

Simple rectangular coupons of the 3-D braided carbon-carbon composite were fabricated and characterized by tensile testing. In the present case, the track/column displacement ratio is 1/1. The material used for this study is T-40 carbon fiber, with a fiber modulus of 276 GPa. The fiber volume fraction of the composite is 35%. The modulus of the carbon matrix is taken as 8.3 GPa for prediction. Since the dimensions of a unit cell are considered to be the center lines of members of the unit cell, part of the bars lie outside the unit cell in real case. An averaging method for the determination of the cross-section areas of the bars was used. Assuming that all the fiber-bars of the composite have the same cross-sectional area, and that all the matrix-bars of the composite have the same cross-sectional area as well. Thus, for a specimen with dimension of $H \times W \times T$, the area of a fiber-bar can be obtained as

$$A_f = 0.35HWT / (\text{total fiber-bar length})$$

the area of a matrix-bar can be expressed as

$$A_m = 0.65HWT / (\text{total matrix-bar length})$$

Accordingly, the unit cell dimension is $0.635 \times 0.22 \times 0.19 \text{ cm}^3$. A_f is 0.0032 cm^2 and A_m is 0.004 cm^2 .

Figure 8 shows the loading condition and boundary conditions of a specimen. A specimen in length of 10 column/track movements is considered for analysis purpose. The applied load was divided into several steps on account of the possible nonlinear load-deformation behavior due to geometrical conformation. Figure 9 shows both experimental and numerical stress-strain curves of c/c composites under simple tension. From the figure, the stiffness of the composites predicted from FCM showed a lower value than experimental results; while FGM predicted a higher value. For the FCM, the consideration of yarns and matrix as structural bars may result in a lower stiffness in matrix-bar axis. Although the matrix-bars play the role in restricting the free deformation of the yarns in FCM, they show larger deformation under tensile load. Consequently, the nature of the finite cell modelling tends to predict a lower value of stiffness of a structure. Further studies on this model to investigate the interaction between fiber and matrix have to be conducted. The load transfer mechanism between fibers and matrix as well as the effect of fiber architecture in a unit cell needs to be explored. This may lead to a 3-D solid element modelling on the unit cell of a braid composite. For the FGM, the higher predicted stiffness may be attributed to the use of fiber data as an input for our prediction. In order to reflect the fiber breakage and degradation during manufacturing, the use of processed yarn data may be more appropriate.

CONCLUDING REMARKS

A unified mechanistic method, incorporating the computer aided geometric modelling and finite element procedure, has been presented to predict the mechanical behavior of 3-D braid composites. The CAGM has been shown to provide the detailed information of the fiber architecture of 3-D braid composites. The present analysis includes the consideration of the interior and boundary elements of the entire cross-section, and consideration of bending moment of the yarns. By appropriate choice of yarn mechanical properties and

precise determination of dimension of a unit cell, the finite cell modelling has been shown to be an adequate model for 3-D braided composites as a first approximation. The precision of the model may be further modified by an alternate method of representing the matrix effect.

In order to expand the usefulness of the FCM to more complex modes of deformation such as bending and shear, the interaction between reinforcing yarns and the matrix must be examined. The prediction of the stress-strain curve up to failure requires the establishment of a suitable failure criterion.

REFERENCES

1. Ko, F. K. Developments of High Damag  Tolerant, Net Shape Composites Through Textile Structural Design, Proceedings of ICCM-V, (ED. Harigan, W. C., Strife J. and Dhingra, A. K.), pp. 1201-1210, San Diego, CA, 1985.
2. Rosen, B. W. Chatterjee S. N. and Kibler J. J., An Analysis Model for Spatially Oriented Fiber Composites, Composite Materials: Testing and Design (Fourth Conference), ASTM STP 617, pp. 243-254 American Society for Testing and Materials, 1977.
3. Ko, F. K. Three-Dimensional Fabrics for Composites, Chapter 5, Textile Structural Composites, (ED. Chou, T. W. and Ko, F. K.), Elsevier Science Publishers B. V., Amsterdam, 1989.
4. Ma, C. L., Yang, J. M. and Chou, T. W. Elastic Stiffness of Three-Dimensional Braided Textile Structural Composites, Composite Materials: Testing and Design (Seventh Conference), ASTM STP 893, (ED. Whitney, J. M.), pp. 404-421, American Society for Testing and Materials, Philadelphia, 1986.
5. Yang, J. M., Ma, C. L. and Chou, T. W. Fiber Inclination Model of Three-Dimensional Textile Structural Composites, J. of Composite Materials, Vol 20, pp. 472-484, 1986.
6. Ko, F. K., Pastore, C. M., Lei, C. and Whyte, D. W. A Fabric Geometry

Model for 3-D Braid Reinforced FP/AL-Li Composites, Competitive Advancements in Metals/Metals Processing, SAMPE Meeting, Aug. 18-20, Cherry Hill, NJ, 1987.

- 7. Byun, J. H., Du, G. W and Chou T. W. Analysis and Modeling of 3-D Textile Structural Composite, ACS Conference, Florida, September 1989.**
- 8. Lei, S. C., Wang, A. S. D. and Ko, F. K. A Finite Cell Model for 3-D Braided Composites, ASME Winter Annual Meeting, Chicago IL, Nov. 27 - Dec. 2, 1988.**
- 9. Lei, S. C., Ko, F. K. and Wang, A. S. D. Micromechanics of 3-D Braided Hybrid MMC, Symposium on High Temperature Composites, Dayton, Ohio, June 13-15, 1989, pp.272-281, Proceedings of the American Society for Composites, Technomic Publish Co., 1989.**
- 10. Pastore, C. M. and Cai, Y. J. Applications of Computer Aided Geometric Modelling for Textile Structural Composites, Composite Materials Design and Analysis, (ED. W. P. de Wilde and W. R. Blain), pp.127 - 141, Computational Mechanics Publications, Springer-Verlag, 1990.**

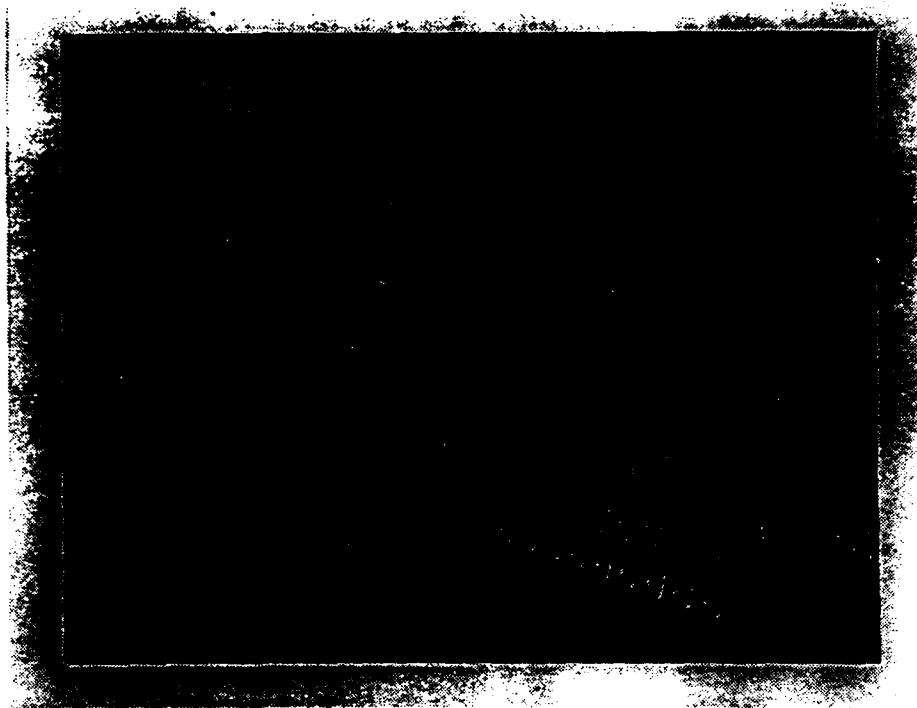


Figure 1. Fiber Architecture of a 3-D braid and a cut-out view generated by CAGM.

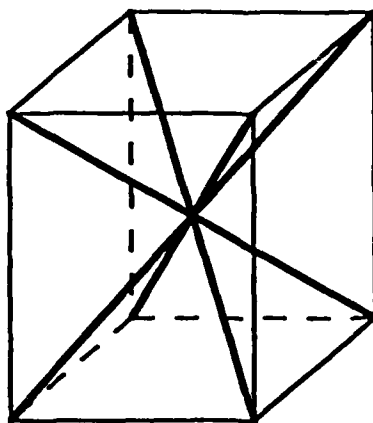


Figure 2. Unit Cell Structure presented in [9]

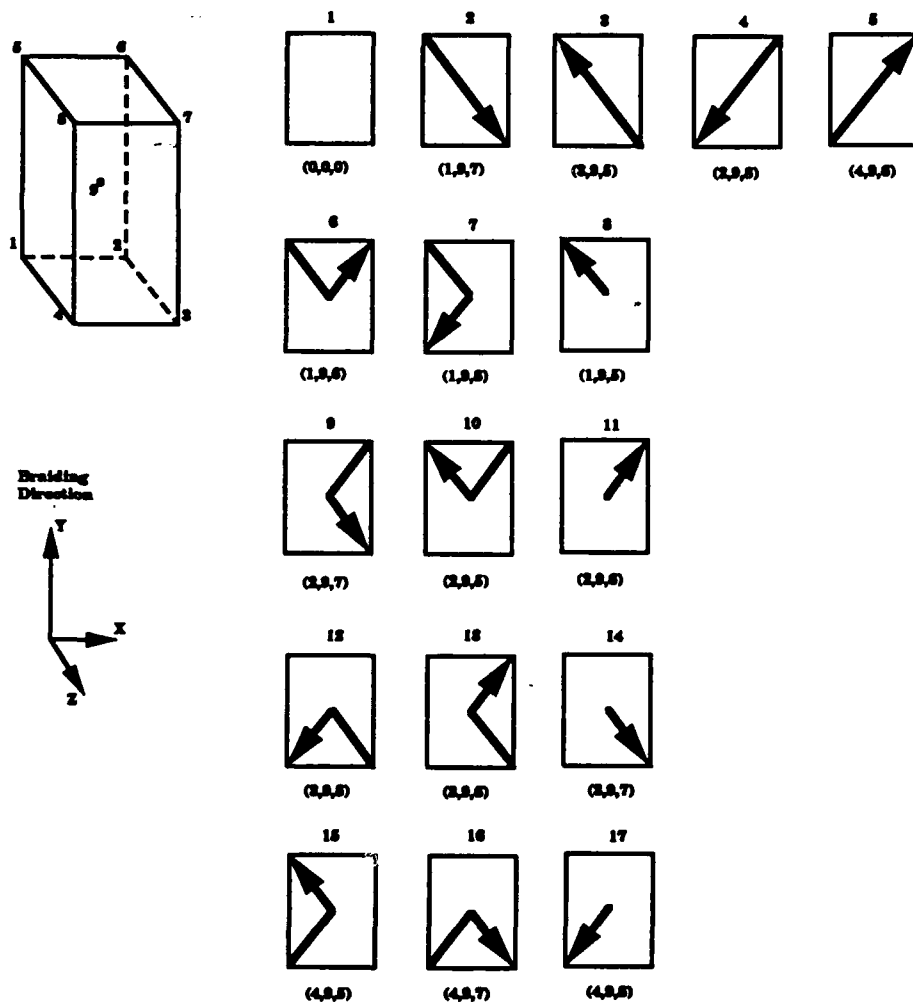
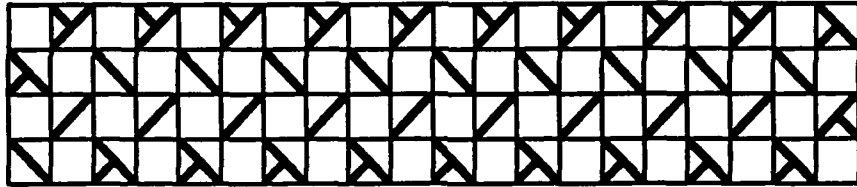


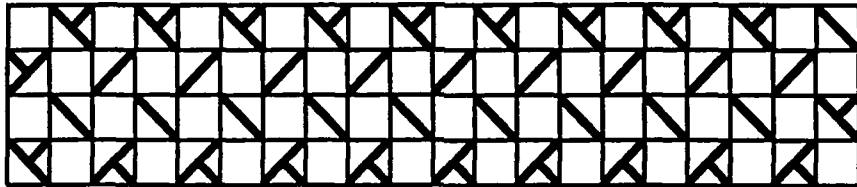
Figure 3. Element Patterns of a 3-D (1x1) braid



(a)

	7,5		7,5		7,5		7,5		7,5		7,5		7,5		7,5		7,16
2,13		2,3		2,3		2,3		2,3		2,3		2,3		2,3		2,3	
	4,5		4,5		4,5		4,5		4,5		4,5		4,5		4,5		4,16
3		2,15		2,15		2,15		2,15		2,15		2,15		2,15		2,15	

(b)



(c)

	3,9		3,9		3,9		3,9		3,9		3,9		3,9		3,9		3
5,10		5,4		5,4		5,4		5,4		5,4		5,4		5,4		5,4	
	2,3		2,3		2,3		2,3		2,3		2,3		2,3		2,3		3,6
6,13		4,13		4,13		4,13		4,13		4,13		4,13		4,13		4,13	

(d)

Figure 4. A cross sectional cell patterns generated by two column/track movements.

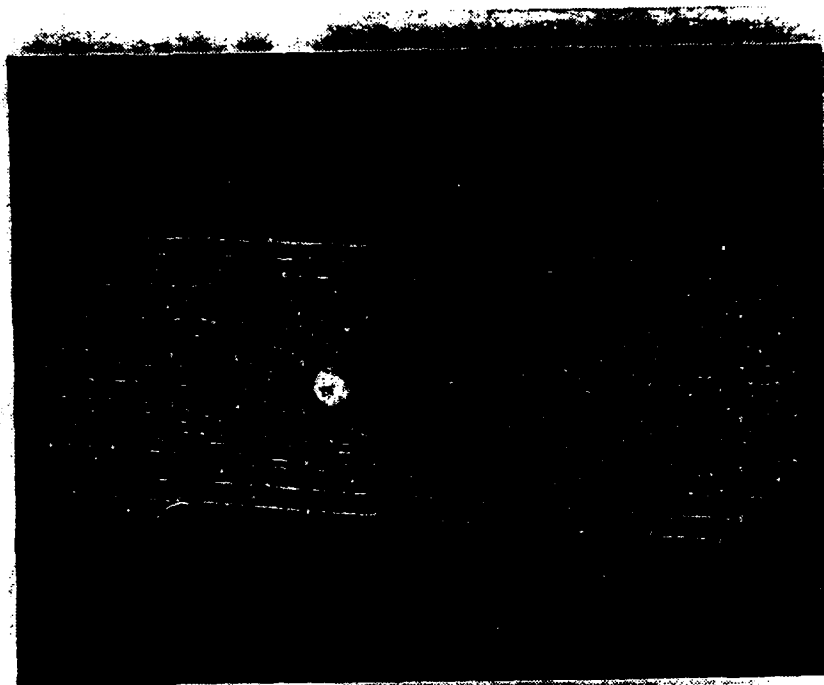


Figure 5. Unit cell Structures formed by a loom of 10 tracks and 4 columns under 4 column/track movements.

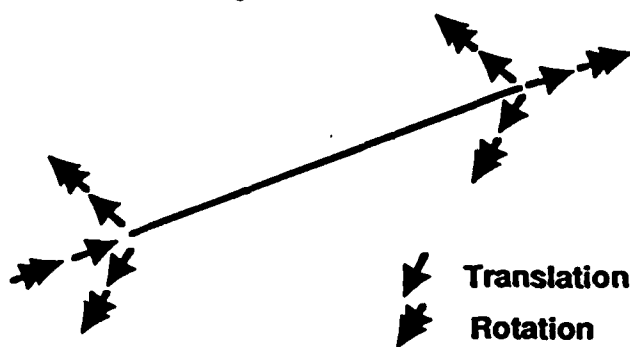


Figure 6. Twelve possible displacements of two joints

KP	0	0	0	0	0	-KP	0	0	0	0	0
0	KS	0	0	0	KF	0	-KS	0	0	0	KF
0	0	KS	0	-KF	0	0	0	-KS	0	-KF	0
0	0	0	KG	0	0	0	0	0	-KG	0	0
0	0	-KF	0	2KM	0	0	0	KF	0	KM	0
0	KF	0	0	0	2KM	0	-KF	0	0	0	KM
-KP	0	0	0	0	0	KP	0	0	0	0	0
0	-KS	0	0	0	-KF	0	KS	0	0	0	-KF
0	0	-KS	0	KF	0	0	0	KS	0	KF	0
0	0	0	-KG	0	0	0	0	0	KG	0	0
0	0	-KF	0	KM	0	0	0	KF	0	2KM	0
0	KF	0	0	0	KM	0	-KF	0	0	0	2KM

$$KP = EA/L ; KS = 12EI/L^3 ; KF = 6EI/L^2 ; KM = 2EI/L ; KG = GJ/L$$

Figure 7. Stiffness matrix of a member in a unit cell.

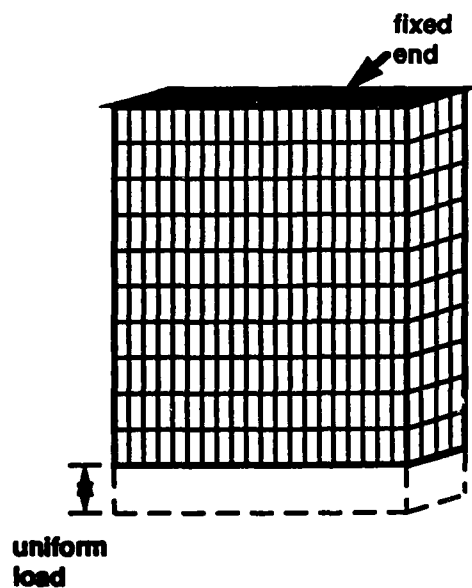


Figure 8. A specimen of ten column/tracks movements under uniform tension

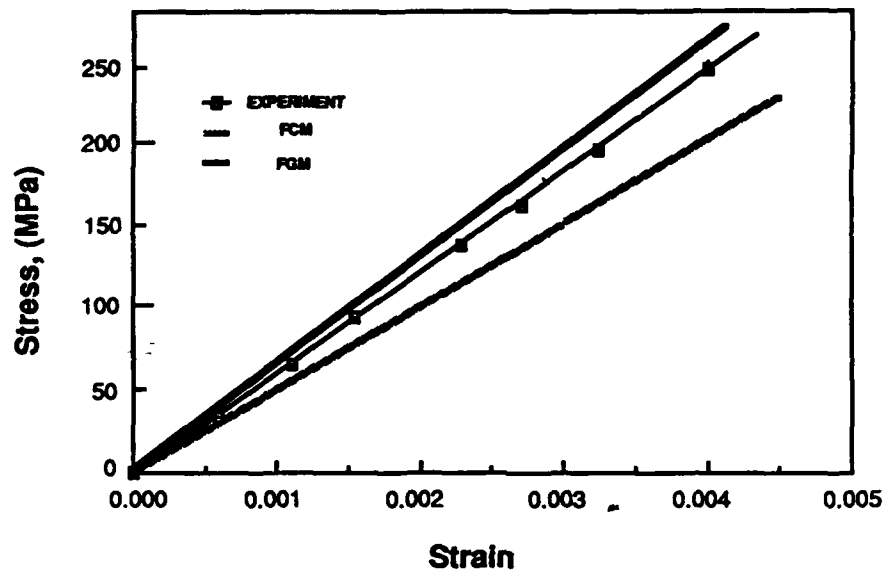


Figure 9. Comparison between experimental and numerical results of 3-D braided carbon/carbon composites.